Identification and assessment of antigens involved in membrane traversal by malaria parasites as vaccine candidates

A thesis submitted in fulfilment of the requirements for the degree of Doctor of Philosophy

Florian Brod

St Edmund Hall, University of Oxford

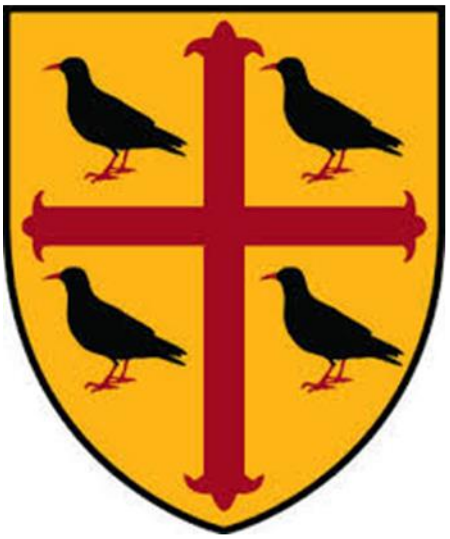



January 2018

Word count: circa 38,000 words excluding tables, figure legends and references

Abstract

Doctor of Philosophy – Infection, Immunology and Translational Medicine

Identification and assessment of antigens involved in membrane traversal by malaria parasites as vaccine candidates

By Florian Brod

St Edmund Hall

Michaelmas Term 2017

Malaria is a mosquito borne disease caused by parasites of the genus *Plasmodium*, inflicting a high number of infections and deaths each year. Since the end of the last century incidence rates were reduced significantly, but control measures that facilitated this decrease are starting to fail. An effective vaccine against malaria, particularly one with a marked effect on disease transmission, would undoubtedly be an invaluable tool for control, elimination and finally eradication of this ancient scourge of humankind. Consensus is that a vaccine containing multiple antigens from different life-cycle stages has the most realistic chance of success. Development of an effective malaria vaccine therefore requires two things, identification of critical antigens to be included in the vaccine as well as the assessment of ways to generate multi-antigen vaccines which are effective. During their complex lifecycle, *Plasmodium* parasites cross host cell membranes multiple times, moving between intracellular and extracellular spaces. The short windows of extracellular location represent the only times parasites are directly exposed to components of the human humoral immunity, making them susceptible to antibody mediated neutralisation. In this thesis I developed and tested novel, antibody inducing vaccines targeting multiple proteins of different life cycle stages with a role in membrane traversal. Furthermore, in an effort to find potential novel antigens suitable for inclusion in a vaccine, I identified a novel protein-protein interaction involved in traversal of the mosquito midgut, a natural bottle neck in the *Plasmodium* lifecycle. By expanding our understanding of how malaria is spread, as well as demonstrating new strategies to interfere with the process, I hope information from this thesis will aid the development of an effective malaria vaccine.

Acknowledgements

The preparation of this thesis has been a tremendously challenging, but also a rewarding and at times an outright fun experience. So as is customary, I would like to use these first pages to thank all the people who helped me to overcome any obstacles, supported me in difficult times and shared the joy of the good ones.

Firstly, my gratitude goes to my supervisors Adrian Hill and Sumi Biswas. Adrian, when I came to Oxford and started my rotations I had no intentions of spending my DPhil working on vaccines against malaria. That I ended up doing just that is in large part due to your highly contagious enthusiasm for the matter. Thanks for taking me into the Jenner Institute, for your guidance and support, for replying within five minutes to emails send at 2 o'clock at night and for proofreading parts of this thesis after I sent it to you a week before my submission deadline. Sumi, ending up under your direct supervision was probably one of the luckiest coincidences of my entire PhD, all the more as it happened so early on. I could hardly have wished for a more attentive and approachable supervisor. Particularly when I decided to start a completely new project half way through my time, your support has been invaluable. Thanks for striking the perfect balance between being a friend and a boss, for always keeping an open door, even when the group grew from a handful of people to its current impressive size, for all the small and big things you have done to help this thesis on its way and that I could impossibly list here, and not last for sacrificing a sizeable chunk of your Christmas and New Year's break reading every single chapter of it.

I also have to thank Julie Furze, Ahmed Salman, Jing Jin, Rebecca Dabbs, Marta Ulaszewska, Alex Fyfe and Alex Spencer for a lot of technical and practical support and for teaching me the skills I acquired in the last four years.

My gratitude further extends to external collaborators, namely Kazutoyo Miura, for running all my SMFAs and tirelessly answering every single one of my questions, and Andre Nobrega Pitaluga, Sofia Tapanelli and George Christophides for helping me organise and conduct the RNAi knock down experiment of *MG36*.

Furthermore I want to thank various members of team TBV, the antibody group and the wider Jenner Institute past and present, particularly Darren, Lee, Iona, Jo, Dan, Sarah, Tom, Martino, Anita, Matt, Adam, Pawan, Danny and Jonathan. You made the Jenner Institute a place I happily left the house for (nearly) every morning.

Preparing this thesis was not only a challenge physically and intellectually, but also emotionally, therefore I would like express my gratitude towards my friends without whom I would surely have lost all will to life at least once; to my friends at home, who made me feel like I never left whenever I came to visit, particularly Nickel, John, Keven, Robert, Lena and Jonas, and to my friends here in Oxford, particularly Joe, Simone and Sean with whom I saved humanity from the brink of extinction multiple times, and to Jack for wild parties in Thailand, England and Germany as well as calm walks in the Peak District.

My thanks also go, with love, to the people who contributed most to making me the person I am today, my family; to my uncle and aunt Ossi and Sigi, who always thought I was way more special than I am, to my cousin Malte and my brother-in-all-but-blood Janis, who were there for me from before I can remember, to my little sister Annika, my polar opposite who, like nobody else, reminds me of the things important in life that I naturally tend to neglect, and to my parents Marianne and Gert, thanks for always believing in me, thanks for always supporting me, thanks for being the most wonderful and loving parents a son could wish for!

Finally and most emphatically, my thanks go to my wife Heike and my children Lina and Mio. Heike, you left your beloved Frankfurt to accompany me to Oxford so I could pursue a PhD here, and even when things got unbelievably difficult you stayed here with me and supported me all the way through. I love you! Lina and Mio, you were both born while this thesis was coming to be as well, and as a consequence you might have seen less of me than I would have liked, but knowing you were there was probably the biggest motivation for me to see this through. You too, I love with all my heart!

Table of Contents

Abstract ..... **II**

Acknowledgements ..... **III**

Table of Contents ..... **V**

List of Figures ..... **XII**

List of Tables ..... **XVI**

List of Abreviations ..... **XVII**

Chapter 1 - Introduction **1**

1.1 Malaria - A major challenge to global health 1

1.2 The *Plasmodium* lifecycle 4

1.2.1 The pre-erythrocytic stage 6

1.2.2 The asexual blood stage 10

1.2.3 The sexual stage 14

1.3 Immunity against malaria 20

1.3.1 Immunity against pre-erythocytic parasites 20

1.3.2 Immunity against the blood stage of malaria infection 21

1.3.3 Immune responses against gametocytes 24

1.4 Vaccines against malaria 25

1.4.1 Pre-erythrocytic vaccines 27

1.4.2 Blood stage vaccines 30

1.4.3 Transmission blocking vaccines 31

1.5 Thesis outline and aims 34

Chapter 2 - Material and Methods 36

2.1 Materials 36

2.1.1 Buffers 36

2.1.2 Media 37

2.1.2.1 Bacterial growth media and agars 37

2.1.2.2 *Pichia* growth media and agars 37

2.1.3 Antibodies 38

2.1.4 Primers 38

2.1.5 Plasmids 40

2.1.6 Expression systems 40

2.1.6.1 PichiaPink 40

2.1.6.2 GS115 41

2.1.6.3 Drosophila Schneider-2 (S2) cells 41

2.1.7 Adjuvants 41

2.1.7.1 Alhydrogel 41

2.1.7.2 AS01 42

2.1.7.3 Matrix-M 42

2.1.7.4 AddaVax 42

2.1.8 Vaccines 43

2.1.8.1 RTS,S 43

2.1.8.2 Pfs25-IMX313 43

2.1.9 Parasites 43

2.1.10 Gene synthesis 44

2.1.10.1 GeneArt Strings DNA Fragments 44

2.1.10.2 GeneArt Gene Synthesis 44

2.2 Molecular Biology 45

2.2.1 Polymerase chain reaction (PCR) 45

2.2.1.1 PCR for subcloning 45

2.2.1.2 Colony PCR 46

2.2.1.3 qPCR 47
2.2.2 Subcloning 47
2.2.2.1 Subcloning by restriction digest and ligation 47
2.2.2.2 Subcloning by In-Fusion cloning 47
2.2.3 Cloning of expression vectors 48
2.2.3.1 Cloning of the R21c expression vector 48
2.2.3.2 Cloning of SPECT1-VLP expression vectors 48
2.2.3.3 Cloning of the SPECT1-6xHis expression vector 49
2.2.3.4 Cloning of Pfs25-VLP expression vectors 49
2.2.3.5 Cloning of AVEXIS plasmids 49
2.2.4 Transformation of *E. coli* 51
2.2.4.1 Generation of competent Top10 *E. coli* cells 51
2.2.4.2 Re-transformation of plasmids 52
2.2.4.3 Transformation of newly cloned plasmids 52
2.2.5 Plasmid preparation 53
2.2.6 Sequencing 53
2.2.7 Transformation of *Pichia pastoris* 53
2.2.7.1 Generation of electrocompetent *Pichia* cells 53
2.2.7.2 Electroporation of *Pichia* pastoris 54
2.3 Protein Biochemistry 54
2.3.1 Protein expression from *Pichia pastoris* 54
2.3.1.1 Small scale protein expression for analysis of expression 54
2.3.1.2 Large scale protein expression 55
2.3.1.3 Glass beads lysis of *Pichia* pastoris for VLP purification 56
2.3.1.4 High pressure lysis of *Pichia* pastoris for VLP purification 56
2.3.2 Protein expression in *Drosophila* Schneider-2 (S2) cells 57
2.3.3 Protein characterisation by SDS polyacrylamide gel electrophoresis 58
2.3.3.1 SDS page 58
2.3.3.2 Detection of proteins using unspecific protein stains 58
2.3.3.3 Detection of proteins by Western blot 59

2.3.4 Fast protein liquid chromatography (FPLC) 59
2.3.4.1 C-Tag affinity chromatography 59
2.3.4.2 Immobilised metal ion affinity chromatography (IMAC) 59
2.3.4.3 Size exclusion chromatography (SEC) 60
2.3.5 Protein quantification 60
2.3.6 SpyTag-SpyCatcher/SnoopTag-SnoopCatcher conjugation 60
2.3.7 Transmission electron microscopy (TEM) 61
2.3.8 Avidity-based extracellular interaction screen (AVEXIS) 61
2.3.8.1 Quantification of prey proteins 61
2.3.8.2 Quantification of bait proteins 62
2.3.8.3 AVEXIS assay 63
2.3.8.4 IgG competition AVEXIS 64
2.3.9 Surface plasmon resonance 64
2.4 Immunology 65
2.4.1 ELISA 65
2.4.1.1 Endpoint ELISA 65
2.4.1.2 Standard ELISA 66
2.4.1.3 NANP Avidity ELISA 67
2.4.1.4 NANP Isotype ELISA 68
2.5 Animals and Parasitology 69
2.5.1 Immunisation 69
2.5.2 Blood sampling 69
2.5.2.1 Blood sampling by tail tip amputation and thin film preparation 69
2.5.2.2 Blood sampling by tail bleeding 70
2.5.2.3 Blood sampling by cardiac puncture (exsanguination) 70
2.5.3 Parasite production 70
2.5.4 Malaria challenge 71
2.5.5 Standard membrane feeding assay (SMFA) 71
2.5.6 Inhibition of sporozoite invasion assay (ISI) 72

2.5.7 Mosquito RNAi 73
2.5.7.1 cDNA synthesis 73
2.5.7.2 dsRNA synthesis 74
2.5.7.3 Gene knockdown in mosquitoes 74
2.6 Statistical Analysis 75
Chapter 3 - Pre-clinical assessment of the malaria vaccine candidate R21 76
Authorship statement 76
3.1 Introduction 76
3.2 Results 80
3.2.1 R21 can be purified by affinity chromatography 80
3.2.2 Priming with Hepatitis-B vaccine, Engerix-B affects immune responses to R21..... 83
3.2.3 R21 elicits durable anti-CSP antibody responses in mice 85
3.2.4 Lower doses of R21 correlate with better protection 87
3.3 Discussion 95
Chapter 4 - Generation and characterisation of dual antigen malaria vaccines 98
Authorship statement 98
4.1 Introduction 98
4.2 Results 102
4.2.1 Dual antigen VLP design 102
4.2.2 R21-SPECT1, an improved sporozoite vaccine 104
4.2.2.1 SPECT1 can be expressed on the surface of HBsAg-VLPs 104
4.2.2.2 Optimisation of R21-SPECT1 particle production 108
4.2.2.3 Anti-SPECT1 antibodies induced by R21-SPECT1 have protective efficacy against malaria in mice 112
4.2.3 R21-Pfs25, a multi-stage vaccine 116

4.2.3.1 Pfs25 and CS vaccines can be combined without interference 116

4.2.3.2 Expression of Pfs25 on the surface of HBsAg results in decreased particle yields..... 120

4.2.3.3 Generation of a CS-Pfs25 dual antigen VLP using Spy/Snoop technology.... 124

4.2.3.4 CS-Snoop-HBsAg-Spy-Pfs25 induces a functional antibody response against both antigens 127

4.2.4 Triple vaccine combinations 130

4.3 Discussion 132

4.4 Appendices 138

Chapter 5 - Identification of protein-protein interactions between the ookinete and the mosquito midgut surface 143

Authorship statement 143

5.1 Introduction 143

5.2 Results 145

5.2.1 Generation of ookinete and mosquito midgut epithelium surface protein libraries. 145

5.2.2 Expression of library proteins for AVEXIS screen 150

5.2.3 AVEXIS screen of ookinete and mosquito midgut epithelium surface proteins. 155

5.2.4 Characterisation of the Pfs28-MG36 interaction 164

5.2.5 Pfs28 only binds to full length MG36, not to either of its two transferrin like domains 167

5.2.6 The interaction of Pfs28 and MG36 can be specifically inhibited by anti-Pfs28 antibodies 169

5.2.7 Assessment of MG36 as a novel target for transmission blocking vaccines 170

5.2.8 Knockdown of *MG36* in mosquitoes reduces their susceptibility to malaria infection 173

5.2.9 The interaction of P28 and MG36 cannot be detected in other parasite-vector pairs 176

5.3 Discussion 180

Chapter 6 - Concluding remarks and future directions 187

6.1 Summary of findings 187

6.1.1 Novel vaccination strategies to target membrane traversal 187

6.1.2 Identification of novel protein-protein interaction involved in midgut traversal 190

6.1.2.1 A new hypothesis for the role of Pfs28 during midgut traversal 190

6.2 Future directions 192

6.2.1 Prospects of multi-antigen malaria vaccines 192

6.2.2 Defining the role of the Pfs28-MG36 interaction during midgut traversal 193

6.3 Conclusion 195

References 196

List of Figures

Figure 1.1: Spatial distribution of malaria transmission. 2

Figure 1.2: The *Plasmodium* lifecycle. 5

Figure 1.3: Liver infection by sporozoites 9

Figure 1.4: The bloodstage of *Plasmodium* infection. 13

Figure 1.5: The sexual stage of the malaria parasite life cycle. 19

Figure 1.6: Age distribution of malaria burden in stable transmission settings. 22

Figure 3.1: Lower doses of RTS,S and R21 correlate with better protection against challenge with transgenic *Plasmodium* parasites in mice. 79

Figure 3.2: Comparison of virus like particles based on the Hepatitis B surface antigen 81

Figure 3.3: R21 can be purified by C-Tag affinity chromatography 83

Figure 3.4: Pre-existing antibody titres against HBsAg have a moderate effect on the immune response to R21 84

Figure 3.5: R21 elicits long lasting antibody responses in mice. 86

Figure 3.6: Higher efficacy of low doses of R21 and RTS,S is not correlated with antibody isotype or avidity. 87

Figure 3.7: Higher efficacy of lower vaccine doses is not preserved in a subsequent malaria challenge 89

Figure 3.8: R21 and RTS,S are highly immunogenic at low doses. 91

Figure 3.9: High protection of RTS,S and R21 against transgenic malaria challenge is maintained at reduced vaccine doses. 93

Figure 3.10: High protection conferred by low doses of RTS,S and R21 against transgenic malaria challenge is maintained over two subsequent challenges. 94
Figure 4.1: Displaying antigens at the C–terminus of HBsAg- VLPs.....103
Figure 4.2: SPECT1 can be fused to HBsAg to be displayed on VLPs. 105
Figure 4.3: R21-SPECT1 induces antibody responses against both antigens in mice...106
Figure 4.4: Comparison of original and modified VLP purification process. 109
Figure 4.5: Maturation of R21-SPECT1 improves particle uniformity and immunogenicity 111
Figure 4.6: R21-SPECT1 induces functionally active antibodies against CSP and SPECT1 in Balb/c mice 113
Figure 4.7: R21-SPECT1 induces functionally active antibodies against CSP and SPECT1 in CD1 mice 115
Figure 4.8: RTS,S and Pfs25-IMX313 can be combined without reducing the antibody response to Pfs25 118
Figure 4.9: RTS,S and Pfs25-IMX313 can be combined without reducing the anti NANP-repeat immune response.....119
Figure 4.10: Insertion of NANP repeats between HBsAg and Pfs25 allows its expression on a VLP 122
Figure 4.11: R21-NANP-Pfs25 induces antibody responses against both antigens in mice.....123
Figure 4.12: Conjugation of Pfs25-SpyTag and CS-SnoopTag to Snoop-HBsAg-Spy produces dual antigen VLPs.....126
Figure 4.13: CS-Snoop-HBsAg-Spy-Pfs25 induces a functional antibody response against Pfs25. 128

Figure 4.14: CS-Snoop-HBsAg-Spy-Pfs25 induces a functional antibody response against CSP 129
Figure 4.15: Triple vaccine combination 131
Figure 5.1: AVEXIS constructs 150
Figure 5.2: Quantification of proteins for AVEXIS 151
Figure 5.3: Western blot of AVEXIS prey and bait constructs 153
Figure 5.4: AVEXIS of Ook1, Ook2 and Ook3 against all 38 midgut proteins 156
Figure 5.5: AVEXIS of Ook4, Ook5 and Ook6 against all 38 midgut proteins. 157
Figure 5.6: AVEXIS of Ook7, Ook8 and Ook9 against all 38 midgut proteins 158
Figure 5.7: AVEXIS of Ook10, Ook11 and Ook12 against all 38 midgut proteins. 159
Figure 5.8: AVEXIS of Ook13, Ook14 and Ook15 against all 38 midgut proteins 160
Figure 5.9: AVEXIS of Ook16 and Ook17 against all 38 midgut proteins 161
Figure 5.10: Confirmation of the Pfs28-MG36 interaction 164
Figure 5.11: Characterisation of the Pfs28-MG36 interaction 166
Figure 5.12: MG36 is made up of two Transferrin like domains, which are both required for binding of Pfs28 168
Figure 5.13: Anti-Pfs28 antibodies specifically inhibit the interaction of Pfs28 with MG36 170
Figure 5.14: Assessment of MG36 as a novel target for transmission blocking vaccines 171
Figure 5.15: Anti-MG36 antibodies are less capable of blocking interaction between MG36 and Pfs28 than anti-Pfs28 antibodies 173
Figure 5.16: Knockdown of *MG36* reduces the susceptibility to malaria infection in A. gambiae mosquitoes 175

Figure 5.17: Sequence alignment of P28 and MG36 from three parasite-vector pairs 177

Figure 5.18: Interaction between P28 and MG36 were not detected in other parasite-vector pairs 179

List of Tables

Table 2.1: Buffers 36

Table 2.2: Bacterial growth media and agars 37

Table 2.3: *Pichia* growth media and agars 37

Table 2.4: Antibodies 38

Table 2.5: Primers for cloning, sequencing, qPCR and RNAi 38

Table 2.6: Plasmids used as backbones for the cloning of expression vectors used in this thesis 40

Table 2.7: Transgenic P. berghei parasites 43

Table 2.8: Phusion PCR thermo cycle 45

Table 2.9: Colony PCR thermo cycle 46

Table 2.10: Coating antigens and internal controls used in endpoint ELISAs in this thesis. 66

Table 2.11: Coating antigens, internal controls and standard curves used in standard ELISAs in this thesis. 67

Table 5.1: Proteins included in the ookinete surface library. 147

Table 5.2: Proteins included in the mosquito midgut surface library. 148

Table 5.3: Dilution factor and molecular weight of AVEXIS bait and prey proteins. 152

Table 5.4: Dilution factor and molecular weight of Pfs28-bait and MG36-prey 163

Table 5.5: Relative expression level and molecular weight of MG36-TFL-bait proteins 167

Table 5.6: Dilution factor and molecular weight of MG36 and Pfs28 orthologous proteins for AVEXIS 178

List of Abreviations

ACT	Artemisinin-based combination therapies
AMA	Apical membrane antigen
AOX	Alcohol oxidase
APC	Antigen presenting cell
APN	Aminopeptidase
AVEXIS	Avidity-based extracellular interaction screening
BAP	Biotin acceptor peptide
BirA	Biotin ligase
bp	base pairs
CBF	Clinical BioManufacturing Facility
cDNA	Complementary DNA
CelTOS	Cell-traversal protein for ookinetes and sporozoites
ChAd	Chimpanzee adeno viral vector
CHMI	Controlled human malaria infection
CI	Confidence interval
COMP	Cartilage oligomeric matrix protein
Crt	Calreticulin
CSP	Circumsporozoite protein
CTRP	Circumsporozoite TRAP-related protein
CyRPA	Cysteine-rich protective antigen
DBL	Duffy-binding-like protein
dsRNA	double stranded RNA
EBA	Erythrocyte binding antigen
EBL	Erythrocyte-binding-like protein
EBP	Enolase binding protein
EFF	Exoerythrocytic forms

EGF	Epidermal growths factor
ELISA	Enzyme-linked immunosorbent assay
EMA	European Medicines Agency
EPA	Pseudomonas aeruginosa exoprotein A
EphA2	EphrinA2
EPI	Expanded Program on Immunisation
FPLC	Fast protein liquid chromatography
GAMA	GPI-anchored micronemal antigen
GAPDH	Glyceraldehyde 3-phosphate dehydrogenase
giRBC	Gametocyte infected red blood cell
GLURP	Glutamate rich protein
GMEP	Global malaria eradication program
GMP	Good manufacturing practice
GSK	GlaxoSmithKline
HBsAg	Hepatitis B surface antigen
HGF	Hepatocyte growth factor
HSPG	Heparan sulfate proteoglycans
ifu	Infectious units
IM	Intramuscular
IMAC	Immobilised metal ion affinity chromatography
ISCOM	immune stimulating complex adjuvant
ISI	Inhibition of sporozoite invasion
IV	Intravenous
iRBC	Infected red blood cell
LLIN	Long-lasting insecticide-treated nets
LSA	Liver stage antigen
MAOP	Membrane-attack ookinete protein
ME	Multi epitope string

MHC	Major histocompatibility complex
MJ	Moving junction
MPL	3-O-desacyl-4'-monophosphoryl lipid A
MSP	Merozoite surface protein
MSPDBL	Merozoite surface protein Duffy binding-like
MVA	Modified vaccinia Ankara
MVI	Malaria Vaccine Initiative
MW	Molecular weight
OD	Optical density
PAMP	Pathogen associated molecular pattern
Pb	*Plasmodium berghei*
PBS	Phosphate buffered saline
PCR	Polymerase chain reaction
Pf	*Plasmodium falciparum*
PfEMP	*Plasmodium falciparum* erythrocyte membrane protein
pfu	plaque forming units
PLP1	Perforin like protein
PSOP	Putative secreted ookinete proteins
PTM	Peritrophic matrix
PVM	Parasitophorous vacuole membrane
RBC	Red blood cell
Rh	Reticulocyte-binding-like homolog protein
RIFIN	Repetitive interspersed families of polypeptides
Ripr	Rh5 interacting protein
RDT	Rapid diagnostic tests
RON	Rhoptry neck complex protein
S2	*Drosophila* Schneider-2 cells
SCRBQ	Scavenger receptor croquemort homologue

SEC	Size exclusion chromatography
SERA	Serine repeat antigen
SMFA	Standard membrane feeding assay
SOAP	Secreted ookinete adhesive protein
SPECT	Sporozoite microneme protein essential for cell traversal
SPR	Surface plasmon resonance
STEVOR	Subtelomeric variable open reading frame proteins
Sub	Subtilisin-like protease
SURFIN	Surface-associated interspersed gene family proteins
TBS	Tris-buffered saline
TBV	Transmission blocking vaccines
TEM	Transmission electron microscopy
TFH	T follicular helper
TFL	Transferrin like
TRA	Transmission reducing activity
TRAP	Thrombospondin-related-anonymous protein
TRI	Transmission reducing immunity
WARP	von Willebrand factor A domain-related protein
WB	Western blot
WHO	World health organisation
WRAIR	Walter Reed Army Institute of Research
VIMT	Vaccines that interrupt malaria transmission
VLP	Virus like particle
VSA	variant surface antigen
XA	Xanthurenic acid

Chapter 1 - Introduction

1.1 Malaria - A major challenge to global health

Malaria is simultaneously one of the world's oldest and deadliest diseases. Human malarial parasites most likely evolved alongside humans themselves some 6-10 million years ago [1] and are transmitted through the bite of an infected mosquito. While malaria is often thought of as a tropical disease today, at the beginning of the 20th century it was much more widely prevalent, reaching latitudinal extremes of 64° north and 32° south, covering more than 50% of the world's land area and putting 77% of its population at risk. The main determinant for malaria transmission is the presence of a good malaria vector, and it was indeed the elimination of the vector that facilitated elimination of malaria in most non-tropical counties in the first half of the 20th century [2]. Out of over 500 species of *Anopheles* mosquitoes, approximately 70 are capable of transmitting malaria and 41 are considered capable of transmitting malaria at a level of major concern to public health [3]. In sub-Saharan Africa, malaria is predominantly spread by *A. gambiae*, whose longevity, robustness and preference to bite humans make it an ideal vector. Here, the entomological inoculation rate, the number of infectious mosquito bites a person receives on average per year, can be as high as 1000 (***Figure 1.1***). In these areas of high transmission, the majority of malaria is caused by *P. falciparum,* one of six species of *Plasmodium* parasites capable of causing disease in human hosts. The other species are *P. vivax*, the zoonotic *P. knowlsei*, *P. malariae*, *P.*

ovale curtisii and *P. ovale wallikeri* [4]. Out of these *P. falciparum* causes the most severe form of malaria.

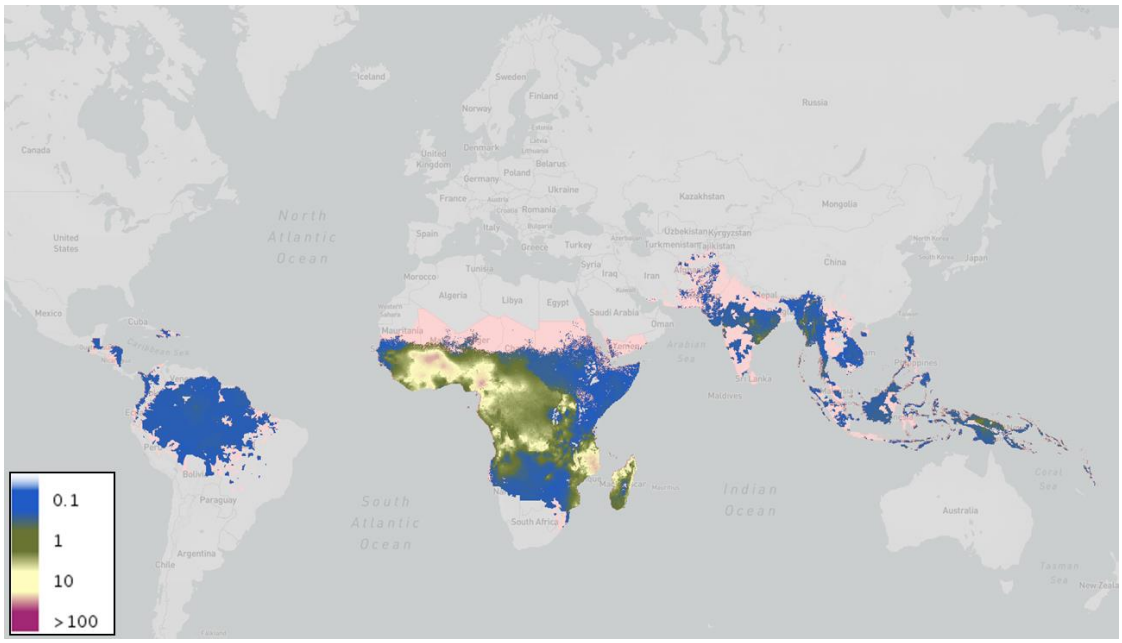

Figure 1.1: Spatial distribution of malaria transmission. The heat map shows the entomological inoculation rate of *P. falciparum*, the causative parasite of the most severe form of human malaria in 2010. Areas shaded in light red are areas of unstable transmission with incident rates of < 0.1%. (Map generate with: https://map.ox.ac.uk/explorer)

The symptoms of uncomplicated malaria are non-specific and include a vague absence of wellbeing, headache, fatigue, muscle aches, and abdominal discomfort, which are followed by regularly reoccurring bouts of fever. Severe *P. falciparum* malaria manifests differently depending on the age of the host, with severe anaemia and hypoglycaemia common in children, pulmonary oedema, jaundice and acute kidney injury more common in adults and acidosis and coma, caused by cerebral malaria, occurring in all age groups [5]. While the case fatality rate of uncomplicated *P. falciparum* malaria can be as low as 0.1% if treated promptly with effective anti-malarial drugs, the mortality rate of severe falciparum malaria is strongly dependent on the manifestation of symptoms and can exceed 80%. The global number of malaria

deaths reached 445 000 in 2016, with 91% of deaths occurring in the WHO African region [6].

The overall spatial distribution of malaria cases closely follows the distribution of fatalities from malaria with over 90% of malaria cases occurring in sub-Saharan Africa. According to estimates in the WHO world malaria report 2017 [6] there were a total of 216 million cases of malaria in 2016, an increase of 5 million cases over 2015. This is the first time since 2010 that case numbers increased in respect to the estimates of the previous year. While the increase was only by 5 million cases, less than 2.5%, this is still cause for great concern as it indicates that current control mechanisms, which helped to drastically reduce malaria prevalence over the last decade are starting to fail.

From its most widespread, pre-intervention distribution in 1900, malaria could be significantly reduced globally in the decades following Ronald Ross's discovery that the disease was transmitted through the bite of Anopheline mosquitoes [7]. Simple, environmental control of mosquito breeding sites resulted in elimination of malaria in 10 countries, reducing the land mass and population exposed to malaria by 13% and 9%, respectively in the years between 1900 and 1946 [2]. Efforts to protect soldiers stationed in areas of high malaria transmission during WWII led to the discovery of two of the first highly efficacious means for malaria elimination, the residual insecticide DTT and the anti-malarial drug chloroquine. In its 1955-1969 global malaria eradication program (GMEP), the WHO relied heavily of both of these tools, using DDT to interrupt transmission in an "attack phase" and chemoprophylaxis to eradicate malaria in the later "consolidation phase" [8]. Despite its failure to eradicate malaria

GMEP, together with less centrally organised national efforts, by 1975 had reduced the number of malaria endemic countries by 39 and the world's land mass and population exposed to malaria by 7% and 16%, respectively [2]. Unfortunately, the failed attempt at malaria eradication, for which, the rapid rise of insecticide resistant mosquitoes and chloroquine resistant parasites were thought to be the main contributing factors, resulted in a drop in enthusiasm and therefore funding for malaria control [8]. As a direct consequence of this no more dramatic impact was made on the world wide distribution of malaria until the end of the last century. The turn of the millennium however brought with it a renewed interest in malaria elimination and a number of programs and initiatives were brought to life with the aim to reduce the global prevalence of the disease [9]. Increased investment and funding yielded a number of new and highly effective tools against malaria, most notably long-lasting insecticide-treated nets (LLINs), rapid diagnostic tests (RDTs) and artemisinin-based combination therapies (ACT). The large scale roll out of these control tools reduced malaria incidence rate by 37% between 2000 and 2015 [10]. The increase in incidence rate in 2016 over 2015 therefore conjures uneasy images of the final days of GMEP. The spread of artemisinin resistant parasites in Southeast Asia [11-14] and pyrethroid resistance arising in mosquitoes in Africa [15], make clear the dire need for novel intervention tools if the failure of GMEP is not to repeat itself.

1.2 The *Plasmodium* lifecycle

Plasmodium parasites have an exquisitely complex lifecycle with obligate developmental steps in the human host as well as in the mosquito vector. Roughly, it

can be broken down in three different stages, the pre-erythrocytic stage, the erythrocytic stage or asexual blood stage and the sexual or sporogonic stage (***Figure 1.2***). Our current understanding of the *Plasmodium* lifecycle at a molecular level, arise partially from observations made directly in human parasites, but to a large extent also from studies in mouse malaria model parasites such as *P. berghei* and the chicken malaria parasite *P. gallaniceum*. While many processes are conserved between these different parasites, significant differences have also been demonstrated, and it is important to keep in mind that it is not always possible to infer information about one parasite from experiments conducted in another.

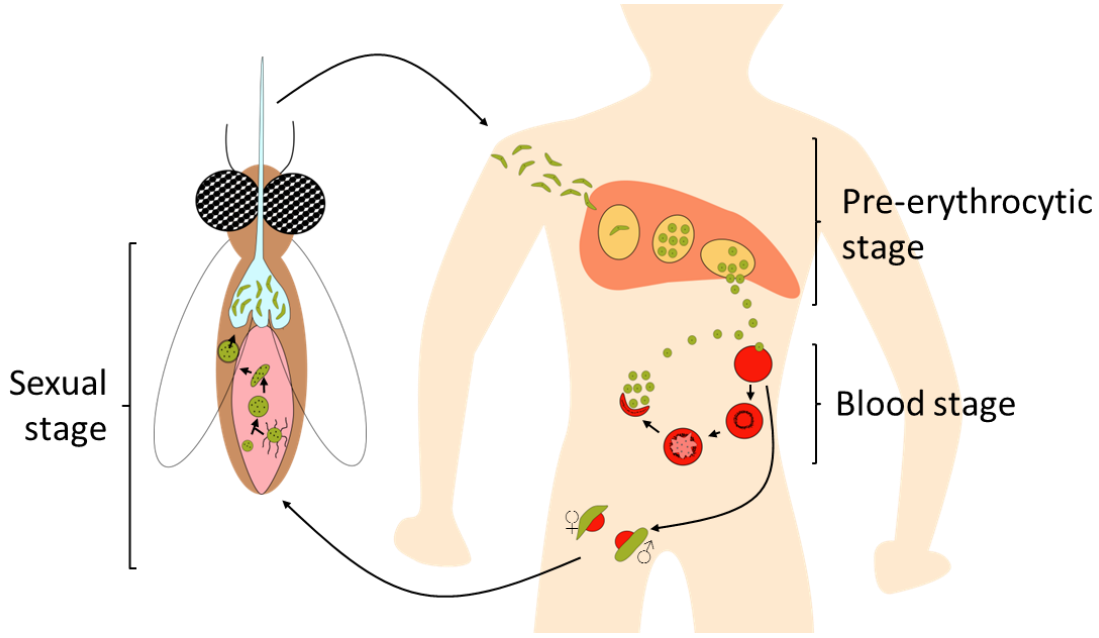

Figure 1.2: The Plasmodium lifecycle. Sporozoites are injected into a human host during the blood meal of an infected *Anopheles* mosquito. In the pre-erythrocytic phase, sporozoites invade hepatocytes of the liver where they develop into exoerythrocytic forms (EFFs) and undergo schizogenous replication. When the hepatic schizont bursts it releases up to 30.000 merozoites, which then infect erythrocytes and initiate the symptomatic blood stage of malaria infection. Merozoites replicate inside the infected erythrocyte until it bursts and releases between 16 and 32 new merozoites. A small subset of merozoites does not undergo schizogenous replication upon erythrocyte infection, but develop into long lived gametocytes that circulate in the bloodstream. When a mosquito feeds on a gametocytemic host, gametocytes in the mosquito midgut differentiate and fuse to form a zygote which then differentiates into the motile ookinete. Ookinetes cross the mosquito midgut epithelium and form oocysts at the midgut basal lamina. Midgut sporozoites are formed inside the oocyst through schizogenous replication. Upon their release they invade the mosquito's salivary gland where they reside as salivary gland sporozoites, ready to initiate a new round of infection.

1.2.1 The pre-erythrocytic stage

Infection of the human host starts with the bite of an infected anopheline mosquito. While the mosquito is probing for the blood meal, motile sporozoites from the mosquito's salivary gland are deposited in the dermis from where they embark to infect the liver. Sporozoites are extremely efficient at this process, and as little as 10 sporozoites have been shown to be sufficient to establish malaria infection [16]. Upon their deposition in the skin, sporozoites move randomly until they contact the endothelium of a blood vessel along and around which they then migrate before finally invading it [17]. Once they enter a capillary they are rapidly transported to the liver via the blood stream where they invade a hepatocyte and develop into exoerythrocytic forms (EFF) (***Figure 1.3***). After reaching the blood stream, the process of liver infection is normally completed within a few minutes [18].

Like the invasive stages of all apicomplexan parasites, generally called zoites, sporozoites are motile despite not possessing cilia or flagella, instead relying on a process termed gliding motility. The gliding motility of zoites is dependent on a subpellicular actomyosin motor, often referred to as the glidosome [19], that transports surface adhesins, like the thrombospondin-related-anonymous protein (TRAP) [20] or the circumsporozoite protein (CSP) [21], from the apical pole, from where they are secreted to the posterior pole, resulting in a forward movement [22, 23]. This gliding motility is essential for the sporozoite to complete its journey from the dermis to the liver, allowing for three important processes: movement along non-permissive barriers, cell invasion [22], and egress from invaded cells [24].

Invasion is a process that is highly conserved across all apicomplexan zoites. Other than intracellular bacteria or viruses, apicomplexans invade host cells not through passive uptake, but by actively moving into the cell. Gliding motility is therefore essential for the process, and zoites in which gliding motility is disabled through mutation of TRAP, the protein linking extracellular adhesion to a substrate to the intracellular actomyosin motor, are completely incapable of cell invasion [20]. In the first step of the process, the zoite attaches itself to the host cell, where the release of adhesive proteins from micronemes and rhoptries results in the formation of a tight junction [25]. The proteins that form the tight junction, which is therefore also referred to as the moving junction (MJ), are then translocated along the anteroposterior axis of the cell. This results in the zoite pushing against the host cell plasma membrane which invaginates and surrounds the invading parasite. Once the parasite has moved completely into the cell, the MJ, which is now positioned at its posterior end, is sealed off, resulting in the intracellular zoite being surrounded by a tightly fitting parasitophorous vacuole. The membrane of the parasitophorous vacuole (PVM) is non-fusogenic, and therefore provides a safe space for the parasite to replicate [26].

Sporozoites differ from most other zoites by not being released in close proximity to their target cells. Before sporozoites can invade a hepatocyte they therefore have to cross a number of cells including fibroblasts and phagocytes in the dermis [27] as well as Kupffer cells [28] and sinusoidal epithelial cells [29] in the capillaries of the liver. Passage of these barriers occurs by an active process called cell traversal and is associated with cell wounding [30]. A number of proteins have been shown to be

essential for cell traversal [31, 32], two of which, SPECT1 (Sporozoite microneme protein essential for cell traversal) [33] and SPECT2 [34] a membrane attack complex containing protein also referred to as PLP1 (perforin like protein 1), are exclusively active in the pre-erythrocytic stage. Both appear to play a role in escape from invaded cells rather than in entry [27] and were demonstrated to be important for the ability of sporozoites to establish liver infection *in vivo*, but are dispensable for hepatocyte invasion *in vitro* [35]. Indeed it was shown that sporozoites enter cells for traversal in transient vacuoles that are distinct from parasitophorous vacuoles and independent of microneme and rhoptry secretion as well as MJ formation [36]. In contrast to the parasitophorous vacuole these transient vacuoles do not provide a protected environment for the parasite, and have to be evaded quickly to avoid degradation by host lysozymes, a process in which SPECT1 and SPECT2 appear to be involved [35, 36]. It is very likely that escape from phagocytes occurs by a similar mechanism. Cell traversal therefore appears to have two related but distinct functions, escape from phagocytosis, as well as penetration of cellular barriers on route to the liver. Recently it could be shown that glyceraldehyde 3-phosphate dehydrogenase (GAPDH) on the surface of sporozoites binds CD68 on the surface of Kupffer cells, macrophage like cells in the liver sinusoid, during cell traversal, making CD68 the receptor for sporozoite invasion of Kupffer cells and a gateway for malaria infection of the liver [37, 38].

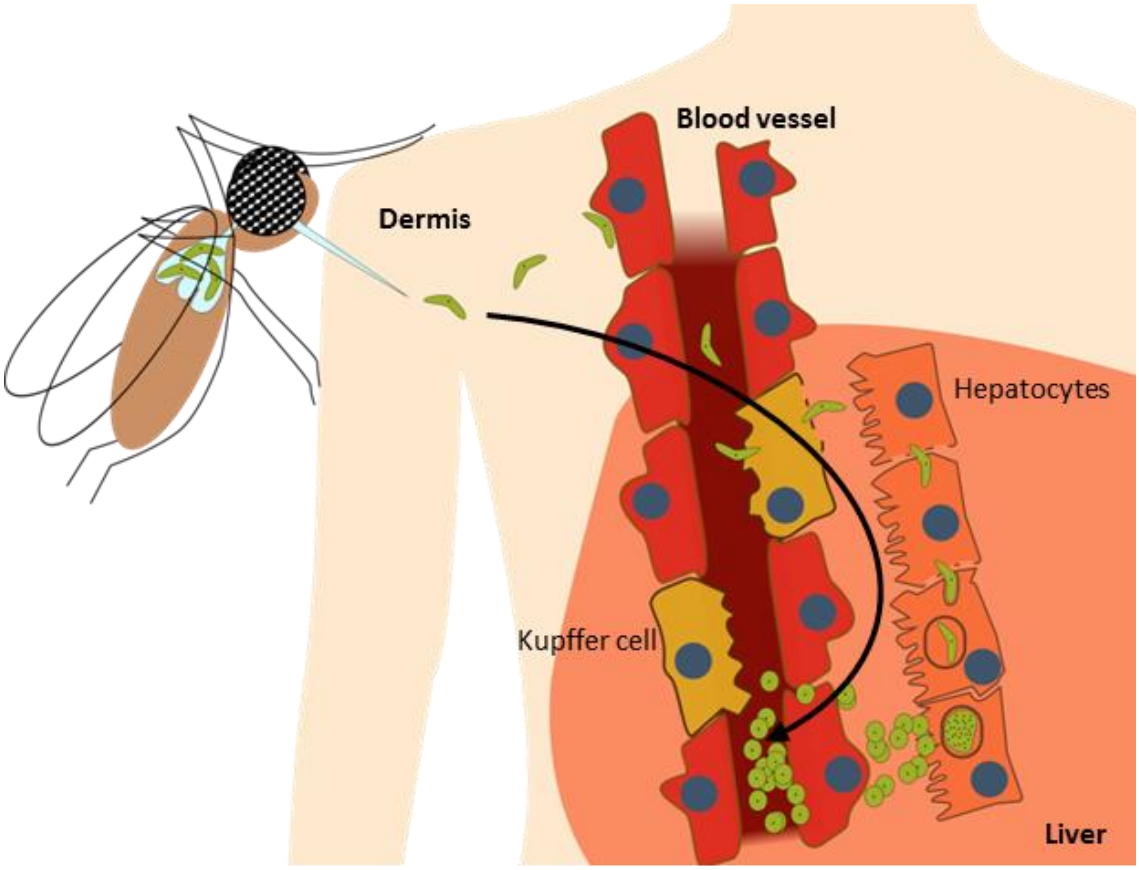

Figure 1.3: Liver infection by sporozoites. Sporozoites are injected into the dermis of a human host by a blood feeding mosquito. They then invade blood vessels in which they are transported to the liver. Sporozoites cross the liver sinusoidal epithelium through Kupffer cells and subsequently traverse through a number of hepatocytes before infecting one and developing into the exoerythrocytic form (EFF). The parasite then undergoes schizogenous replication before releasing up to 30,000 merozoites into the blood stream.

Interestingly, upon infection of the liver, sporozoites continue to traverse through a number of hepatocytes before finally invading one in which they then develop into exoerythrocytic forms EFFs and undergo schizogenous replication in prepataion of blood stage infection. It was hypothesised that this traversal of hepatocytes primes sporozoites for invasion by activating apical exocytosis [39] or make neighbouring hepatocytes more susceptible for invasion through release of hepatocyte growth factor (HGF) from wounded cells [40]. More recent studies however suggest that it simply takes some time for sporozoites to switch from the cell traversal to the invasion machinery [41].

The molecular basis of cell traversal and invasion by sporozoites is incompletely understood, but heparan sulfate proteoglycans (HSPGs) appear to play a role in the switch between the two processes as it was shown that sporozoites preferentially traverse cells with low-sulfated HSPGs but preferentially invade cells with high-sulfated HSPGs. Interestingly CSP has been shown to bind to HSPGs [42] and is specifically proteolytically processed to activate sporozoites for cell invasion [43], implicating a likely role as a mediator of productive hepatocyte invasion. Other hepatocyte proteins potentially involved in hepatocyte traversal or invasion are CD81 [44] and the scavenger receptor SR-BI [45, 46] as well as the *Plasmodium* proteins p36 and p52 [47-49]. Finally EphrinA2 (EphA2) on hepatocytes was recently suggested as a receptor for hepatocyte invasion [50]. All of these proteins appear to form an intricate interaction network involved in productive invasion of hepatocytes and PV formation, but the underlying molecular processes are to date not well characterised.

Once the sporozoite has completed its journey and finally invaded a hepatocyte, it replicates inside the parasitophorous vacuole developing into a schizont containing many thousands merozoites which are then released into the blood stream to initiate the blood stage of the parasite's life cycle.

1.2.2 The asexual blood stage

The asexual blood stage of malaria infection is initiated when liver schizonts burst and release thousands of merozoites into the blood stream where they invade erythrocytes. The process of erythrocyte invasion by merozoites is better understood than cell traversal and invasion by the other two motile forms of the *Plasmodium*

parasite, which is largely owed to the possibility of culturing blood stage parasites *in vitro*. Video microscopy shows that the invasion process occurs in three, distinct phases [51, 52], primary attachment and erythrocyte deformation, apical attachment and erythrocyte invasion and finally echinocytosis, a state of dramatic, dehydration like, morphological changes of the red blood cell (RBC). The first two steps, during which the merozoite is exposed to the host immune system in the blood stream, are on average completed within less than a minute.

On a molecular level, erythrocyte invasion begins with the attachment of the merozoite to the erythrocyte surface in a random orientation. The merozoite surface protein 1 (MSP1) as well as its associated proteins MSPDBL1 and 2 (merozoite surface protein duffy binding-like) have been suggested to be involved in this process [53, 54] but other observations suggest that the role of MSP1 is in egress from the erythrocyte rather than in its invasion [55]. There are other MSPs than MSP1, which together with other proteins form the dense protein coat that covers the merozoite surface, but which of these are involved in merozoite attachment is only incompletely understood. A number of merozoite surface proteins including MSP1 [56] and the glutamate rich protein (GLURP) [57, 58], have been shown to be the target of antibodies that inhibit merozoite invasion, but whether this effect is due to active blockage of the invasion or merozoite inhibition by complement fixation is not clear [59].

After initial attachment, adhesin containing micronemes are secreted from the merozoite, resulting in tight attachment to the erythrocyte and reorientation so that the apical tip is in contact with the membrane [51, 52]. This process seems to involve gliding motility and specific proteolytic cleavage of adhesion complexes on the side of

the merozoite [60] as well as membrane wrapping on the side of the erythrocyte [61]. Two classes of micronemal adhesins are predominantly involved in erythrocyte binding, the Duffy- or erythrocyte-binding-like proteins (DBL or EBL) and the reticulocyte-binding-like homolog proteins (Rh) (reviewed in: [62]). They bind a number of known and unknown receptors, and while overall important appear to be highly redundant and not individually essential for erythrocyte invasion. An exception from this is Rh5, which binds basigin (CD147) on the erythrocyte surface [63]. It forms a complex with Ripr (Rh5 interacting protein) and CyRPA (cysteine-rich protective antigen) and is involved in a separate, essential step during merozoite attachment [64, 65]. Reorientation is followed by secretion of the merozoite rhoptry content and the establishment of a tight junction between the RBC and the parasite. The Rh5-Ripr-CyRPA complex has been shown to be present of the merozoite's apical tip during tight junction formation and was suggested to be involved in inserting a pore into the erythrocyte membrane through which proteins can be injected into the RBC [66, 67]. Rhoptry neck complex proteins (RON) are among the first proteins that are injected into the RBC from the rhopthries, one of which is RON2, the receptor for AMA1 (apical membrane antigen 1). The AMA1-RON2 interaction is at the core of the MJ between the merozoite and the erythrocyte [68]. Fascinatingly, this means that the merozoite provides itself with its own invasion receptor. The merozoite then moves through the MJ by gliding motility as during the invasion of hepatocytes by sporozoites (***Figure 1.4***).

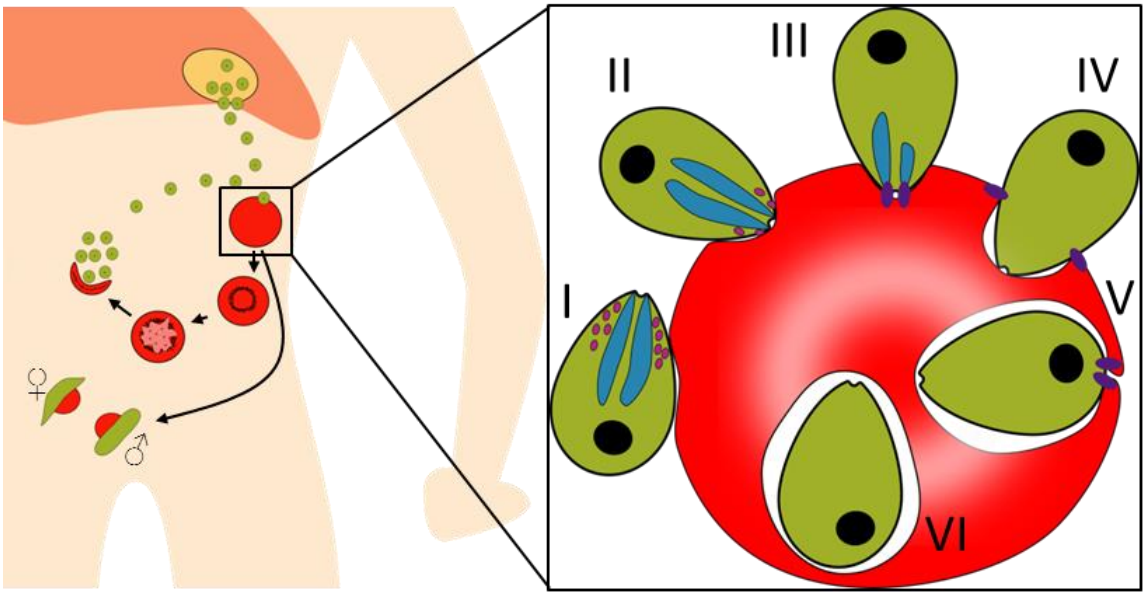

Figure 1.4: The bloodstage of Plasmodium infection. Merozoites egress from the liver and then invade erythrocytes. The invasion is initiated by the merozoite making loose contact with the RBC (I). Adhesins secreted from the micronemes then reorientate the merozoite so that the apical tip is in contact with the membrane (II). Secretion of the contents of the merozoite rhoptries then results in the formation of a tight junction between the parasite and the erythrocyte (III) through which the merozoite moves (IV) until it is completely encapsulated by the erythrocyte's cell membrane (V). This will later form the parasitophorus vacuole (VI). Inside the red blood cell the merozoites develop into ring stages, trophozoites and finally schizonts containing 16-32 merozoites which are released into the bloodstream ready to once again infect erythrocytes. A small subset of merozoites leave the asexual replication cycle, develop along a different pathway and differentiate into gametocytes instead.

Once inside the erythrocyte the merozoite develops into a ring, and subsequently into a trophozoite until it finally becomes a schizont containing 16-32 new merozoites, which are released in a concerted manner to initiate a new round of the blood stage infection cycle. During these developmental stages the parasite consumes and remodels the RBC, and it is during this stage that pathogenesis manifests. Using a highly complex machinery, the parasite exports proteins from the parasitophorous vacuole into the erythrocyte's cytosol and into its plasma membrane (reviewed in [69]). Among the exported proteins is PfEMP1 (*Plasmodium falciparum* erythrocyte membrane protein 1) as well as other adhesins that allow attachment of the parasitised erythrocyte to the vascular epithelium, thereby preventing transport to the

spleen and clearing in splenic macrophages [70-72]. Adherence causes sequestration of infected RBCs (iRBCs) in the peripheral circulation and contributes to organ dysfunction in patients with severe *falciparum* malaria, as sequestered parasites can block blood vessels and induce the production of pro-inflammatory cytokines that damage endothelial cells and increase vascular permeability [73, 74]. Other exported proteins are involved in accessing nutrients from the blood plasma and increasing the rigidity of the infected erythrocyte. It has been estimated that as many as 25% of the genes encoding exported proteins may be essential for parasite survival [75].

During each round of the blood stage infection cycle, a small proportion of invaded merozoites do not develop into ring stages, trophozoites and schizonts, but differentiate into the sexual stages of the malaria parasite known as gametocytes. Uptake of gametocytes by a blood feeding mosquito initiates the sexual stage of the *Plasmodium* life cycle.

1.2.3 The sexual stage

Switching from asexual development to gametocytogenesis by malaria parasites occurs in mature trophozoites or early during schizogony, and is regulated by the transcription factor AP2-G [76-78]. This means by the time a merozoite invades an RBC it is already determined whether it is to continue with asexual replication or to differentiate into a male or female gametocyte. Which environmental factors induce the switch is poorly understood. Commitment to gametocytogenesis could be purely stochastically driven, but a number of host and parasite factors have been implicated to potentially drive the decision, all of them in some form related to increased stress

[79, 80]. Once a merozoite, programmed for gametocytogenesis, invades an RBC, it goes through five developmental stages [81, 82]. From stage I gametocytes, which are indistinguishable from asexual parasites, they develop into stage IV gametocytes via two intermediate stages (stage II and III). All of these stages are characterised by high rigidity of the iRBC and are found sequestered in the bone marrow parenchyma were they avoid splenic clearance [83, 84]. Stage V iRBCs regain flexibility and return into the circulation where they can be taken up by a blood feeding *Anopheles* mosquito.

In the mosquito midgut, a drop of temperature of > 5°C and the presence of the mosquito waste product xanthurenic acid (XA) induce dramatic changes in the gametocytes within minutes after the blood meal [85, 86]. The male gametocyte undergoes three rounds of rapid genomic replication and assembly of flagella, resulting in eight flagellated microgametes emerging from the gametocyte, a process called exflagellation [87]. Male and female gametocytes then both escape the RBC in a process mediated by the release of osmiophilic bodies, vesicular structures in the gametocytes, containing the perforin like protein PLP2 (a homolog of SPECT2) that induces pore formation in the erythrocyte membrane [88]. The microgamete then fuses with the female macrogamete to form a diploid zygote. The process of attachment of the micro- to the macrogamete are incompletely understood, but two of the three proteins first shown to be a target of transmission blocking antibodies [89, 90], Pfs48/45 and Pfs230 appear to be involved in the process [91-93]. Once in close proximity, fusion of the gametes is catalysed by the conserved membrane fusion protein HAP2 [94]. Shortly after gamete fusion, their nuclei fuse within the zygote, which then undergoes two-step meiotic division. Interestingly, the meiosis is not

accompanied by cell division, resulting in the ookinete containing four haploid sets of chromosomes within a single nucleus [95]. The ookinete, like the two zoites from earlier lifecycle stages, is motile and relies on gliding motility to move in the blood meal and traverse through the midgut epithelium. Before reaching the epithelium the ookinete has to cross the peritrophic matrix (PTM), a chitinous layer secreted by the mosquito that surrounds the blood meal [96]. A process that is facilitated by secretion of chitinase from the ookinete [97].

Molecular processes at the midgut epithelium are only poorly understood, and whether a specific ligand-receptor interaction between the ookinete and the midgut takes place is a matter of ongoing debate. However, the ability of antibodies directed against Pfs25, Pfs28, PfEnolase and AgAPN1 to block infection of the mosquito lends some weight to the arguments in favour of the presence of one such interaction [90, 98-100]. Pfs25 and its paralogue Pfs28 are the two predominant proteins on the ookinete surface, but also present on the surface of the macrogamete and the zygote. Both share a similar structure containing multiple disulphide-bond-rich, epidermal growth factor (EGF) domains and have been reported to have multiple, partially overlapping functions [101]. These functions potentially include a role in structuring the ookinete outer membrane, protecting against lethal factors in the mosquito midgut, or in recognition of and attachment to the midgut epithelium. Particularly the last of these possibilities has been subject of vivid debates, which are still unresolved [102, 103]. Furthermore, Pfs25 is involved in anchoring large adhesion protein complexes to the surface of gametes and the ookinete [104] and binds laminin on the basal lamina side of the midgut epithelium [105]. Enolase has two separate functions

important for mosquito infection, first it binds plasminogen whose conversion to active plasmin promotes the invasion process [99], second it binds to enolase binding protein (EBP) on the midgut epithelium, which acts as an entry receptor for a subset of *P. berghei*, but not for *P. falciparum* ookinetes [106]. Finally, AgAPN1 is a mosquito amino peptidase that contains an epitope that is the target of transmission blocking antibodies, but its function in the interplay with the parasite has so far not been further characterised. Opsonisation with antibodies alone could theoretically be sufficient to block transmission of the parasite, even if the target of the antibodies is not involved in specific ligand-receptor interactions. But the presence of specific transmission blocking epitopes in APN1 and Pfs25 suggest a more specific mechanism [100, 107]. Early *in vitro* studies showed specific adherence of ookinetes to the luminal side of midgut epithelium but not to the basal lamina side [108], suggesting a mechanism for ookinete recognition of the epithelial brush border. Later it could be shown that chondroitin sulfate proteoglycans might be the target of ookinete attachment on the epithelial surface [109]. The varying and partially contradictory data available on molecular interactions between the ookinete and the midgut epithelium illustrate the gaps in understanding the process of midgut traversal and gave rise to a number of different hypotheses. The “Ross cell model” arose from observations in *P. gallaniceum* and suggested that *Plasmodium* parasites preferentially traverse a specific V-ATPase-positive type of midgut epithelial cells (Ross cells) [110, 111]. This model has however been fiercely contested by others [112, 113], who presented evidence that all mosquito midgut cells are highly uniform, and invasion occurs through or in between any regular epithelial cell.

The contesting “Time bomb model” of ookinete invasion presented evidence that invasion occurs predominantly by the traversal of cells which do not express high levels of vesicular ATPase. Invaded cells are severely wounded in the process, undergo apoptosis, and are rejected from the epithelium by an actin purse-string-mediated restitution mechanism, which allows the epithelium to 'bud off' the damaged cells without losing its integrity [113, 114]. To avoid being rejected from the epithelium in the budding cadaver of the invaded cell, the ookinete traverses laterally into neighbouring epithelial cells until finally emerging on the basal lamina [115]. Two perforin-like proteins, PLP3 (also called MAOP, membrane-attack ookinete protein) and PLP5 have been shown to be essential for epithelial cell traversal by ookinetes [116, 117]. Interestingly, the two membrane attack complex containing proteins are not redundant, and knock out of each individual PLP results in ookinetes that are attached to brush border microvilli of midgut epithelial cells, but unable to cross this barrier. The fact that ookinetes incapable of cell traversal are found attached to the midgut epithelium further supports the hypothesis that there is a specific interaction between the two cell types. A number of other proteins have been implicated to be involved in traversal of the mosquito midgut, but for many of them the molecular function remains elusive [118]. A selection of sexual stage antigens, containing numerous proteins suggested to be involved in mosquito midgut traversal, was recently screened for their potential as transmission blocking vaccines (TBV), but other than Enolase found no new antigens that could be targeted through TBVs [119].

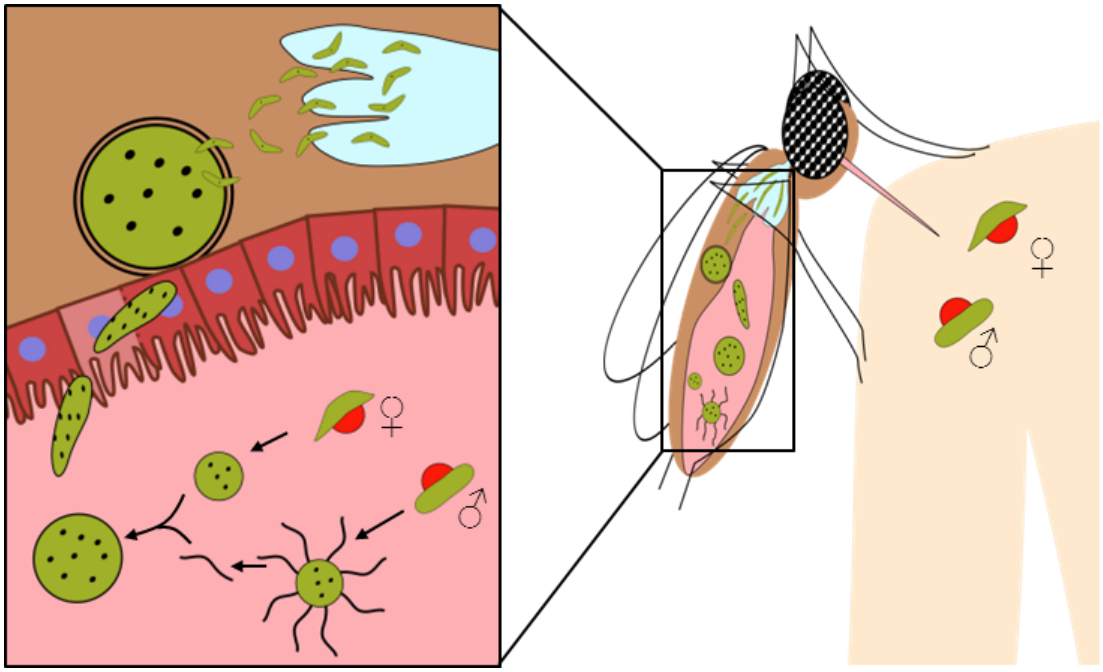

Figure 1.5: The sexual stage of the malaria parasite life cycle. Upon the uptake of mature gametocytes by a blood feeding mosquito, male and female gametocytes differentiate into micro- and macrogametes respectively. They then fuse to form a zygote that differentiates into a motile ookinete. The ookinete crosses the midgut epithelium by traversing through a number of epithelial cells, which are wounded in the process and undergo apoptosis. On the basal lamina side of the midgut epithelium the ookinetes differentiates into a sessile oocyst, inside which sporozoites are formed. Once released from the oocyst, sporozoites migrate through the hemolymph to the mosquitoes salivary glands, in which they reside after invasion until being injected into a new host during a blood meal.

Upon successful traversal of the midgut epithelium, the ookinete remains in the space between the epithelium's basal membrane and the basal lamina where it differentiates into a sessile ookinete, producing hundreds of sporozoites. Once matured, the sporozoites are released into the haemolymph and migrate to the mosquito salivary glands which they then invade. During the blood meal of the infected mosquito, these sporozoites are injected into the dermis of a host were they initiate a new round in the *Plasmodium* lifecycle.

1.3 Immunity against malaria

The first systematic analysis of immunity against malaria was carried out by Robert Koch in the late 1800s in Papua New Guinea. It was here that he observed that in endemic areas, malaria is most apparent in young children, while the parasites may be completely absent from the blood of adults and that individuals who are constantly exposed to infection develop immunity to malaria [120]. His observations from more than 100 years ago laid the foundation for our current understanding of immunity against malaria. More than 60 years later it was shown that antibodies are the main protective component in the blood of malaria immune adults [121], and that passive transfer of IgG from the serum of immune individuals can reduce parasitaemia in non-immune children. This indicates that the protective component of naturally acquired immunity against malaria is predominantly directed against parasites in the blood stage of the *Plasmodium* lifecycle. While subsequent analysis of the immune response against malaria widely confirmed these observations, other lifecycle stages were also shown to be targeted by the human immune system.

1.3.1 Immunity against pre-erythocytic parasites

There are two potential targets for naturally acquired immunity against pre-erythrocytic stages of malaria. Free sporozoites could be susceptible to neutralisation by antibodies en route to the liver, and infected hepatocytes could be targeted by cytotoxic T-cells. To what extent such immune responses play a role in protection acquired from natural exposure to malaria is unclear, but observation of re-infection shortly after clearing of parasites by drug treatment in immune individuals indicates

that the effect of naturally acquired immunity against pre-erythrocytic stages is limited [122, 123]. Some studies however reported a delay in re-infection in immune individuals [123] and a recent study of antibodies in immune individuals showed the existence of protective anti-CSP antibodies induced from natural exposure to parasites [124]. Other sporozoite proteins targeted by naturally acquired antibodies are the liver stage antigen 1 (LSA1) and TRAP [125], but there has to date not been any clear evidence that would suggest a protective effect from serum titres of those antibodies.

While there is at least some evidence for naturally acquired antibodies against pre-erythrocytic parasites to contribute to immunity, reports on protective cellular responses are even rarer. The presence of CD8+ T-cell responses against CSP and LSA1 in naturally acquired immunity has been reported [126, 127], but to date there is no clear evidence for a protective function of naturally acquired cytotoxic T-cells against intrahepatic parasites.

1.3.2 Immunity against the blood stage of malaria infection

Although immune responses against blood stage parasites have conclusively been shown to be predominantly responsible for naturally acquired immunity, the target of these responses is still only partially understood. Considering the age distribution of disease burden in stable transmission settings, with a majority of severe cases occurring in infants, and a majority of mild cases occurring in children until immunity is developed to a level were parasitaemia remains at sub-microscopic levels even after infection (***Figure 1.6***), it seems very plausible that there are two distinct mechanisms for

naturally acquired immunity, one that develops quickly and protects from disease and one that develops more slowly and is capable of controlling parasitaemia.

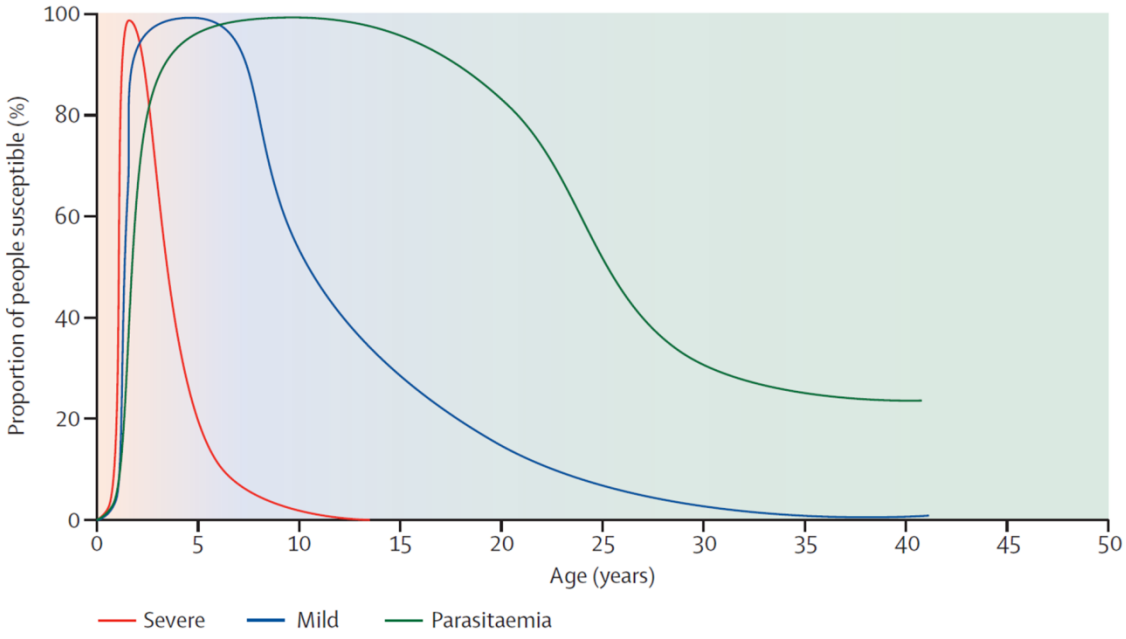

Figure 1.6: Age distribution of malaria burden in stable transmission settings. Natural immunity against malaria is acquired over repeated exposure, first against severe malaria, then against illness with malaria, and finally against microscopy-detectable parasitaemia. Figure from: [5]

The ability to protect from symptomatic disease is likely dependent on immunity against proteins displayed on the surface of iRBC such as PfEMP1 [128]. Other adhesins such as RIFINs (repetitive interspersed families of polypeptides), STEVORs (Subtelomeric variable open reading frame proteins) and SURFINs (Surface-associated interspersed gene family proteins) have also been implicated to play a role as targets for naturally acquired immunity [129-132]. These adhesins are collectively referred to as variant surface antigen (VSAs) and are all in some form involved in adhesion of iRBCs to the vascular endothelia and other RBCs (rosetting), key processes in the pathogenesis of malaria. There is some evidence that the protective potential of anti-VSA antibodies is dependent on their ability to interfere with iRBC cytoadherence

[133], but opsonisation-induced phagocytosis could also play a role [134]. Among the VSAs, PfEMP1 seems to be the most important target of naturally acquired immunity [132], as is illustrated by the loss of protection from severe malaria in pregnant women, facilitated through the placenta-specific PfEMP-1 variant VAR2CSA against which no antibodies exist in first time mothers [135, 136]. VSAs are highly variable and highly strain specific. PfEMP1 alone is encoded in over 60 so-called var genes, each able to recombine, demonstrating the extent of VSA variability [137, 138]. Immune responses following infection are limited to the VSA variants of the specific parasite strain, explaining why strain transcending immunity is only acquired after repeated exposure to a variety of parasites [139]. There is however evidence for heterologous boosting after infection with different parasite strains, suggesting the presence of conserved, cross reactive epitopes within these proteins [140]. These conserved epitopes could be responsible for the protection from severe malaria that is acquired following only one or two exposures to *P. falciparum* [141], while a more general protection from illness has to be acquired over larger numbers of infections[142-144]. There is evidence that control of parasitaemia through naturally acquired immunity is primarily conferred by antibodies that target proteins on the merozoite surface and interfere with RBC invasion [145]. This is consistent with the observation that reduction in parasitaemia after passive transfer of IgG from malaria immune adults to non-immune children, occurs following schizogony, while the antibodies do not appear to be effective against developing or mature trophozoites [121]. A variety of proteins from the merozoite surface, micronemes and rhoptries have been implicated to be targeted by this type of naturally acquired immunity, including AMA-1, MSP1, MSP2, MSP3 and Rh5 [146-150]. Interestingly, RIFINs, STEVORs and SURFINs are also present on the surface of merozoites where

they could play a role in erythrocyte binding [131, 151]. There are two different mechanisms by which antibodies against these antigens could inhibit erythrocyte invasion, facilitating phagocytosis by macrophages or neutrophils [152, 153] and inducing complement-mediated cell damage by opsonisation [59], or direct neutralisation by preventing processing of invasion proteins or blocking their erythrocyte-binding sites. Interestingly, it was recently shown that merozoites actively fix human factor H, a regulator of the complement system, on their surface through interaction with Pf92, underlining the role complement fixation plays in immunity against blood stage parasites [154]. Like VSAs most merozoite surface antigens, with the exception of the highly conserved Rh5, show distinct strain specific variability, explaining the delay in developing a strain transcending immunity with an effect on parasitaemia.

Taken together, these observations suggest that naturally acquired immunity is dependent on the interplay of immune responses against different targets and by different mechanisms, which are only acquired by repeated exposure to *Plasmodium* parasites [155].

1.3.3 Immune responses against gametocytes

Immune responses to gametocyte antigens clearly differ from immunity to earlier lifecycle stage in that they do not appear to provide any direct benefit to the immune individual. Transmission reducing immunity (TRI) nonetheless does exist, and there are two possible mechanisms by which it might interfere with transmission of malaria. Antibodies directed against surface antigens of gametocyte infected RBCs (giRBCs),

some of which are distinct from those expressed on iRBCs, could theoretically lead to opsonisation and subsequently complement fixation or phagocytosis. But while antibody binding to giRBCs has been reported, evidence to support this mechanism of TRI conclusively has not yet been presented [156-158]. Most evidence point towards antibodies directed against pre-fusion antigens of *Plasmodium* gametes to be the major facilitator of naturally acquired TRI. Gamete antigens are presented to the host's immune system when gametocytes fail to be transmitted to a mosquito and subsequently break down in the host where they can induce an antibody response. These antibodies can be taken up together with gametocytes by a blood feeding mosquito, and then become functional in the mosquito midgut once gametes are released from RBCs and therefore become susceptible to immune effectors in the plasma [159]. The best characterised targets of this kind of TRI are the male gamete antigens Pfs48/45 and Pfs230 [89, 160]. The exact mechanism of Pfs48/45 and Pfs230 mediated TRI is not clearly defined, but opsonisation followed by complement fixation [161] as well as direct blocking of macrogamete-microgamete fusion [93] have both been implicated to play a role.

In summary, these observations suggest that, while immune responses against giRBCs and gamete antigens do not provide a direct benefit to the host, naturally acquired TRI could have a substantial effect on malaria transmission.

1.4 Vaccines against malaria

Vaccines are undoubtedly one of the most successful public heath interventions of all time. They are usually cheap and highly effective, and because they often protect an

individual from infection for a long time or even their entire life, they can be an invaluable tool in disease control. The eradication of small-pox and rinderpest, as well as the elimination of measles, rubella and polio from wide parts of the world would not have been possible without vaccines. It is therefore evident that an efficacious malaria vaccine would be of immense value to all efforts to contain and eventually eradicate this ancient scourge of humankind. An ideal malaria vaccine would have to have two characteristics. It would protect a vaccinated individual from illness as well as have an impact on malaria transmission. For a number of factors this has been difficult to achieve. One is the complex lifecycle of the *Plasmodium* parasite, as a result of which the immune system encounters five very different forms of the parasite instead of only one, sporozoites, intrahepatic EEFs, merozoites, blood-stage parasites in iRBCs and gametocytes, each presenting a distinct set of antigens. Furthermore, *Plasmodium* parasites have evolved active immune evasion mechanisms, particularly during the blood stage of infection, which is the target of naturally acquired immunity. In spite of the obvious difficulties, huge efforts have been made to develop a malaria vaccine, and there are now vaccine candidates targeting each of the different life cycle stages in humans as well as in the mosquito, some of which show very promising results. Incidentally, when Robert Koch first observed acquired immunity to malaria at the turn of the 19th century, one of his predictions was that, when enough is known about the involved mechanisms, it should be possible to immunise against malaria [120]. All his other observations have been confirmed over the last 100 years, so maybe there is cause for optimism that also the last one will be proven true in the near future.

1.4.1 Pre-erythrocytic vaccines

The first vaccines that were successfully used in humans were live organisms, similar to the pathogen, but less likely to cause illness or causing a milder form of disease. Similarly the first malaria vaccine tested in humans were gamma irradiated sporozoites delivered to the human host by mosquito bite [162]. The concept of vaccination with whole sporozoites has since been advanced significantly, either with irradiated sporozoites, genetically attenuated sporozoites, or with unattenuated sporozoites delivered under chloroquine cover, and holds promise as one of the most efficacious vaccine strategies for malaria today [163-166]. However, there are also significant drawbacks to this immunisation procedure. Mosquito bites are not a viable route of vaccine delivery, therefore sporozoites have to be obtained from dissected mosquito salivary glands, a process that is not easily scalable to production for the vaccine market. Cryopreserved sporozoites are extremely temperature sensitive and have to be transported in liquid nitrogen which makes their deployment in endemic settings in deprived, rural areas practically impossible. Finally, the protection conferred through immunisation with whole sporozoites does not appear to be very long lived, and is reduced drastically against heterologous parasite strains [165].

Despite all these factors, which make whole sporozoites a suboptimal vaccine candidate, these studies show that it is possible to induce strong immune responses against pre-erythrocytic lifecycle stages, something that is not induced by natural infection, most likely due to the much higher number of sporozoites delivered in the vaccine than in a mosquito bite, and that the induced immunity can confer sterile protection from the disease. Analysis of the immune responses to whole sporozoite

vaccines in mice revealed certain antigens as targets of protective antibodies, including CSP [167].This encouraged research into subunit vaccines, which consisted of only one pre-erythrocytic antigen. Early clinical trials with CSP showed no protective efficacy [168], and it was hypothesised that this was due to an insufficient magnitude of the induced antibody response. RTS,S, currently the most advanced malaria vaccine candidate, was developed in an attempt to increase antibody titres to CSP following vaccination. It presents parts of CSP on a Hepatitis B vaccine virus like particle (VLP), which appeared to increase the induced antibody titres [169, 170]. The phenomenon of increased immunogenicity through display of antigens on VLPs has been observed in other contexts as well [171], and seems to be due to a combination of factors including the regular array of the antigen, which acts as a pathogen associated molecular pattern (PAMP) and increased draining to the lymphatics because of the particles size [172, 173]. Furthermore, RTS,S is delivered with a highly potent adjuvant (AS01) specifically developed for this purpose. Despite inducing extremely high antibody titres, recently concluded phase III clinical trials of RTS,S in AS01 showed only around 25% and 50% sterile protection from malaria in infants and young children, respectively [174, 175]. Furthermore, antibody titres were poorly maintained and efficacy waned quickly over the course of a year. Despite its disappointing efficacy, the development of RTS,S and completion of phase III clinical trials mark a milestone in the road to an effective malaria vaccine, but also makes it clear that the end of that road is not yet reached.

Other evidence from studies in mice infected with sporozoites suggest an important role for cytotoxic CD8+ T-cells in protection from malaria at the intrahepatic stage of

infection, mediated through effector molecules and cytokines like perforin, FAS ligand, granzymes, IFN-γ and TNF [176-180]. Considerable effort therefore went into the development of T-cell inducing vaccines that might be able to complement an RTS,S-like antibody inducing vaccine. Immunisation with plasmid DNA or viral vectors have long been known to induce potent T-cell responses, as they are able to enter cells and hijack their cellular protein production machinery resulting in intracellular expression of the encoded antigen and hence its presentation on major histocompatibility complex (MHC) class I and II molecules [181]. Despite the role anti-CSP effector T-cells appear to play in the immune response to sporozoites in animal models [177, 178], heterologous prime boost experiments using DNA and modified vaccinia Ankara (MVA) vectors encoding CSP, showed only partial protection in humans [182]. The most advanced T-cell vaccine to date encodes a multi epitope string (ME) followed by TRAP, and heterologous prime boost experiments using DNA followed by MVA showed promising results in Phase II clinical trials [182, 183]. The magnitude of the T-cell response to ME-TRAP could be further improved by priming with chimpanzee adenovirus (ChAd) vectors instead of DNA, resulting in increased CD8+ T-cell responses as well as inducing a moderate antibody response. In a controlled human malaria infection (CHMI) challenge trial, 58% of volunteers showed evidence of parasite control after ChAd-MVA ME-TRAP immunisation and 21% were sterilely protected [184]. These studies show the potential of T-cell inducing vaccines against malaria, and combinations with antibody inducing vaccines such as RTS,S are currently being tested with highly promising results [185].

1.4.2 Blood stage vaccines

While targeting the pre-erythrocytic stage with malaria vaccines is highly appealing, as this means eliminating the parasite before it causes symptoms or can be transmitted, it also means that only a single parasite needs to escape immune detection to cause fully symptomatic disease. As the target of naturally acquired immunity, the blood stage of infection presents a logical alternative to pre-erythrocytic stages as a vaccine target. Two broadly separate classes of molecules offer themselves for the use as antigens in blood stage vaccines. VSAs appear to be mainly responsible for sequestration of iRBCs and therefore pathogenesis of malaria. Neutralising antibodies against VSAs could potentially prevent sequestration and therefore protect from severe disease. Furthermore antibody mediated complement fixation and phagocytosis could reduce the number of iRBCs and thereby aid the clearance of parasites from the blood. Alternatively, antibodies directed against proteins involved in merozoite invasion of erythrocytes could interfere with this process and therefore interrupt the exponential growth of the parasite within the host.

Immunisation against VSAs has not yet picked up much traction in human vaccine trials, mainly due to the obvious problems encountered when trying to immunise against an extremely variable group of antigens. While there is some evidence that it is possible to protect from disease from a homologous strain there does not appear to be any effect against heterologous parasite strains [186].The fact that immunity against severe malaria is acquired after only one or two infections [141] does however suggest that there are conserved regions in VSAs that could be the target of future VSA vaccines. Nonetheless, efforts to generate a blood stage malaria vaccine have mainly

focused on merozoite surface proteins and a number of them, including MSP1, MSP2, MSP3, GLURP, AMA1, the serine repeat antigen 5 (SERA5) and the 175 kDa erythrocyte binding antigen (EBA-175), have been tested in clinical trials, all without reporting significant success [187-192]. Rh5 differs from these blood-stage invasion ligands, in that it plays an essential role in the RBC invasion process, is highly conserved, non-redundant and susceptible to strain-transcending antibody-mediated immunity [193-195]. Vaccines targeting Rh5 and its associated merozoite invasion complex therefore hold the potential to overcome the limitations of previous blood stage vaccine candidates.

1.4.3 Transmission blocking vaccines

Together with pre-erythrocytic vaccines, transmission blocking vaccines are referred to as VIMT (vaccines that interrupt malaria transmission) [196]. Some blood stage vaccines could also interfere with gametocyte development and hence be considered a VIMT, but the role of blood stage immunity on gametocytogenesis is not yet clearly defined. Classical, sexual stage transmission blocking vaccines differ from pre-erythrocytic and blood stage vaccines in that they do not confer any immunity against illness. While this may be less attractive from an individual's perspective, on a population level these vaccines could have a big impact on malaria prevalence and could be an invaluable tool in malaria elimination and eradication campaigns, therefore protecting the individual as part of a protected community. Consequently, transmission blocking vaccines are the only type of malaria vaccine that have the potential to protect at risk infants and young children by immunisation of fully immunocompetent adults.

There are two groups of transmission blocking antigens. Pre-fusion antigens are expressed on gametocytes and therefore encountered by the human immune system during malaria infection, which could result in boosting of antibody titres during an infection. Pfs48/45 and Pfs230 are the most extensively characterised antigens in this category. Post-fusion antigens are never encountered by the human immune system as they are expressed on later forms of the parasite during the sexual stage, such as activated gametes, zygotes and ookinetes. Another potential target for transmission blocking vaccines are proteins on the mosquito midgut. Pfs25 and Pfs28 are examples for well-studied post fusion antigens, and APN1 is the most studied mosquito antigen as a vaccine candidate. All of these vaccines induce an antibody response in the human host, but the antibodies only become functional in the mosquito midgut after they have been ingested by a blood feeding mosquito alongside gametocytes. As a consequence of this, most transmission blocking antigens have never been under immune selection pressure and are therefore remarkably conserved, making them susceptible to cross strain neutralisation [197]. As transmission blocking activity of a vaccine cannot be assessed directly, surrogate *ex vivo* assays were developed and qualified [198]. The most used is the standard membrane feeding assay, where parasites are mixed with serum or purified IgG from vaccinees and then fed to mosquitoes through a thin membrane. Six to eight days after the feed oocyst numbers in the mosquitoes are counted as a measure of parasite burden [199].

Of all transmission blocking antigens Pfs25 is probably the best characterised, and has been tested in clinical trials. In the first clinical trial, Pfs25 was administered adjuvanted with Montanide (ISA720) and the trial had to be stopped prematurely due

to adverse effects, probably as a result of the combination of the antigen and adjuvant [200]. Nonetheless it was possible to correlate transmission blocking activity with antibody titres in volunteers who had completed the trial, which showed that high antibody titres would be required for a vaccine targeting Pfs25 to block transmission. This was confirmed by a subsequent study where Pfs25 was conjugated to the exoprotein A of *Pseudomonas aeruginosa* [201, 202]. Even though display of Pfs25 on a particulate platform could substantially increase antibody titres against Pfs25, transmission blocking activity determined by SMFA was only moderate. These disappointing results might be explainable through the observation that IC50 values for Pfs25 antibodies vary significantly between species. In humans they are more than five times higher than in mice and twenty times higher than in rabbits, which might explain the different results seen in pre-clinical studies in mice [203]. However, it has to be noted that the trial, possibly because of the bad experiences with montanide, used the weak adjuvant alhydrogel. It is therefore possible that the use of a strong adjuvant would result in a more favourable outcome. Another platform to increase immune responses to Pfs25 with imminent translation into clinical trials is based on the multimerisation platform IMX313, which when fused to Pfs25 results in increased antibody titres in mice after immunisation, either when encoded in viral vectors or as protein in adjuvant formulations [204].

A number of transmission blocking vaccine candidates with promising pre-clinical results are due to be tested in clinical trials in the near future including further constructs containing Pfs25 and vaccines targeting Pfs48/45 and Pfs230 [205, 206]. If limitations encountered during the previous clinical trials with Pfs25 can be overcome

they could quickly earn their place among the available tools to eliminate and eventually eradicate malaria.

1.5 Thesis outline and aims

Considering the most recent developments in malaria elimination campaigns, it is clear that novel control measures are desperately needed. Given the role vaccines played in previous disease eradication and elimination campaigns, it appears obvious that an effective malaria vaccine could play a similar role in campaigns to contain this ancient disease. Traversal of cellular barriers is an essential step at multiple points of the *Plasmodium* lifecycle. Sporozoites traverse fibroblasts, phagocytes, epithelial cells and hepatocytes, and egress of merozoites from hepatocytes and RBCs also involves membrane traversal. Finally, ookinetes cross the mosquito midgut epithelium, traversing a number of epithelial cells in the process. Interfering with membrane traversal therefore presents an attractive strategy for developing effective vaccines against malaria. Several proteins have been implicated to play a role in membrane traversal at different lifecycle stages and in this thesis I aimed to assess the potential of some of them as vaccines for malaria, individually as well as in combination with each other. For vaccines with and impact on malaria transmission, protein-protein interactions involved in cell traversal by sporozoites and ookinetes particularly offer themselves as targets. Contrasting with the important role this process could play for the development of novel malaria vaccines, very little is known about the molecular interactions underlying the crossing of the mosquito midgut by ookinetes. I therefore aimed to extend the current understanding of the ookinete traversal of the mosquito

midgut by identifying previously undescribed ligand-receptor pairs between the surface of the ookinete and the midgut epithelium. Putative interactors would then be assessed for their potential as vaccine candidates and their physiological role in crossing of the midgut epithelium.

These ambitions resulted in the formulation of the following list of aims for this thesis:

1. Pre-clinical assessment of the CSP displaying VLP vaccine candidate, R21 (Chapter 3)
2. Assessment of SPECT1 as a pre-erythrocytic antigen for inclusion in a malaria vaccine and potential combination with CSP (Chapter 4)
3. Assessment of combination of CSP and Pfs25 vaccines as a multi-stage malaria vaccine (Chapter 4)
4. Screening for novel protein-protein interaction between the ookinete and the mosquito midgut epithelium by AVEXIS (Chapter 5)
5. Characterisation of identified ligand-receptor pairs between the parasite and mosquito midgut (Chapter 5)

Chapter 2 - Material and Methods

2.1 Materials

2.1.1 Buffers

Table 2.1: Buffers

Name	Components	Use
Yeast breaking buffer	0.1% Triton X-100 1mM EDTA 1 mM MgCl2 10 mM Tris pH (7.8)	Lysis of *Pichia pastoris* using glass beads
Yeast resuspension buffer	20 mM Tris (pH 8) 5 mM EDTA	Resuspension of *Pichia pastoris* pellets prior to lysis by high pressure homogenisation
Liberation buffer	20 mM Tris (pH 8) 5 mM EDTA 0.5 % Tween-20	Liberation of VLPs from membrane fractions of yeast homogenate
His running buffer	20 mM NaH_2PO_4 (pH 7.4) 300 mM NaCl 20 mM Imidazol	Running buffer for IMAC
His elution buffer	20 mM NaH_2PO_4 (pH 7.4) 300 mM NaCl 500 mM Imidazol	Elution buffer for IMAC
10x Spy/Snoop conjugation buffer	40 mM Na_2HPO_4 200 mM sodium citrate pH 6.2	Conjugation of SpyTagged/SnoopTagged proteins to SpyCatcher/SnoopCatcher displaying VLPs

2.1.2 Media

2.1.2.1 Bacterial growth media and agars

Table 2.2: Bacterial growth media and agars

Name	Components	Use
LB medium/agar	LB Broth (Lennox) (Sigma, L7275 (medium), L7025 (agar))	Growth of untransformed *E. Coli* cultures
LB-Kan	LB medium/agar + 25 µg/ml Kanamycin (Sigma, K0254)	Growth of *E. Coli* cultures, transformed with a plasmid containing a Kanamycin resistance cassette
LB-Carb	LB medium/agar + 100 µg/ml Carbenicillin (Sigma, C1613)	Growth of *E. Coli* cultures, transformed with a plasmid containing an Ampicillin resistance cassette
SOC	SOC Outgrowth medium (NEB, B9035)	Recovery of freshly transformed *E. Coli* cultures

2.1.2.2 Pichia growth media and agars

Table 2.3: Pichia growth media and agars

Name	Components	Use
YPD medium/agar	YP or YP agar (Invitrogen, A11156) + 2% Dextrose	Growth of PichiaPink strains prior to transformation, growth of GS115.
YPDS	YPS (Invitrogen, A11156) + 2% Dextrose	Recovery of cells after electroporation.
PAD agar	PAD agar (Invitrogen, A11156) + 2% Dextrose	Lacks adenine, is used for selecting transformants in the PichiaPink system.
BMGY	1% yeast extract 2% peptone 100 mM potassium phosphate, pH 6.0 1.34% YNB 0.0004% biotin 1% glycerol	Growth of *Pichia pastoris* for protein expression

BMMY	1% yeast extract 2% peptone 100 mM potassium phosphate, pH 6.0 1.34% YNB 0.0004% biotin 0.5% methanol	Induction of protein expression in *Pichia pastoris*

2.1.3 Antibodies

Table 2.4: Antibodies

Name	Use
Mouse anti Hepatitis B Surface Antigen (BioRad, MCA4658)	WB (1:1000)
CaptureSelect™ Biotin Anti-C-tag Conjugate (Thermo Scientific, 7103252100)	WB (1:1000)
Anti-Mouse IgG (whole molecule)−Alkaline Phosphatase antibody produced in goat (Sigma, A3562)	WB (1:1000) ELISA (1:3000)
Streptavidin-ALP (Mabtech, 3310-8)	WB (1:1000)
2A10 (anti NANP mAb from hybridoma supernatant)	ELISA (different dilutions)
CD4 Antibody (OX68) (Santa Cruz Biotechnology, sc-53042)	WB (1:1000) AVEXIS

2.1.4 Primers

Table 2.5: Primers for cloning, sequencing, qPCR and RNAi

Name	Sequence	Use
Cloning primers		
R21c for	CCAGTTTGTCCATTGATTCCAG	Cloning of pPink-HC-R21c
R21c rev	GCTCGAGGTACCTTAAGCTTCTGGTTCAATGTAAACCCACAAGCAAAAG	Cloning of pPink-HC-R21c
SPECT1 for	GCTAGTCTCGAGAAAAGGTACAACTTGAACAACGACTTGTCC	Cloning of pPink-alpha-HC-SPECT1-6xHis
SPECT1 rev	GCACGTGGTACCCTATTAGTGGTGGTGATGGTGATGAGACAAAGCCATGTTCAAGTCC	Cloning of pPink-alpha-HC-SPECT1-6xHis

Sequencing primers		
pPink-HC for	TGCGACTGGTTCCAATTGACAAGC	Sequencing of inserts in pPink-HC, reads forward from AOX1 promoter
pPink-HC rev	GTTACATGCGTACACGCGTTTGTACAG	Sequencing of inserts in pPink-HC, reads backwards from CYC1 region
pXKP for	GCAAAGTGAACACGTCGCTAAGCG	Sequencing of inserts in pExpres2-KanPac, reads forward from Actin promoter
CD4-Tag rev	GTTCGCCCTGCAGGCTCTCTTCG	Sequencing of inserts in pExpres2-KanPac, reads backwards from CD4-Tag
pXKP rev	GTCAGATATCGATCGATCCGCGG	Sequencing of inserts in pExpres2-KanPac, reads backwards from region at 3' end of stop codon
MG36 rev	CGATCGAAGATGCCGCGGCTG	Sequencing of MG36 constructs, reads backwards from a region in MG36 conserved over *A. albimanus, A. stephensi* and *A. gambiae*
RNAi primers		
MG36 ds for	TAATACGACTCACTATAGGGCTCGAATCTCTGCTCGCTCT	Generation of a template for dsRNA synthesis for the knockdown of *MG36* in *Anopheles gambiae,* contains T7 promoter
MG36 ds rev	TAATACGACTCACTATAGGGCACGTCACACTTGTCCTGCT	Generation of a template for dsRNA synthesis for the knockdown of *MG36* in *Anopheles gambiae,* contains T7 promoter
qPCR primers		
MG36 for	CGGAGTTTGGTGGAATTGCTTC	Quantification of *MG36* mRNA
MG36 rev	AGAACTCGCTCATCAGGTGG	Quantification of *MG36* mRNA
S7 for	GGTGCACCTGGATAAGAACCA	Internal reference for qPCR[207]
S7 rev	CGGCCAGTCAGCTTCTTGTAC	Internal reference for qPCR[207]

2.1.5 Plasmids

Table 2.6: Plasmids used as backbones for the cloning of expression vectors used in this thesis

Name	Expression System	Promoter	Use
pPink-HC-S	PichiaPink	AOX1	Contains HBsAg gene. Used as backbone for pPink-HC-S-SPECT1 and pPink-HC-S-Pfs25
pPink-HC-R21	PichiaPink	AOX1	Contains R21 gene. Used as backbone for pPink-HC-R21c, pPink-HC-R21-SPECT1 and pPink-HC-R21-Pfs25
pPink-HC-alpha	PichiaPink	AOX1	Contains alpha mating factor secretion signal. Used for cloning of pPink-HC-alpha-SPECT1-6xHis
pPIC9K	*Pichia* (GS115)	AOX1	Contains alpha mating factor secretion signal. Used for cloning of pPIC9K-CS-SnoopTag-CTag
pExpreS2-KanPac	S2	Actin	Contains a puromycin resistance cassette for selection of transfected S2 cells and a BIP signal peptide for expression of secreted proteins. Used as backbone for all AVEXIS plasmids

2.1.6 Expression systems

2.1.6.1 PichiaPink

The PichiaPink expression system is a eukaryotic protein expression system based on *Pichia pastoris*. Transformation with expression vectors based on pPink-HC or pPink-HC-alpha allows the expression of proteins under the methanol inducible AOX1 promoter. PichiaPink varies from *Pichia pastoris* by gene deletion knock out of *ade2*, which make PichiaPink an adenine auxotroph that is unable to grow on medium lacking adenine and has a slow growth phenotype on rich medium. Furthermore, knock out of *ade2* leads to the accumulation of purine precursors in the vacuole,

which causes the colony to be red in colour. Both of these characteristics can be used for selection of transformants. Two strains of PichiaPink were used in this thesis. In strain 1 only *ade2* is knocked out, strain 4 furthermore carries gene deletions of the two protease genes *PEP4* and *PRB1*.

2.1.6.2 GS115

GS115 is a *Pichia pastoris* strain. Secreted proteins can be expressed under methanol induction by transformation with expression vectors based on pPIC9K.

2.1.6.3 Drosophila Schneider-2 (S2) cells

S2 cells are a *Drosophila* cell line used to express proteins after non-viral transfection with expression vectors based on pExpreS2 (ExpreS2ion Biotechnology).

2.1.7 Adjuvants

2.1.7.1 Alhydrogel

Alhydrogel (Invivogen, vac-alu-250) contains 2% (10 mg/ml) Aluminium hydroxide ($Al(OH)_3$) as an active component, which acts primarily through the formation of a depot at the injection site, enabling enhanced antigen availability, activation of antigen presenting cells (APCs) and uptake by immune cells [208]. As aluminium ions react with phosphate to form $AlPO_4$, alhydrogel was only used with Tris-buffered antigens. Vaccines were formulated by mixing 8.5 µl (8.5 µg $Al(OH)_3$) per dose with 16.5 µl TBS. After 15 minutes at room temperature, 25 µL of the antigen at double the final concentration was added to the adjuvant preparation. The formulated vaccine

was incubated at room temperature for one hour and then injected into mice within 2 hours.

2.1.7.2 AS01

AS01 is a strong, antibody and T-cell inducing adjuvant proprietary to GlaxoSmithKline Biologicals S.A. (GSK). It is a liposome-based adjuvant system containing two immunostimulants: 3-O-desacyl-4'-monophosphoryl lipid A (MPL) and the saponin QS-21 [209]. AS01E was provided by GSK under an MTA. AS01 was pre formulated at double the final concentration. Upon mixing 25 µl of AS01E per dose with 25 µL of the antigen at double the final concentration, the formulated vaccine was stored on ice and injected into mice within 1 hour.

2.1.7.3 Matrix-M

Matrix-M is a strong, antibody and T-cell inducing adjuvant proprietary to Novavax. It is made up from liposomes containing phospholipids, cholesterol and saponin [210]. Matrix-M was provided by Novavax under an MTA. 5 µl of Matrix-M per dose were mixed with the diluted antigen. The formulated vaccine was stored on ice and injected into mice within 1 hour.

2.1.7.4 AddaVax

AddaVax (Invivogen, vac-adx-10) is a squalene-based oil-in-water nano-emulsion similar to MF59, and is thought to act through recruitment and activation of APCs and stimulation of cytokine and chemokine production by macrophages and granulocytes [211]. Vaccines were formulated by mixing antigen pre diluted to double the final

concentration with the same amount of AddaVax. The formulated vaccine was stored on ice and injected into mice within 1 hour.

2.1.8 Vaccines

2.1.8.1 RTS,S

RTS,S was provided by GlaxoSmithKline Biologicals S.A under an MTA. RTS,S was pre diluted so that upon mixing 25 µl of RTS,S per dose with 25 µL AS01E both vaccine and adjuvant would be at the concentration required for each experiment.

2.1.8.2 Pfs25-IMX313

Pfs25-IMX313 was expressed and purified by Yuanyuan Li as described previously [204]. In brief: Pfs25-IMX313 was expressed in *Pichia pastoris* under the control of the methanol inducible promoter AOX1. N-terminal fusion to the alpha-mating factor secretion signal sequence allowed secretion into the culture media. Following expression nanoparticles were purified from the culture supernatant using a 5 ml CaptureSelect™ C-tag affinity matrix column.

2.1.9 Parasites

Table 2.7: Transgenic P. berghei parasites

Name	Description	Use
PfCSP@PbUIS4	*P. berghei* expressing PfCSP under control of the PbUIS4 promotor in addition to PbCSP	Malaria challenge to assess efficacy of RTS,S and R21
PfCSP@PbCSP	*P. berghei* expressing PfCSP under control of the PbCSP promotor, replacing PbCSP	Assessment of RTS,S and R21 efficacy by ISI

PfSPECT1@PbUIS4	*P. berghei* expressing PfSPECT1 under control of the PbUIS4 promotor in addition to PbSPECT1	ISI to assess efficacy of SPECT1-VLP vaccines
PfSPECT1@PbSPECT1	*P. berghei* expressing PfSPECT1 under control of the PbSPECT1 promotor, replacing PbSPECT1	Malaria challenge and ISI to assess efficacy of SPECT1-VLP vaccines
PfCSP@PbCSP+ PfSPECT1@PbSPECT1	*P. berghei* expressing PfSPECT1 under control of the PbSPECT1 promotor, as well as PfCSP under control of the PbCSP promotor, replacing both of the *P. berghei* sporozoite proteins	ISI to assess efficacy of R21-SPECT1 dual-VLP vaccines

2.1.10 Gene synthesis

2.1.10.1 GeneArt Strings DNA Fragments

Genes of low complexity and lengths of below 3000 base pairs (bp) were ordered from GeneArt (Invitrogen) as GeneStrings. Proteins to be synthesised were designed on the amino acid level and then back translated into DNA using the GeneArt ordering software, which allowed to codon optimise the sequence for the relevant expression systems. DNA overhangs were added to both ends of the GeneStrings to allow direct subcloning by In-Fusion cloning.

2.1.10.2 GeneArt Gene Synthesis

Genes that could not be synthesised as GeneStrings, because of complexity or size, as well as all AVEXIS constructs were synthesised as fully sequence confirmed plasmids. Genes were normally delivered in the GeneArt standard cloning vectors. Proteins to be synthesised were designed on the amino acid level and then back translated into DNA

using the GeneArt ordering software, which allowed to codon optimise the sequence for the relevant expression systems. Restriction sites were added to both ends of the synthesised genes to allow subcloning by restriction digest and ligation.

2.2 Molecular Biology

2.2.1 Polymerase chain reaction (PCR)

PCRs for subcloning and colony PCRs were run on a programmable Biometra T professional Thermocycler. qPCR was run on a Applied Biosystems® 7500 Fast Real-Time PCR System.

2.2.1.1 PCR for subcloning

To generate PCR products that would subsequently be used for cloning into expression plasmids, Phusion DNA polymerase was used (Phusion® High-Fidelity PCR Master Mix, NEB, M0531). Reactions were set up by mixing the master mix with primers, template DNA and nuclease free water. Because of the high speed and high fidelity of Phusion DNA polymerase, 32 amplification cycles were run routinely (Table 2.8).

Table 2.8: Phusion PCR thermo cycle

Initial denature	98°C	2 minutes	
Denature	98°C	20 seconds	┐ x 32
Primer anealing	(Lowest T_m of any primer) - 2°C	10 seconds	┘
Elongation	72°C	15 seconds per kb	
Final elongation	72°C	5 minutes	

For primer pairs with melting temperatures more than 5°C apart, the primer annealing step was replaced with a temperature ramp. The annealing temperature was decreased from 70°C to 54°C in 2°C steps, with each step being held for 5 seconds.

For challenging PCRs with low product yields, Betaine was added to the PCR reaction to a final concentration of 1 M.

Before further processing, DNA was purified from the PCR using the QIAquick PCR Purification Kit (Qiagen, 28104).

2.2.1.2 Colony PCR

Colony PCRs to screen for successfully transformed *E. coli* clones from an agar plate were performed with Phire DNA polymerase (Thermo Scientific, F122). For each reaction a single colony was picked from an agar plate and resuspended in 10 µl nuclease free water. 2 µl of the suspension were transferred to a fresh agar plate to allow recovery of the clone, the remaining 8 µl were boiled for 10 minutes at 98°C. 5 µl of the boiled suspension was then mixed with the reaction mix containing, primers, Phire reaction buffer, 10 mM dNTPs, Phire DNA polymerase and nuclease free water. 24 reaction cycles normally produced enough DNA for detection on an agarose gel.

Table 2.9: Colony PCR thermo cycle

Initial denature	98°C	10 minutes	
Denature	98°C	5 seconds	┐
Primer anealing	(Lowest T_m of any primer) - 2°C	10 seconds	├ x 24
Elongation	72°C	15 seconds per kb	
Final elongation	72°C	5 minutes	

2.2.1.3 qPCR

qPCR was run using Fast SYBR™ Green Master Mix (Applied Biosystems, 4385616) according to the manufacturer's instructions.

2.2.2 Subcloning

2.2.2.1 Subcloning by restriction digest and ligation

PCR products and plasmids for subcloning were digested using NEB restriction enzymes. After incubation at appropriate temperature and buffer for the used enzymes, as determined by the NEB double digest finder, digested PCR products were purified using the QIAquick PCR Purification Kit (Qiagen, 28104). Digested plasmids were electrophoresed in 1% Agarose gels containing 0.01% SYBR™ Safe DNA Gel Stain (Invitrogen, S33102) alongside GeneRuler 1 kb DNA Ladder (Thermo Scientific, SM0313). Bands of the correct size were excised from the gel and the DNA purified using the QIAquick Gel Extraction Kit (Qiagen, 28704). Plasmid backbone and insert were then mixed in a molar ratio of 1:3 and ligated using T4 DNA ligase. Ligation reactions were set up in nuclease free water and T4 ligase buffer and incubated at room temperature for 10 minutes before being transformed into competent *E. coli* cells.

2.2.2.2 Subcloning by In-Fusion cloning

DNA fragments ordered as GeneStrings from GeneArt were subcloned using the In-Fusion® HD Cloning Kit (Takara Bio, 638916). In brief, genestrings were designed to have a 15 bp extension on each end, homologous to the ends of the digested plasmid

backbone. Insert and vector were mixed in a ratio of 1:2 in In-Fusion master mix and nuclease free water. The reaction was incubated at 50°C for 15 minutes and then transformed into competent *E. coli* cells.

2.2.3 Cloning of expression vectors

2.2.3.1 Cloning of the R21c expression vector

The gene for expression of R21c was cloned by primer extension PCR from the R21 expression plasmid pPink-HC-R21. The reverse primer bound the plasmid just before the R21 stop codon and contained the DNA sequence of the C-Tag followed by a stop codon and a NotI restriction site. The forward primer bound the plasmid within the R21 coding region and covered a KpnI restriction site present in the sequence. The PCR product was cloned into pPink-HC-R21 via a NotI-KpnI double digest, generating the R21c expression plasmid pPink-HC-R21c. The sequence of the cloned gene was confirmed by sequencing.

2.2.3.2 Cloning of SPECT1-VLP expression vectors

A gene string was ordered containig the C-terminus of HBsAg from the internal KpnI restriction site onwards, followed by the gene of SPECT1 followed by the DNA sequence of the C-Tag, a stop codon and a NotI restriction site. Overhangs were added to the 5'- and 3'-ends of the string to allow in Fusion cloning into pPink-HC-R21 for a dual antigen VLP and pPink-HC-S for a VLP displaying only SPECT1. The generated plasmids were named pPink-HC-R21-SPECT1 and pPink-HC-S-SPECT1. The sequence of the cloned genes was confirmed by sequencing.

2.2.3.3 Cloning of the SPECT1-6xHis expression vector

The insert for expression of His-tagged SPECT1 was cloned by primer extension PCR from the R21-SPECT1 expression plasmid pPink-HC-R21-SPECT1. The reverse primer bound the plasmid just before the R21-SPECT1 stop codon and contained the DNA sequence of the His-tag followed by a stop codon and a KpnI restriction site. The forward primer bound the plasmid at the beginning of the SPECT1 gene and contained the C-terminus of the alpha mating factor which contained an XhoI restriction site. The PCR product was cloned into pPink-HC-alpha by XhoI-KpnI double digest to generate the SPECT1-6xHis expression plasmid pPink-HC-alpha-SPECT1-6xHis. The sequence of the cloned gene was confirmed by sequencing.

2.2.3.4 Cloning of Pfs25-VLP expression vectors

A genestring was ordered encoding the C-terminus of HBsAg from the internal KpnI restriction site onwards, followed by the gene of Pfs25 followed by the DNA sequence of the C-Tag, a stop codon and a NotI restriction site. Overhangs were added to the 5'- and 3'-ends of the string to allow in Fusion cloning into pPink-HC-R21 for a dual antigen VLP and pPink-HC-S for a VLP displaying only Pfs25. The generated plasmids were named pPink-HC-R21-Pfs25 and pPink-HC-S-Pfs25. The sequence of the cloned genes was confirmed by sequencing.

2.2.3.5 Cloning of AVEXIS plasmids

Codon optimised genes for expression in *Drosophila* were synthesised by GeneArt. The AVEXIS-plasmid generation was performed in two steps, with all subcloning steps being performed by GeneArt. First, three expression plasmids were generated,

pExpreS2-KanPac-Prey+, pExpreS2-KanPac-Bait+ and pExpreS2-KanPac-BirA-His. All three plasmids used the pExpreS2-KanPac backbone (ExpreS2ion biotechnologies) and were cloned via SacII and HindIII restriction sites. These restriction enzymes were chosen as their usage would remove a NotI restriction site from the pExpreS2-KanPac backbone, which was important for the next step of subcloning.

pExpreS2-KanPac-Prey+ contained a NotI restriction site followed by a Drosophila Kozack consensus sequence followed by the BIP signal peptide followed by the gene for the ectodomain of rat CD200, followed by an AscI restriction site, followed by a CD4-Tag (rat CD4 domains 3 and 4), followed by a flexible linker (SGGGSGGGTGGG), followed by a gene for the oligomerisation domain of the rat cartilage oligomeric matrix protein (COMP), followed by a flexible linker (LDRNLPPLAPLGPH), followed by the gene for beta-lactamase followed by a stop codon. The plasmid design was based on the original AVEXIS prey positive control expression plasmid for HEK cells (Addgene plasmid ID 32405) [212] .This plasmid was used to express the positive control prey protein as well as to act as a backbone for the cloning of all other prey plasmids.

pExpreS2-KanPac-bait+ contained a NotI restriction site followed by a Drosophila Kozack consensus sequence followed by the BIP signal peptide followed by the gene for the ectodomain of rat CD200 receptor, followed by an AscI restriction site, followed by a CD4-Tag (rat CD4 domains 3 and 4), followed by the gene for a biotin acceptor peptide (BAP) followed by a stop codon. The plasmid design was based on the original AVEXIS bait positive control expression plasmid for HEK cells (Addgene plasmid ID 32406) [212] .This plasmid was used to express the positive control bait protein as well as to act as a backbone for the cloning of all other bait plasmids.

pExpreS2-KanPac-BirA-His contained a NotI restriction site followed by a Drosophila Kozack consensus sequence followed by the BIP signal peptide followed by the gene for a biotin ligase (BirA), followed by an AscI restriction site, followed by a 8xHis-Tag followed by a stop codon. The plasmid design was based on the original AVEXIS BirA-His expression plasmid for HEK cells (Addgene plasmid ID 32408) [212] .This plasmid was co-transfected with the bait protein plasmids to allow biotinylation of the bait proteins at the BAP, as well as to act as a backbone for the cloning of plasmids for proteins that should be purified for further analysis.

In the second cloning step the genes of all the selected ookinete proteins were cloned into the pExpreS2-KanPac-prey backbone, and the genes of all the selected mosquito midgut proteins were cloned into the pExpreS2-KanPac-bait backbone using NotI and AscI. This plasmid design allowed for all proteins to be shuttled between the three different AVEXIS backbones by a simple NotI-AscI double digest.

2.2.4 Transformation of *E. coli*

2.2.4.1 Generation of competent Top10 E. coli cells

Competent *E. coli* cells were generated using $CaCl_2$ [213]. In brief, a 10ml sterile LB (no antibiotic) culture was inoculated with a single colony of JM109/TOP10 *E. coli* from a freshly streaked agar plate and grown over night at 37°C. The following morning, 1ml of the overnight culture was used to inoculate a 100ml LB culture, which was grown to an OD_{600} of 0.5. The culture was pelleted at 4000rpm for 10min at 4˚C in a pre-cooled centrifuge and the supernatant discarded. The pellet was resuspended in 10ml ice-cold, filter sterilised 0.1M CaCl2 and incubated on ice for 15 minutes. Bacteria were

pelleted as before, resuspended in 4ml ice cold, filter sterilised 0.1M CaCl2 with 20% glycerol and frozen at -80°C in 200 µl aliquots. 50 µl of competent cells were used per transformation.

2.2.4.2 Re-transformation of plasmids

To grow a new culture from a previously prepared culture, 0.1 µg of plasmid was added to 50 µl of a freshly thawed aliquot of Top10 competent *E. coli*. The bacteria were incubated at room temperature for 5 minutes and then spread on a LB-Agar plate containing the appropriate antibiotic.

2.2.4.3 Transformation of newly cloned plasmids

Plasmids generated by restriction digest and ligation were transformed into Top10 competent *E. coli*. Plasmids generated by In-Fusion were transformed into stellar competent *E. coli* supplied as part of the In-Fusion® HD Cloning Kit (Takara Bio, 638916). Transformation into both *E. coli* strains followed the same protocol.

5 µl of a ligation reaction or 2.5 µl of an In-Fusion reaction were added to 50 µl of a freshly thawed aliquot of competent cells. The mixture was incubated on ice for 30 minutes and then heat shocked for 30 seconds at 42°C. After heat shocking the cells were immediately returned on ice and recovered for 3 minutes. Cells were then recovered by adding 250 µl of SOC medium and incubating for 1 hour at 37°C. The complete 300 µl transformation reaction was then spread on a LB-Agar plate containing the appropriate antibiotic.

2.2.5 Plasmid preparation

Depending on the required amount of DNA plasmids were prepped using the QIAprep Spin Miniprep Kit (Qiagen, 27104), the QIAGEN Plasmid Plus Midi Kit (Qiagen, 12943) or the QIAGEN Plasmid Plus Maxi Kit (Qiagen, 12963).

2.2.6 Sequencing

All sequencing was carried out either by GATC-biotech or by Source bioscience by Sanger (dye-termination) sequencing.

2.2.7 Transformation of *Pichia pastoris*

All work in PichiaPink was performed using the PichiaPink expression system (Invitrogen, A11150, A11151, A11152, A11153, and A11154), all work in GS115 was performed using the same media and agars, but with the expression vector pPIC9K (Invitrogen, V17520).

2.2.7.1 Generation of electrocompetent Pichia cells

A 10 ml YPD culture was inoculated in a sterile 125 mL baffled flask with a single colony of the required *Pichia* strain from a freshly steaked YPD agar plate and grown for 2 days under shaking at 300 rpm at 28°C. The entire culture was then used to inoculate 100 mL of YPD media in a sterile 1 liter flask. The culture was then grown for 1–2 days at 28°C until it reached an OD_{600} of 1.3–1.5 (log phase growth). The cells were pelleted by cetrifugation at 1,500 × g at 4°C for 5 minutes four times and resuspended in 250 ml ice cold, sterile water, 50 ml ice-cold, sterile water, 10 ml ice-cold 1 M

sorbitol and finally 300 µl ice-cold 1 M sorbitol for a final volume of approximately 500 µl. Cells were used on the same day and leftover cells were stored at -80 °C.

2.2.7.2 Electroporation of Pichia pastoris

DNA used for transformation of electrocompentent *Pichia* cells was linearised by digesting with EcoNI, which cuts pPink plasmids a single time in the TRP2 region or SalI which cuts pPIC9K a single time in the His4 region. This allows integration of the linearised plasmid into the TRP2 locus of PichiaPink strains and the His4 locus of GS115 via homologous recombination, respectively. After purification using the QIAquick PCR Purification Kit (Qiagen, 28104), 5–10 µg of linearised plasmid DNA was mixed with a freshly prepared or freshly thawed aliquot of electrocompetent *Pichia* cells in an ice-cold 0.2 cm electroporation cuvette. The cuvette was incubated with the cells on ice for 5 minutes and then pulsed in a BioRad gene pulser Xcell using the pre-installed *P. pastoris* programme. Immediately after pulsing 1 mL of ice-cold YPDS media was added to the cuvette and the cells were incubated at 28°C for 2 hours without shaking. After incubation 50 ml, 250 ml and 750 ml were spread on PAD selection plates and incubated at 28°C for 3–10 days until distinct colonies were formed.

2.3 Protein Biochemistry

2.3.1 Protein expression from *Pichia pastoris*

2.3.1.1 Small scale protein expression for analysis of expression

To express small amounts of proteins to screen for protein expression in individual *Pichia* clones, a 5 ml BMGY culture was inoculated with a single, white colony from a

PAD agar plate for PichiaPink strain, or a single colony from a YPD agar plate for GS115, and grown for 2 days at 28°C, 280 rpm. The culture was then pelleted by centrifuging at 1500 x g and the pellet resuspended in 1 ml BMMY. The culture was grown for 2 more days at 28°C, 280 rpm, with 40 µl of 100% methanol being added after 24 hours. After pelleting cells by centrifuging at 1500 x g secreted proteins can be detected in the supernatant and intracellularly expressed proteins in the pellet by Western blot.

Glycerol stocks of *Pichia* clones with confirmed protein expression were generated by growing a 25 ml BMGY culture for 3 days at 28°C, 280 rpm, pelleting cells by centrifuging at 1500 x g and resuspending the pellet in BMGY + 20% glycerol. Glycerol stocks were stored at -80°C.

2.3.1.2 Large scale protein expression

To express larger quantities of proteins from transformed *Pichia* strains, using a single colony from an agar plate, or 10 µl of a glycerol stock, a 25 mL BMGY starter culture was inoculated in a 250 mL baffled flask. The starter culture was grown at 28°C in a shaking incubator at 280 rpm for 2 days and then used to inoculate 2 x 500 ml of BMGY in 2.5 l baffled flasks. The BMGY cultures were grown for 2 days at 28°C with vigorous shaking and then pelleted by centrifuging in sterile centrifuge bottles at 1,5000 × g for 5 minutes at room temperature. The pellets were resuspended in 200 ml of BMMY medium to induce protein expression, pooled and grown in one of the flasks for three more days. 24 and 48 hours after induction methanol was added to the culture to a final concentration of between 0.5% - 4%. Cells were then harvested by centrifuging at 3,000 × g for 5 minutes at room temperature.

Supernatants containing secreted proteins were either stored at -20°C or used straight away for protein purification via FPLC. Pellets containing intracellularly expressed VLPs were either stored at -20°C or lysed using glass beads or high pressure for subsequent protein purification from the lysate by FPLC.

2.3.1.3 Glass beads lysis of Pichia pastoris for VLP purification

Up to 120 ml of BMMY culture (4 x 30 ml aliquots in 50 ml falcon tubes, equivalent of 300 ml BMGY culture) were lysed using glass beads. Each aliquot was pelleted by centrifugation at 3000 x g for 5 minutes and the pellet resuspended in 0.3 ml of yeast breaking buffer per ml of culture volume. 0.5 g acid washed glass beads (Sigma, G8772) were added to each tube as well as 25 units of benzonase (Sigma, E1014) per ml of lysis buffer. Cells were lysed by vortexing for 1 minute followed by incubation on ice for one minute for a total of 10 cycles. To allow digest of nucleic acids by benzonase the lysate was incubated at room temperature for 15 minutes. Glass beads and cell debris were removed by centrifugation at 3000 x g for 20 minutes, the supernatants pooled and 2 mg of Amberlite XAD4 (Sigma, XAD4) were added per ml of lysate to remove free detergent. Lysate was incubated with XAD4 for 2 hours at room temperature with vigorous shaking and then filtered through a 0.2 µm filter before protein purification by FPLC.

2.3.1.4 High pressure lysis of Pichia pastoris for VLP purification

Larger culture volumes (up to 200 g of pellet wet weight) were lysed using high pressure homogenisation. The pellet's wet weight was determined by weighing and it was then resuspended in 100 ml of yeast resuspension buffer per 25 g of pellet. High

pressure homogenisation was performed in an APV Lab 2000 homogeniser at 1000 bar. The homogenate was immediately cooled on ice and then centrifuged at 12000 x g for 30 minutes to pellet cell debris as well as the VLP containing membrane fractions. The supernatant was discarded and the pellet washed twice in 50 ml 20 mM Tris pH 8 per 25 g of cell weight by centrifuging as before. After the washes the pellet was resuspended in 4 x cell weight volume of liberation buffer and homogenised a second time at 1000 bar. After being cooled on ice the homogenate was incubated for 30 minutes at room temperature with vigorous shaking. Cell debris was removed by centrifugation at 12000 x g for 30 minutes. The pellet was discarded and 1.1g of XAD4 per 100 ml were added to the supernatant. After incubation for 2 hours at room temperature with vigorous shaking the lysate was filtered through a 0.2 µm filter before protein purification by FPLC.

2.3.2 Protein expression in *Drosophila* Schneider-2 (S2) cells

To express small quantities of proteins from S2 cells, cells were transiently transfected with pExpres2 plasmids using Expres2 Insect-TR (ExpreS2ion biotechnology, received under MTA). S2 cells were grown in Excell420 containing 1% Pen/Strep. On day 1, 8 ml of an $8x10^6$ cells/ml cell suspension were mixed with 100 µl of ExpreS2 Insect-TR 5x and then mixed with 20ug DNA. To express monobiotinylated proteins, the plasmid encoding a biotin acceptor peptide containing protein was mixed with the plasmid pExpres2-KanPac-BirA-His in a ratio of 10:1. Transfected cells were recovered for 5 minutes in vented cap 50 ml conical centrifuge tubes (Sigma, Z761028) before being incubated at 200 rpm at 25°C in a rack, inclined at an angle of 45°. Supernatants were harvested by centrifugation on day 4 post transfection. Supernatants were filtered

through 0.22 µm syringe filters and then used straight away, further processed or frozen at -20°C.

When larger quantities of protein were required cell numbers and reagent quantities were scaled up proportionally to culture volumes of up to 50 ml. Cultures of 15-25 ml were cultured in 125 ml conical flasks at 115 rpm, culture volumes of 25-50 ml were cultured in 250 ml conical flasks at 115 rpm.

2.3.3 Protein characterisation by SDS polyacrylamide gel electrophoresis

2.3.3.1 SDS page

Proteins samples for SDS page were prepared in 4 x Laemmli buffer (BioRad, 1610747). If protein samples should be reduced prior to electrophoresis 250 mM DTT was added to the sample. Before loading on polyacrylamide gels, the samples were boiled at 95°C for 3 minutes. Pre cast NuPAGE™ 4-12% Bis-Tris Midi Protein Gels (Invitrogen, WG1403) and NuPAGE™ MES SDS Running Buffer (Invitrogen, NP0002) were used for most proteins. Occasionally gels with other concentrations of polyacrylamide were also used.

2.3.3.2 Detection of proteins using unspecific protein stains

Total protein in a gel was visualised either by Coomassie staining (Quick Coomassie, Generon, GEN-QC-STAIN) for high protein concentrations, or by silver staining (Pierce™ Silver Stain Kit, Thermo Scientific, 24612) for low protein concentrations.

2.3.3.3 Detection of proteins by Western blot

Proteins were blotted on nitrocellulose membranes using the BioRad TransBlot Turbo Transfer System (BioRad, 17001915). Antibodies were bound to the membrane using the iBind Flex western system (Invitrogen, SLF2000S). Western blots were developed using SIGMAFAST™ BCIP®/NBT (Sigma, B5655).

2.3.4 Fast protein liquid chromatography (FPLC)

FPLC was used to purify protein from cell lysates and supernatant. All size exclusion chromatography (SEC) was performed using an Äkta Pure Chromatography system (GE Healthcare Life Sciences), all affinity chromatography was performed either using an Äkta Pure Chromatography system (GE Healthcare Life Sciences) or an Äkta Start Chromatography system (GE Healthcare Life Sciences).

2.3.4.1 C-Tag affinity chromatography

As pre-packed C-Tag affinity columns are not commercially available, CaptureSelect™ C-tag Affinity Matrix (Thermo Scierntific, 191307005) was packed into empty XK16 columns (GE Healthcare Life Sciences, 28988937). Between 5 ml and 20 ml affinity Matrix was packed per column, depending on the desired purification scale. TBS was used as running and wash buffer. Protein was eluted from the column using 2 M $MgCl_2$.

2.3.4.2 Immobilised metal ion affinity chromatography (IMAC)

IMAC was used to purify His-tagged proteins from supernatants or lysates over HisTrap HP 5 ml columns (GE Healthcare Life Sciences, 17-5248-01). To reduce unspecific

binding to the column, Imidazol was added to the supernatant to a final concentration of 20 mM. His running buffer was used as a running and wash buffer; His elution buffer was used as elution buffer. After each run the column was stripped with 200 mM EDTA and reloaded with 0.1 M $NiCl_2$.

2.3.4.3 Size exclusion chromatography (SEC)

Small sample volumes (up to 500 µl) were run over a Superdex 200 Increase 10/300 GL column (GE Heathcare Life Sciences, 28990944). Bigger sample volumes (up to 5 ml) were run over a HiLoad 16/600 Superdex 200 pg column (GE Heathcare Life Sciences, 28989335). Depending on the downstream application of the sample either TBS or PBS was used as a running buffer.

2.3.5 Protein quantification

Purified proteins were quantified by measuring absorption at a wavelength of 280 nm, or by using the Pierce™ BCA Protein Assay Kit (Thermo Scientific, 23225) according to the manufactures microplate procedure protocol.

2.3.6 SpyTag-SpyCatcher/SnoopTag-SnoopCatcher conjugation

SpyCatcher/SnoopCatcher displaying HBsAg VLPs were conjugated to SpyTagged/SnoopTagged antigens by incubating the VLP with a 1.5-fold molar excess of the antigen in Spy/Snoop conjugation buffer over night at room temperature. Unconjugated antigen was removed by dialysis or by using 100K MWCO spin concentrators.

2.3.7 Transmission electron microscopy (TEM)

TEM of R21c and HBsAg-VLPs was performed under the supervision of Juha Huiskonen at the Wellcome Trust Centre for Human Genetics. All other TEM was performed by Errin Johnson at the Sir William Dunn School of pathology EM core facility. VLPs were applied to carbon coated copper grids and stained with 2% uranylacetate to allow imaging by transmission electron microscopy.

2.3.8 Avidity-based extracellular interaction screen (AVEXIS)

AVEXIS was performed as described previously [214] with minor modifications.

2.3.8.1 Quantification of prey proteins

AVEXIS prey proteins were expressed in S2 cells were they were secreted into the culture supernatant. Protein containing supernatant was sterile filtered and then used straight away for quantification. For that, 60 µl of supernatant were transferred into microtitre plates in duplicates and diluted down the plate in a 1:3 dilution series. 20 µl from each well were then transferred into a fresh 96 well microtitre plate. 60 µl of 125 ug/ml nitrocefin solution were added to the wells and the plate was instantly transferred into a Varioskan Flash plate reader (Thermo Scientific) were the OD_{482} was measured every minute for 20 minutes. Proteins were normalised by diluting or concentrating them using 10K molecular weight cut off (MWCO) spin concentrators (Merck Milipore, UFC901008) so they would reach saturation after 7 minutes. The highest dilution at which saturation was reached in less than 7 minutes was used to calculate the dilution factor. If undiluted sample did not reach saturation within 20 minutes, the time to saturation was calculated by linear regression and the

concentration factor determined accordingly. Where 8 ml of supernatant were not sufficient, supernatants from up to 3 individual transfections were pooled prior to concentration.

2.3.8.2 Quantification of bait proteins

Supernatants from transiently transfected S2 cells containing monobiotinylated AVEXIS bait proteins were dialysed three times against an excess volume of PBS in 12 ml, 10K MWCO Slide-A-Lyzer™ Dialysis Cassettes (Thermo Scientific, 66810) to remove free biotin. Bait proteins were then quantified by an anti-CD4-Tag ELISA. To bind biotinylated proteins, streptavidin coated 96-well microritre plates (Thermo Scientific, 15500) were blocked with 200µl Blocker Casein in PBS (Thermo Scientific, 37528) for 30min at room temperature, and then incubated with dialysed supernatants at different concentrations. 75 µl of undiluted supernatant was added to the top row of wells in duplicates and then diluted down the plate in a 1:3 dilution series. Proteins were allowed to bind to the plate for 1 hour at room temperature. After washing plates 6 times with PBS-T 50 µl of OX68 anti CD4-Tag antibody was added to each well at a concentration of 1µg/ml and incubated at room temperature for 1 hour. To allow quantification of bound protein, the plates were washed 6 times with PBS/T and then incubated with 50 µl/well goat anti-mouse AP and incubated at room temperature for 1 hour. To develop the ELISA, plates were washed 6 times with PBS-T and two times with PBS without Tween. After washing, 100 µl p-nitrophenylphosphate (Sigma, N2765) at 1mg/mL in diethanolamine buffer (Sigma, 34064) were added to each well and optical density at 405nm (OD_{405}) was read after 1 hour. Samples were normalised by dilution or concentration using 10K MWCO spin

concentrators (Merck Milipore, UFC901008) so the signal saturated upon the time of reading. Where 8 ml of supernatant were not sufficient, supernatants from up to 3 individual transfections were pooled prior to concentration.

2.3.8.3 AVEXIS assay

To screen for interactions between bait and prey proteins, threshold dilutions of bait proteins were coupled to steptavidine coated 96-well microritre plates (Thermo Scientific, 15500) that had previously been blocked with 200µl Blocker Casein in PBS (Thermo Scientific, 37528) for 30min at room temperature. Biotinylated OX68 was coupled to the plate to confirm the presence of prey proteins. Furthermore, 4 wells were coupled with bait+ control protein. After washing the plates 6 times with PBS-T they were probed with threshold dilutions of the different prey proteins for two hours at room temperature. One of the bait+ wells was also probed with prey protein (negative control), the other three were probed with prey+ at threshold dilution as well as a 1:10 and a 1:100 dilution of it (positive controls). After 6 washes with PBS-T and two more with PBS, 60 µl of nitrocefin (TOKU-E, N005) at a concentration of 125 µg/ml were added to each well and hydrolysis by beta-lactamase was quantified by measuring the OD at 485nm two hours after the substrate was added to the plates. To confirm detected signals and detect low intensity signals, plates were stored over night at 4°C and then read a second time. A signal was considered as positive when the OD485 was higher than the average OD485 within the same screen plus five times the standard deviation.

2.3.8.4 IgG competition AVEXIS

To assess the ability of IgG directed against one of the interaction partners to interfere with the interaction in AVEXIS, normalised amounts of Bait+ as well as the bait-protein to be tested were coated to streptavidin coated microtitre plates (Thermo Scientific, 15500) that had previously been blocked with 200µl Blocker Casein in PBS (Thermo Scientific, 37528) for 30min at room temperature. A 1:3 dilution series of purified IgG was set up at starting at 1 mg/ml and mixed with an equal volume of Prey+ and the to be tested prey-protein, normalised to double concentration. After washing the plates 6 times with PBS-T the mixture was added to the prepared wells in duplicate and the plates incubated for 2 hours at room temperature. After 6 washes with PBS-T and two more with PBS, 60 µl of nitrocefin (TOKU-E, N005) at a concentration of 125 µg/ml were added to each well and hydrolysis by beta-lactamase was quantified by measuring the OD at 485nm two hours after the substrate was added to the plates. The ability of IgG to inhibit the interaction was calculated as the reduction in signal intensity relative to the signal in the absence of IgG.

2.3.9 Surface plasmon resonance

SPR was performed on a Biacore X100 (GE healthcare life sciences). Monobiotinylated Ook12 was immobilised on flow cell 2 of a CAP sensor chip to a level of >2500 RU. Flow cell 1 was only conjugated with capture reagent but no protein. Purified MG36 protein was then run over both flow cells in concentrations ranging from 40 µM to 1.25 µM in 1:2 dilutions. Changes in RU on flow cell 2 relative to flow cell 1 were recorded. Steady state affinity was analysed to determine the K_D of the interaction.

2.4 Immunology

2.4.1 ELISA

2.4.1.1 Endpoint ELISA

Antibody responses in mouse sera were assessed by endpoint total IgG ELISA. ELISAS were carried out in Nunc-Immuno Maxisorp 96 well plates (Thermo Scientific, 442404) coated with 2µg/ml of the relevant coating antigen in carbonate-bicarbonate coating buffer (Sigma Aldrich, C3041) overnight at 4°C. Plates were washed with PBS-Tween and blocked with 10% Casein Block (Thermo Scientific, 37528). Sera were diluted at a starting concentration between 1:100 and 1:3000, added to the top row of the plate in duplicate, and serially diluted 3-fold down the plate. Plates were incubated for 2 hours at room temperature and then washed as before. Goat anti-mouse whole IgG conjugated to alkaline phosphatase was added for 1 hour at room temperature. Following a final wash, plates were developed by adding p-nitrophenylphosphate (Sigma, N2765) at 1mg/mL in diethanolamine buffer ((Sigma, 34064)) and OD_{405} was read. Serum antibody endpoint titres were taken as the x-axis intercept of the dilution curve at an absorbance value of the background plus three standard deviations or a minimum of 0.15. If a 1:100 dilution of a serum sample did not develop a signal above background, the IgG titre in this sample was considered to be 0. To make results comparable an internal control was included on each plate. Coating antigens and internal controls are listed in Table 2.10.

Table 2.10: Coating antigens and internal controls used in endpoint ELISAs in this thesis.

ELISA	Coating antigen	Internal control
HBsAg endpoint	HBsAg (India Immunologicals)	Reference serum pool (starting dilution 1:1000)
NANP endpoint	$(NANP)_6C$ peptide	2A10 (starting dilution 1:1000)
Pfs28 endpoint	Pfs28-His produced in S2	Reference serum pool (starting dilution 1:1000)
MG36 endpoint	MG36-His produced in S2	Reference serum pool (starting dilution 1:1000)

2.4.1.2 Standard ELISA

Alternatively, immune responses were assessed by a standardised total IgG ELISA. ELISAs were carried out in Nunc-Immuno Maxisorp 96 well plates (Thermo Scientific, 442404) coated with 1µg/ml of the relevant coating antigen in carbonate-bicarbonate coating buffer (Sigma Aldrich, C3041) overnight at 4°C. Plates were washed with PBS-Tween and blocked with 5% milk in PBS-Tween. Sera were diluted to reach an OD_{405} in the linear range of the standard curve at the same time an internal control reaches an OD_{405} of 1. Samples were added in triplicates. An internal control was added in six replicates. A standard curve was added in duplicates, by serial dilution along the plate in 1:2 steps ten times. Plates were incubated for 2 hours at room temperature and then washed as before. Goat anti-mouse whole IgG conjugated to alkaline phosphatase was added for 1 hour at room temperature. Following a final wash, plates were developed by adding p-nitrophenylphosphate (Sigma, N2765) at 1mg/mL in diethanolamine buffer (Sigma, 34064) and OD_{405} was read. ELISA units were extrapolated from the samples OD on the linear range of the standard curve.

Table 2.11: Coating antigens, internal controls and standard curves used in standard ELISAs in this thesis.

ELISA	Coating antigen	Internal control	Standard curve
NANP standard	$(NANP)_6C$ peptide	2A10 (1:14000)	2A10 (starting dilution 1:500)
Pfs25 standard	Pfs25-His produced in *Pichia*	Reference serum pool (1:33,161)	Reference serum pool (starting dilution 1:1000)
SPECT1 standard	SPECT1-6xHis produced in *Pichia*	Reference serum pool (1:32,000)	Reference serum pool (starting dilution 1:1000)

2.4.1.3 NANP Avidity ELISA

Avidity of anti-NANP-repeat antibodies was determined by chaotropic salt displacement ELISA. Serum samples whose endpoint titres had been determined previously were diluted to the dilution at which the OD_{405} in the endpoint ELISA had been 1. 50 µl of diluted sera were then added to two columns of a Nunc-Immuno Maxisorp 96 well plates (Thermo Scientific, 442404) that had been coated with 2µg/ml NANP6C peptide in carbonate-bicarbonate coating buffer (Sigma Aldrich, C3041) overnight at 4°C. Plates were incubated for 2 hours at room temperature and then washed 6 times in PBS-T. Afterwards, increasing concentrations of NaSCN diluted in PBS was added down the plate (0, 1, 2, 3, 4, 5, 6, and 7M NaSCN). Plates were incubated with the chaotropic salt for 15 minutes at room temperature before plates were washed again 6 times in PBS-T. Goat anti-mouse whole IgG conjugated to alkaline phosphatase was added for 1 hour at room temperature. Following a final wash (6 times PBS-T, twice PBS) plates were developed by adding p-nitrophenylphosphate (Sigma, N2765) at 1mg/mL in diethanolamine buffer (Sigma, 34064) and OD_{405} was read. Avidity was calculated as the IC_{50} of NaSCN, i.e. the

concentration of NaSCN at which the signal is exactly half the intensity of the signal when no NaSCN was added.

2.4.1.4 NANP Isotype ELISA

Isotypes of anti-NANP-repeat antibodies were quantified using a standardised isotype ELISA. ELISAS were carried out in Nunc-Immuno Maxisorp 96 well plates (Thermo Scientific, 442404). The top 6 rows of wells were coated with 2µg/ml NANP6C peptide in carbonate-bicarbonate coating buffer (Sigma Aldrich, C3041) overnight at 4°C. The two bottom rows were coated with as 1:2 dilution series of isotype control IgG (IgG2a or IgG1) in duplicates starting at 2 µg/ml. The last well of the two rows only contained PBS. The next day, plates were washed with 6 times with PBS-Tween and blocked with 10% Casein Block (Thermo Scientific, 37528). Sera were tested at two dilutions, each in triplicates. If anti-IgG1-Biotin was used for detection, sera were diluted 1:10,000 and 1:40,000, if anti-IgG2a-Biotin was used for detection sera were diluted 1:5,000 and 1:10,000. Diluted sera were added to the top six rows, only PBS was added to the bottom two rows. Plates were incubated for 2 hours at room temperature and then washed as before. Secondary antibodies were added to the corresponding plates e.g. anti-mouse-IgG1-Biotin was added to the plate were mouse IgG1 was used for standard curve and anti-mouse-IgG2a-Biotin was added to the plate were mouse IgG2a was used. Both biotin-conjugated secondary antibodies were used at a dilution of 1:5,000. Plates were incubated for another hour at room temperature, washed as before and Extravidin-AP was added at a dilution of 1:5,000. After 30 minutes of incubation the plates were washed 6 times with PBS-T and twice with only PBS before they were developed by adding p-nitrophenylphosphate (Sigma, N2765) at 1mg/mL in

diethanolamine buffer (Sigma, 34064) and OD_{405} was read. Plates were read until the 4th IgG1 standard (0,25 µg/ml) and the 2nd IgG2a standard (1 µg/ml) had reached an OD_{405} of 1.5, respectively. ELISA units for each Isotype were extrapolated from the samples OD on the linear range of the standard curve.

2.5 Animals and Parasitology

All animal experiments and procedures were performed according to the UK Animals (Scientific Procedures) Act Project Licences (PPL 30/2889, PA7D20B85 and P9804B4F1) and approved by the Oxford University Local Ethical Review Body.

2.5.1 Immunisation

Age-matched female CD1 or Balb/C mice (Envigo), housed in specific pathogen-free environments, were vaccinated under Isoflurane induced general anaesthesia by intramuscular injection of 50 µl vaccine formulation into one leg (IM). If more than one immunisation was performed as part of one experiment, injections were alternated between the left and the right hind leg.

2.5.2 Blood sampling

2.5.2.1 Blood sampling by tail tip amputation and thin film preparation

To monitor parasitaemia in a malaria infected mouse the tip of the tail was amputated. This allowed collecting a single drop of blood on multiple consecutive days by removing the scab from the wound with a clean tissue. Blood was collected on microscopy slides to prepare thin blood films. Films were fixed with methanol for 1

minute and subsequently stained with 5% Giemsa stain for up to 1 hour. The proportion of infected erythrocytes was then counted to calculate the level of parasitaemia.

2.5.2.2 Blood sampling by tail bleeding

To obtain small blood samples mice were warmed to 37°C in a heat box. A small incision was made laterally in the tail and blood was collected into capillary tubes. If the bleeding did not stop naturally after enough blood was obtained, pressure was applied to the wound until the bleeding ceased. Obtained blood samples were allowed to clot at 4 °C overnight before centrifugation at 13,000 x *g* in a benchtop centrifuge and removal of serum for testing.

2.5.2.3 Blood sampling by cardiac puncture (exsanguination)

To obtain larger blood samples mice were anesthetised using Isoflurane and then exsanguinated by cardiac puncture. Blood was removed by a 1 ml syringe using a 25 G needle. Once blood was removed death was confirmed by dislocation of the neck. Blood was then transferred into 1.5 ml Eppendorf tubes and allowed to clot at 4 °C overnight before centrifugation at 13,000 x *g* in a benchtop centrifuge and removal of serum for testing.

2.5.3 Parasite production

To produce parasites for malaria challenge, inhibition of sporozoite invasion assay or generation of new blood stocks, one or two mice were intraperitoneally injected with a parasite bloodstock. Parasitaemia was monitored through blood sampling by tail tip

amputation and thin film preparation. As soon as the parasitaemia exceeded 1%, the mouse was anaesthetised by intra muscular injection of ketamine and placed on top of a pot containing approximately 50 female *A. stephensi* mosquitoes. Mosquitoes were allowed to feed through the mesh covering the pots for at least 10 minutes. If large numbers of parasites were required, a second pot of mosquitoes was fed on the same mouse. 10-12 days after the bloodmeal mosquitoes were allowed to feed on an uninfected mouse, as this had been shown to increase the number of parasites per mosquito. 21 days after the initial feed salivary glands were dissected from the mosquitoes to obtain sporozoites.

2.5.4 Malaria challenge

To assess vaccine efficacy *in vivo*, mice were challenged with transgenic rodent parasites expressing human malaria antigens (Table 2.7). Mice were injected intravenously with 1000 sporozoites and parasitaemia monitored daily from day 5 after challenge until day 12 after challenge. As soon as parasitaemia exceeded 1%, mice were euthanised by dislocation of the neck. Parasitaemia over at least three consecutive days was plotted by linear regression to determine the time to 1% parasitaemia. If no infected erythrocytes were detected at 12 days after challenge, the mouse was considered protected from the challenge.

2.5.5 Standard membrane feeding assay (SMFA)

SMFAs were performed to assess the ability of vaccine-induced antibodies to block the development of *P. falciparum* strain NF54 oocysts in the mosquito midgut as described in [215]. All SMFAs were performed at the MVI SMFA reference lab at NIH/NCAID by

Kazutoyo Miura and co-workers. In brief, stage V gametocytes from a mature gametocyte culture were mixed with normal human serum and normal red blood cells to make a feeding mixture with 0.15% - 0.2% stage V gametocytemia. Purified IgG was added to these at the concentrations shown in the figures and then fed to 3–6 day old starved female *A. stephensi* (SDA 500) via a parafilm® membrane. The mosquitoes were maintained for 8 days and then dissected to count the number of oocysts per midgut in 20 mosquitoes. Percent reduction in infection intensity was calculated relative to the respective control IgG tested in the same assay.

2.5.6 Inhibition of sporozoite invasion assay (ISI)

Functional activity of anti-sporozoite antibodies was assessed by ISI using transgenic parasites expressing the relevant vaccine antigen as well as GFP to allow detection of infected cells by flow cytometry.

One day prior to mosquito dissection for isolation of sporozoites, HUH7 cells were seeded in a 96 well plate at a concentration of 300.000 cells/ml in a volume of 100 µl/well, resulting in a concentration of 30.000 cells per well.

One day later mosquitoes were dissected and salivary glands collected in ice cold RPMI without FCS. Sporozoites were released from salivary glands by tissue disruption using a pestle and mortar, and counted in a hemocytometer.

Sera and antibodies were diluted to double the required concentration in 120 µl complete RPMI. The medium was removed from the HUH7 cells seeded the day before, and 50 µl of diluted serum was added to the wells in duplicates. Sporozoites were then diluted to 300.000 sporozoites per ml in complete RPMI and 50 µl were

added to each well, resulting in 15.000 sporozoites per well and a ratio of cells to sporozoites of 2:1. To aid sporozoite invasion of the cells, the plate was centrifuged at 500xg for 5 minutes before incubation at 37°C and 5% CO_2 overnight in a tissue culture incubator.

After 24h of incubation, cells were detached from the plate by removing medium from the plate and then adding 100 µl of TrypLE™ Express (Gibco, 12604013) to the wells. Cells were incubated with Trypsin for 5 minutes at 37°C and then transferred into cluster tubes. The empty wells were washed twice with 200 µl FACS buffer (PBS +0.5% BSA +0.05% Azide). Both washes were added to the cluster tubes. Cells were pelleted in the cluster tubes by centrifuging at 2000 rpm for two minutes and the supernatant discarded. Cells were then resuspended in 80 µl FACS buffer. Directly before running cells on an LSR II flow cytometer (BD Biosciences), 5 µl DAPI (1:1000) was added to the cells to allow separation of live from dead cells. Each sample was run for 1 minute on the LSR. Inhibition was calculated as reduction in viable, GFP positive hepatoma cells in comparison to cells infected with sporozoites in the absence of serum.

2.5.7 Mosquito RNAi

Mosquito RNAi experiments were conducted at Imperial College (London) in the laboratory of George K Christophides.

2.5.7.1 cDNA synthesis

To generate *A. gambiae* cDNA whole bodies of 5-15 mosquitoes were collected into TRIzol (Invitrogen, 15596026) and total mRNA extracted according to the manufacturer's instructions. Potential DNA contaminations were removed using the

TURBO DNA-free™ Kit (Invitrogen, AM1907). cDNA was synthesised from the purified RNA using SuperScript™ III Reverse Transcriptase (Invitrogen, 18080093) according to the manufacturer's instructions.

2.5.7.2 dsRNA synthesis

A template for dsRNA synthesis was synthesised from *A. gambiae* cDNA as described in (PCR for subcloning) using an annealing temperature gradient and primer MG36 ds for and MG36 ds rev. After size and quality of the obtained PCR product was confirmed by gel electrophoresis on a 1% agarose gel, and it was used as a template in the TranscriptAid T7 High Yield Transcription Kit (Thermo Scientific, K0441). The kit was used as in the manufacturer's instructions but the reaction was incubated at 37°C overnight instead of 2 hours. dsRNA was purified from the reaction using the RNeasy Mini Kit (Qiagen, 74104) according to the maufacturer's RNA clean up protocol.

2.5.7.3 Gene knockdown in mosquitoes

To knock down genes in *A. gambiae*, 69 µl dsRNA at a concentration of 3 µg/µl were injected into the thorax of 0-2 day old, CO_2-anesthetized mosquito females using a Drummond Nanoject II Auto-Nanoliter Injector. Two days after injection whole bodies as well as midguts of a small number of mosquitoes were collected intoTRIzol and cDNA was synthesised as described in 2.5.7.1. The obtained cDNA was then used to determine the efficiency of the knockdown by qPCR as described in 2.2.1.3.

To assess the effect of the knock down on ookinete to oocyst development, mosquitoes were fed on cultured *P. falciparum* NF54 gametocytes via a parafilm® membrane two days after injection. Seven days later, midguts were dissected from the

mosquitoes, stained in 0.5% mercurochrome (Sigma Aldrich, M7011) and oocysts were counted under a light microscope.

2.6 Statistical Analysis

Comparison of antibody titres between two groups was performed by Mann-Whitney test. Comparison of antibody titres between more than two groups was performed using a Kruskal-Wallis test, which was followed up by a Dunn's multiple comparison post-test, if significant.

Differences in survival following malaria challenge between two groups was calculated using Mantel-Cox signed-rank test.

Transmission reducing activity (TRA) was calculated from SMFA data, as 100 x (mean number of occysts in test/mean number of oocysts in control) and 95% confidence intervals (95%CIs) of % inhibition in oocyst density from a single or multiple feeding experiments for each test antibody at each concentration were calculated using a zero inflation negative binomial model, as described in [215]. Oocyst densities of two groups were compared using the same model, and Holm corrected p-values were calculated for multiple comparisons.

Statistical tests were performed using Prism 6 (GraphPad Software Inc, USA), or JMP11 (SAS Institute Inc, USA). P-values <0.05 were considered significant.

Chapter 3 - Pre-clinical assessment of the malaria vaccine candidate R21

Authorship statement

Transmission electron micrographs of R21c and HBsAg (***Figure 3.3*** **C,D**) were acquired under direct supervision and with assistance of Prof. Juha Huiskonen. Immunisations and blood sampling of mice for the antibody persistence study after immunisation with R21 and RTS,S (***Figure 3.5***) were conducted by Marta Ulaszewska. All malaria challenges were conducted with assistance from Dr. Ahmed Salman.

3.1 Introduction

The first step of the P*lasmodium* lifecycle in the human host is the progression from the bloodstream, which the parasite invades after being deposited in the skin by a blood feeding mosquito, into hepatocytes of the liver. This is achieved by sporozoites, one of the three motile forms in the *Plasmodium* lifecycle, and in rats normally completed within 2 minutes after inoculation into the blood stream [18]. Sporozoites cross the liver sinusoidal epithelium and traverse through a number of hepatocytes before establishing within one hepatocyte in which they then undergo schizogonous replications in preparation for the blood stage of infection [29, 30, 35]. The process by which sporozoites engage and penetrate sinusoidal epithelial cells and hepatocytes is only poorly understood but a number of proteins on the surface of host cells and sporozoites have been implicated in the process, amongst which the circumsporozoite protein (CSP), the first protein on the sporozoite surface to be found as a target of a

host immune response [216], and a highly abundant sporozoite protein, has received most attention.

The to date most advanced malaria vaccine candidate RTS,S targets CSP with the aim to interrupt the *Plasmodium* lifecycle before the establishment of liver stage infection. It was developed by GlaxoSmithKline (GSK) and the Walter Reed Army Institute of Research (WRAIR) in the late 1980s and early 1990 [217]. It is the only malaria vaccine to have completed Phase III clinical trials [174, 175, 218, 219] and to have obtained a positive scientific opinion from the European Medicines Agency (EMA) [220]. Since most fatalities caused by malaria occur in African children under the age of 5, RTS,S was tested in two age groups: 6-12 week-olds and 5-17 months-olds at first immunisation. In the latter age group vaccine efficacy was 45.7% over 18 months following three immunisations. This dropped to 26.2% over a time of 48 months, but could be increased to 39% when a fourth dose of vaccine was administered 18 months past the third dose [174, 175]. In the 6-12 weeks old group efficacy was lower at all time points (26.6% over 18 months, 18.2% and 26.7% over 38 months without or with a fourth immunisation after 18 months, respectively) [174, 175]. As a result of this limited efficacy, challenges with deploying a vaccines outside the standard EPI (Expanded Program on Immunisation) regimen time points, and a possible safety signal with increased female mortality in vaccinees, the World Health Organisation (WHO) has, after assessing the feasibility and cost effectiveness of the implementation of RTS,S, recommended further large scale pilot implementation studies over the next five years prior to potential pre-qualification and licensure for use in disease prevention in African countries [221].

R21 is a rationally improved version of RTS,S that was developed recently in the Jenner institute [222]. This virus like particle (VLP) is, like RTS,S, based on the Hepatitis B virus surface antigen (HBsAg) and displays part of CSP. But unlike RTS,S R21 is not comprising a 4:1 mixture of HBsAg and the CSP-HBsAg fusion protein, but is made up entirely from the fusion protein, therefore likely displaying CSP at 4-fold higher density on the VLP surface (***Figure 3.2***). First studies in mice showed R21 to be highly immunogenic, and when administered with immune stimulating complex adjuvants (ISCOMs), such as Matrix M, to provide sterile protection against challenge with transgenic rodent parasites [222].

While RTS,S induces an immune response against CSP as well as HBsAg, R21 on its own does only generate a significant immune response against the malaria antigen. This is most likely due to the higher proportion of CSP in relation to HBsAg in R21 than in RTS,S. Since the efficacy of RTS,S correlates broadly with the magnitude of the antibody response against the central NANP repeats of CSP [223], it was hypothesised that immune responses to R21 could, at a similar dose, induce better protection than RTS,S. To test this hypothesis R21 and RTS,S were compared at different doses, but no significant difference between the two vaccines could be detected (Katharine Collins, unpublished data)(***Figure 3.1***).

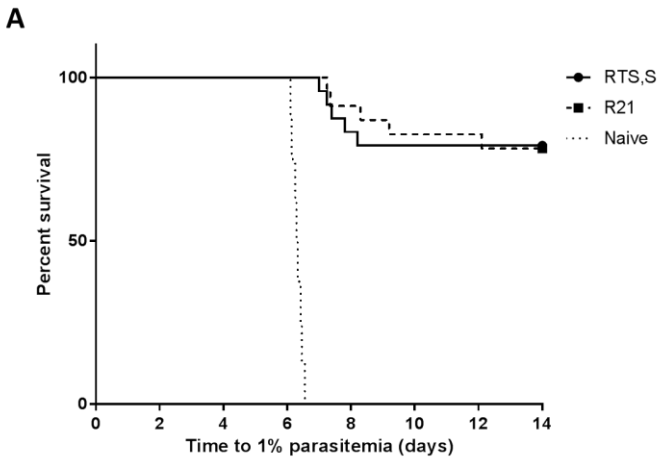

B

	RTS,S	R21
5 µg	4/8	4/8
1.6 µg	8/8	8/8
0.5 µg	7/8	6/7

Figure 3.1: Lower doses of RTS,S and R21 correlate with better protection against challenge with transgenic Plasmodium parasites in mice. Balb/C mice that had received three intra muscular injections of either RTS,S or R21 in AS01 at different doses were challenged with *P. berghei* parasites expressing the *P. falciparum* circumsporozoite protein (PfCSP) under the PbUIS4 promotor. **A** Kaplan-Meier survival curves of naïve mice and mice immunised with different doses of RTS,S or R21, with pooled groups for all doses of the two different vaccines. **B** Number of protected out of total mice for each vaccine regimen. (Katherine Collins, unpublished data).

Interestingly, while there is no statistically significant difference between mice immunised with RTS,S and mice immunised with R21, for both vaccines there is a correlation between lower vaccine doses and increased protection from malaria (Katharine Collins, unpublished data).

Additional studies showed that R21, at least in a less potent adjuvant, can be combined with TRAP-based viral vectors, concurrently inducing a strong humoral and cellular immune response and enhancing efficacy significantly [222]. Based on the promising results of these early pre-clinical evaluations of R21 it was decided to proceed with clinical assessment of this new vaccine candidate. These aspirations where however inhibited by the fact that yield of R21 was modest and the purification of R21 was dependent on CsCl gradient ultracentrifugation and could not be transferred into a good manufacturing practice (GMP) process.

In the early stages of my PhD I developed a new, affinity chromatography based purification process for R21. This has allowed R21 to progress to GMP manufacture and entering phase I clinical trials. In parallel to the ongoing trials, the properties of R21 were further assessed in mouse models with as focus on antibody persistence after immunisation and the effects of low dose administration of the vaccine. All those studies were done side by side with RTS,S to allow comparison of the two vaccines.

3.2 Results

3.2.1 R21 can be purified by affinity chromatography

C-tag, a four amino acid affinity tag consisting of glutamic acid-proline-glutamic acid-alanine (EPEA) expressed at the C-terminus of a protein, had recently been used to purify the protein vaccine antigen Rh5, and was suggested to have the potential to form the basis of a good manufacturing practice-compliant platform [224]. To allow for an easier purification process of R21 than had been previously described [222], and that would allow for production of R21 under GMP conditions, C-tag was fused to the C-terminus of R21 (R21c) (***Figure 3.2***). It had previously been shown that HBsAg VLPs tolerate the addition of small peptides at the C-terminus and that peptides added there are exposed on the surface of the particle [225]. The presence of the C-Tag on the surface of R21 should then allow purification of the particle from yeast lysate by affinity chromatography using the commercially available C-Tag affinity matrix, which consists of a camelid antibody (nanobody) directed against the C-Tag coupled to a stationary phase which can be packed into fast protein liquid chromatography (FPLC) columns.

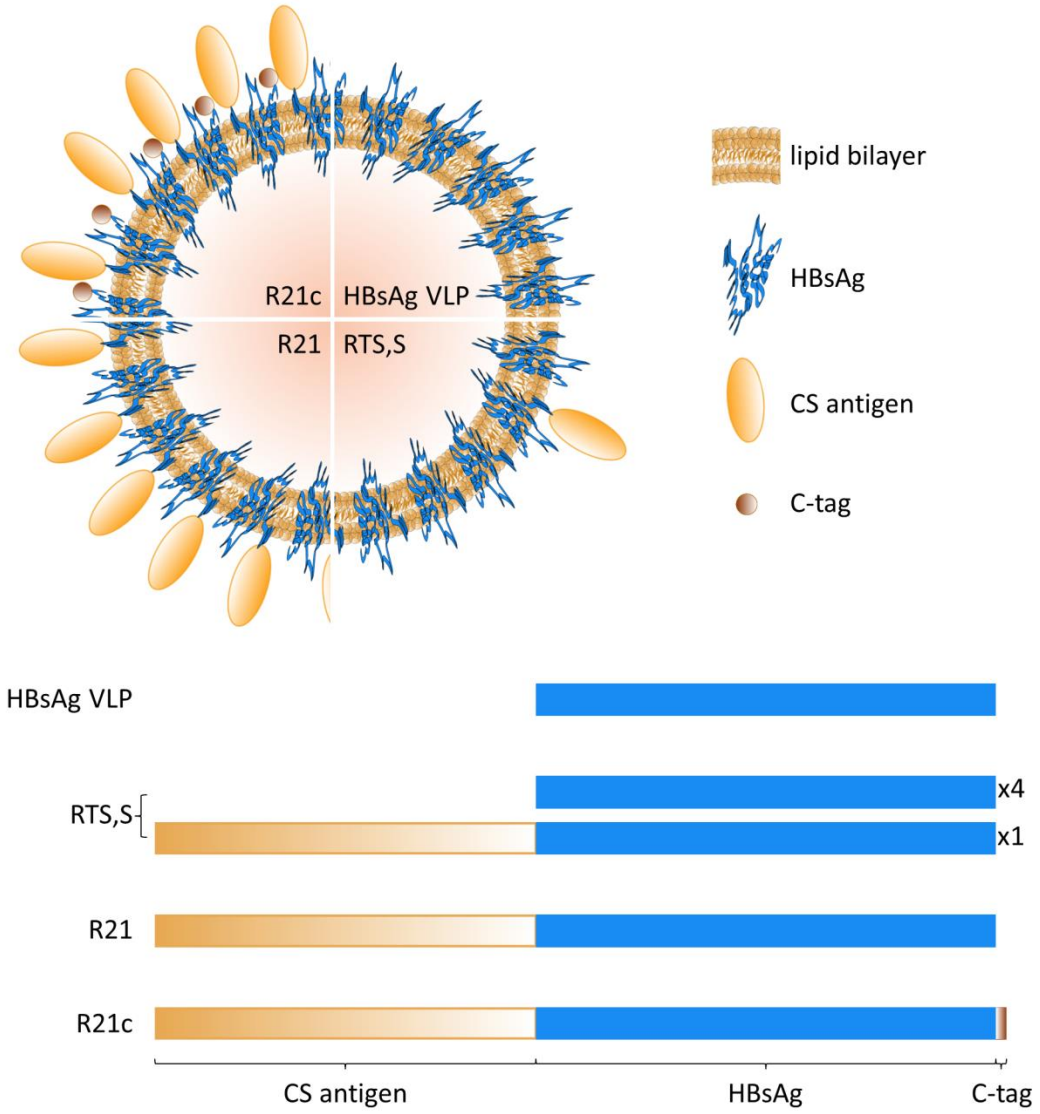

Figure 3.2: Comparison of virus like particles based on the Hepatitis B surface antigen. Hepatitis B surface antigen VLPs (HBsAg VLPs) form the antigenic component of all current Hepatitis B vaccines. Upon expression in yeast cells HBsAg is incorporated into membranes of the Golgi apparatus and assembles into lipoprotein particles during cell lysis. The malaria vaccine candidate RTS,S, is generated from yeast cells expressing HBsAg (S) and the circumsporozoite-HBsAg fusion protein RTS at a ratio of 4:1. RTS contains the antigenic NANP repeat regions (R) and a C-terminal T-cell epitope (T) of CSP fused to the N-terminus of HBsAg (S). By coexpressing S and RTS from the same cell mixed lipoprotein particles are formed that make the antigenic component of GSKs RTS,S ("Mosquirix") vaccine. R21 is a rationally improved version of RTS,S that contains only the CSP-HBsAg fusion protein, therefore likely displaying the malaria antigen at a 4-fold higher density on the VLP surface. R21c is identical to R21 but contains the four amino acids EPEA (C-tag) fused to the C-terminus of the CSP-HBsAg fusion protein, which allows for the particle to be purified by affinity chromatography.

The plasmid for expression of R21c was cloned as described in 2.2.3.1 and used to transform PichiaPink strain 1 and strain 4 cells as described in 2.2.7. A single clone of

the strain 1 transformants was selected and used for expression of R21c at a larger scale as described in 2.3.1.1 and 2.3.1.2. Using a C-tag affinity column, C-tag binding proteins could be purified from the glass bead lysate of this culture. The purified protein was confirmed to be the monomeric R21 protein by anti-HBsAg Western blot and silver staining (***Figure 3.3*** **A**), where a band is detected at 50 kDa, which correlates with the molecular weight of the R21c monomer. In the silver stained gel a second band is detected at 100 kDa which approximates the molecular weight of the R21 dimer. In subsequent preparative size exclusion chromatography (SEC) the VLP leaves the column in a single peak earlier than monomeric protein was expected to elute, indicating that most monomeric protein detected in WB contributes to VLP formation (***Figure 3.3*** **B**). To finally confirm presence of intact VLPs negative staining transmission electron microscopy (TEM) was performed showing distinct particles of similar size and shape as a vaccine grade preparation of HBsAg VLPs provided by India Immunologicals (***Figure 3.3*** **C**).

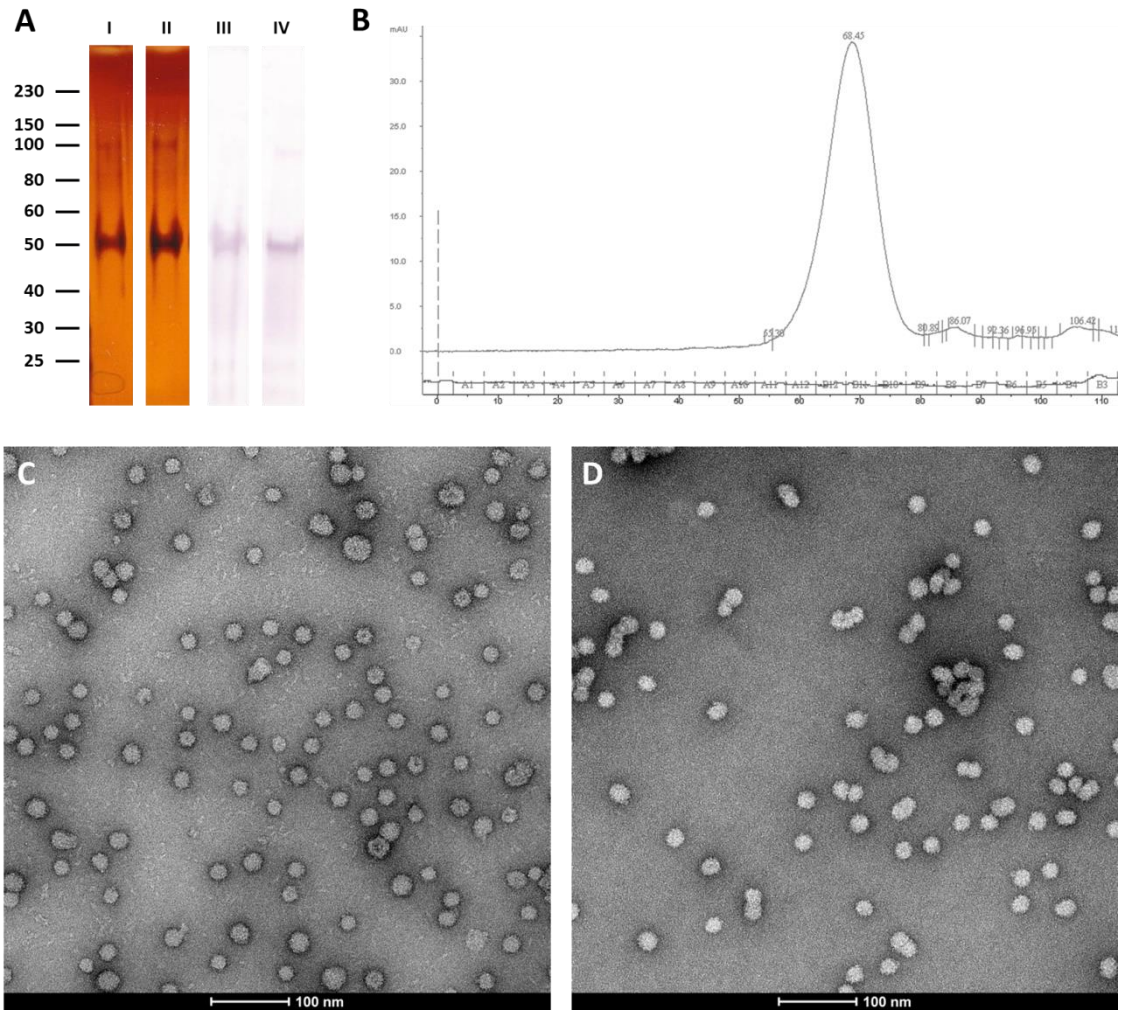

Figure 3.3: R21 can be purified by C-Tag affinity chromatography. **A** Silver stained gel and Western blot of R21. R21 was purified by C-Tag affinity chromatography (lanes I and III) followed by size exclusion chromatography (lanes II and IV) and visualised by silver staining (lanes I and II) and anti-HBsAg Western blot (lanes III and IV) after being run on 12% polyacrylamide gels. **B** Size exclusion chromatogram of C-Tag affinity purified R21. **C,D** Transmission electron micrographs of C-tag affinity purified R21c (C) and HBsAg VLPs (D).

3.2.2 Priming with Hepatitis-B vaccine, Engerix-B affects immune responses to R21

Previous experiments had shown that in contrast to RTS,S, R21 does not induce an immune response to the HBsAg carrier VLP [222]. An effect of pre-existing anti-HBsAg titres as induced by routine Hepatitis B vaccination with Engerix-B on the immune response to RTS,S has been observed but never comprehensively analysed [226, 227]. To assess whether the immune response to R21 was similarly affected by pre-existing

HBsAg titres Balb/c mice (n = 8 per group) were immunised twice by intramuscular injection of the Hepatitis-B vaccine Engerix-B (1 µg HBsAg in Alhydrogel) or with Alhydrogel in TBS in a four week interval. Four weeks later both groups were immunised with R21 adjuvanted with 12 µg Matrix M. The antibody titres against HBsAg and the NANP repeats of the R21 CSP antigen were measured by ELISA before and after the immunisation with R21 (***Figure 3.4***).

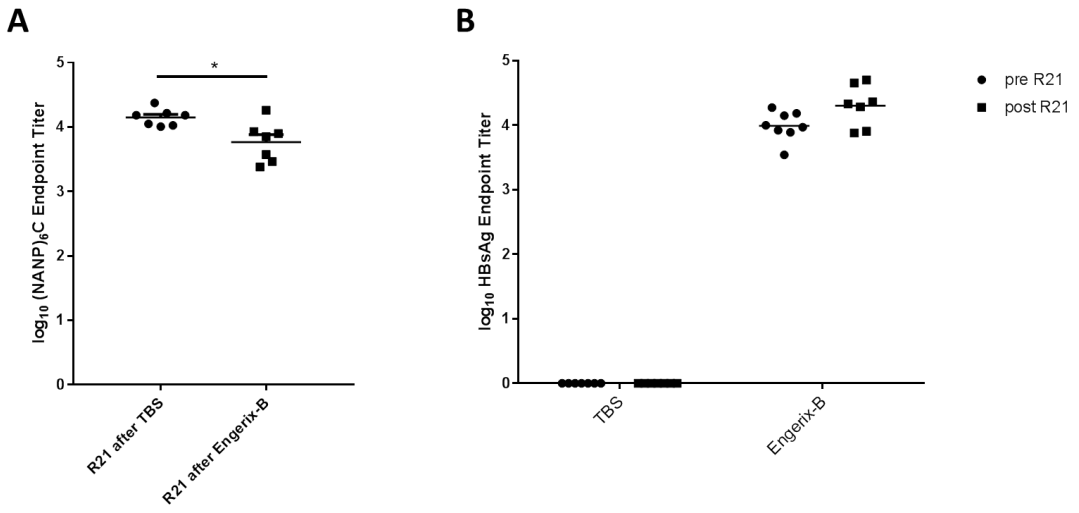

Figure 3.4: Pre-existing antibody titres against HBsAg have a moderate effect on the immune response to R21. Balb/C mice were immunised twice with the Hepatitis B vaccine Engerix-B or with a no protein mock vaccine. One month later mice of both groups were immunised with R21. **A** Antibody responses to CSP were assessed by NANP endpoint ELISA. **B** Antibody responses to HBsAg were determined by HBsAg endpoint ELISA. Data points show endpoint titres in individual mice, lines show the median. Groups were compared by Mann-Whitney test. * = $p < 0.05$.

High antibody titres against the carrier antigen HBsAg slightly but significantly reduced anti-NANP endpoint titres in mice primed with Engerix-B by about 2-fold (15240 after TBS + Alhydrogel versus 7098 after Engerix-B, difference between medians = 8141, p = 0.0175, Mann-Whitney test) (***Figure 3.4*** **A**). Similarly there is a trend for existing antibody responses against HBsAg to be boosted by R21 although this effect is not significant (9617 before R21, 21382 after R21, difference between medians = 11766, p

= 0.0939, Mann-Whitney test). In mice with no pre-existing HBsAg titres R21 did not induce a measurable immune response against HBsAg (***Figure 3.4*** **B**), confirming previous observations by Collins et al. [222].

3.2.3 R21 elicits durable anti-CSP antibody responses in mice

Previous comparisons between R21 and RTS,S in AS01 could not conclusively show a difference between the two vaccines, mostly due to the fact that the protection induced by both vaccines was too high to detect any difference (Katharine Collins, unpublished data). To assess potential differences under conditions where protection would be more limited, immune responses induced by both vaccines were followed over one year and the protective efficacy after that period was assessed by malaria challenge with transgenic rodent parasites. As phase III clinical trials had shown antibody titres induced by RTS,S and the associated protection from malaria to wane quickly over time, durability is - alongside overall efficacy - the main point on which future malaria vaccines need to be improved. Therefore, Balb/c mice (n = 12 per group) were immunised with two doses of 1.6 µg R21 or RTS,S adjuvanted with AS01 at an eight week interval and the immune response monitored over a period of twelve months. Subsequently the mice were challenged with P. *berghei* sporozoites expressing *P. falciparum* circumsporozoite protein (PfCSP) under the PbUIS4 promotor by intravenous injection of 1000 sporozoites per mouse.

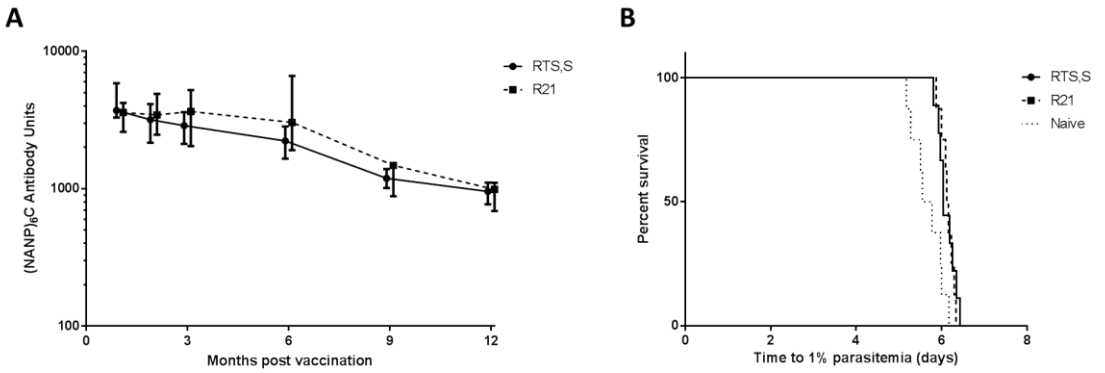

Figure 3.5: R21 elicits long lasting antibody responses in mice. **A** Antibody responses to CSP in mice immunised with RTS,S or R21 over a course of 12 months. Antibody responses were assessed by NANP standard ELISA in serum samples collected 1, 2, 3, 6, 9 and 12 months after the immunisation. Plotted values = median, error bars = interquartile range. **B** Kaplan-Meier survival curve of the mice challenged with *P. berghei* sporozoites expressing PfCSP under the PbUIS4 promotor, twelve months after the second immunisation with R21 or RTS,S.

In the twelve months following vaccination antibody titres against the protective NANP repeats of CSP dropped significantly in mice immunised with either vaccine (***Figure 3.5*** **A**), from 3709 AU to 957 AU after immunisation with RTS,S and from 3591 AU to 988 AU after immunisation with R21 (median antibody titres one month and twelve months after immunisation, $p < 0.0005$, Mann-Whitney test). Although there is a trend for titres to be maintained at a higher level after immunisation with R21 than after immunisation with RTS,S, there is no time point at which there is a statistically significant difference between the titres. Despite antibody titres being maintained at high levels at the time of malaria challenge, no mice were sterilely protected. However, in both groups a statistically significant delay in time to 1% parasitaemia was observed in comparison to naïve mice (delay of median time to 1% parasitaemia = 0.38 days, $p = 0.0108$ for RTS,S and 0.48 days, $p = 0.0078$ for R21, log-rank (Mantel-Cox) test) (***Figure 3.5*** **B**). It is therefore apparent that even relatively small drops in antibody

titres have a substantial effect on protective efficacy, highlighting the importance but also the difficulty of maintaining high antibody titres against CSP at all times.

3.2.4 Lower doses of R21 correlate with better protection

In previous experiments a correlation was observed between lower doses of R21 and RTS,S with higher protection from transgenic parasite challenge (Katharine Collins, unpublished data). To elucidate the mechanism of higher protection upon immunisation with a lower vaccine dose avidity of antigen specific antibodies in serum of those mice was determined by NANP avidity ELISA. Furthermore the ratio of IgG2a and IgG1 as markers of a Th1 and Th2 response was determined by NANP isotype ELISA (***Figure 3.6***).

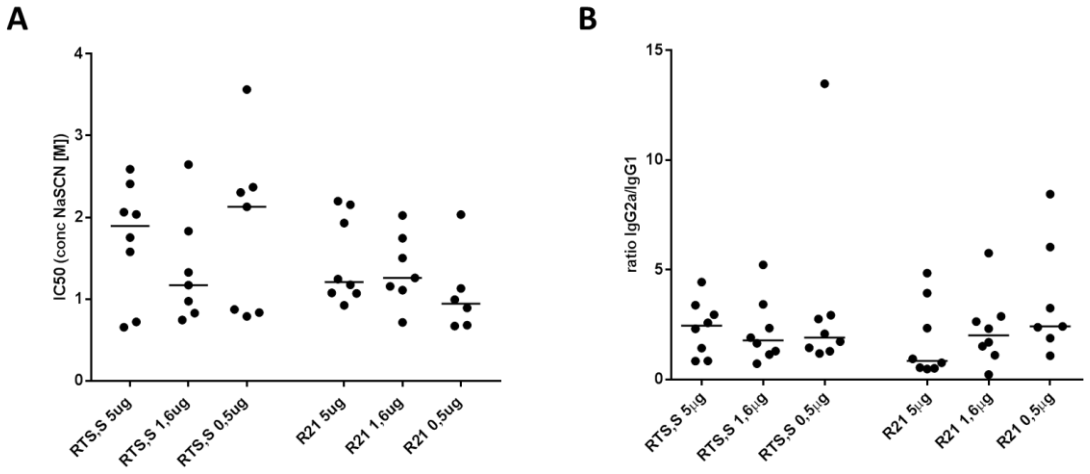

Figure 3.6: Higher efficacy of low doses of R21 and RTS,S is not correlated with antibody isotype or avidity. **A** Avidity of antigen specific IgG in serum of mice immunised with different doses of RTS,S or R21 was determined by chaotropic salt displacement ELISA. **B** Ratio of IgG2a and IgG1 in serum of mice immunised with different doses of RTS,S or R21 as determined by NANP isotype ELISA. Data points show avidity and IgG ratio in serum of individual mice, lines show the median.

Avidity of anti NANP antibodies were similar in all groups (differences in antibody avidity between different doses of the same vaccine were analysed by Dunn's multiple

comparisons test, differences between identical doses of the two different vaccines were analysed by Mann-Whitney test) (***Figure 3.6*** **A**). Similarly, no statistically significant differences could be detected in IgG2a/IgG1 ratios induced in the different groups, indicating that reducing the dose of the immunogen did not skew the CD4+ T-cell response towards a Th1 or Th2 phenotype (differences in IgG2a/IgG1 ratios between different doses of the same vaccine were analysed by Dunn's multiple comparisons test; differences between identical doses of the two different vaccines were analysed by Mann-Whitney test) (***Figure 3.6*** **B**). Neither of these factors therefore seem to be causally involved in the enhanced efficacy observed after low dose vaccine administration.

As survival rates after malaria challenge in these mice were high, it was assessed whether protection would be maintained over a prolonged period of time and so the mice were re-challenged with transgenic *P. berghei* parasites expressing PfCSP under the PbUIS4 promotor by intravenous injection of 1000 sporozoites per mouse six months after being challenged for the first time (***Figure 3.7***).

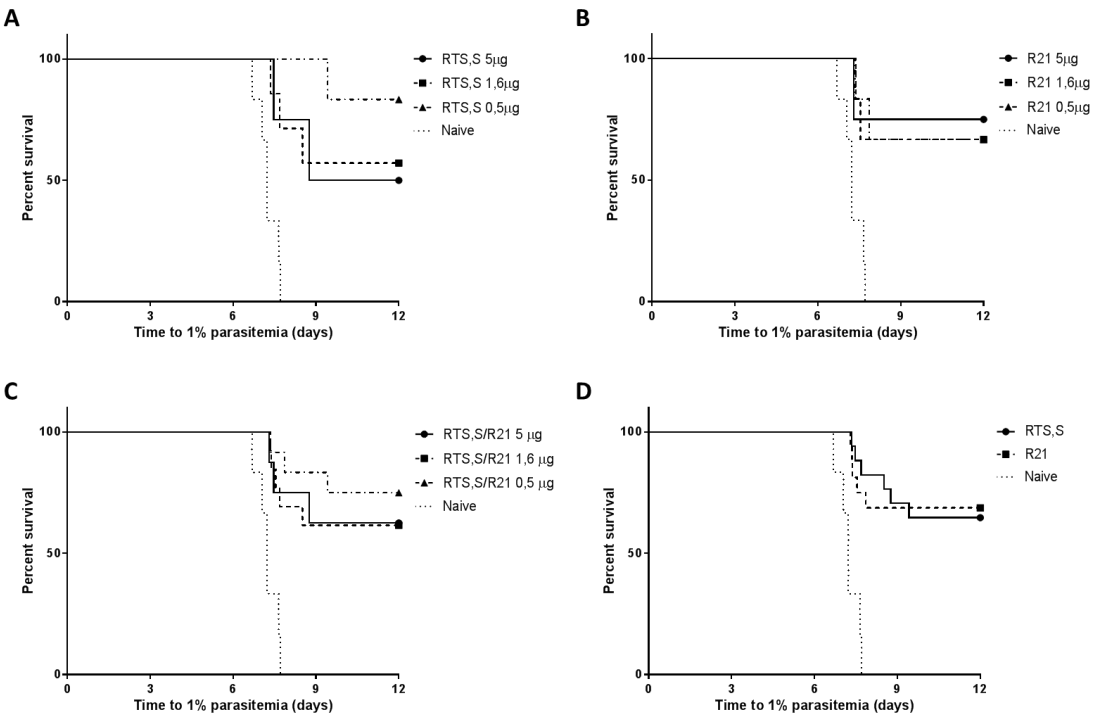

E

	RTS,S	R21
5 µg	2/4	3/4
1.6 µg	4/7	4/6
0.5 µg	5/6	4/6

Figure 3.7: Higher efficacy of lower vaccine doses is not preserved in a subsequent malaria challenge. Balb/c mice that were protected in the first challenge were challenged a second time with *P. berghei* parasites expressing PfCSP under the PbUIS4 promotor. **A** Kaplan-Meier survival curves of naïve mice and mice immunised with different doses of RTS,S. **B** Kaplan-Meier survival curves of naïve mice and mice immunised with different doses of R21. **C** Kaplan-Meier survival curves of naïve mice and mice immunised with different doses of RTS,S or R21, with pooled groups for identical doses of the two different vaccines. **D** Kaplan-Meier survival curves of naïve mice and mice immunised with different doses of RTS,S or R21, with pooled groups for all doses of the two different vaccines. **E** Number of protected out of total mice for each vaccine regimen.

Six months after the original challenge protection conferred by immunisation with both vaccines was still high, although lower than at the original challenge. When data from all different doses was pooled protection was 65% for RTS,S and 69% for R21 (***Figure 3.7*** **D**). Comparison of survival curves by Log-rank (Mantel-Cox) test showed them to not be significantly different (p=0.9521). Similarly there was no longer a significant difference between different vaccine doses (***Figure 3.7*** **A,B**). When data from

the same doses of the two different vaccines is pooled there is a trend for the lowest doses to confer higher protection than the two higher doses (***Figure 3.7*** **C**), but this is not statistically significant.

To follow up on these observations an additional experiment was performed and the amount of immunogen given to each mouse was further reduced by a factor of 10. 10 Balb/C mice per group were immunised by three intra muscular injections of either RTS,S or R21 in AS01 at different doses (0.5 µg 0.16 µg and 0.05 µg) using a two week interval. 13 days after each immunisation a blood sample was collected and antibody responses to CSP assessed by NANP endpoint ELISA. Avidity of antigen specific IgG in serum of mice after the third immunisation was assessed by NANP avidity ELISA (***Figure 3.8***).

Even at 10-fold reduced doses both vaccines induce very high antibody responses after three immunisations (***Figure 3.8*** **C**). There is however a trend for higher doses to induce higher antibody titres than lower doses, but this is only statistically significant for RTS,S where 0.5 µg of vaccine induce higher antibody titres than 0.05 µg. The same can be observed after one and two immunisations (***Figure 3.8*** **A,B**). After the first immunisation, the same effect can also be observed for R21, which induces a significantly stronger antibody response at 0.5 µg than at 0.16 µg and 0.05 µg. Differences between identical doses of the two different vaccines are less pronounced and are completely lost after the third immunisation. As had been observed with the previous dose escalation study, reducing the amount of immunogen in each dose did not have a detectable effect on antibody avidity (***Figure 3.8*** **D**).

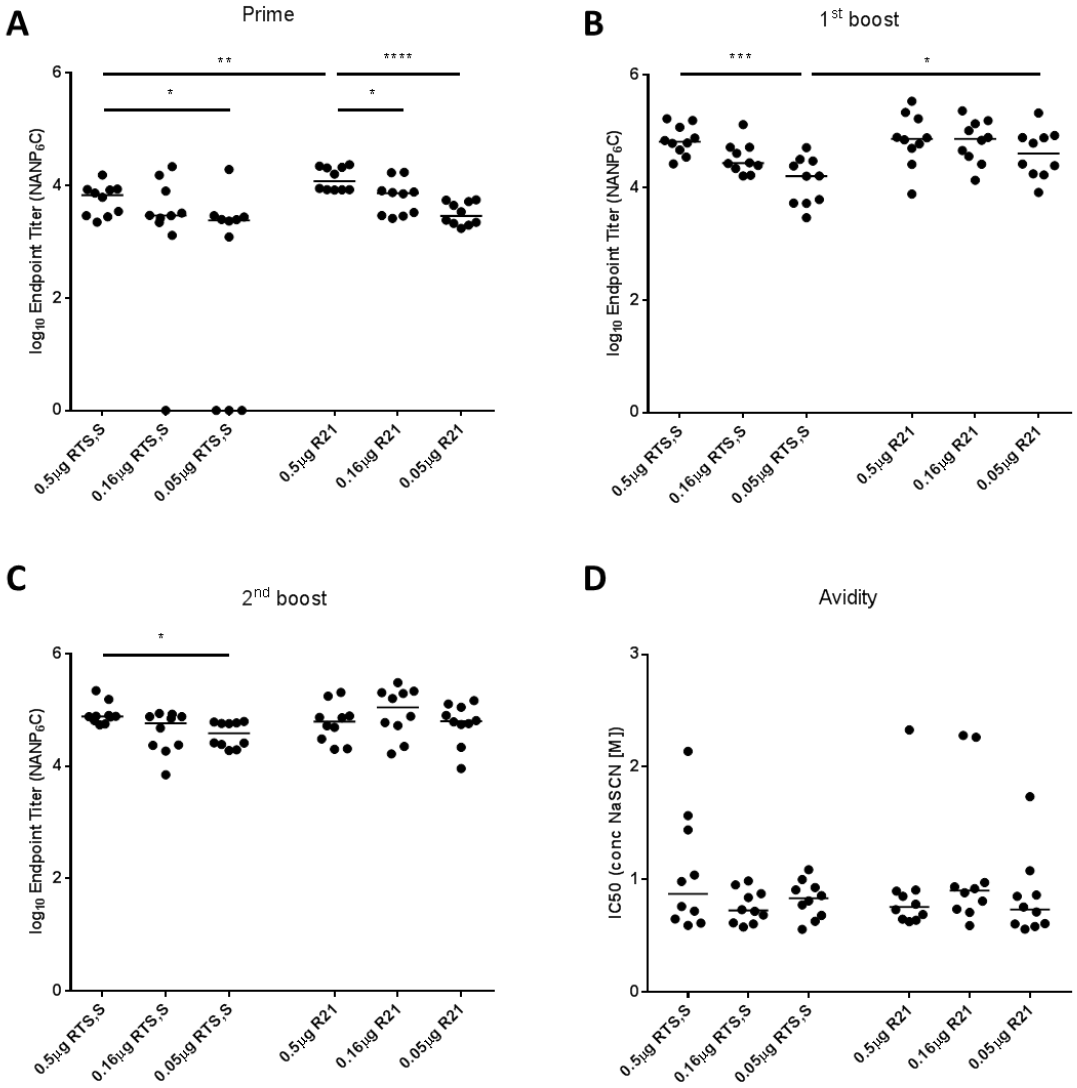

Figure 3.8: R21 and RTS,S are highly immunogenic at low doses. Antibody responses against CSP were assessed in Balb/C mice immunised with different doses of RTS,S or R21. **A,B,C** Antibody responses to CSP after one, two and three immunisations were assessed by NANP endpoint ELISA. **C** Avidity of antigen specific IgG in serum of mice after the third immunisation was determined by NANP avidity ELISA. Antibody responses to similar doses of R21 and RTS,S were compared by Mann-Whitney test. Differences in antibody responses between different doses of the same vaccine were compared by ANOVA followed by Dunn's multiple comparison test. * = $p \leq 0.05$, ** = $p \leq 0.01$, *** = $p \leq 0.0005$, **** = $p \leq 0.0001$.

The ability of reduced vaccine doses to induce a protective antibody response against malaria was assessed by challenge with transgenic *P. berghei* parasites expressing PfCSP under the PbUIS4 promotor two weeks after the final immunisation (***Figure 3.9***).

Protection from malaria challenge conferred by immunisation with low doses of RTS,S and R21 was very high, exceeding the levels observed in the experiment with 10-fold higher doses and showing at least 80% sterile protection in all groups (***Figure 3.9*** **A,B**). There was no statistically significant difference between any of the vaccinated groups, but all vaccinated groups are significantly different from the naïve group ($p < 0.0001$, (Mantel-Cox) Log-rank test). Even the 0.05 µg RTS,S regime which had induced significantly lower antibody titres after three injections than 0.5 µg RTS,S induced a similar level of protection from malaria challenge (90% and 100% respectively). Even when data from the same doses of the two different vaccines was pooled there was no correlation between vaccine dose and protection (***Figure 3.9*** **C**). When data from all different doses was pooled protection was 90% for RTS,S and 97% for R21 (***Figure 3.9*** **D**).

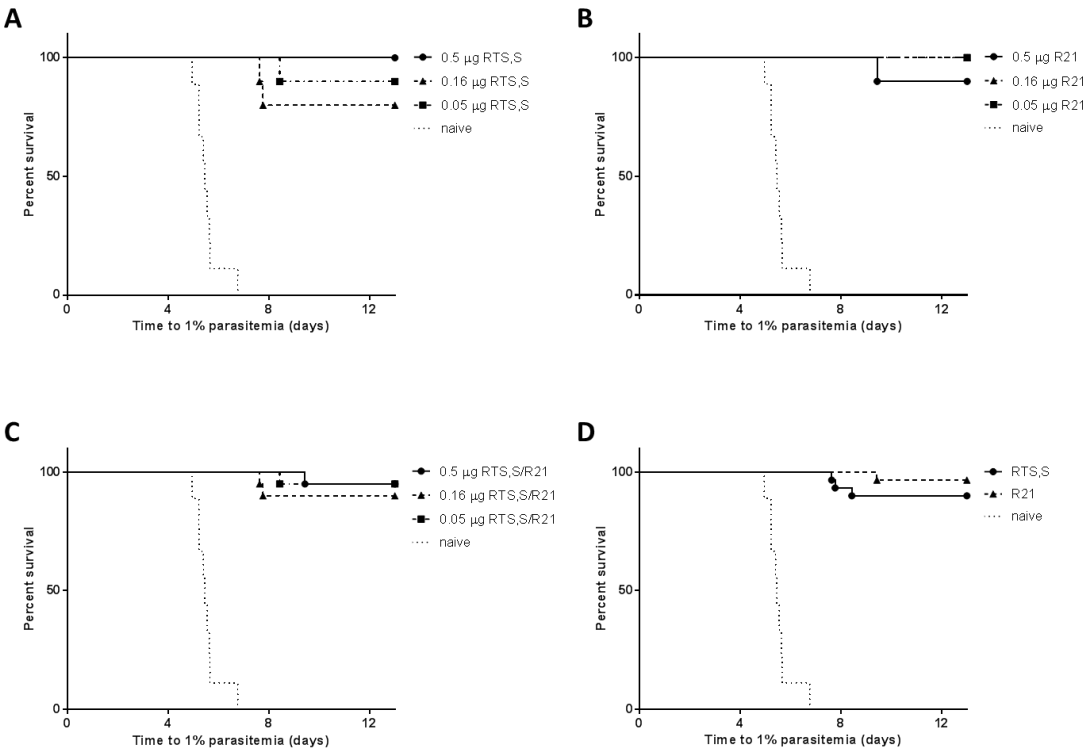

Figure 3.9: High protection of RTS,S and R21 against transgenic malaria challenge is maintained at reduced vaccine doses. Mice immunised with low doses of RTS,S or R21, were challenged with *P. berghei* sporozoites expressing PfCSP under the PbUIS4 promotor. **A** Kaplan-Meier survival curves of naïve mice and mice immunised with different doses of RTS,S. **B** Kaplan-Meier survival curves of naïve mice and mice immunised with different doses of R21. **C** Kaplan-Meier survival curves of naïve mice and mice immunised with different doses of RTS,S or R21, with pooled groups for identical doses of the two different vaccines. **D** Kaplan-Meier survival curves of naïve mice and mice immunised with different doses of RTS,S or R21, with pooled groups for all doses of the two different vaccines.

With protection from malaria challenge not reduced and potentially even improved by reducing vaccine doses, it was assessed whether low doses had an effect on the durability of protection. To that end, mice that were protected during the challenge were challenged again four months after the original challenge and a third time four months after the re-challenge.

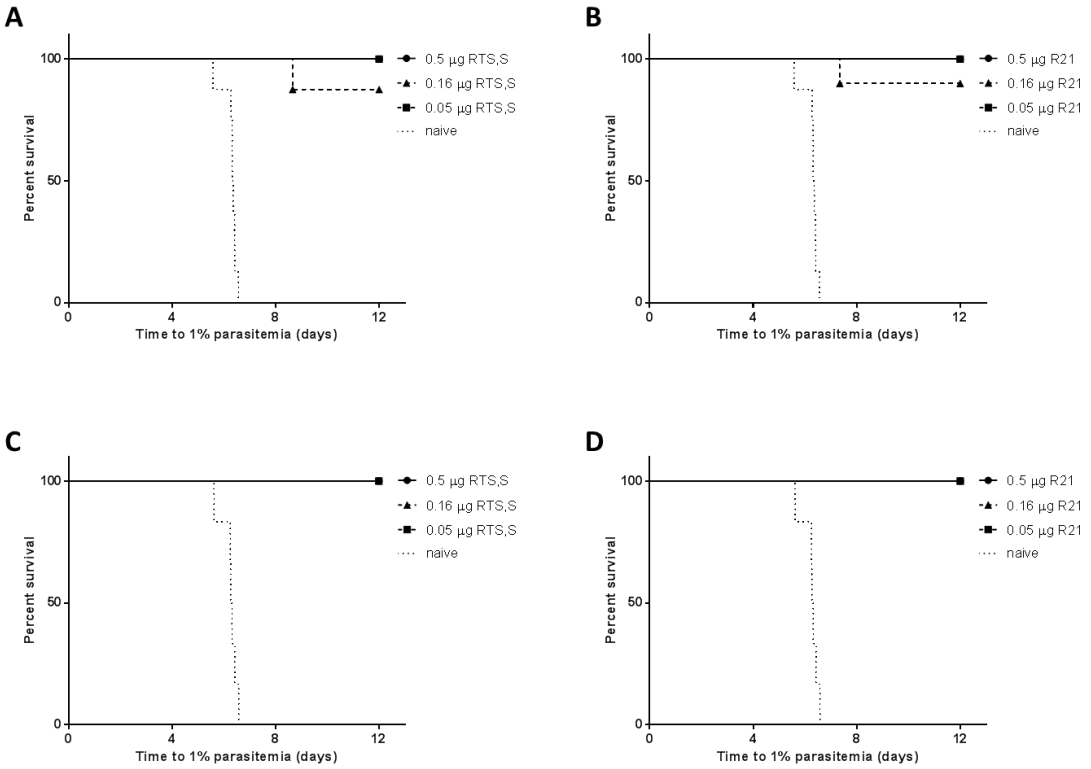

Figure 3.10: High protection conferred by low doses of RTS,S and R21 against transgenic malaria challenge is maintained over two subsequent challenges. Mice protected from malaria in the first challenge were challenged again with *P. berghei* sporozoites expressing PfCSP under the PbUIS4 promotor, four and eight months later. **A** Kaplan-Meier survival curves of naïve mice and mice immunised with different doses of RTS,S in the second challenge. **B** Kaplan-Meier survival curves of naïve mice and mice immunised with different doses of R21 in the second challenge. **C** Kaplan-Meier survival curves of naïve mice and mice immunised with different doses of RTS,S in the third challenge. **D** Kaplan-Meier survival curves of naïve mice and mice immunised with different doses of R21 in the third challenge.

Protection remained at very high levels in both subsequent challenges with sterile protection levels above 88% in all groups in the first, and 100% in all groups in the second re-challenge. Only two out of 53 mice succumbed during the second challenge, one in the 0.16 µg group of RTS,S and R21 each and there is no statistically significant difference between any of the vaccinated groups in this or the final challenge, but all vaccinated groups are significantly different from the naïve groups ($p < 0.0001$, (Mantel-Cox) Log-rank test).

The levels of protection observed in this dose escalation study over three consecutive malaria challenges exceed protection in any other previous experiment, although the collected data does not suggest a conclusive mechanism for the correlation between reduced vaccine doses and increased protection.

3.3 Discussion

RTS,S is the most advanced malaria vaccine candidate to date, and although its completion of phase III clinical trials presents a major milestone on the road to a vaccine capable of eliminating and eventually eradicating this devastating disease, its limitations are still severe. This became all too apparent in the very cautious endorsement of RTS,S by the WHO in its 2016 report [221]. R21 is a rationally improved version of RTS,S and might be able to overcome some of the limitations that prevent GSK's vaccine from being successful in all respects.

The affinity purification process established as part of this PhD thesis (***Figure 3.3***) allowed for the first time the manufacture of R21 under GMP conditions. This has led to R21 being tested in a number of phase I and phase IIa clinical trials with a sterile efficacy rate of up to 82 % (Navin Venkatraman, unpublished data) and further trials are planned for the near future. A head to head comparison with RTS,S in humans has not yet been conducted, but all pre-clinical comparisons in mice suggest that R21 performs at least equivalent to RTS,S, but there is no statistically significant data to confirm observed trends in superiority.

The effect of pre-existing HBsAg titres in vaccinees has only sporadically been taken into account during clinical trials with RTS,S, and when it was considered the conclusions drawn were conflicting [226, 227], but Aide et al. [227] found evidence that somewhat lower CS antibody titres may be induced in Mozambique 1-4 year olds with antibodies to HBsAg at the time of RTS,S/AS02 immunisation. In mouse experiments conducted as part of this thesis, pre-existing HBsAg titres appeared to have a statistically significant inhibitory effect on R21's ability to prime an anti-NANP antibody response, halving the induced antibody titres (***Figure 3.4***). If this effect was observed to a similar extent in human infants, this could have a significant effect on the ability of the vaccine to prevent malaria infection. Nonetheless priming was successful even in the presence of anti HBsAg antibodies in the serum suggesting that the ability of R21 to boost this response would not be reduced. Additionally, the fact that R21 does not prime a HBsAg response on its own [222], suggests that it would be less affected by pre-existing HBsAg titres than RTS,S which induces a strong anti-HBsAg response.

One of the most puzzling, but also one of the most exciting findings of this part of my PhD was the observation that reduced vaccine doses of RTS,S and R21 correlate with better protection from malaria challenge in mice (***Figure 3.9*** and ***Figure 3.10***). The collected data suggests that this effect is not correlated with antibody avidity measured by a chaotropic salt displacement assay or Th1-Th2 phenotype of the CD4+ T-cell response (***Figure 3.6*** and ***Figure 3.8***). This makes the mechanism of the observed correlation somewhat enigmatic. Nonetheless these findings were subsequently also assessed in ongoing clinical trials where apart from 50 µg per dose, which is the dose

used in the phase III RTS,S trial, doses of 10 µg and even 2 µg were tested with promising results (unpublished data). Ongoing work with samples from these clinical trials, gave rise to the hypothesis that lower doses of vaccine modulate the T folicullar helper (TFH) cells response to favour germinal centre formation and resulting in a more balanced and more durable antibody response (Georgina Bowyer, personal communication).

On the whole, results from this chapter of my thesis facilitated the GMP manufacture of R21, as R21c, and hence its assessment in first clinical trials. Particularly results from dose escalation studies in mice further informed the design of these clinical trials with positive dose sparing and efficacy outcomes. All this contributed substantially to the translation of R21 from the lab into the clinic and to making it the promising vaccine candidate that it is today.

Chapter 4 - Generation and characterisation of dual antigen malaria vaccines

Authorship statement

Transmission electron micrographs of dual antigen VLPs (***Figure 4.2*** **B,C**; ***Figure 4.5*** **A**; ***Figure 4.10*** **B**) were acquired by Errin Johnson (Sir William Dunn School of Pathology, EM core facility). All malaria challenges were conducted with assistance from Dr. Ahmed Salman. SMFA was performed at the Malaria Vaccine Initiative (MVI) SMFA reference laboratory at the National Institute of Health, USA by Dr. Kazutoyo Miura and co-workers. Rh5-ELISAs for the triple vaccine combination experiment (***Figure 4.15*** **C**) were performed by Sarah Silk.

4.1 Introduction

The shortcomings of RTS,S in the recently concluded phase III clinical trial made it clear that a highly efficacious malaria vaccine will not be available in the near future. Second generation vaccines currently in development are designed to overcome some of the problems that prevented RTS,S from being more successful, but none seems to be the proverbial silver bullet against malaria. One reason for this could be that most vaccines currently focus on only one antigen of one lifecycle stage, and for a highly complex parasite like *Plasmodium*, this might just not be enough. Recent clinical trials conducted using more complex immunogens, such as irradiated sporozoites, or completely viable parasites administered under drug coverage, showed higher efficacy

than single antigen vaccines, but face other potentially prohibitive limitations, such as high production costs and demanding storage conditions [164-166]. The most viable option might therefore lie in between the two approaches, in the combination of a few antigens from one or more lifecycle stages, which could work additively or even synergistically, and therefore have high efficacy with limited cost and more achievable logistics [228, 229]. Particularly for a vaccine against *P. falciparum*, which would mainly be deployed in regions with very limited financial and infrastructural resources, these factors are of the highest importance. In a recent study from the Jenner Institute a favourable effect of combining viral vectors with an antibody inducing VLP like RTS,S or R21 was demonstrated [185, 222] and others showed that even antigens from all three lifecycle stages can be combined in single vaccine [230]. Combining multiple antigens in a single vaccine could be achieved either by mixing two or more single antigen vaccines and administering them as one injection, or by combining multiple antigens within a single immunogen. As part of my DPhil thesis I assessed the feasibility of combining two or three leading malaria vaccine candidates within a single, multi-component injection. Furthermore, I tested to what extent R21 could be used as a platform for a single-immunogen, dual-antigen VLP vaccine. VLPs induce strong antibody responses and therefore offer themselves as a platform for an antibody inducing multi-antigen vaccine. As the parasite resides most of the time within host cells, shielded from the host's humoral immunity, antigens of the motile lifecycle stages of the malarial parasite, during which the parasite briefly occupies an extracellular space before invading a new cell, are the most promising antigens for such a vaccine. I therefore chose antigens implicated with a role in membrane

traversal of motile sporozoites or ookinetes, hence susceptible to antibody mediated neutralisation, and expressed them as additional antigens on R21.

SPECT1 (sporozoite microneme protein essential for cell traversal), is a sporozoite antigen that was first discovered in *P. berghei* in 2004 [33]. Its precise mode of action is not well characterised and it appears to be not involved in hepatocyte infection, but together with PLP1 (also called SPECT2) it has been demonstrated to be essential for crossing the liver sinusoid [33, 34, 231]. Cell traversal describes the process of entering and leaving cells that precedes infection of a hepatocyte, and has been shown to be of importance for efficient malaria infection in a number of studies [27, 35]. A recent study using *P. falciparum* in a humanised mouse models suggests that the role of PLP1 and SPECT1 is in exiting rather than entering cells. The same study showed SPECT1 to be localised on the *P. falciparum* sporozoite surface as well as inside micronemes [35]. Its presence on the parasite surface and its implication in an important process during liver infection make SPECT1 a promising target for an antibody inducing vaccine. In first immunisation studies, mice were immunised with a heterologous prime boost regimen using chimpanzee adenoviral vectors (ChAd63) and modified vaccinia Ankara (MVA) expressing SPECT1. In 40% of the mice this provided sterile protection from challenge with transgenic rodent parasites expressing *P. falciparum* SPECT1 (PfSPECT1) under the *P. berghei* UIS4 (PbUIS4) promotor and antibodies were implicated in the observed protection by depletion studies (Ahmed Salman, unpublished data). Expressing SPECT1 as part of a strongly antibody inducing VLP, rather than in a mainly T-cell inducing viral vector was therefore expected to result in similar or even better protection. If this protection was to be additive or even synergistic with the protection

induced by the CS-antigen in R21 this could be a significant improvement to one of today's most promising malaria vaccine candidates.

Pfs25 is to date the most advanced candidate antigen for a transmission blocking malaria vaccine (TBV). It was identified more than 30 years ago by a monoclonal antibody that reduced infectivity when it was fed to mosquitoes alongside a parasitized blood meal [90], and first assessed as a TBV in 1994 [232]. Pfs25 has since been characterised extensively and tested in clinical trials, which showed that antibodies against Pfs25 reduce malaria transmission in standard membrane feeding assays (SMFA) [200]. As had been observed earlier with vaccines targeting CSP, vaccine efficacy correlated with the magnitude of the induced antibody response. Because of this, a number of strategies have been applied to increase the antibody response against Pfs25 containing vaccines [233], including multimerisation of the antigen by fusion to IMX313, or conjugation to a detoxified form of Pseudomonas aeruginosa exoprotein A (EPA). Both strategies resulted in increased immunogenicity and efficacy in mice [201, 204] and for conjugation to EPA these findings could be replicated in humans [202]. Expressing Pfs25 on the surface of an HBsAg-VLP, which had helped overcome the problem of insufficient immunogenicity for CSP vaccines [169], was expected to have a similar effect. In addition to that, combining the CS-antigen and Pfs25 in a single vaccine could overcome one of the biggest drawbacks of transmission blocking vaccine, which is the absence of a direct protective effect on the vaccinee.

As part of this thesis, I generated dual-antigen VLPs that expressed SPECT1 or Pfs25 in addition to the CS antigen of R21 and used them to assess the feasibility of multi-antigen VLPs as malaria vaccines in mouse models.

4.2 Results

4.2.1 Dual antigen VLP design

R21 is one of the Jenner Institute's leading malaria vaccine candidates and was therefore used as a platform for the first generation of dual antigen VLPs generated as part of this thesis. To achieve expression of a second antigen on the surface of R21, the additional antigen was fused to the C-terminus of the monomeric subunit of R21, which I had shown to be susceptible to modification by expression of the C-tag there. To generate suitable single antigen control VLPs the same antigens were also fused to the C-terminus of HBsAg without an N-terminal CS antigen (S). This would allow assessing whether expression of two antigens on a single VLP had an effect on the immune response to each individual antigen by comparing responses induced by the dual and the single antigen VLP. R21 was used as a single antigen control for the CS antigen of the dual VLPs. The VLP design is depicted in ***Figure 4.1***.

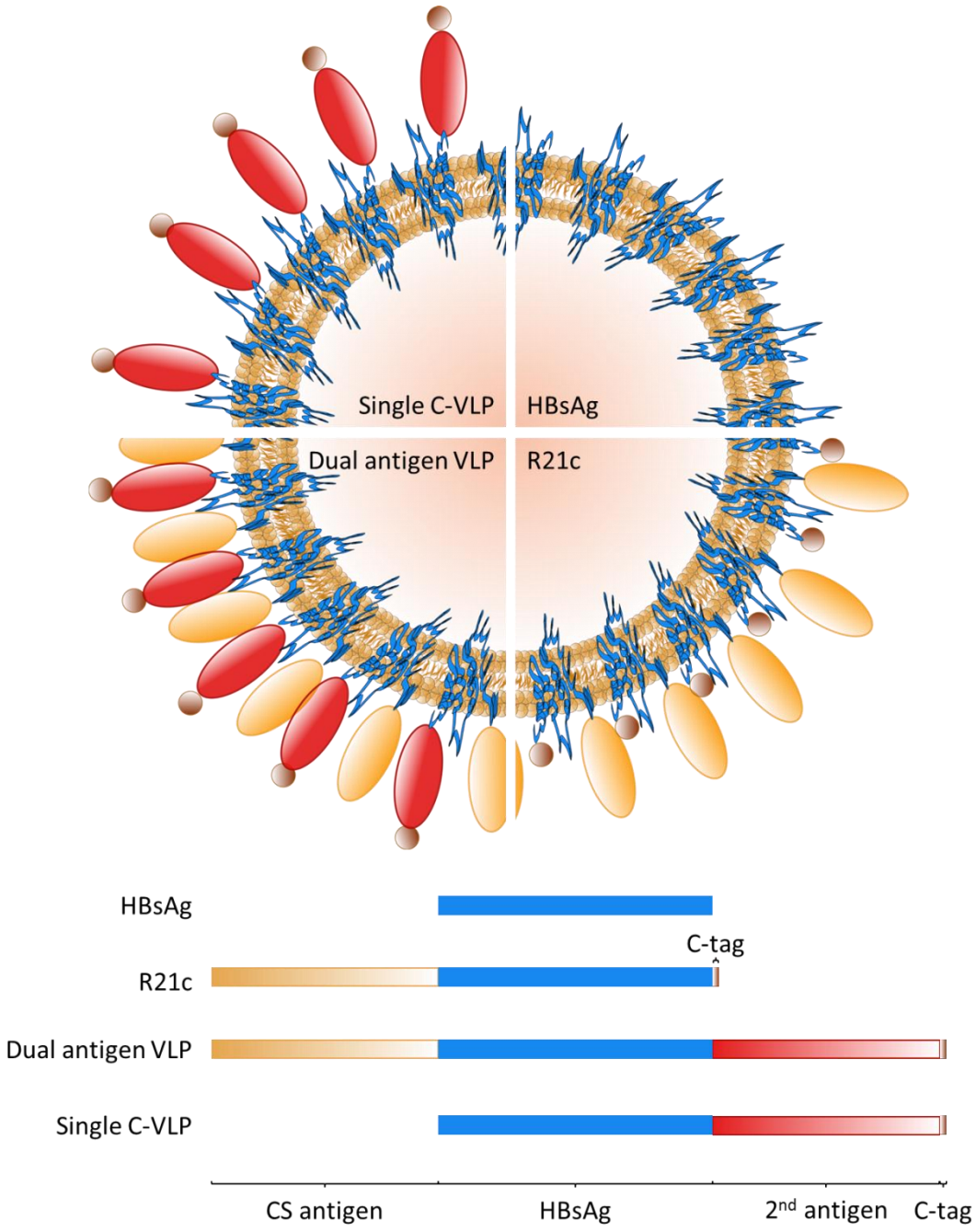

Figure 4.1: Displaying antigens at the C–terminus of HBsAg- VLPs. R21c was used as a platform for the generation of dual antigen VLPs. Its monomeric subunit consists of the Hepatitis B surface antigen (HBsAg) with an N-terminally fused CS antigen and a C-terminally fused C-tag. Dual antigen VLPs are made up from a similar monomeric subunit, with an additional antigen being fused between HBsAg and the C-tag. By fusing the same antigens in a similar fashion to HBsAg (S) instead of R21c, single antigen VLPs are generated displaying an antigen C-terminally (Single C-VLPs).

4.2.2 R21-SPECT1, an improved sporozoite vaccine

4.2.2.1 SPECT1 can be expressed on the surface of HBsAg-VLPs

Plasmids for the expression of HBsAg-VLPs displaying SPECT1 were generated by fusing SPECT1 to the C-terminus of HBsAg as described in 2.2.3.2. One of the generated plasmids, pPink-HC-R21-SPECT1 was used to clone a plasmid for expression of monomeric, His-tagged SPECT1 to be used as ELISA antigen as described in 2.2.3.3. The generated plasmids were used to transform PichiaPink strain 1 cells, and a protein expressing clone was selected and used to express the VLPs as well as the monomeric protein at large scale as described in 2.2.7, 2.3.1.1 and 2.3.1.2. Monomeric protein was purified from culture supernatant by immobilised metal ion chromatography (IMAC) followed by size exclusion chromatography (SEC). C-tag binding proteins were purified from glass bead lysates of cultures using a C-tag affinity column. The purified proteins were confirmed to be the monomeric R21-SPECT1 and S-SPECT1 subunits by Western blot and Coomassie staining (***Figure 4.2*** **A**). In both Coomassie and Western blot of R21-SPECT1, a band was detected at 80 kDa, which correlates with the molecular weight of the R21-SPECT1 monomer. In the Western blot a second band is detected at 50 kDa which could arise from a degradation product of the monomer. S-SPECT1 could not be detected by Coomassie staining, but in the Western blot a band can be detected at 50 kDa, correlating with the S-SPECT1 monomer. Additional bands can be detected at higher and lower molecular weights which could be formed from degradation and aggregation products or multimers of the S-SPECT1 monomer. Before being electrophoresed, C-Tag eluates were buffer exchanged and concentrated using 100K MWCO spin concentrators, which should remove protein not assembled into particles.

The concentration process could also have caused the aggregation/degradation detected in the Western blot. Nonetheless, the dominant band detected in Western blot of both particles was of the expected size, as was the only band detected by Coomassie staining of R21-SPECT1, indicating expression of the correct proteins. Yields were determined by BCA, and found to be significantly lower than for R21c, particularly for S-SPECT1, which could explain why S-SPECT1 could not be detected by Coomassie staining. Despite concentration, yields were too low at this stage to allow further purification and analysis by SEC, therefore assembly of the proteins into VLPs was confirmed by transmission electron microscopy (TEM) (***Figure 4.2*** **B,C**).

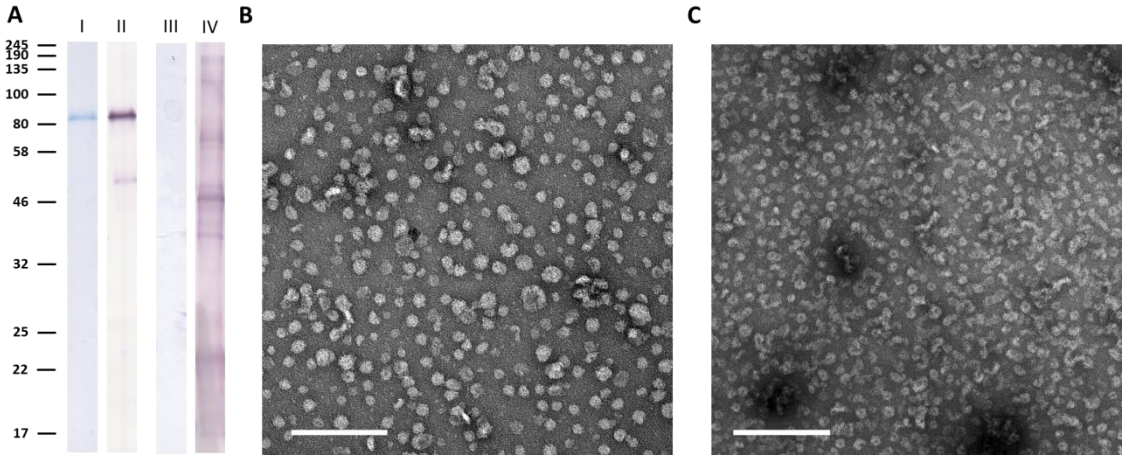

Figure 4.2: SPECT1 can be fused to HBsAg to be displayed on VLPs. **A** Coomassie stained gel and Western blot of R21-SPECT1 and S-SPECT1. R21-SPECT1 (lanes I and II) and S-SPECT1 (lands III and IV) were purified by C-Tag affinity chromatography and visualised by Coomassie staining (lane I and III) and anti-HBsAg Western blot (lane II and IV) after being electrophoresed over a 4-12% polyacrylamide gel. **B,C** Transmission electron micrographs of R21-SPECT1 (B) and S-SPECT1 (C). Scale bar = 200 nm.

Electron micrographs of both VLPs showed assembly into particles although the size and shape of the particles were heterogeneous within both samples. The average particle diameter of R21-Spect was of 25 nm (average diameter of 30 randomly selected particles = 24.8 nm ± 9.5 nm), which is slightly larger than the 20 nm expected for HBsAg VLPs. The average S-SPECT1 diameter was lower, but closer to the expected

20 nm (average diameter of 30 randomly selected particles = 17.8 nm ± 3.6 nm). The data from gel electrophoresis and TEM suggest that VLPs displaying SPECT1 could be generated, but the presence of SPECT1 at the C-terminus of HBsAg lowered expression yields as well as the ability to assemble into particles.

To further analyse the newly generated VLPs, they were tested for their immunogenicity in mice. 5 Balb/c mice per group were immunised with 2.5 µg of S-SPECT1, R21-SPECT1 or R21 adjuvanted with 8.5 µg Alhydrogel. Three doses of each vaccine were administered using a three week interval. 20 days after each immunisation a blood sample was collected and CSP and SPECT1 antibody titres in the serum quantified by NANP and SPECT1 standard ELISA (***Figure 4.3***). Due to the limited quantity of some serum samples the antibody response to SPECT1 could not be determined for all five serum samples of each group.

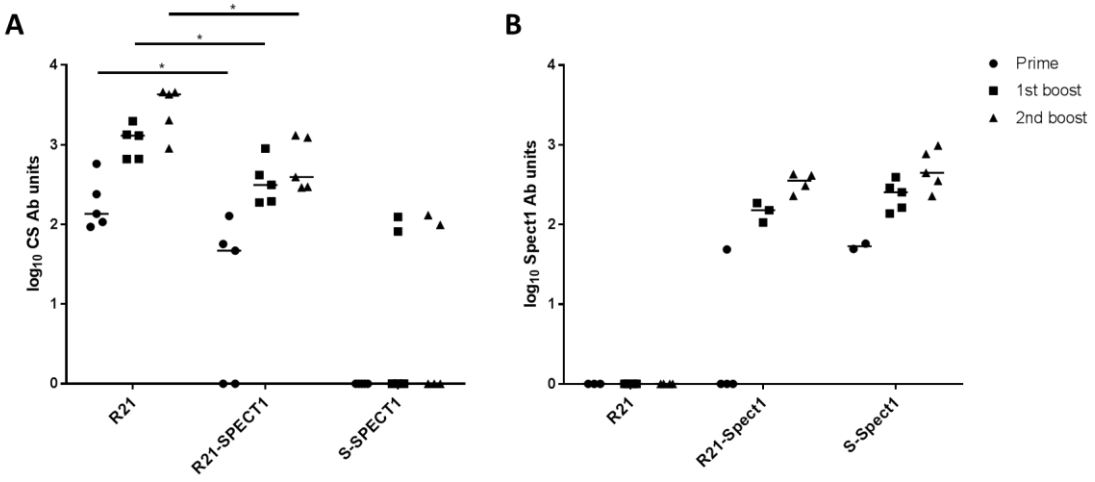

Figure 4.3: R21-SPECT1 induces antibody responses against both antigens in mice. Balb/c mice (n = 5 per group) were immunised with three doses of S-SPECT1, R21-SPECT1 or R21 in Alhydrogel and antibody titre determined by ELISA. **A** Antibody responses to CSP were assessed by NANP standard ELISA. **B** Anti-SPECT1-antibody responses were assessed by SPECT1 standard ELISA. Antibody titres induced by the dual antigen VLP at each time point were compared to titres induced by the appropriate single VLP control at the same time point by Mann-Whitney test. * = $p < 0.05$. Bars indicate median.

The first analysis of R21-SPECT1 *in vivo* showed that dual antigen VLPs are capable of inducing an immune response against both of the displayed antigens. However, anti-NANP antibody titres induced by immunisation with R21-SPECT1 were significantly lower than antibody titres induced by immunisation with R21 at all time points tested (difference between median after prime, 1st boost and 2nd boost, respectively = 0.4641, p = 0.0317, 0.6181, p = 0.0317 and 1.037, p = 0.0317) (***Figure 4.3*** **A**). Anti-SPECT1 antibody titres were of similar levels following immunisation with R21-SPECT1 and S-SPECT1 (***Figure 4.3*** **B**). The detection of an anti NANP antibody response in two of the mice immunised with S-SPECT1 following the second immunisation is very surprising, as no NANP repeats are present in this VLP. The response is only at low level above background, and not boosted by the third immunisation, but was confirmed when the ELISA was repeated and therefore appears to be genuine.

Two different hypotheses are conceivable to explain the reduced anti-NANP antibody titres induced by R21-SPECT1 when compared to R21. Either, the presence of a second antigen on the VLP causes antigenic competition, resulting in lower antibody titres against the individual antigens, or the apparent lower quality of the SPECT1 VLPs makes them less immunogenic. The second hypothesis is supported by the fact anti-SPECT1 antibody titres induced by the dual antigen VLP are similar to the ones induced by the single antigen S-SPECT1 VLPs. It seemed likely that in order to generate a highly immunogenic dual antigen VLP, it would first be necessary to improve the quality of the produced VLPs.

4.2.2.2 Optimisation of R21-SPECT1 particle production

To address the low yields of HBsAg VLPs expressing SPECT1 at the C-terminus the VLP purification process was modified. First, the process of lysing the yeast cells was changed from using glass beads to a high pressure homogeniser. In addition to lysing cells more efficiently and reproducibly than using glass beads, this allowed to lyse up to 200 g of pelleted yeast culture, equivalent to approximately 4 l of shake flask culture as compared to a maximum of 300 ml of shake flask culture using glass beads.

Furthermore, the process of cell lysis and VLP liberation were separated into two individual steps. HBsAg VLPs are not secreted when expressed in yeast cells, instead the protein assembles into multi-layered, lamellar structures and accumulate in the Golgi apparatus. By performing the cell lysis in the absence of detergent and collecting the membrane fraction of the lysed cells by centrifugation at 12,000 x g, soluble cytosolic proteins can be separated from the VLP preparation. VLPs are then released from the membrane fractions by performing another high pressure homogenisation, this time in the presence of detergent. This is relevant as experiments to scale up the expression of R21c conducted at the Clinical BioManufacturing Facility (CBF) had shown contamination of particle preparations with alcohol oxidase 1 (AOX1) to be a reoccurring problem even after C-Tag purification (CBF, personal communication). AOX1 is the natural gene of the AOX1 promoter, the promoter used for VLP expression in PichiaPink, and therefore induced by methanol. As AOX1 is a soluble protein, it can be removed by washing the pelleted membrane fractions multiple times before particle liberation, therefore allowing the use of higher percentages of methanol

during the induction phase, resulting in higher VLP yields. A comparison of the original and the modified VLP purification process is given in the flow chart in ***Figure 4.4***.

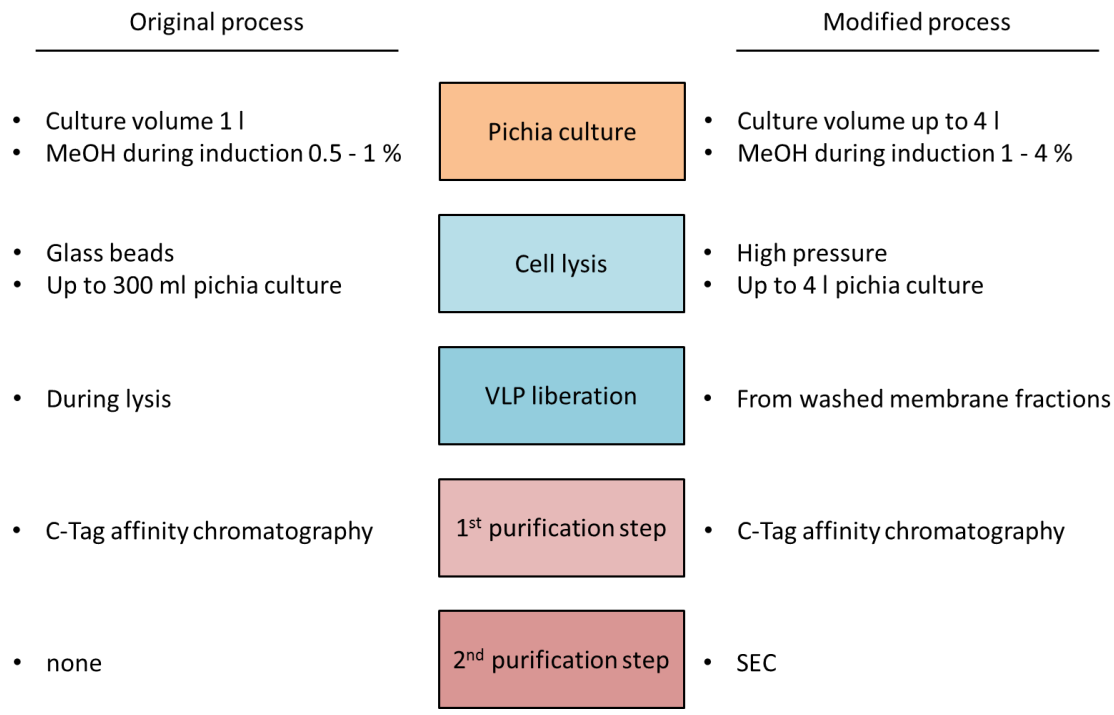

Figure 4.4: Comparison of original and modified VLP purification process. Use of a high pressure homogeniser allowed processing of larger culture volumes at a time. Separation of cell lysis and VLP liberation allowed washing of membrane fractions from yeast cell lysate, and therefore the use of higher percentages of methanol during induction. Taken together these changes increased the particle yield after C-tag affinity chromatography, therefore allowing further purification by SEC.

Finally, a particle maturation step was introduced following the purification of particles by C-tag affinity chromatography and SEC. It had previously been shown that maturation of HBsAg VLPs with KSCN followed by heat treatment induced oxidative refolding resulting in formation of additional intra- and inter-molecular disulphide bonds and improvement of particle uniformity and regularity [234]. To assess whether a similar improvement on particle uniformity could be observed for R21-SPECT1, and to further assess whether such morphological changes would have an effect on immunogenicity of the particles, purified R21-SPECT1 was mixed with KSCN to a final concentration of 3 M. After 24 hours at 4°C, KSCN was removed by dialysis and the VLP

incubated at 37°C for 10 days. Samples were taken before and after KSCN treatment as well as 1, 5 and 10 days after incubation. All samples were analysed by TEM to assess morphological changes, as well as injected into Balb/c mice (n = 5 per group), at a concentration of 0.4 μg per dose and adjuvanted with 5 μg Matrix M, to assess the effect on immunogenicity. 21 days after the immunisations a blood sample was collected and CSP and SPECT1 antibody titres in the serum quantified by NANP and SPECT1 standard ELISA.

Both, particle morphology and immunogenicity were improved by the maturation process. Particle uniformity improved greatly after KSCN treatment and further after heat treatment over 5 days. Changes between 5 and 10 days of heat treatment were less pronounced (***Figure 4.5*** **A)**. Similarly anti-NANP antibody responses appeared to be improved after KSCN treatment and were significantly higher than the ones induced by unmatured particles after 5 and 10 days of heat treatment (***Figure 4.5*** **B**). Antibody titres against SPECT1 appeared to be less affected by KSCN treatment alone, but became significantly improved after 1 day of heat treatment (***Figure 4.5*** **C**). Surprisingly, antibody titres appeared to drop after 5 days but were detected at a similar level after 10 days. As there is no conceivable mechanism to explain a decline in immunogenicity followed by recovery of full immunogenicity over a continuous course of heat treatment, the observed reduced immunogenicity after five days of maturation is likely due to limitations of the experimental setup, rather than a true effect of the heat treatment. A certain degree of variability of immune responses in mice after a single immunisation with a low dose of antigen can perhaps be expected. Furthermore, all antibody titres in this experiment were at the lower end of the detection range,

therefore even a fractionally weaker immune response in some mice might be detected as negative, resulting in an over exaggeration of differences between groups. Based on these observations all further VLP preparations were matured by KSCN treatment followed by heat maturation for 3 days.

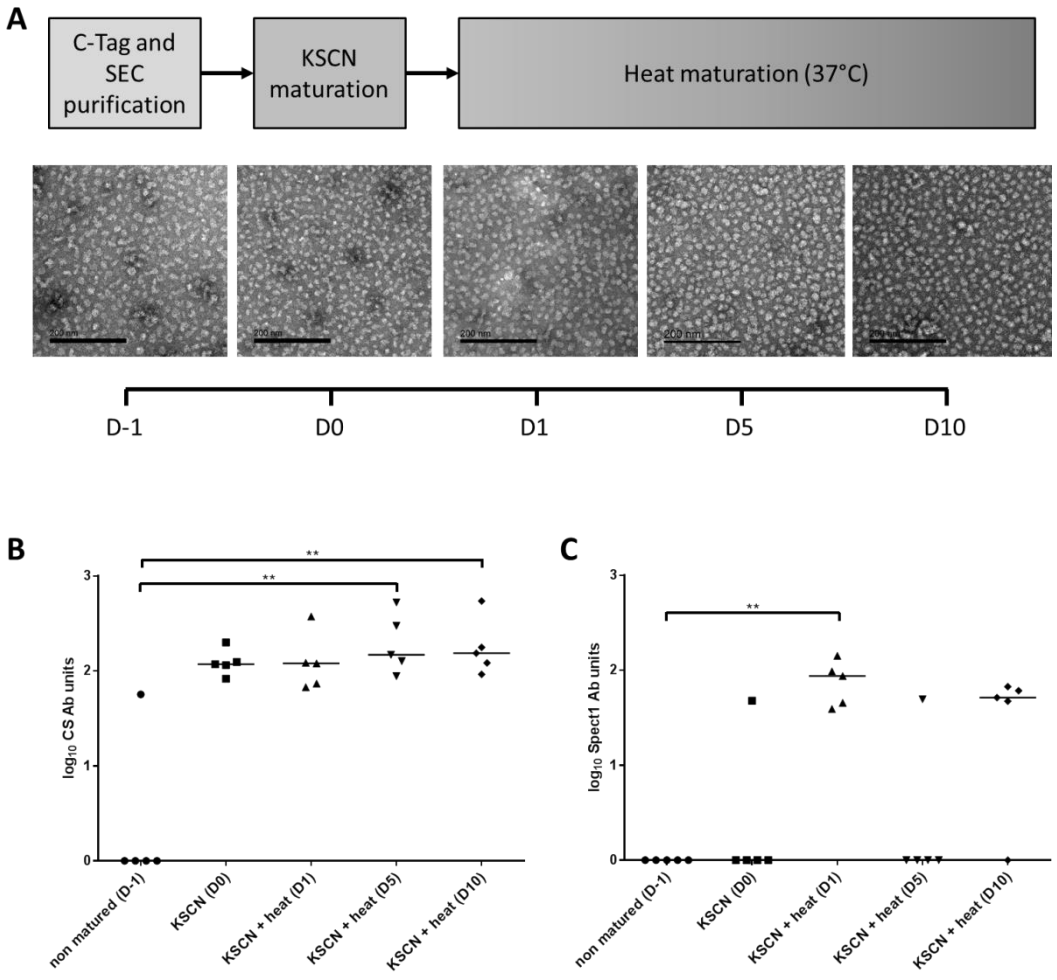

Figure 4.5: Maturation of R21-SPECT1 improves particle uniformity and immunogenicity. **A** Effect of KSCN and heat maturation on particle morphology. R21-SPECT1 was purified using the modified purification process (D-1) and incubated with KSCN 24 hours (D0). The VLP was then incubated at 37°C for 10 days, with samples taken after 1 (D1), 5 (D5) and 10 days (D10). Samples from all time points were imaged by TEM. Scale bar = 200 nm. Larger versions of the micrographs can be found in the appendix. **B,C** Effect of KSCN and heat treatment on R21-SPECT1 immunogenicity. Balb/c mice (n=5 per group) were immunised with samples collected at the different time points in the maturation process. Anti-NANP-antibody responses were assessed by NANP standard ELISA.(B). Anti-SPECT1-antibody responses were assessed by SPECT1 standard ELISA (C). Antibody titres induced by samples of each time point in the maturation process were compared by ANOVA followed by Dunn's multiple comparison test. ** = $p < 0.01$. Bars indicate median.

4.2.2.3 Anti-SPECT1 antibodies induced by R21-SPECT1 have protective efficacy against malaria in mice

To assess the ability of anti-SPECT1 antibodies induced by R21-SPECT1 to protect from malaria, Balb/c mice were immunised twice with 0.5 µg R21-SPECT1, adjuvanted with 5 µg Matrix M, in a three week interval and serum samples were collected 20 days after each immunisation. Antibody titres against NANP repeats and SPECT1 were determined by ELISA. Functional activity of antibodies induced against either of the antigens or both antigens in combination was assessed by inhibition of sporozoite invasion (ISI) assay using *P.berghei* sporozoites expressing PfCSP under the PbCSP promoter, PfSPECT1 under the PbSPECT1 promoter or both. Four weeks after the second immunisation mice were challenged with *P.berghei* expressing PfSPECT1 under the PbSPECT1 promoter, by intravenous injection of 1000 sporozoites per mouse. Parasitaemia in mice was followed by microscopy of thin blood films (***Figure 4.6***).

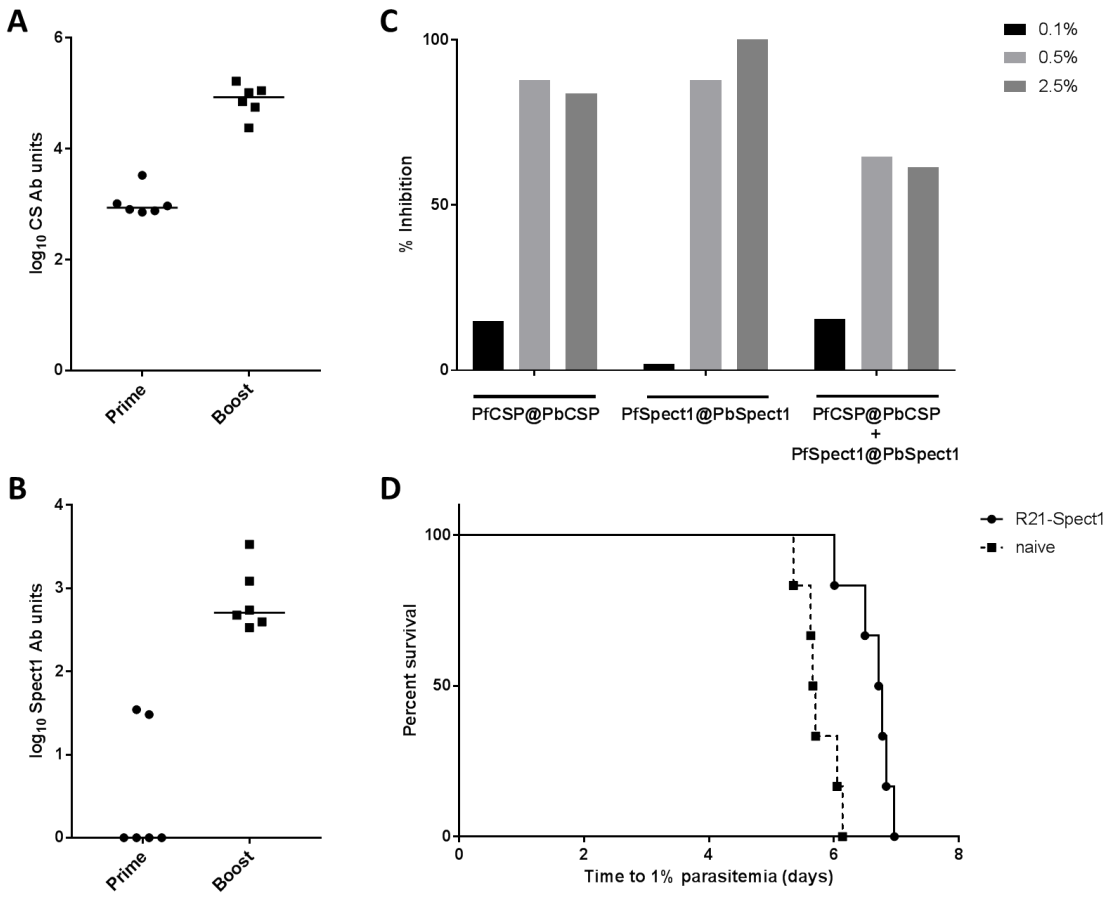

Figure 4.6: R21-SPECT1 induces functionally active antibodies against CSP and SPECT1 in Balb/c mice. Balb/c mice (n = 6 per group) were immunised twice with R21-SPECT1. **A** Antibody responses to CSP were assessed by NANP standard ELISA. **B** Antibody responses to SPECT1 were assessed by SPECT1 standard ELISA. **C** The ability of the induced antibodies to reduce hepatocyte invasion by sporozoites was assessed by ISI using *P.berghei* sporozoites expressing PfCSP under the PbCSP promoter, PfSPECT1 under the PbSPECT1 promoter or both. Post-boost serum pools were tested 2.5%, 0.5% and 0.1% of the total culture medium. Inhibition was calculated as reduction in infected hepatoma cells in comparison to cells infected with sporozoites in the absence of serum. Bars are representative of the mean of two experimental replicates. **D** Four weeks after the second immunisation the mice were challenged with *P. berghei* parasites expressing PfSPECT1 under the PbSPECT1.

The first dose of R21-SPECT1 induced a detectable antibody response against CSP NANP repeats in all mice and against SPECT1 in two out of six mice. The immune response was boosted after the second immunisation and responses were detected against both antigens in all mice (***Figure 4.6*** **A,B**). Serum dilutions of down to 0.5% showed high inhibition of sporozoite invasion in ISI assays and blocking is of similar levels against the two different single gene replacement parasites, but reduced against

the double gene replacement parasites (***Figure 4.6*** **C**). It should be noted that at serum concentrations of 2.5% the viability of the hepatocytes was very low and calculated inhibition is based on less than 500 events in flow cytometry. Results at this concentration are therefore prone to errors, which could be the reason for the lower inhibition observed against the double transgenic parasite at this serum dilution. Disappointingly, no mice were sterilely protected from challenge with PfSPECT1 gene replacement *P. berghei* transgenic parasites. There is however a significant delay in time to 1% parasitaemia of 1.1 days in the vaccinated group when compared to naïve mice ($p = 0.0031$, log-rank (Mantel-Cox) test).

This was the first time a challenge experiment had been conducted using a PfSPECT1 gene replacement transgenic parasite. Previous experiments using *P. berghei* expressing PfSPECT1 under the PbUIS4 promoter, had shown 40% sterile protection in CD1 mice immunised with viral vectors expressing PfSPECT1. To assess whether the absence of any sterile protection after immunisation with R21-SPECT1 was due to inferiority of the VLP when compared to viral vectors, the different mouse strain, or a more stringent challenge using the gene replacement parasite, CD1 mice (n =10 per group) were immunised with 3 µg R21-SPECT1 adjuvanted with 5 µg Matrix-M twice in an eight week interval. A second group was primed with 10^8 infectious units (ifu) ChAd63 and boosted with 10^7 plaque forming units (pfu) MVA, both encoding SPECT1. 14 days after the second immunisation a blood sample was collected and the immune response, inhibition of sporozoite invasion and protection from challenge were compared (***Figure 4.7***).

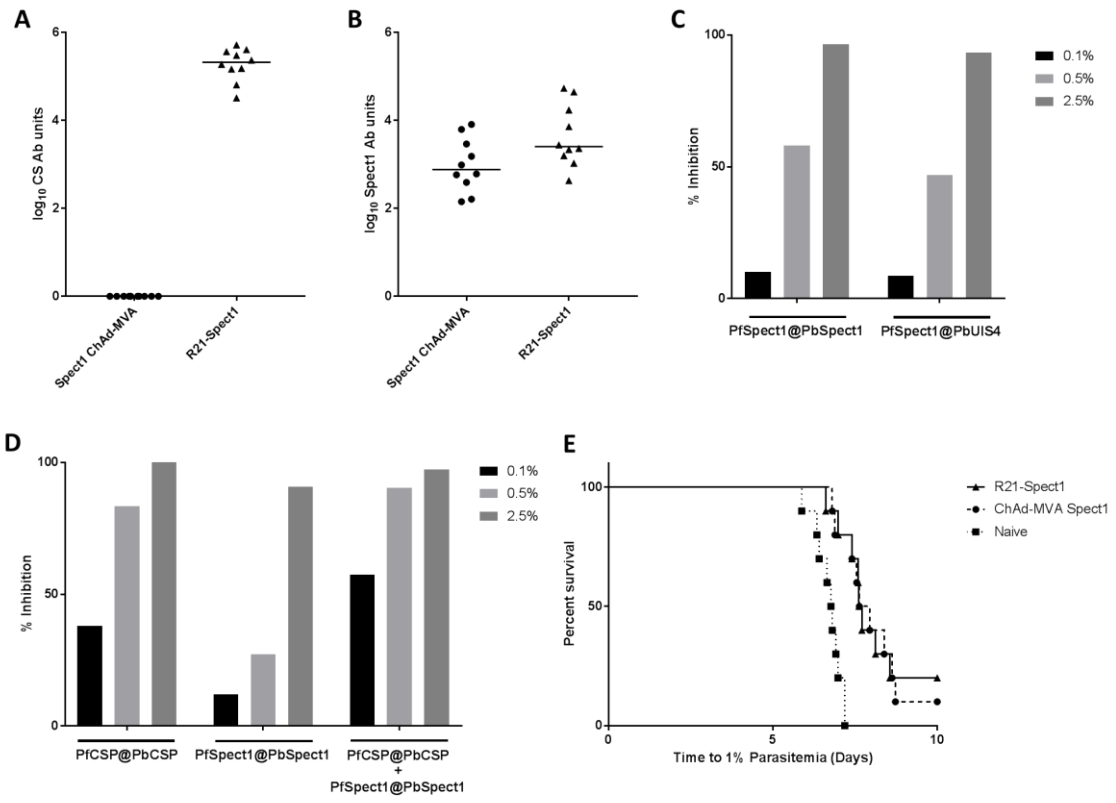

Figure 4.7: R21-SPECT1 induces functionally active antibodies against CSP and SPECT1 in CD1 mice. CD1 mice were immunised with two doses of R21-SPECT1 or with ChAd63 and MVA, both encoding SPECT1. **A** Anti-NANP-antibody responses in post boost serum. **B** Anti-SPECT1-antibody responses in post boost serum. Data points show responses in individual mice, lines show the median. **C** ISI assay measuring functional activity of antibodies induced by vaccination with viral vectors against *P. berghei* sporozoites expressing PfSPECT1 either under the PbSPECT1 promoter or under the PbUIS4 promoter. **D** ISI assay measuring functional activity of antibodies induced by vaccination with R21-SPECT1 against *P. berghei* sporozoites expressing PfSPECT1 under the PbSPECT1 promoter, PfCSP under the PbCSP promoter or both. Post-boost serum pools were tested 2.5%, 0.5% and 0.1% of the total culture medium. Inhibition was calculated as reduction in infected hepatoma cells in comparison to cells infected with sporozoites in the absence of serum. Bars are representative of the mean of two experimental replicates. **E** Three weeks after the second immunisation the mice were challenged with *P. berghei* parasites expressing PfSPECT1 under the PbSPECT1 promotor.

As expected, viral vectors encoding SPECT1 did not induce an immune response against CSP, while R21-SPECT1 induced strong antibody titres against this antigen (***Figure 4.7*** **A**). Both vaccine regimen induced an antibody response against SPECT1 and there is a trend for higher titres being induced by the VLP than by the viral vectors although this was not statistically significant (***Figure 4.7*** **B**). There was no statistically significant difference between vaccinated groups in protection against challenge (20%

sterile protection in the VLP group and 10% sterile protection in the viral vector group)(***Figure 4.7*** **E**). The two vaccinated groups were significantly different from naïve mice ($p<0.0001$, Log-rank Mantel-Cox test). Surprisingly serum from mice vaccinated with viral vectors inhibits sporozoite invasion into hepatocytes to very similar extent, whether the gene addition or the gene replacement parasite is used (***Figure 4.7*** **C**). Therefore, ability to inhibit sporozoite invasion cannot explain the reduced protection observed upon challenge with the gene replacement parasite. Interestingly, serum from mice immunised with the dual antigen VLP showed high inhibition of sporozoite invasion against the two single gene replacement parasite lines, but even better inhibition of the double gene replacement sporozoites (***Figure 4.7*** **D**). This data therefore gives a first indication that immune responses against CSP and SPECT1 can work together to efficiently reduce liver infectivity of sporozoites, meriting further investigation of the R21-SPECT1 dual antigen VLP.

4.2.3 R21-Pfs25, a multi-stage vaccine

4.2.3.1 Pfs25 and CS vaccines can be combined without interference

To initially assess whether it would be feasible to combine vaccines against two different lifecycle stages, two well established vaccine candidates were mixed or co-administered to assess whether a strong immune response against both antigen would be maintained. Therefore, we collaborated with GlaxoSmithKline, and combined RTS,S the most advanced sporozoite vaccine with Pfs25-IMX313, our most advanced transmission blocking vaccine. The vaccines were adjuvanted with AS01E. Ten Balb/c mice per group were immunised either with 5 µg RTS,S and 4 µg Pfs25-IMX313

combined into a single injection (mixed) or with each vaccine injected separately into the left and the right hind leg (co-administered), respectively. In the co-administered group, each injection was adjuvanted with only half a dose of AS01E, to keep the total amount of administered adjuvant constant. As a control a group of mice were immunised with either RTS,S alone or Pfs25-IMX313 alone. A final control group received only PBS with adjuvant. Mice were immunised twice in a four week interval and blood samples were collected on days 27 and 42. Antibody titres against Pfs25 and NANP repeats were quantified by ELISA at each of the time points and serum from the final time point was used to assess vaccine efficacy *ex vivo* by SMFA and ISI.

All Pfs25-IMX313 containing vaccine formulations in AS01 induced strong anti-Pfs25 antibody responses in mice (***Figure 4.8*** **C**). Mixing or co-administration of RTS,S and Pfs25-IMX313 did not have a significant effect on anti Pfs25 antibody titres when compared to the group that received Pfs25-IMX313 alone. Assessment of functional activity by SMFA, however, showed significantly higher blocking for the Pfs25-IMX313 alone group in the two lowest IgG concentration tested in the second assay (83.3 µg/ml and 27.8 µg/ml) (***Figure 4.8*** **B**), while at higher IgG concentration there was no difference between groups. Interestingly, no significant difference between any group was detected in the first SMFA (***Figure 4.8*** **A**). Correlation of antibody titres with functional activity did not indicate a difference in antibody quality between combination and individually administered vaccine (***Figure 4.8*** **D**).

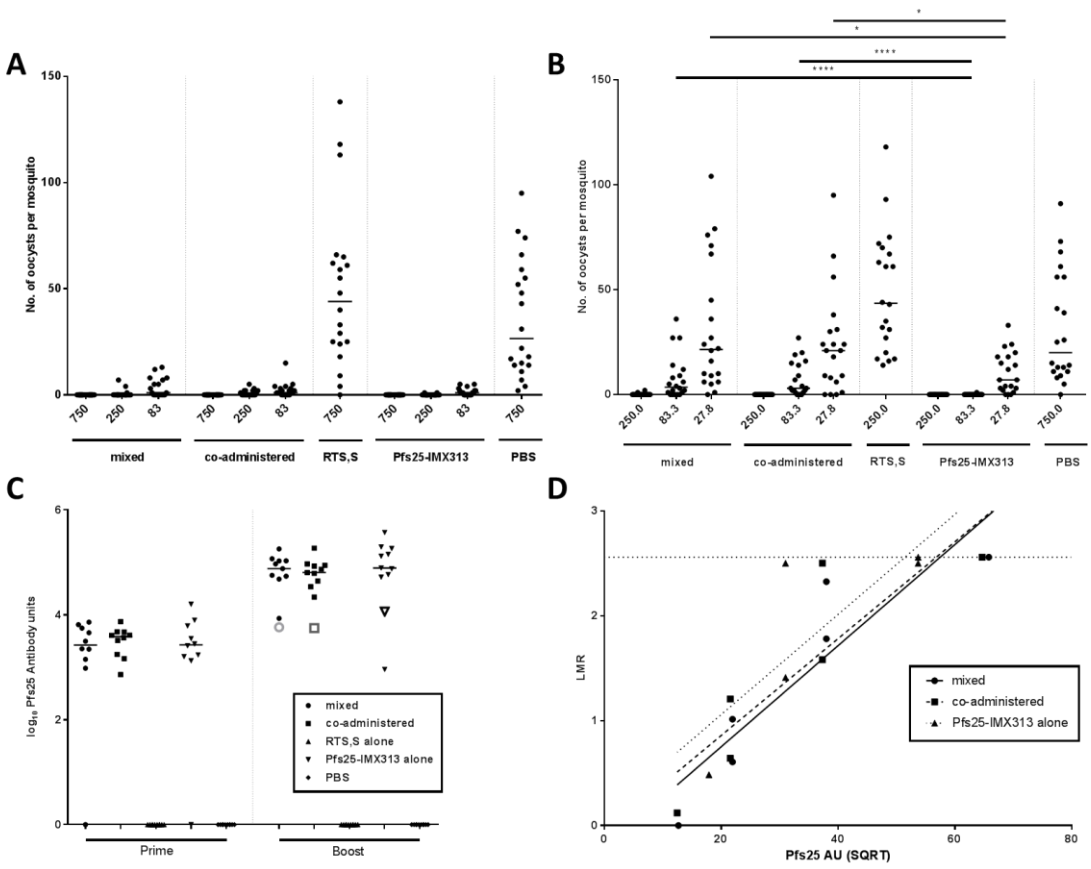

E

Sample name		PBS	mixed				Co-administered				RTS,S alone		UOXJ214Pfs25-IMX313 alone			
IgG conc [ug/ml]		750	750.0	250.0	83.3	27.8	750.0	250.0	83.3	27.8	750.0	250.0	750.0	250.0	83.3	27.8
SMFA 1	Average Oocyst count	36.2	0.0	0.6	3.5		0.0	0.9	2.3		49.6		0.0	0.1	1.4	
	TRA (%)		100.0	98.3	90.3		100.0	97.4	93.8		-37.0		100.0	99.7	96.1	
	p		0.001	0.001	0.001		0.001	0.001	0.001		0.443		0.001	0.001	0.001	
SMFA 2	Average Oocyst count	31.8		0.2	7.9	31.8		0.0	7.3	24.1		48.8		0.0	0.1	10.4
	TRA (%)			99.5	75.0	-1.3		100.0	76.9	23.3		-55.7		100.0	99.8	66.8
	p			0.001	0.002	0.973		0.001	0.001	0.527		0.295		0.001	0.001	0.007
2 feeds	Estimated TRA (%)			99.1	84.5			99.5	88.1					99.9	99.2	
	95%CI Lo			98.1	72.9			98.9	78.6					99.5	98.3	
	95%CI Hi			99.7	91.9			99.8	93.7					99.9	99.7	
	p-value			0.001	0.001			0.001	0.001					0.001	0.001	

Figure 4.8: RTS,S and Pfs25-IMX313 can be combined without reducing the antibody response to Pfs25. BALB/c mice were immunised with combinations of RTS,S and Pfs25-IMX313 or with each vaccine alone. **A,B** Transmission blocking activity of the induced antibodies was assessed by SMFA. Data points show the number of oocysts in individual mosquitoes, lines show the median. SMFA results at similar IgG concentrations were compared by Mann-Whitney test. * = $p < 0.05$, **** = $p < 0.0001$. **C** Anti Pfs25 antibody titres in serum samples as well as in the purified IgG used in SMFA were determined by Pfs25 standard ELISA. Filled shapes show serum titres in individual mice, lines show the median, empty shapes show the antibody units of a 1 mg/ml solution of purified IgG. **D** Functional activity per antibody unit of IgG induced through different vaccination regimen was assessed through correlation of transmission blocking activity with antibody titres by LMR/SQRT analysis. **E** The table shows the average number of oocysts per mosquito and percentage of transmission reducing activity in each of the two SMFAs and gives an estimate of transmission reducing activity from both feeds combined. Given p-values are in respect to the negative control.

Similarly, no significant reduction in anti NANP-repeat antibody titres could be observed upon mixing or co-administration of RTS,S and Pfs25-IMX313 when compared to administration of RTS,S alone, and all RTS,S containing vaccine formulations in AS01 induced strong antibody responses (***Figure 4.9*** **A**). Functional activity of anti-CSP antibodies was assessed by inhibition of sporozoite invasion (ISI) assay using *P.berghei* sporozoites expressing PfCSP under the PbCSP promoter. At 1% serum concentration inhibition of sporozoite invasion is detectable in all groups, and there is no statistically significant difference between groups immunised with RTS,S alone or mixed or co-administered with Pfs25-IMX313.

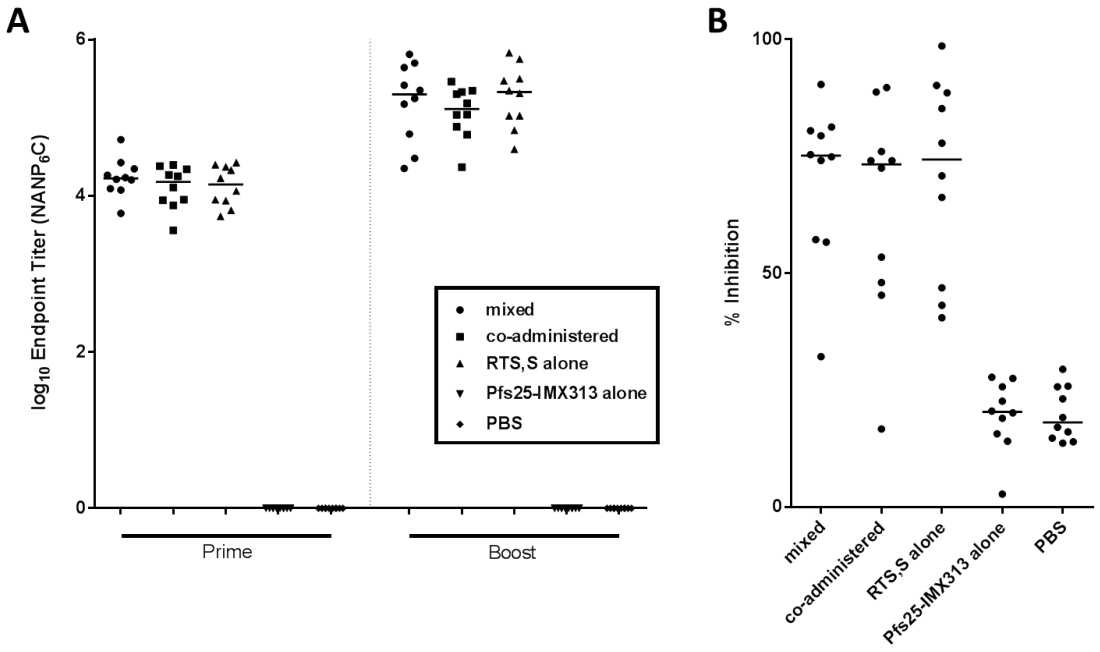

Figure 4.9: RTS,S and Pfs25-IMX313 can be combined without reducing the anti NANP-repeat immune response. BALB/c mice were immunised with combinations of RTS,S and Pfs25-IMX313 or with each vaccine alone. **A** Antibody responses against CSP in serum samples from both time points were assessed by NANP endpoint ELISA. **B** ISI assay measuring functional activity of induced antibodies against *P. berghei* sporozoites expressing PfCSP under the PbCSP promoter. Data points show inhibition of individual serum samples at 1% serum concentration and the lines show the median.

Taken together, data obtained from combination of RTS,S with Pfs25-IMX313 suggests that sporozoite and sexual stage antigens can be combined in a single vaccine formulation without strong antigenic interference and further experiments, aiming at displaying the two antigens on a single VLP vaccine appeared justified.

4.2.3.2 Expression of Pfs25 on the surface of HBsAg results in decreased particle yields

Plasmids for expression of HBsAg-VLPs displaying Pfs25, either as a single antigen at the C-terminus or in addition to the R21 CSP antigen, were generated as described in 2.2.3.4. The generated plasmids were used to transform PichiaPink strain 1 cells, and a protein expressing clone was selected and used to express the VLPs at large scale as described in 2.2.7, 2.3.1.1 and 2.3.1.2. C-tag binding proteins were purified from glass bead lysates of the cultures using a C-tag affinity column. Unfortunately, yields after C-Tag affinity chromatography were too low even to be detected by anti HBsAg Western blot, and it was therefore assumed that the process would have to be adapted before sufficient amounts of VLP could be produced to allow testing as a vaccine.

Previous attempts to produce Pfs25 displaying particles by N-terminal fusion to HBsAg had failed due to similarly low particle yields (Yuanyuan Li, personal communication), suggesting there are intrinsic properties of Pfs25 that prevent its expression on the surface of HBsAg-VLPs. Since Pfs25 contains a very large number of paired cysteine residues (22 out of 180 amino acids in the mature ectodomain), and HBsAg VLPs also require the formation of inter and intramolecular disulphide bonds, it was hypothesised that formation of incorrectly paired disulphide bonds between HBsAg and Pfs25 could result in incorrect folding and protein degradation, explaining the low yields.

To test this hypothesis, a rigid linker was inserted in between the HBsAg and Pfs25. Based on the predicted, elongated Type I β-Turn structure of the CSP NANP repeats, four of those repeats were chosen to be used as the linker. Plasmids expressing the linker containing VLP monomers (pPink-HC-S-NANP-Pfs25 and pPink-HC-R21-NANP-Pfs25) were cloned and transformed into yeast as described above, but using a genestring encoding the HBsAg C-terminus, followed by 4x(NANP) followed by Pfs25 and a C-Tag. Expression of these constructs at larger scale yielded a small amount of protein from the R21-NANP-Pfs25 culture, but yields from the S-NANP-Pfs25 culture were again too low to allow further characterisation. After buffer exchanging and concentration using 100 kDa MWCO spin concentrators, the purified protein was confirmed to be the monomeric R21-NANP-Pfs25 subunit by Coomassie staining and Western blot, where a band of approximately 80 kDa could be detected at the predicted molecular weight of R21-NANP-Pfs25 (***Figure 4.10*** **A**). Because of the very low product yield, further purification by SEC was not performed at this stage. Assembly of the proteins into virus like particles was confirmed by TEM (***Figure 4.10*** **B**).

The electron micrograph confirmed assembly into particles, but as had been observed with unmatured SPECT-1 VLPS obtained from glass bead lysate, the size and shape of the particles were highly variable (average diameter of 30 randomly selected particles = 24 nm ± 9 nm). This data suggests that while the addition of an NANP-linker allowed for the first time the expression of Pfs25 on the surface of an HBsAg particle, the additional C-terminal antigen has a negative impact on particle assembly.

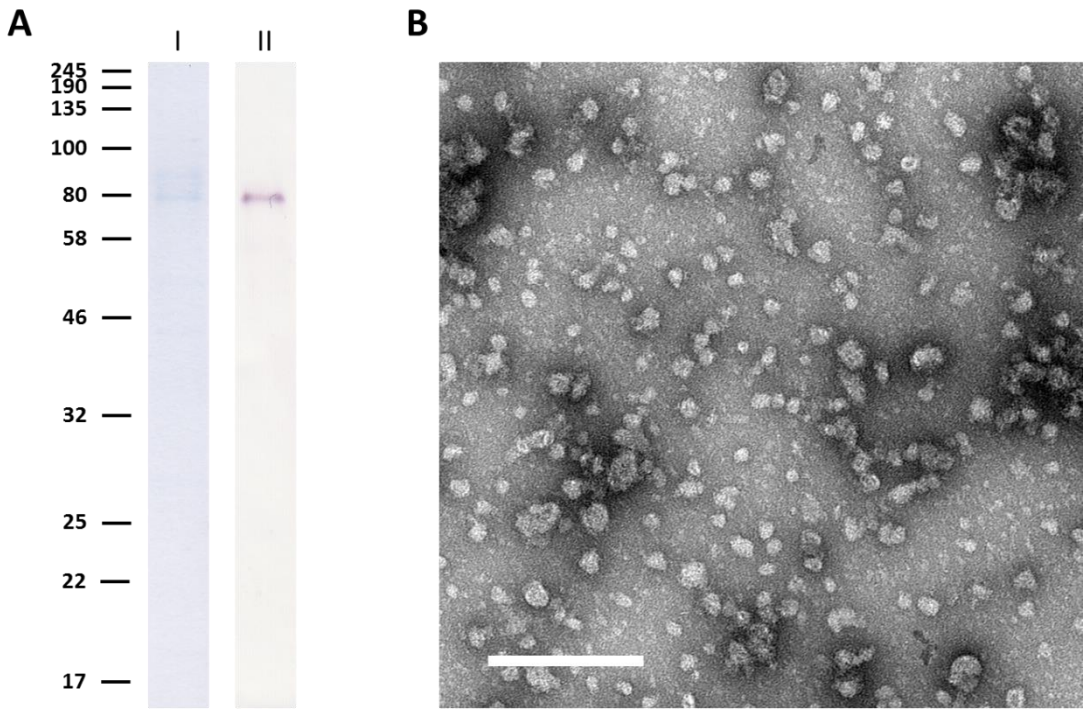

Figure 4.10: Insertion of NANP repeats between HBsAg and Pfs25 allows its expression on a VLP. **A** Coomassie stained gel and Western blot of R21-NANP-Pfs25. R21-NANP-Pfs25 was purified by C-Tag affinity chromatography and visualised by Coomassie staining (lane I) and anti-HBsAg Western blot (lane II) after being electrophoresed over a 4-12% polyacrylamide gel. **B** Transmission electron micrograph of R21-NANP-Pfs25. Scale bar = 200 nm.

Despite the observed heterogeneity of the VLPs it was decided to assess their immunogenicity in mice, to get a first impression of the ability of the multi stage VLP to induce an antibody response *in vivo*. Therefore, 5 Balb/c mice per group were immunised with 2.5 µg of R21-NANP-Pfs25 or R21 adjuvanted with 8.5 µg Alhydrogel. As production of S-NANP-Pfs25 as a single antigen control had not been successful a third group of mice was immunised with 2.5 µg Pfs25 in 8.5 µg Alhydrogel. Three doses of each vaccine were administered in total in a three week interval. 20 days after each immunisation, a blood sample was collected and antibody titres in the serum quantified by NANP and Pfs25 standard ELISA (***Figure 4.11***).

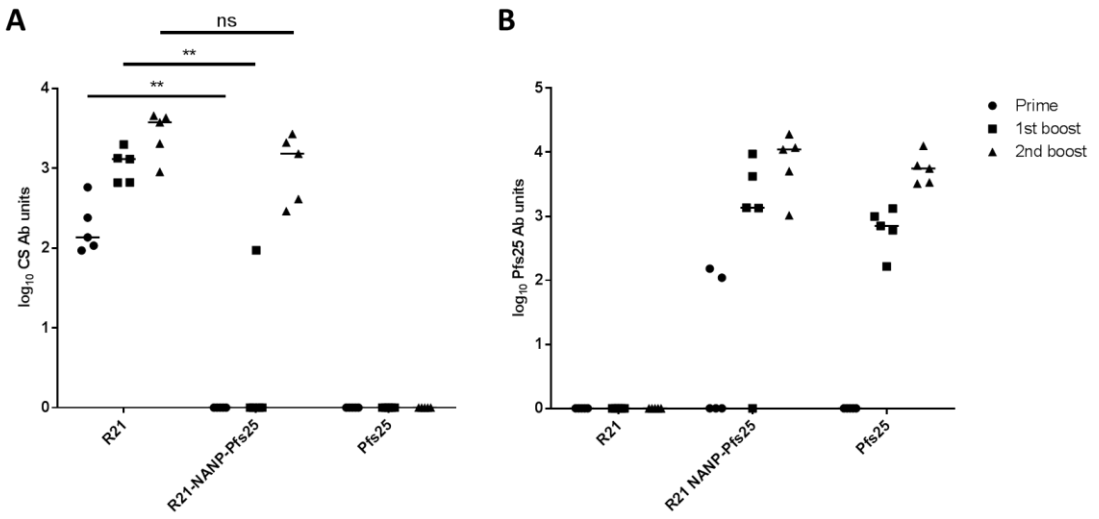

Figure 4.11: R21-NANP-Pfs25 induces antibody responses against both antigens in mice. Balb/c were immunised with R21-NANP-Pfs25, R21 or Pfs25. **A** Antibody responses to the CSP were assessed by NANP standard ELISA**. B** Antibody responses to Pfs25 were determined by Pfs25 standard ELISA. Data points show antibody responses of individual mice, line show the median. Antibody responses induced by the dual antigen VLP at each time point were compared to titres induced by the appropriate single antigen control vaccine at the same time point by Mann-Whitney test. ** = $p < 0.01$. Bars indicate median.

Immunisation with R21-NANP-Pfs25 induced an immune response against both of the displayed antigens. However, antibody responses to the CS antigen after the first and second immunisation were significantly lower than the responses induced after immunisation with R21 (difference between median after prime = 2.134, p = 0.0079, difference between median after 1st boost = 3.115, p = 0.0079). After the third immunisation, antibody responses induced by the two vaccines were not significantly different, but there was still a trend for a higher response from immunisation with R21 (difference between medians = 0.393). Antibody responses against Pfs25 and R21-NANP-Pfs25 are not significantly different at any time point. As anti-Pfs25 antibody responses are normally improved by displaying the antigen on a VLP, the observed titres are indicative of non-optimal particle formation. While establishing the possibility to generate an HBsAg VLP displaying a CS antigen as well as Pfs25 on its

surface, taken together, immune responses to R21-NANP-Pfs25 and analysis of electron micrographs suggest that the particle quality would have to be improved before a more in depth assessment of this particle as a vaccine candidate could be conducted.

To improved particle yield and quality, the production of Pfs25-NANP-Pfs25 was therefore changed to the optimised method established for the production of R21-SPECT1. Unfortunately, even processing of large culture volumes of up to two litres using a high pressure homogeniser and maturation of purified particles did not improve the yield of high quality particles sufficiently to allow further experiments with this vaccine candidate.

4.2.3.3 Generation of a CS-Pfs25 dual antigen VLP using Spy/Snoop technology

As genetic fusion of Pfs25 to HBsAg VLPs had proven challenging, it was assessed whether it would be possible to generate a CSP-Pfs25 dual antigen VLP by covalent conjugation of the antigens to the VLP, using Spy/Snoop technology. The SpyTag-SpyCatcher/SnoopTag-SnoopCatcher system takes advantage of an isopeptide bond formed within some bacterial adhesins. Tag and catcher were generated by splitting the fibronectin binding protein of *Streptococcus pyogenes* (Spy) or *Streptococcus pneumoniae* (Snoop), into a larger protein (Catcher) and a small peptide (Tag). By fusing one protein to the Catcher, another protein to the Tag, the two proteins can be selectively and covalently conjugated after being expressed separately [235, 236]. We had shown earlier that a fusion of SpyCatcher and SnoopCatcher to IMX313 can be used as a platform for a dual antigen vaccine [237]. A dual SpyCatcher-SnoopCatcher HBsAg VLP was being developed and Pfs25-SpyTag had been produced before [238].

Therefore a genestring was ordered encoding the CS-antigen as encoded in R21, followed by a $(GSG)_2$-linker, followed by SnoopTag followed by C-Tag. The genestring was cloned into the pPIC9K vector and transformed into *Pichia pastoris* strain GS115 as described in 2.2.7. A protein expressing clone was selected and used to express the protein at large scale as described, 2.3.1.1 and 2.3.1.2. Since the pPIC9K vector contains an alpha mating factor secretion signal, CS-SnoopTag could be purified from culture supernatant by C-Tag affinity chromatography. The purified protein was confirmed to be the CS-antigen by Western blot using the NANP-repeat specific monoclonal antibody 2A10. A single band was detected in the Western blot, but while the molecular weight of the CS-SnoopTag protein was predicted to be ~22 kDa the band was detected at a significantly higher molecular weight (~50 kDa), as can also be seen in the Coomassie gel in ***Figure 4.12***. Nonetheless, as the protein was recognised by 2A10 it was assumed to be CS-SnoopTag, and detection at higher molecular weight might be caused by the reported elongated structure of the NANP-repeats which could influence its migration in a polyacrylamide gel.

The generated CS-SnoopTag and Pfs25-SpyTag were conjugated to an HBsAg VLP expressing SnoopCatcher at its N-terminus and SpyCatcher at its C-terminus (Snoop-HBsAg-Spy) to generate dual antigen VLPs. The conjugation was performed over two consecutive steps, following each step unconjugated antigens were removed using 100K MWCO spin concentrators. In the first step either Pfs25-SpyTag or CS-SnoopTag was conjugated with Snoop-HBsAg-Spy. Some of the conjugation product was kept as a single antigen control, the remainder was conjugated with the respective other antigen to make the dual antigen VLP. To assess conjugation efficiency, all substrates

and conjugation products were electrophoresed over a polyacrylamide gel, stained with Coomassie stain and analysed by densitometry (***Figure 4.12***).

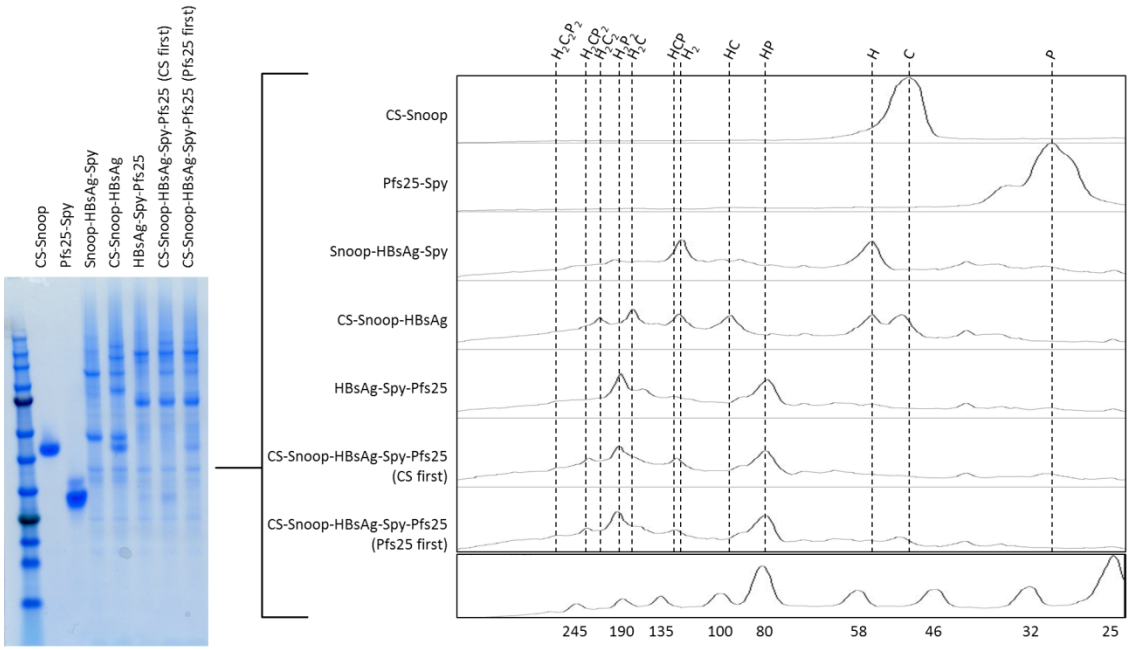

Figure 4.12: Conjugation of Pfs25-SpyTag and CS-SnoopTag to Snoop-HBsAg-Spy produces dual antigen VLPs. CS-Snoop-HBsAg-Spy-Pfs25 dual antigen VLPs as well as intermediate conjugation products and unconjugated proteins were electrophoresed over a 4-12% polyacrylamide gel. The gel was stained with Coomassie stain and individual lanes were plotted in ImageJ. H = Snoop-HBsAg-Spy, C = CS-SnoopTag, P = Pfs25-SpyTag.

This analysis showed that the conjugation efficiency of Pfs25-SpyTag with Snoop-HBsAg-Spy was close to 100%, as no unconjugated VLP monomer or dimer could be detected in the Coomassie stained gel after conjugation with this antigen. The conjugation efficiency of CS-SnoopTag with Snoop-HBsAg-Spy was calculated to be 51.5% and therefore a lot lower than that seen with Pfs25-SpyTag. This conjugation efficiency appeared to be further reduced when CS-SnoopTag was conjugated to the VLP previously conjugated with Pfs25-SpyTag (HBsAg-Spy-Pfs25). The conjugation efficiency of Pfs25-SpyTag on the other hand remained at approximately 100% even when CS-SnoopTag had been conjugated to the VLP before. It was therefore decided

to use the dual antigen VLP which had first been conjugated to CS-SnoopTag and then to Pfs25-SpyTag (CS-Snoop-HBsAg-Spy-Pfs25 (CS first)) for subsequent immunogenicity experiments.

4.2.3.4 CS-Snoop-HBsAg-Spy-Pfs25 induces a functional antibody response against both antigens

To assess the ability of the dual Spy/Snoop VLP to induce an immune response against the two conjugated antigens, five groups of BALB/c mice (n = 5 per group) were primed by intramuscular administration of 3 µg of the dual VLP, a mixture of the intermediate product single antigen VLPs as well as each individual single antigen VLP and the carrier Snoop-HBsAg-Spy VLP (mixed single VLP group received 1.5 µg of each VLP to bring the total dose to 3 µg). All VLPs were adjuvanted with 5 µg Matrix M. 14 days later mice were boosted with the same vaccine formulation. Serum samples were collected on day 13 (prime) and day 28 (boost). The transmission blocking component of the VLPs was assessed by anti-Pfs25 ELISA and SMFA (***Figure 4.13***), while the targeting of sporozoite was assessed by NANP-endpoint ELISA and ISI assay (***Figure 4.14***).

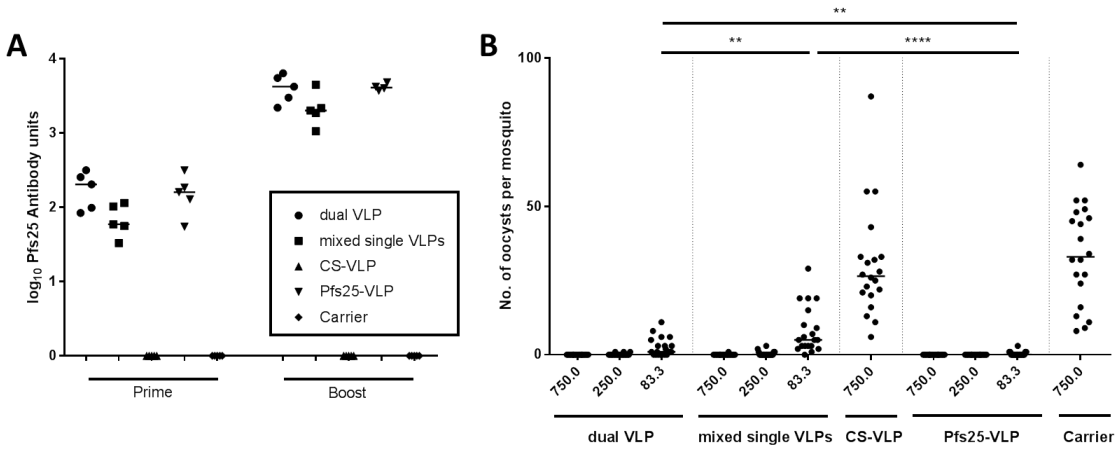

C

Sample name	Dual VLP			Mixed single VLPs			CS-VLP	Pfs25-VLP			carrier
IgG conc [ug/ml]	750.0	250.0	83.3	750.0	250.0	83.3	750.0	750.0	250.0	83.3	750.0
Average Oocyst count	0	0.2	2.6	0.1	0.4	8.3	30.4	0	0	0.4	33.6
TRA (%)	100	99.6	92.4	99.9	98.8	75.4	9.7	100	100	99.0	
p	0.001	0.001	0.001	0.001	0.001	0.002	0.8066	0.001	0.001	0.001	

Figure 4.13: CS-Snoop-HBsAg-Spy-Pfs25 induces a functional antibody response against Pfs25. BALB/c mice immunised with dual or single antigen VLPs **A** Anti Pfs25 antibody responses were quantified by Pfs25 standard ELISA. **B** Functional activity of induced anti-Pfs25 antibodies was assessed by SMFA. Data points show the number of oocysts in individual mosquitoes and the lines show the median. SMFA results at similar IgG concentrations were compared by Mann-Whitney test. ** = $p < 0.01$, **** = $p < 0.0001$. E Average number of oocysts per mosquito and percentage of transmission reducing activity in SMFA. Given p-values are in respect to the negative control.

All Pfs25 containing VLP formulations induce a detectable antibody response against Pfs25 after the first immunisation, which was further boosted by the second immunisation (***Figure 4.13*** **A**). There was no significant difference after prime or after boost in antibody titres induced by either of the Pfs25 containing VLP formulations. In contrast to the induced antibody titres there are significant differences between SMFA results for the three Pfs25 vaccines at the lowest tested concentration (83.3 µg/ml) (***Figure 4.13*** **B**). HBsAg-Spy-Pfs25 (Pfs25-VLP) exhibited higher TRA than CS-Snoop-HBsAg-Spy-Pfs25 (dual VLP), and the dual VLP exhibited higher TRA than CS-Snoop-HBsAg mixed with HBsAg-Spy-Pfs25 (mixed single VLPs). Inferiority of the mixed VLPs is likely due to the halved dose of Pfs25-VLP, while the better SMFA result from the

Pfs25-VLP could be due to a higher percentage of anti-Pfs25 IgG of total IgG in the absence of strongly induced IgG directed against a different antigen, at similar anti-Pfs25 titres in serum.

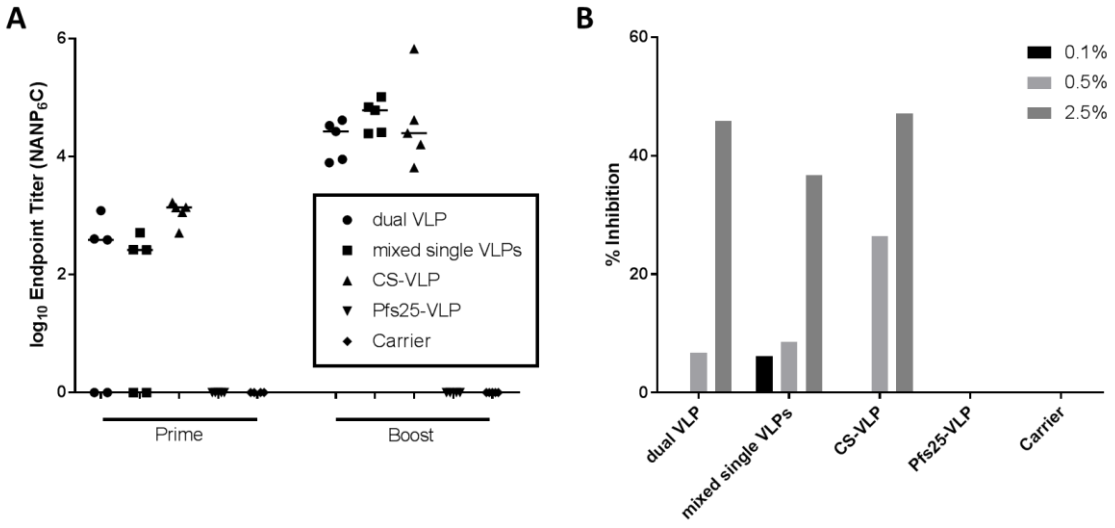

Figure 4.14: CS-Snoop-HBsAg-Spy-Pfs25 induces a functional antibody response against CSP. BALB/c mice immunised with dual or single antigen VLPs. **A** Antibody responses to CSP were quantified by NANP endpoint ELISA. **B** ISI assay measuring functional activity of induced anti-CSP antibodies against *P. berghei* sporozoites expressing PfCSP under the PbCSP promoter. Post-boost serum pools were tested 2.5%, 0.5% and 0.1% of the total culture medium. Inhibition was calculated as reduction in infected hepatoma cells in comparison to cells infected with sporozoites in the absence of serum. Bars are representative of the mean of two experimental replicates.

All CS containing VLP formulations induce an anti NANP antibody response after a single immunisation, although only CS-Snoop-HBsAg (CS-VLP) induces a detectable response in all mice. After boosting however, all mice show similar levels of antibody titres. Inhibition of sporozoite invasion appears to be at similar levels at a serum concentration of 2.5%, although it might be slightly less efficient in the mixed single VLP group, which could again be attributed to the halved dose of CS-VLP in this formulation. At 0.5% CS-VLP shows stronger inhibition than mixed or dual VLPs. As, in contrast to SMFA, ISI uses whole serum and not purified IgG, this cannot simply be attributed to a lower proportion of anti-CSP antibodies of the total IgG. As serum

antibody titres are very similar for all vaccine formulations, only a qualitative difference could explain the observed differences, but this assay would have to be repeated before any definite conclusions can be drawn.

Nonetheless, these data suggest that it is possible to combine pre-erythrocytic and sexual stage antigens on a single VLP without drastically reducing the immunogenicity or functional activity of any of the components.

4.2.4 Triple vaccine combinations

To explore the feasibility of a multi-component vaccine targeting each of the *P. flaciparum* lifecycle stages, the three most advanced vaccine candidates against each lifecycle stage currently under development at the Jenner Institute, R21, Pfs25-IMX313 and Rh5, were combined. Eight groups of BALB/c mice (n = 6 per group) were primed by intramuscular injection of either a mixture of 3 µg R21, 3 µg Pfs25-IMX313 and 3 µg Rh5, a mixture of two of the vaccines or each vaccine individually. The last group received only PBS. All vaccine formulations were adjuvanted with 5 µg Matrix M. 28 days later mice were boosted by intramuscular injection of the same vaccine combination. Serum samples were collected on day 27 (prime) and day 42 (boost). Antibody responses against each antigen were assessed by ELISA.

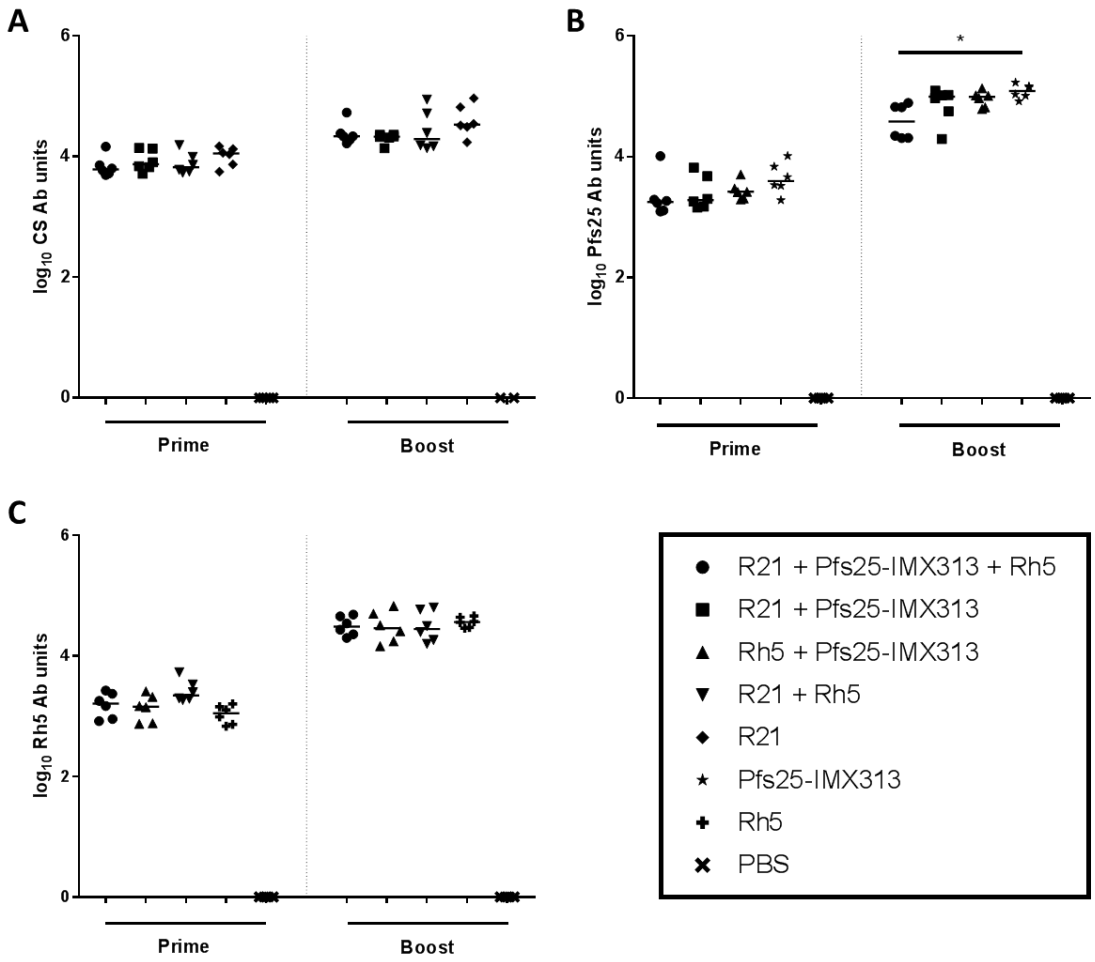

Figure 4.15: Triple vaccine combination. BALB/c mice were immunised with either a mixture of R21, Pfs25-IMX313 and Rh5, a mixture of two of the vaccines or each vaccine individually. **A** Antibody responses to CSP were quantified by NANP standard ELISA. **B** Anti Pfs25 antibody responses were quantified by Pfs25 standard ELISA. **C** Anti Rh5 antibody responses were quantified by Rh5 standard ELISA. Data points show antibody responses in individual mice, bars indicate median. Antibody responses against each antigen were compared by ANOVA followed by Dunn's multiple comparison test . * = $p < 0.05$.

Immunisation with each vaccine combination as well as each individual vaccine induced strong antibody responses against each antigen contained in the administered formulation. Anti NANP-repeat and anti-Rh5 antibody responses were not affected by combination with other antigens, but anti-Pfs25 antibody responses were significantly reduced in the triple combination when compared to Pfs25-IMX313 on its own.

The results of this experiment suggest that combinations of more than two antigens can induce a strong antibody response against each individual antigen, but there is some indication of immune interference.

4.3 Discussion

The shortcomings of recent clinical trials using single antigen subunit vaccines support the development of multi-antigen vaccines for malaria. Work conducted as part of this thesis highlights some of the promises, but also potential pitfalls of combining multiple antigens in a single vaccine, either by expressing them as a part of multi-antigen VLPs or by mixing them into a multi component vaccine formulation.

Mixing vaccines in a multi-component formulation is an easy process that does not require developing a new product. This means that it is possible to draw from previous product development and also allows for production of the individual components in different expression systems, for example yeast for R21 and Pfs25-IMX313 and S2 *Drosophila* cells for Rh5. Additionally, vaccines manufactured to GMP might already be available at sufficient quantity. Therefore, findings in pre-clinical models can quickly be translated into clinical trials. While this is an advantage at early stages of a vaccine development process, it turns into a disadvantage later on, when multiple individual products have to be released to GMP individually, almost definitely increasing the cost of such a multi-component vaccine. For example, a paediatric dose of the single component Hepatitis B vaccine EngerixB costs $12.30 while a dose of the multi component Meningococcus B vaccine Bexsero is priced at $98.51. Additionally, there seems to be some immune interference when multiple vaccines are administered in a

single injection. Particularly anti-Pfs25 antibody titres were reduced when Pfs25-IMX313 was given in combination with R21 and Rh5 (***Figure 4.15***). Interestingly though, there is no reduction in the antibody response against the other two antigens in the formulation, suggesting Pfs25 is immunologically less dominant. Conversely no negative effect on antibody titres or functionality was observed when only two vaccines (RTS,S and Pfs25-IMX313) were combined (***Figure 4.8*** and ***Figure 4.9***). The observed lower activity in SMFA of the combined vaccines is likely due to the relative amount of antigen specific IgG in whole IgG preparations and not an inferior antibody quality. If both antigens in a two component formulation induce similar amount of antibodies upon immunisation, a defined quantity of purified IgG will contain significantly less antigen specific IgG against one of the antigens than if this antigen is the only one against which antibodies are present, as a significant amount of IgG will be directed against the other antigen. This is true even if the serum concentrations of antigen-specific IgG were identical prior to IgG purification. SMFA uses defined quantities of purified IgG rather than serum dilutions, and is therefore prone to underestimating the performance of multi antigen vaccines if the individual antigens have a different degree of transmission blocking activity. In the RTS,S-Pfs25-IMX313 combination experiment this principle is confirmed by the detection of similar antibody titres in serum from all groups, but a nearly three times higher IgG concentration in the purified IgG of the Pfs25-IMX313 alone group than in the groups where the two different vaccines were co-administered or mixed (***Figure 4.8***C). Once this factor is taken into consideration, the transmission blocking activity is practically identical in all three groups (***Figure 4.8***D).

This data suggests that it is feasible to combine multiple antigens in a single vaccine formulation. This is of particular interest when a transmission blocking vaccine is combined with a vaccine that protects from clinical disease, to create a vaccine which reduces severe illness as well as malaria transmission as called for in the malERA research agenda for malaria eradication [239, 240].

Combining multiple antigens within a single VLP proved even more challenging. While the appeal of a single component, multi-antigen vaccine is evident, there are technical hurdles to achieve this. The addition of an antigen to the C-terminus of HBsAg drastically reduced particle yields for all constructs tested in this thesis chapter, but the effect was more pronounced for Pfs25 than for SPECT1. Given the complex assembly of HBsAg particles in yeast it is not surprising that adding an additional protein can negatively affect the yield. In yeast, HBsAg does not naturally form VLPs, rather, the protein accumulates in multi-layered, lamellar structures in the endoplasmatic reticulum, and upon lysis and downstream processing starts to assemble into VLPs [241]. An additional antigen, particularly one as complex and rich in cysteines as Pfs25, could interfere with this process, causing misfolding and degradation of the protein. Nonetheless enough VLP of R21-NANP-Pfs25 and R21-SPECT1 could be obtained to allow initial characterisation of these particles (***Figure 4.2*** and ***Figure 4.10***), and testing of the two dual antigen VLPs in mice yielded encouraging, although weaker than anticipated, immunogenicity results (***Figure 4.3*** and ***Figure 4.11***). As a consequence of protein misfolding, monomeric subunits could present antigens in non-natural conformations, or not on the VLP surface at all, if the topology of the protein was affected, offering a possible explanation for the lower than expected

antibody responses induced by the multi antigen VLPs. Incorrectly folded subunits could be assembled into VLPs alongside successfully folded ones, explaining the irregular appearance of dual antigen VLPs in electron micrographs. Despite substantial efforts R21-NANP-Pfs25 could not be produced in sufficient quantities to allow further testing, so only R21-SPECT1 was tested in further experiments. This revealed that the observed problems, likely caused by protein misfolding, could be overcome by particle maturation through treatment with chaotropic salt (KSCN) followed by incubation at increased temperatures. Both could help misfolded proteins to partially unfold and then refold in the energetically more favourable, natural conformation, a hypothesis supported by the increased immunogenicity and homogenicity of the VLPs after maturation (***Figure 4.5***). Matured R21-SPECT1 was tested in *in vivo* experiments using Balb/c and CD1 mice and transgenic rodent parasites. Unfortunately protection from challenge with transgenic *P. berghei* parasites was much lower than anticipated from previous experiments, although it has to be noted that all previous challenges had used a transgenic *P. berghei* parasite expressing PfSPECT1 under the PbUIS4, rather than the PbSPECT1 promoter (***Figure 4.8*** and ***Figure 4.9***). In other experiments it was recently noted that the expression of a protein under a non-natural promoter induced protein expression at locations, quantities and time points in the lifecycle at which it would normally not be found, therefore not accurately predicting vaccine effects on wild type parasites (personal communication). Nonetheless, this data showed for the first time protection from a malaria challenge by an additional antigen displayed on the surface of R21. Assessment of additivity or synergy between CS and SPECT1 antibodies were hampered by the close to 100% protection from challenge expected from the CS-part of the vaccine alone. ISI might be able to give an estimate on

additivity or synergy, although it had previously been shown that SPECT1 is not essential for hepatocyte invasion [35], potentially making ISI an unsuitable assay. Particularly in the CD1 mouse experiment, which included more mice and induced higher antibody titres due to a higher vaccine dose, there appears to be slightly improved blocking of the dual gene replacement parasite over the two single gene replacement parasite lines, suggesting there might be some additivity or synergy (***Figure 4.7***). Furthermore, the observed functional activity of the vaccine induced antibodies suggests that that they are capable of binding to SPECT-1 and CSP in their natural conformation, as displayed on the parasite surface, indicating that the antigens on the VLP surface are folded correctly. Future work with R21-SPECT1 is therefore merited and should focus on testing three doses instead of two as well as compare the dual VLP to VLPs expressing only one of the antigens. Finally, immunised mice should be challenged with the whole panel of single and double gene replacement parasites and the protection conferred by the different VLPs assessed in respect to the antigen combination.

As generation of a CSP-Pfs25 dual VLP by genetic fusion of both antigens to HBsAg was not feasible, the VLP was generated using Snoop/Spy-catcher technology (***Figure 4.12***). While Pfs25 conjugated very efficiently, the CS antigen conjugated only to around 50 % of the available binding sites. The reduced binding of CS-SnoopTag could be due to co-purified proteins from the yeast supernatant as well as steric hindrance that prevent a more dense coverage of the VLP surface. Despite incomplete conjugation the VLP induced strong and functional antibody titres against both antigens in mice, with no statistically significant differences between the groups (***Figure 4.13*** and ***Figure 4.14***).

SMFA again showed apparent superiority from the single antigen vaccine, but this can most likely be attributed to the relative amount of antigen specific IgG in purified IgG as described in more detail earlier. Furthermore, the “mixed single VLP” group received the same total amount of VLP as all other groups resulting in a lower dose of each antigen, which could reduce the induced titres. In accordance with a similarly pronounced antibody response to CSP in all groups, no significant difference could be detected between groups in the ability of serum to prevent hepatocyte invasion in ISI.

In summary this data suggests that combining multiple antigens to make a more effective malaria vaccine is a feasible strategy. For a limited number of components, competition between antigens and resulting immune interference does not appear to be very pronounced. Furthermore, the inclusion of an additional antigen could in a physiological setting easily overcome a minor drop in antibody titres against one of the components of a multi-component vaccine. Whether it is preferable to combine antigens within a single VLP or by mixing multiple components will mainly depend on the capability of the VLP to assemble and will have to be determined for every individual antigen combination.

4.4 Appendices

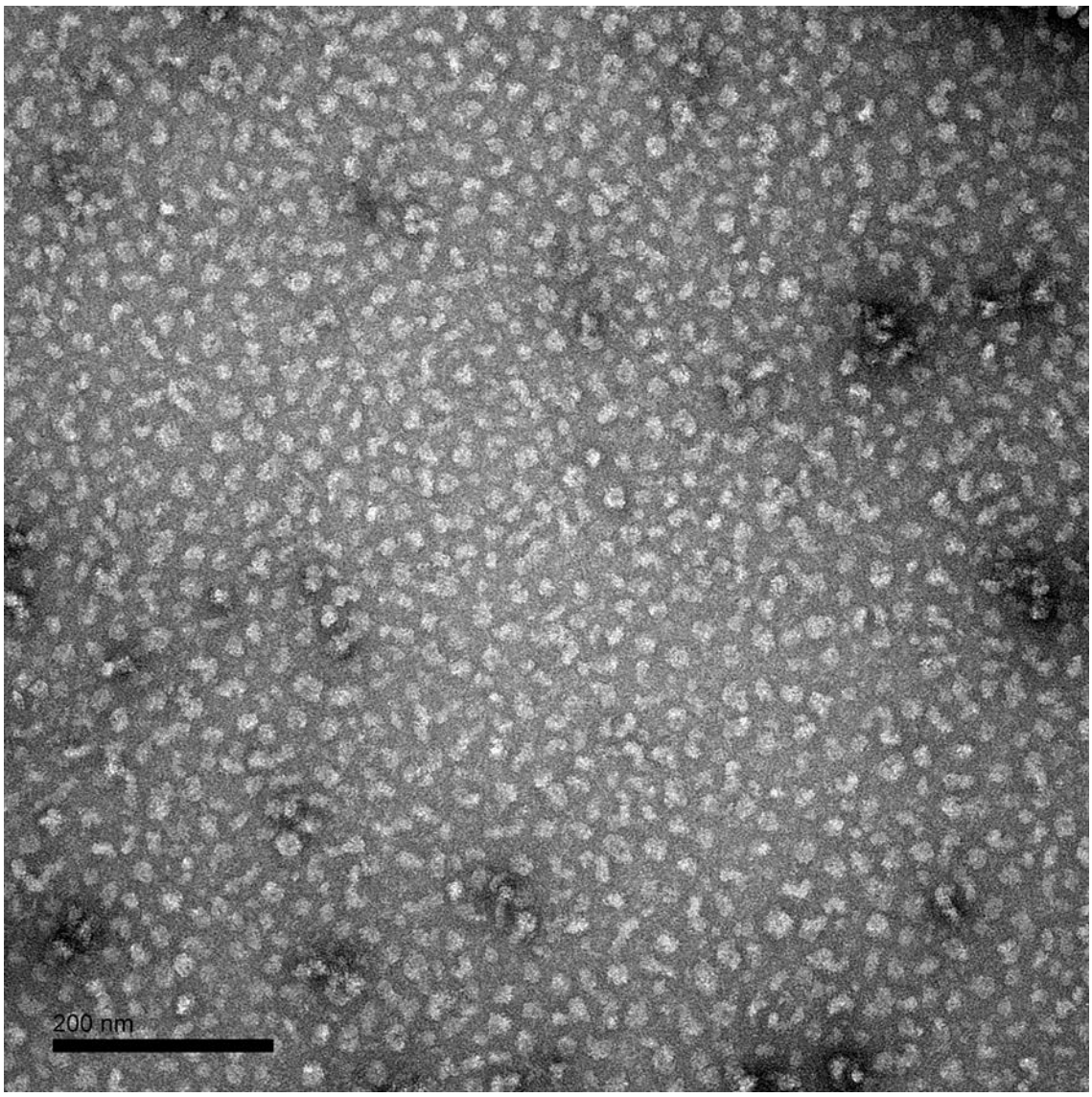

Appendix 4.1: Maturation of R21-SPECT1 improves particle uniformity and immunogenicity. Transmission electron micrograph of D-1 sample

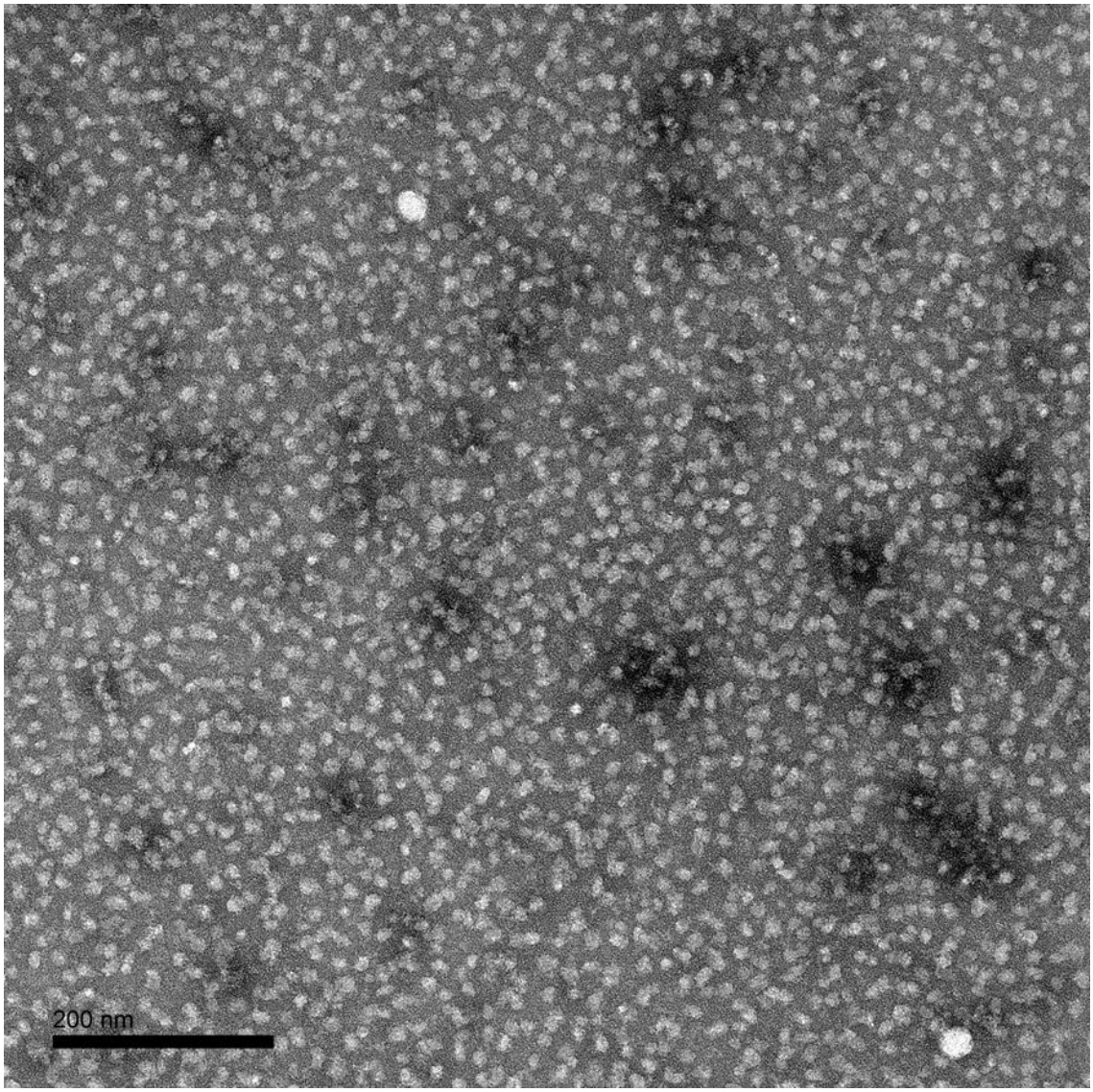

Appendix 4.2: Maturation of R21-SPECT1 improves particle uniformity and immunogenicity. Transmission electron micrograph of D0 sample

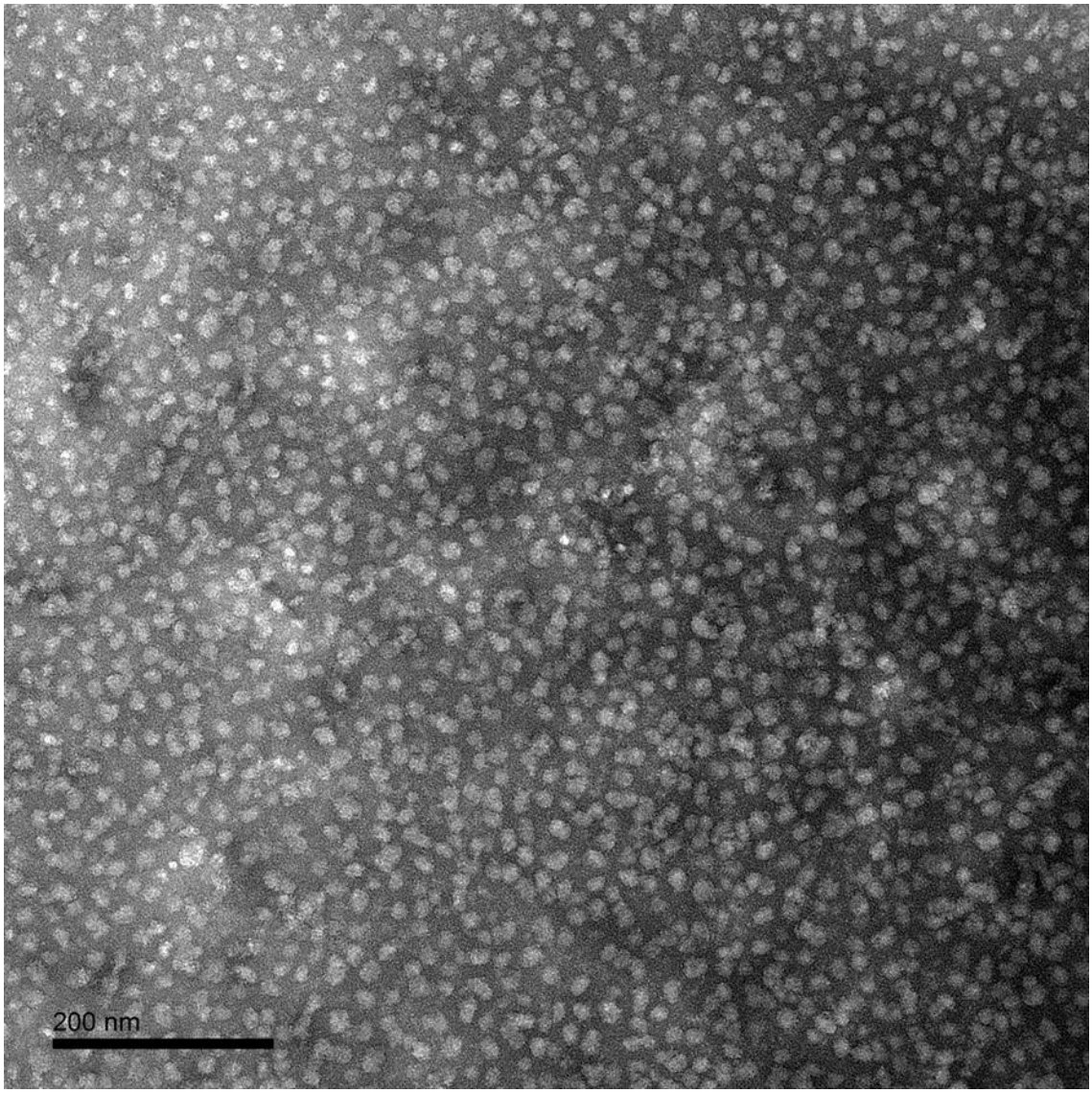

Appendix 4.3: Maturation of R21-SPECT1 improves particle uniformity and immunogenicity. Transmission electron micrograph of D1 sample

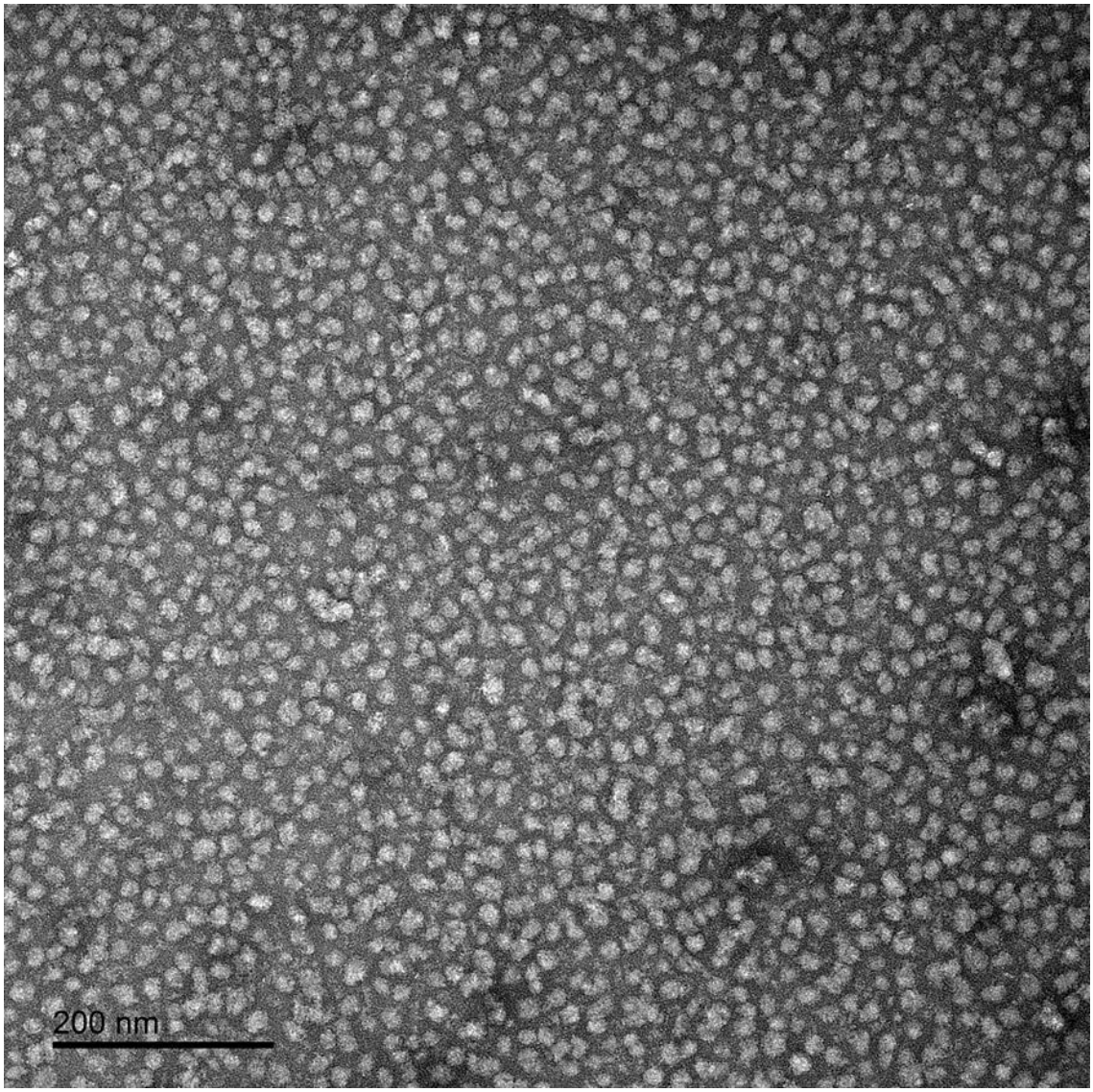

Appendix 4.4: Maturation of R21-SPECT1 improves particle uniformity and immunogenicity. Transmission electron micrograph of D5 sample

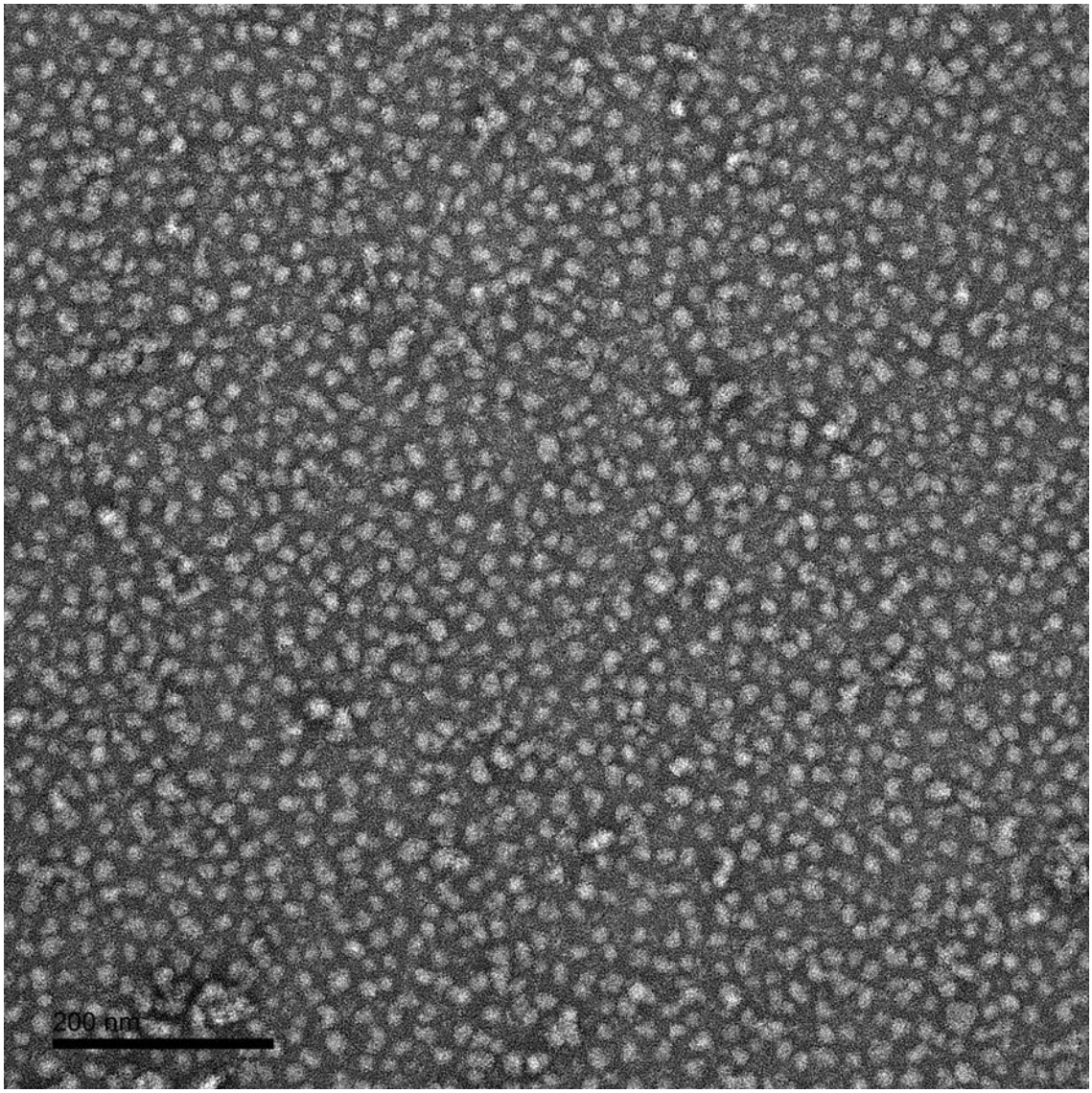

Appendix 4.5: Maturation of R21-SPECT1 improves particle uniformity and immunogenicity. Transmission electron micrograph of D10 sample

Chapter 5 - Identification of protein-protein interactions between the ookinete and the mosquito midgut surface

Authorship statement

SMFA was performed at the Malaria Vaccine Initiative (MVI) SMFA reference laboratory at the National Institute of Health, USA by Dr. Kazutoyo Miura and co-workers. RNAi experiments in mosquitoes were performed with assistance from Dr. Andre Nobrega Pitaluga and Dr. Sofia Tapanelli in the laboratory of Prof. George K Christophides (Imperial College, London).

5.1 Introduction

The passage through the mosquito vector presents a natural bottleneck in the *Plasmodium* lifecycle. Upon ingestion of gametocytes by a mosquito as part of a blood meal, the parasite faces a number of hurdles before it can establish a stable infection of the vector. In the hostile environment of the blood meal inside the mosquito midgut, male and female gametocytes fuse to form a zygote which then matures into the motile ookinete. The ookinete then penetrates the peritrophic matrix, followed by specific attachment to and penetration of the mosquito mitgut epithelial cell layer. Particularly this last step is of interest for transmission blocking interventions and a number of proteins on the surface of the ookinete and the mosquito midgut epithelium have been suggested to be involved in this process. Proteins on the ookinete surface with a potential role in midgut epithelium traversal include (P25 and

P28, circumsporozoite TRAP-related protein (CTRP), von Willebrand factor A domain-related protein (WARP), secreted ookinete adhesive protein (SOAP), two unrelated putative secreted ookinete proteins (PSOP2 and PSOP7), enolase, two *Plasmodium* perforin-like proteins (PPLP3 and PPLP5), subtilisin-like protease (Sub2) and cell-traversal protein for ookinetes and sporozoites (CelTOS)) [32, 99, 101, 113, 116, 117, 242-246], while on the mosquito midgut epithelium (aminopeptidase 1 (APN1), annexin-like proteins, carboxipeptidase B, scavenger receptor croquemort homologue (SCRBQ2), calreticulin (Crt) and enolase binding protein (EBP)) [106, 247-251] have been suggested to play a role. Despite the substantial number of proteins identified as being involved in the process, the only described protein-protein interactions between the ookinete and the mosquito midgut surface are binding of *P. vivax* Pvs25 to *A. albimanus* calreticulin (AnCrt) [251], and binding of enolase to EBP [106]. However, there is to date no direct evidence that the interaction of Pvs25 and surface expressed AnCrt is involved in *Plasmodium* invasion and establishment in the mosquito, and the interaction of enolase and EBP only seems to be essential in a subset of *P. berghei* parasites, but not in *P. falciparum*, the causative agent of the most severe form of human malaria [106].

The identification of novel ligand-receptor-pairs has been hampered by the inability of most conventional assays to detect short lived, low affinity protein-protein interactions. AVEXIS (avidity based extracellular interaction screen) is an assay developed to overcome this limitation by oligomerising one and immobilising the other interaction partner [212]. The assay has been applied to identify a number of previously unknown ligand-receptor interactions including binding of *P. falciparum*

reticulocyte-binding protein homolog 5 (PfRh5) to its erythrocyte receptor basigin, an interaction essential for the invasion of red blood cells by merozoites [63].

As part of my DPhil Thesis, I applied the strategy of screening for novel interaction by AVEXIS to the midgut invasion by the *P. falciparum* ookinete and identified MG36 as an interaction partner for the well described transmission blocking antigen Pfs28. The newly identified interaction was then further characterised by a number of *in vitro* and *in vivo* assays, and found to play a role in the midgut traversal by ookinetes. These findings identify for the first time a ligand-receptor pair between the *P. falciparum* ookinete and the *A. gambiae* midgut surface with a role in mosquito infection and could have implications in the development of novel transmission blocking interventions.

5.2 Results

5.2.1 Generation of ookinete and mosquito midgut epithelium surface protein libraries

To screen for low affinity ligand receptor interactions between the ookinete and the mosquito midgut epithelium using AVEXIS, a library of ookinete and mosquito midgut surface proteins was generated. Proteins to be included in the ookinete surface library were selected from a *P.berghei* ookinete surface proteome [252], (R.E. Sinden, personal communication). Out of 67 proteins for which a signal peptide was predicted by SignalP4.1 [253], 40 were predicted to contain 0-1 transmembrane helices (TMHMM2.0) [254, 255] and 4 were predicted to contain a GPI anchor sequence (big-

PI) [256-258], making them suitable candidates for AVEXIS. The proteome reported a high amount of contamination with intracellular chaperones, therefore all chaperones were excluded from the library as well as all proteins predicted to be targeted to the apicoplast (PlasmoAP) [259] and the mitochondria (targetP1.1) [260]. Finally all proteins that were indicated with a clear role that made their involvement in ligand receptor interactions unlikely such as GAP50, CTRP, chitinase and all perforin like proteins were excluded from the library as well. This left 12 proteins which were increased to a total of 17 by addition of WARP, PSOP2, PSOP7, GAMA and enolase. WARP, PSOP2, PSOP7 and GAMA had been indicated to play a role in mosquito midgut traversal in earlier studies, but were not included in the ookinete surface proteome [246]. Enolase was present in the proteome, but does not contain a signal peptide, it has however been reported to be present on the ookinete surface and to be involved in attachment to the mosquito midgut epithelium [99, 106, 261]. The sequence of *P. falciparum* orthologues of the selected proteins were retrieved from PlasmoDB and the ectodomains identified by signal peptide and transmembrane helix prediction [253] [254, 255] as well as structure prediction by Phyre2 [262]. The signal peptides were replaced with the BIP signal peptide for expression in S2 cells and the proteins truncated at the amino acid preceding any transmembrane helix or GPI-anchor sequence. Finally threonines and serines in a N-X-T/S potential N-glycosylation context were mutated to alanine. All ookinete surface proteins included in the library are listed in ***Table 5.1***.

Table 5.1: Proteins included in the ookinete surface library. Numbers were assigned arbitrarily. Gene identifier lists the unique identifier under which each gene can be found in PlasmoDB. Description lists the description of each protein in PlasmoDB. Ectodomain lists the amino acids of each protein that were expressed for the AVEXIS screen. Type lists the type of protein for each protein, sec = secreted protein, GPI = GPI-anchored protein, I = Type I transmembrane protein (single membrane spanning, secreted N-terminus), IV-B = Type IV-B transmembrane protein (multiple transmembrane spanning, secreted N-terminus).

Number	Gene identifier	Description	Ectodomain	Type
OOK1	PF3D7_0801300	von Willebrand factor A domain-related protein (WARP)	24-290	sec
OOK2	PF3D7_0721700	secreted ookinete protein, putative (PSOP1)	17-467	sec
OOK3	PF3D7_1031000	ookinete surface protein P25 (P25)	23-194	GPI
OOK4	PF3D7_0912400	alkaline phosphatase, putative	21-404	I
OOK5	PF3D7_0504500	MOLO1 domain-containing protein, putative	22-248	I or GPI
OOK6	PF3D7_1015900	enolase (ENO)	1-446	?
OOK7	PF3D7_1455800	LCCL domain-containing protein (CCp2)	24-1617	sec
OOK8	PF3D7_0513700	secreted ookinete protein, putative (PSOP12)	24-735	sec
OOK9	PF3D7_1340000	secreted ookinete protein, putative (PSOP7)	23-618	sec
OOK10	PF3D7_1367800	secreted ookinete protein, putative (PSOP2)	23-1182	sec
OOK11	PF3D7_1002300	conserved *Plasmodium* protein, unknown function	28-406	I or GPI
OOK12	PF3D7_1030900	ookinete surface protein P28 (P28)	23-198	GPI
OOK13	PF3D7_1123500	conserved *Plasmodium* protein, unknown function	24-1222	I or IV-B
OOK14	PF3D7_1351200	conserved *Plasmodium* protein, unknown function	23-1447	I
OOK15	PF3D7_1404300	secreted ookinete adhesive protein, putative (SOAP)	20-202	sec
OOK16	PF3D7_1346800	6-cysteine protein (P47)	27-415	GPI
OOK17	PF3D7_0828800	GPI-anchored micronemal antigen (GAMA)	22-715	GPI

Proteins for the mosquito midgut epithelium library were selected from a detergent resistant membrane proteome of *A. gambiae* brush border microvilli [263]. Proteins

with a GPI anchor or one transmembrane helix and predicted extracellular localisation were selected for the library. Additionally annexin B10B and SCRPQ2 were included in the library as they have been described previously to play a role in ookinete to oocyst conversion [248, 250]. Sequences of the proteins were retrieved from UniProt and ectodomains determined as described for the ookinete library. Signal sequences and N-glycosylation sites were left intact, and proteins were truncated at the amino acid preceding the transmembrane helix or GPI anchor sequence. All ookinete surface proteins included in the library are listed in ***Table 5.2***.

Table 5.2: Proteins included in the mosquito midgut surface library. Numbers were assigned arbitrarily. Gene identifier lists the unique identifier under which each gene can be found in VectorBase. Translation lists the translation of each gene that was used as a basis for the protein to be included in the library. Description lists the description of each protein in VectorBase. Ectodomain lists the amino acids of each protein that were expressed for the AVEXIS screen. Type lists the type of protein for each protein, sec = secreted protein, GPI = GPI-anchored protein, I = Type I transmembrane protein (single membrane spanning, secreted N-terminus), IV-A = Type IV-A transmembrane protein (multiple transmembrane spanning, luminal N-terminus).

Number	Gene identifier	Translation	Description	Ectodomain	Type
MG1	AGAP000032	PA	n.a.	1-1486	I
MG2	AGAP000307	PA	Integrin alpha-PS1	1-1094	I
MG3	AGAP000550	PA	n.a	1-1168	I
MG4	AGAP000720	PA	Neuronal cell adhesion molecule	1-1137	I
MG5	AGAP000815	PA	Integrin beta subunit (INTB)	1-765	I
MG6	AGAP001346	PA	n.a.	1-185	I
MG7	AGAP001613	PA	n.a.	1-176	I
MG8	AGAP001734	PA	Nicastrin	1-670	I
MG9	AGAP002363	PA	n.a.	1-275	I
MG10	AGAP002491	PA	n.a.	1-182	I
MG11	AGAP002643	PA	n.a.	1-131	I
MG12	AGAP002828	PA	n.a.	1-1573	I
MG13	AGAP002848	PA	Niemann-Pick Type C-2	1-132	GPI
MG14	AGAP003647	PA	n.a.	1-888	I
MG15	AGAP003692	PA	n.a.	1-907	I
MG16	AGAP003721	PA	Annexin B10B (ANXB10B)	Full length	sec
MG17	AGAP004303	PA	Integrin alpha-ps	1-1079	I

MG18	AGAP004407	PA	lectin, mannose-binding 2	1-300	I
MG19	AGAP004563	PA	angiotensin-converting enzyme 9 (ANCE9)	1-119	I
MG20	AGAP004809	PA	alanyl aminopeptidase N 1 (APN1)	1-997	GPI
MG21	AGAP005234	PB	copper-zinc superoxide dismutase 2 (CuSOD2)	1-157	GPI
MG22	AGAP005404	PA	lectin, mannose-binding 1	1-491	I
MG23	AGAP005744	PA	leucine-rich immune protein (LRIM26)	1-363	I
MG24	AGAP006280	PA	nuclear pore complex protein Nup210	1-1825	I
MG25	AGAP006400	PA	alkaline phosphatase 2	1-499	GPI
MG26	AGAP006643	PA	n.a.	1-539	I
MG27	AGAP006645	PD	n.a.	1-1032	I
MG28	AGAP006962	PA	multiple inositol polyphosphate phosphatase	1-458	I
MG29	AGAP007256	PA	Multiple epidermal growth factor-like domains 10	1-831	I
MG30	AGAP007612	PA	n.a.	1-851	GPI
MG31	AGAP007665	PA	n.a.	1-300	GPI
MG32	AGAP010133	PA	Class B Scavenger Receptor (SCRPQ2)	33-450	IV-A
MG33	AGAP010233	PA	integrin beta 1	1-730	I
MG34	AGAP010823	PA	n.a.	1-357	I
MG35	AGAP011442	PA	serine carboxypeptidase 1	1-417	GPI
MG36	AGAP011453	PA	n.a.	1-757	I
MG37	AGAP012400	PA	alpha-glucosidase	1-571	GPI
MG38	AGAP013188	PA	aminopeptidase 4 (APN4)	1-912	I

Codon optimised genes for expression in *Drosophila* were synthesised and cloned by GeneArt as described in 2.2.3.5 to generate plasmids for the two AVEXIS control proteins and His-tagged BirA biotin ligase as well as the 38 mosquito midgut bait plasmids and the 17 ookinete prey plasmids (***Figure 5.1***).

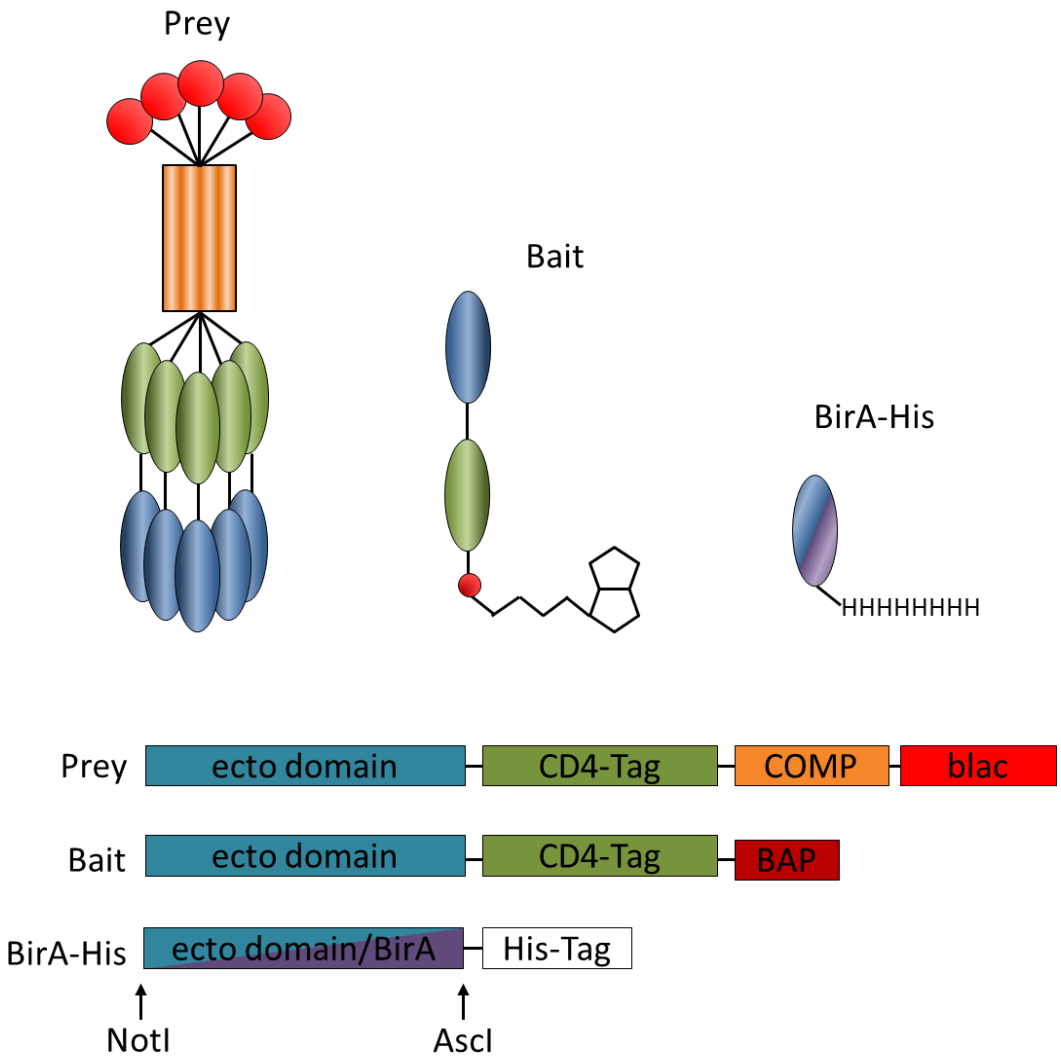

Figure 5.1: AVEXIS constructs. Proteins and DNA sequences of the different AVEXIS constructs are shown as cartoons. The prey construct contains the ectodomain of a protein of interest, a CD4-Tag, the oligomerisation domain of the rat cartilage oligomeric matrix protein (COMP) and beta-lactamase (blac). Upon expression the protein pentamerises at the COMP domain to form the pentameric AVEXIS prey protein. The bait construct contains the ectodomain of a protein of interest, a CD4-Tag and a biotin acceptor peptide (BAP). Upon expression in cells co-transfected with BirA-His, the protein is biotinylated at the BAP to make the monobiotinylated AVEXIS bait protein. The biotin ligase BirA, as well as proteins that should be purified for immunisations or surface plasmon resonance, was expressed with a C-terminal 8xHis-Tag. Different ectodomains can be shuttled between the different constructs by NotI/AscI double digest.

5.2.2 Expression of library proteins for AVEXIS screen

All proteins were expressed from *Drosophila* Schneider-2 (S2) cells by non-viral transient transfection. Proteins were secreted into the cell supernatant, which was collected to be quantified and used in AVEXIS. Upon expression prey protein

containing supernatants were quantified by nitrocefin assay which measures the enzymatic hydrolysis of nitrocefin over time, a reaction catalysed by the beta-lactamase of the prey proteins and accompanied by a colorimetric change of the solution (2.3.8.1). Supernatants containing biotinylated bait proteins were dialysed against PBS to remove excess free biotin and then quantified by ELISA as described in 2.3.8.2. A representative example of prey and bait quantification is shown in ***Figure 5.2***.

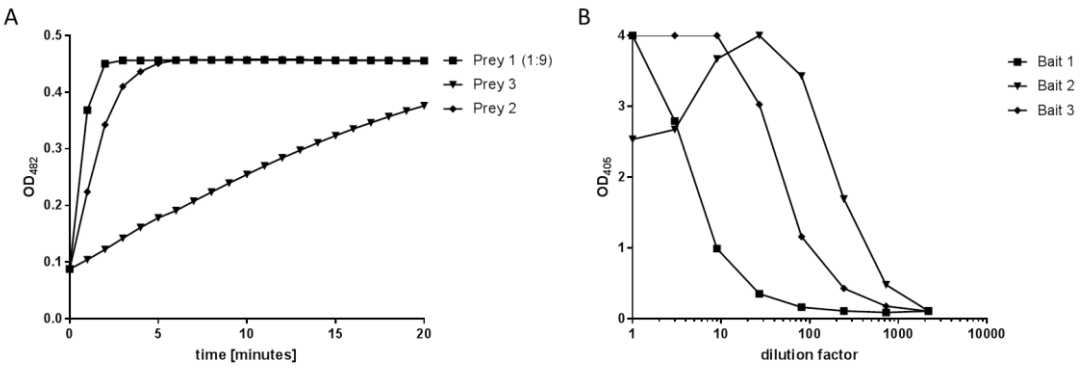

	Prey 1 (1:9)	Prey 2	Prey 3
Time to saturation	2	5	~24
Dilution factor	20	1.4	0.3

	Bait 1	Bait 2	Bait 3
Dilution factor	1	30	10
Fully dialysed	yes	no	yes

Figure 5.2: Quantification of proteins for AVEXIS. **A** Representative example of prey protein quantification. Prey proteins were quantified by nitroceffin assay. Proteins were normalised by concentrating or diluting them so they would reach saturation after 7 minutes. All samples were tested in multiple dilutions and the highest dilution at which saturation was reached in less than 7 minutes was used for to calculate the dilution factor. If undiluted sample did not reach saturation within 20 minutes, the time to saturation was calculated by linear regression (Prey 3). **B** Representative example of bait protein quantification. Bait proteins were quantified by ELISA. Proteins were normalised by concentrating or diluting them so that the signal reached saturation after 1 hour of developing. Lower signal intensity at lower dilution (Bait 2) indicates incomplete removal of free biotin.

Protein expression levels varied widely (around 750-fold between lowest and highest expressing bait protein and around 2000-fold between lowest and highest expressing prey protein), but all proteins could be expressed in sufficient quantities to conduct the complete screen from less than 25 ml of transiently transfected S2 cells. Dilution factors and the molecular weight of all AVEXIS proteins are listed in Table 5.3.

Table 5.3: Dilution factor and molecular weight of AVEXIS bait and prey proteins.

sample	dilution factor	MW [Dalton]
MG1	1	183338
MG2	1	139767
MG3	1	157496
MG4	30	149458
MG5	10	107283
MG6	80	42835
MG7	1	42750
MG8	1	97686
MG9	30	53777
MG10	30	42935
MG11	50	36676
MG12	3	200266
MG13	0.33	36738
MG14	10	119858
MG15	1	126130
MG16	1	60276
MG17	10	142131
MG18	80	56728
MG19	30	162530
MG20	10	133695
MG21	10	39064
MG22	30	76998
MG23	50	62372
MG24	0.11	223637
MG25	30	76672
MG26	30	83028
MG27	10	138817
MG28	30	76379
MG29	10	112354
MG30	20	111991
MG31	50	55412
MG32	30	71935
MG33	15	105164
MG34	30	62173
MG35	15	69433
MG36	30	106145
MG37	30	88155
MG38	10	126936
bait+	50	47175

sample	Dilution factor	MW [Dalton]
Ook1	2.3	88203
Ook2	7	109920
Ook3	7	77348
Ook4	0.4	103799
Ook5	7	84868
Ook6	0.4	107218
Ook7	0.2	240308
Ook8	1.2	143231
Ook9	0.6	128234
Ook10	0.1	191651
Ook11	0.3	102511
Ook12	20	78072
Ook13	0.25	195526
Ook14	0.03	232264
Ook15	1.4	79095
Ook16	0.3	103379
Ook17	16	138801
Prey+	60	80957

To confirm expression of the different AVEXIS constructs, proteins were diluted or concentrated according to Table 5.3, electrophoresed on a 4-12% SDS-polyacrylamide gel and then detected by Western blot (***Figure 5.3***).

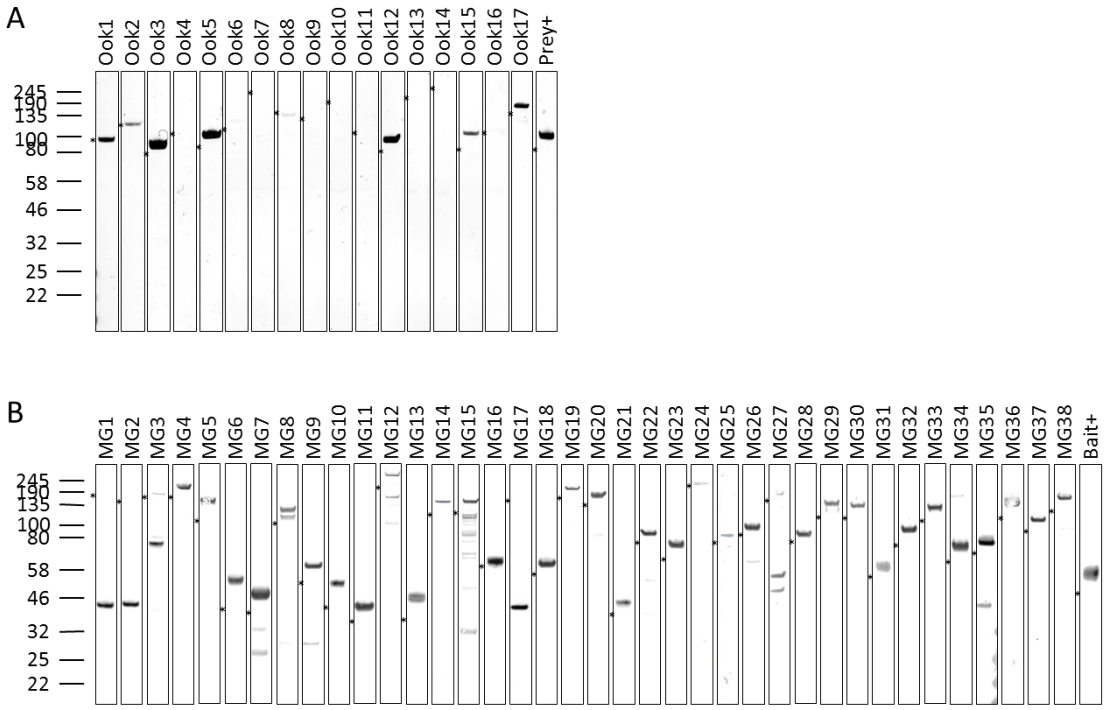

Figure 5.3: Western blot of AVEXIS prey and bait constructs. AVEXIS prey (A) and bait (B) proteins were normalised to similar relative concentrations and then electrophoresed on 4-12% bis-Tris polyacrylamide gels. Prey-proteins were visualised by anti-CD4-Tag Western blot, bait proteins were visualised by Western blot using streptavidin conjugated alkaline phosphatase. Asterisks on the left of each lane indicate the calculated molecular weight of each protein.

Only seven out of the 17 prey proteins (Ook1, Ook2, Ook3, Ook5, Ook12, Ook15 and Ook17), as well as the prey positive control, were detected in a single band of high signal intensity in the Western blot. Three more proteins, Ook6, Ook8 and Ook16 can be detected in a single band with lower signal intensity. All of these proteins were detected with a slightly higher molecular weight than had been calculated, which could be due to an N-glycosylation site within the CD4-Tag. There appears to be a correlation between expression level, as determined by nitrocefin assay, ability to

detect the protein in Western blot, and molecular weight of the protein. All prey-proteins with a molecular weight below 100 kDa could successfully be detected by Western blot, while out of 12 prey-proteins with a higher molecular weight only five could be detected in the Western blot, three of those being Ook6, Ook8 and Ook16 which were only detected faintly. All 7 proteins that could not be detected in the Western blot required concentration before application to Western blot or use in AVEXIS, indicating low expression levels to begin with.

Out of the 38 mosquito midgut bait-proteins, 22 as well as the positive control were detected as a single high intensity band at the correct size. A further 9 (MG7, MG8, MG9, MG20, MG22, MG26, MG34, MG35 and MG38) could be detected in a high intensity band at the correct size, but with one or two additional bands of lower intensity also detected in the sample, indicating aggregation or degradation of a small proportion of the protein. Two proteins (MG3 and MG27) could be detected faintly, with one or two bands of the wrong molecular weight detected with higher intensity in the sample, indicating that a majority of the protein had been degraded. In two samples (MG12 and MG15) bands that could be of the correct size were detected alongside a multitude of additional band, making it difficult to assess whether majority of the protein is intact or degraded. Three proteins (MG1, MG2 and MG17) could not be detected at the expected size at all, but all contained a band at approximately 40 KDa, which could be a degradation product containing the biotinylated CD4-Tag as well as a proportion of the bait-protein. Similar to the prey-proteins, all proteins were detected at a higher molecular weight than calculated. This could be due to the N-

glycosylation site in the CD4-Tag as well as additional N-glycosylation sites within the proteins

5.2.3 AVEXIS screen of ookinete and mosquito midgut epithelium surface proteins

Despite the failure to detect some of the prey- and bait proteins by Western blot, all constructs were taken forward to be tested in AVEXIS, under the premise that results would to be critically assessed in respect to the appearance of the involved proteins in Western blot. The assay was performed as described previously [214] (***Figure 5.4*** to ***Figure 5.9***).

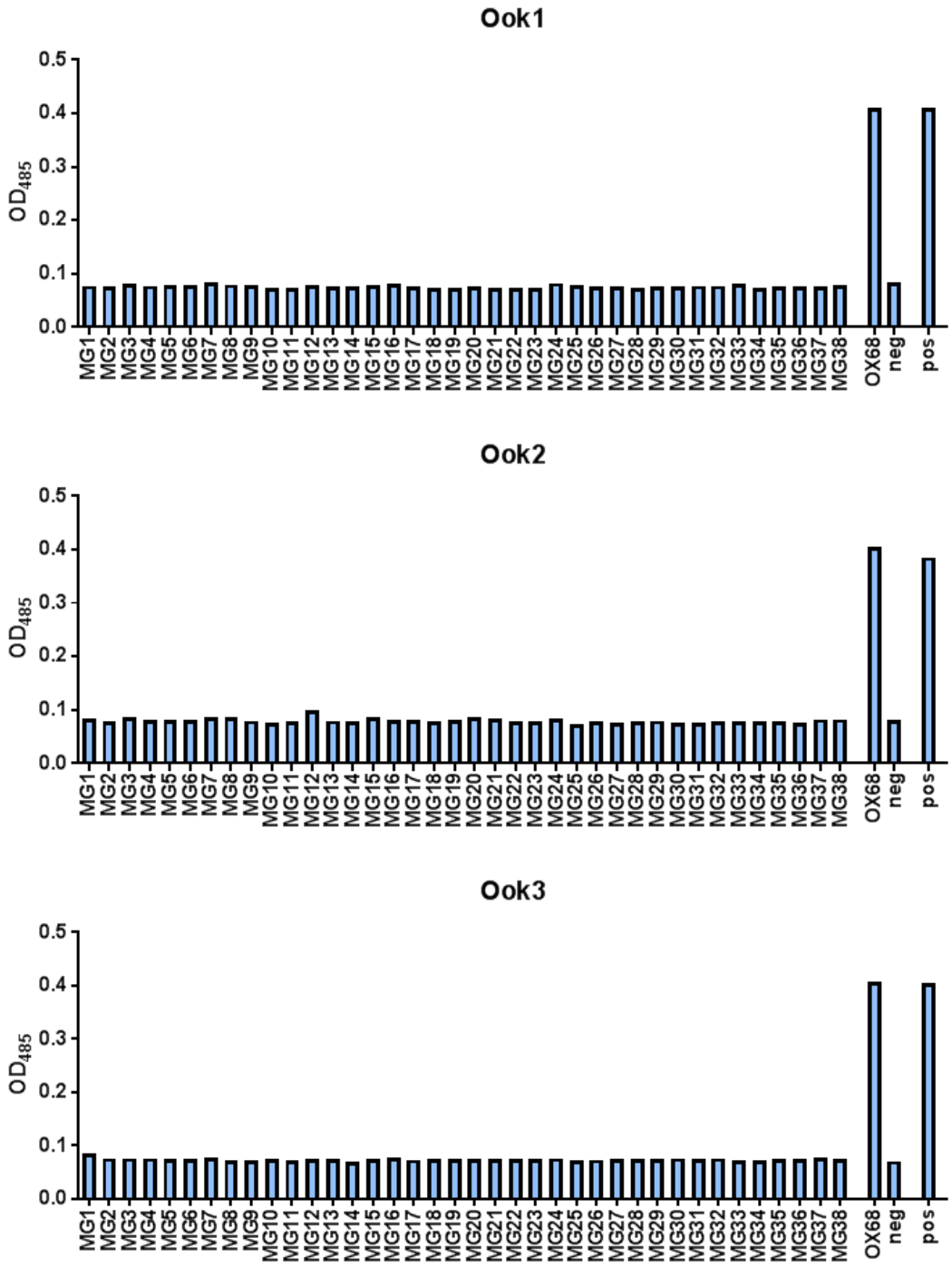

Figure 5.4: AVEXIS of Ook1, Ook2 and Ook3 against all 38 midgut proteins. Midgut bait proteins were coupled to streptavidin coated microtire plates and probed with pentameric prey proteins. Nitrocefin hydrolysis catalysed by the beta-lactamase of the prey proteins was assessed by measuring OD485 2 hours after addition of substrate to the plate. Biotinylated OX68 was coupled to the plate to confirm the presence of prey proteins. As a negative control (neg) Bait+ was coupled to the plate and probed with the ookinete prey protein. As a positive control (pos) Bait+ was coupled to the plate and probed with Prey+.

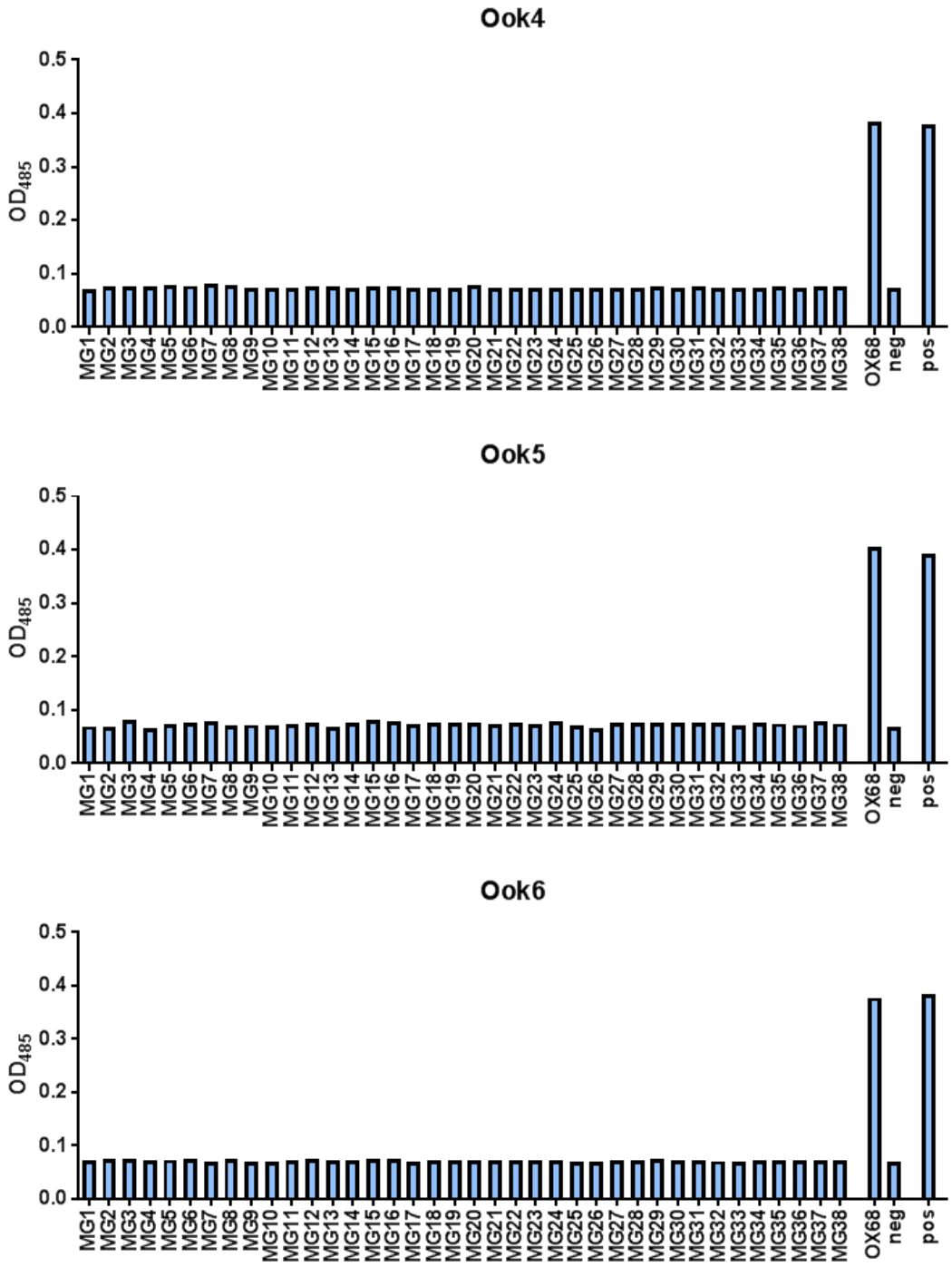

Figure 5.5: AVEXIS of Ook4, Ook5 and Ook6 against all 38 midgut proteins. Midgut bait proteins were coupled to streptavidin coated microtire plates and probed with pentameric prey proteins. Nitrocefin hydrolysis catalysed by the beta-lactamase of the prey proteins was assessed by measuring OD485 2 hours after addition of substrate to the plate. Biotinylated OX68 was coupled to the plate to confirm the presence of prey proteins. As a negative control (neg) Bait+ was coupled to the plate and probed with the ookinete prey protein. As a positive control (pos) Bait+ was coupled to the plate and probed with Prey+.

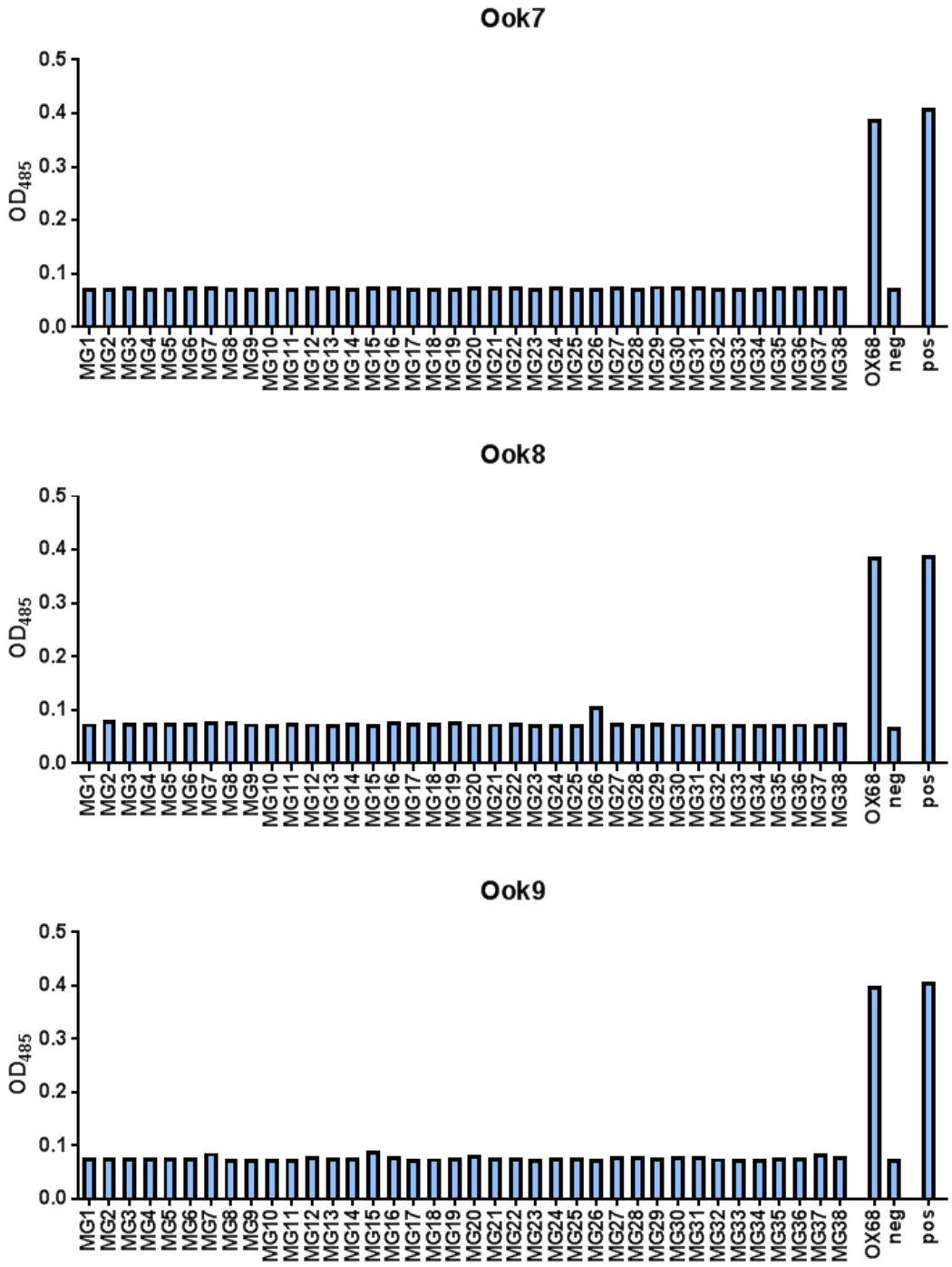

Figure 5.6: AVEXIS of Ook7, Ook8 and Ook9 against all 38 midgut proteins. Midgut bait proteins were coupled to streptavidin coated microtire plates and probed with pentameric prey proteins. Nitrocefin hydrolysis catalysed by the beta-lactamase of the prey proteins was assessed by measuring OD485 2 hours after addition of substrate to the plate. Biotinylated OX68 was coupled to the plate to confirm the presence of prey proteins. As a negative control (neg) Bait+ was coupled to the plate and probed with the ookinete prey protein. As a positive control (pos) Bait+ was coupled to the plate and probed with Prey+.

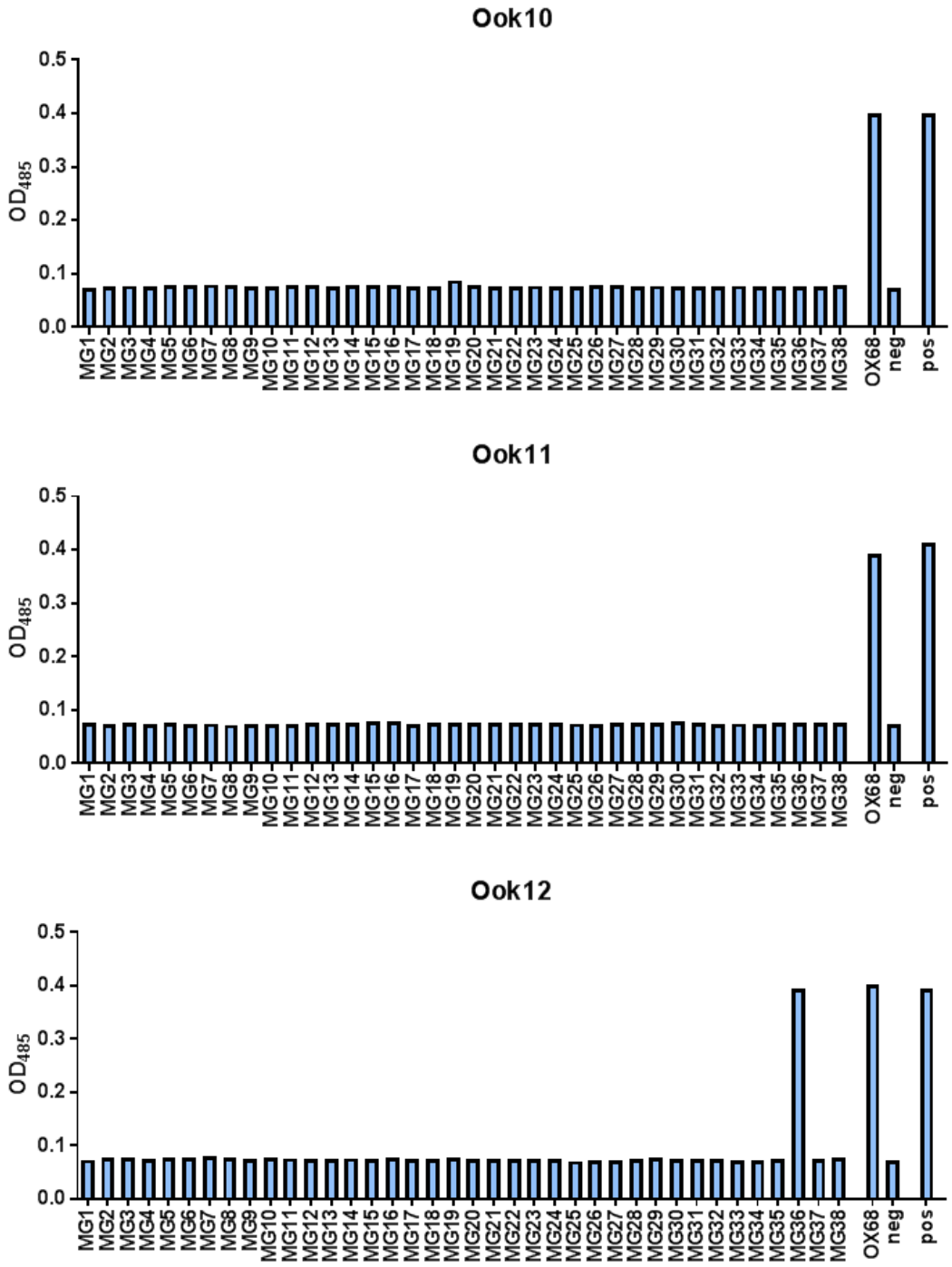

Figure 5.7: AVEXIS of Ook10, Ook11 and Ook12 against all 38 midgut proteins. Midgut bait proteins were coupled to streptavidin coated microtire plates and probed with pentameric prey proteins. Nitrocefin hydrolysis catalysed by the beta-lactamase of the prey proteins was assessed by measuring OD485 2 hours after addition of substrate to the plate. Biotinylated OX68 was coupled to the plate to confirm the presence of prey proteins. As a negative control (neg) Bait+ was coupled to the plate and probed with the ookinete prey protein. As a positive control (pos) Bait+ was coupled to the plate and probed with Prey+.

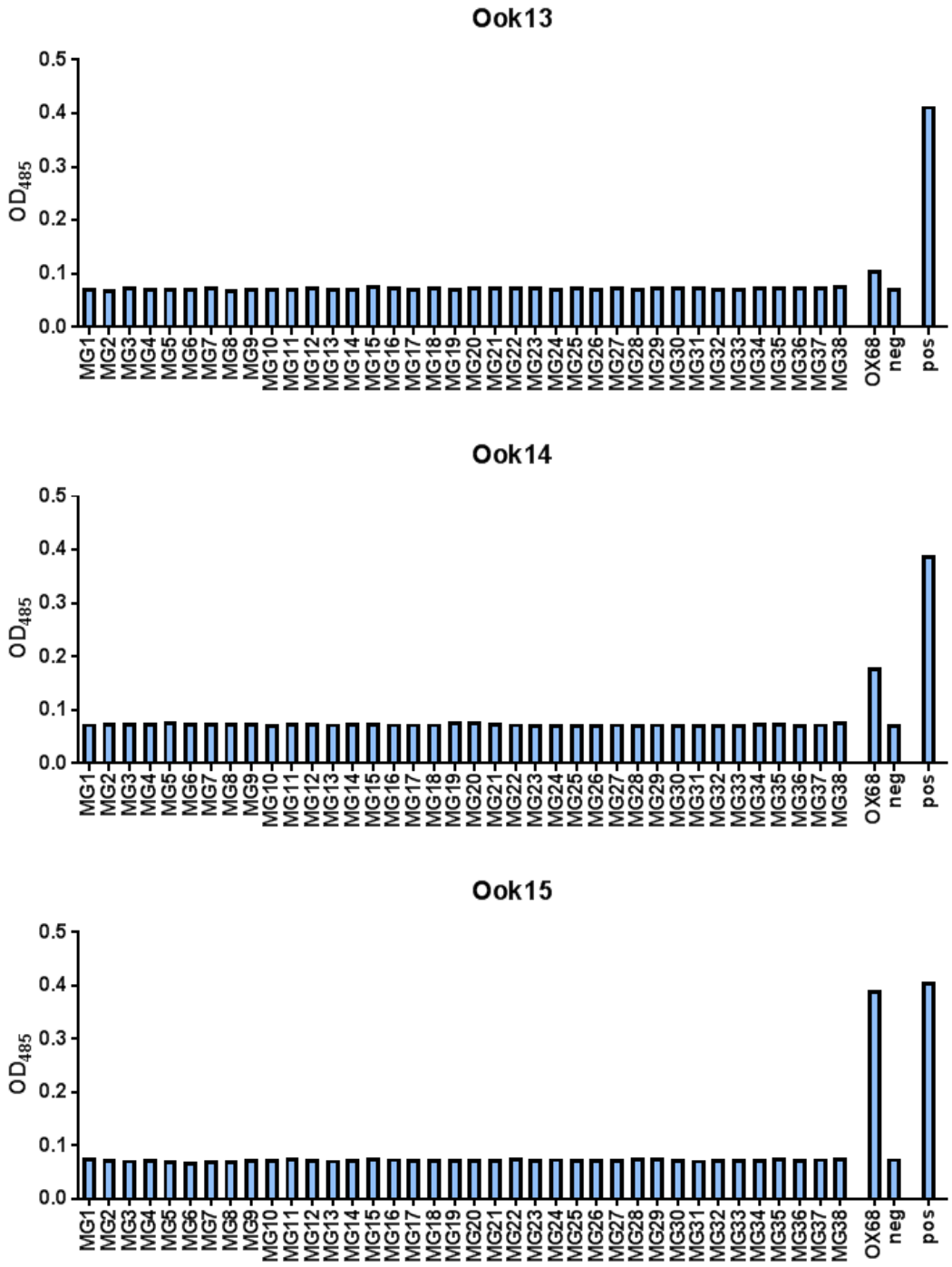

Figure 5.8: AVEXIS of Ook13, Ook14 and Ook15 against all 38 midgut proteins. Midgut bait proteins were coupled to streptavidin coated microtire plates and probed with pentameric prey proteins. Nitrocefin hydrolysis catalysed by the beta-lactamase of the prey proteins was assessed by measuring OD485 2 hours after addition of substrate to the plate. Biotinylated OX68 was coupled to the plate to confirm the presence of prey proteins. As a negative control (neg) Bait+ was coupled to the plate and probed with the ookinete prey protein. As a positive control (pos) Bait+ was coupled to the plate and probed with Prey+.

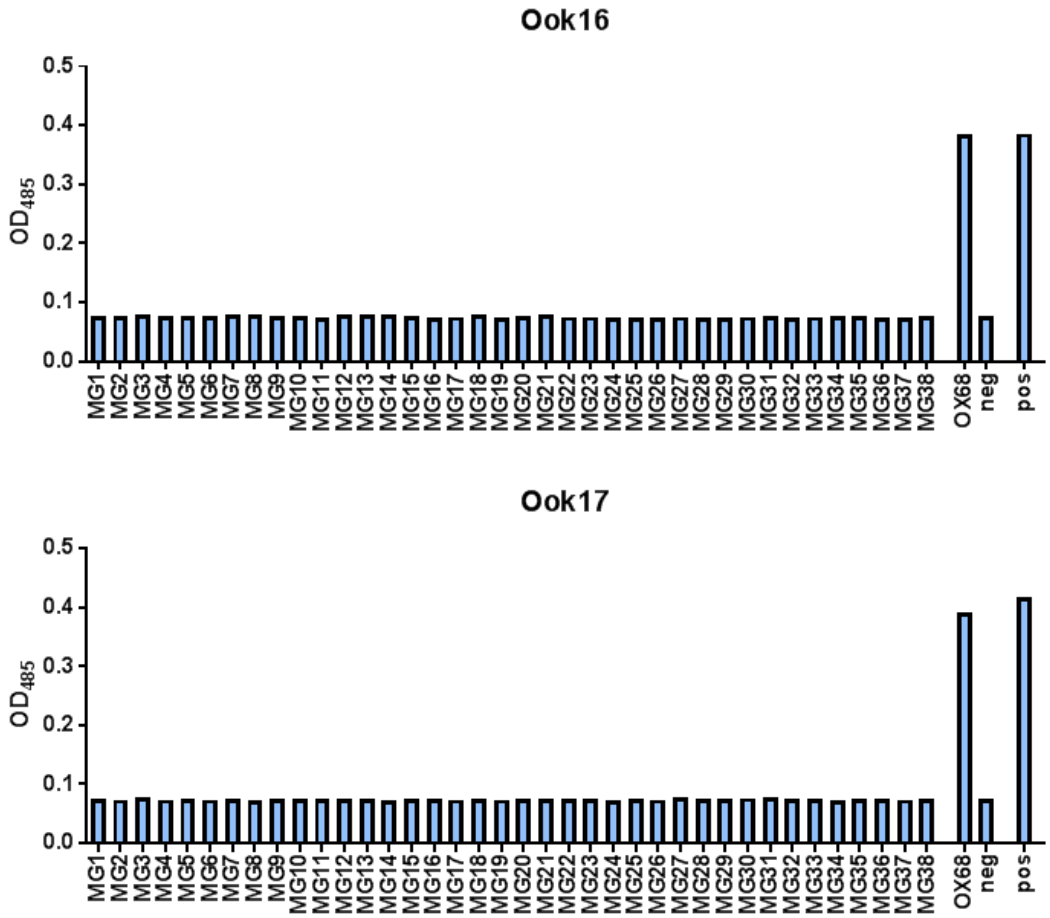

Figure 5.9: AVEXIS of Ook16 and Ook17 against all 38 midgut proteins. Midgut bait proteins were coupled to streptavidin coated microtire plates and probed with pentameric prey proteins. Nitrocefin hydrolysis catalysed by the beta-lactamase of the prey proteins was assessed by measuring OD485 2 hours after addition of substrate to the plate. Biotinylated OX68 was coupled to the plate to confirm the presence of prey proteins. As a negative control (neg) Bait+ was coupled to the plate and probed with the ookinete prey protein. As a positive control (pos) Bait+ was coupled to the plate and probed with Prey+

On all plates the positive control interaction, between rat CD200 and the rat CD200 receptor, showed saturation of signal within two hours of incubation at room temperature, indicating that there were no issues with the assay. On all plates apart from the ones that used Ook13 and Ook14 as prey proteins (***Figure 5.8***), a well coated with biotinylated OX68 reached a similar absorption as the positive control interaction, indicating that sufficient amounts of prey protein were present to catalyse the hydrolysis of nitrocefin, provided there was an interaction between the prey and one

of the bait proteins. Ook13 and Ook14 did not reach saturation of signal in the OX68 control well, therefore there is a high potential for false negative results in their interaction screens. A signal was considered as positive when the OD485 was higher than the average OD485 within the same screen plus five times the standard deviation.

Out of a total of 646 potential interactions, one was detected as positive. The interaction of Ook12 (Pfs28) and MG36 (***Figure 5.7***) produced a signal comparable to the signal of the positive control. Both of the involved proteins passed all the control criteria, i.e. a single band of high intensity was detected in the Western blot for both constructs, and the prey protein was detected in the OX68 control well, indicating that the observed signal was due to a specific interaction of the two proteins. The only other protein pair to show a positive signal, albeit a much weaker one, was Ook8 and MG26 but this was lost when the plates were read a second time after 24 hours of incubation at 4°C. Ook8 had been detected in the OX68 control well with high intensity, but could only be detected as a band of faint intensity in the prey-protein Western blot. Furthermore, in the bait-protein Western blot there were multiple bands observed for MG26. A better quality preparation of both proteins could therefore give a clearer indication whether these two proteins are potential interactors or not. At the time of writing of this thesis this had not been pursued further.

To confirm the interaction of Pfs28 with MG36 the assay was repeated two more times (***Figure 5.10*** **A**). The results were very similar to the original AVEXIS assay, therefore confirming the interaction. Furthermore, the two proteins were expressed in

the reverse orientation, i.e MG36 as prey- and Pfs28 as bait-protein. The expression levels of the two proteins were quantified by nitrocefin assay and CD4-Tag ELISA (Table 5.4).

Table 5.4: Dilution factor and molecular weight of Pfs28-bait and MG36-prey

sample	dilution factor	MW [Dalton]
Pfs28-bait	50	43878
MG36-prey	2	140306

Expression of the two proteins was furthermore confirmed by Western blot (***Figure 5.10*** **B**). In the Western blot of Pfs28-bait, a band was detected at around 50 kDa, the MW of non-glycosylated Pfs28-bait was calculated to be 44kDa and is therefore likely to be the detected band. In the Western blot of MG36-prey, a band was detected at around 140 kDa corresponding to the calculated MW of MG36-prey. AVEXIS between the two proteins was repeated in the reverse configuration (***Figure 5.10*** **C**). Again, the interaction between Pfs28 and MG36 was detected with similar signal intensity to the positive control, further confirming this result.

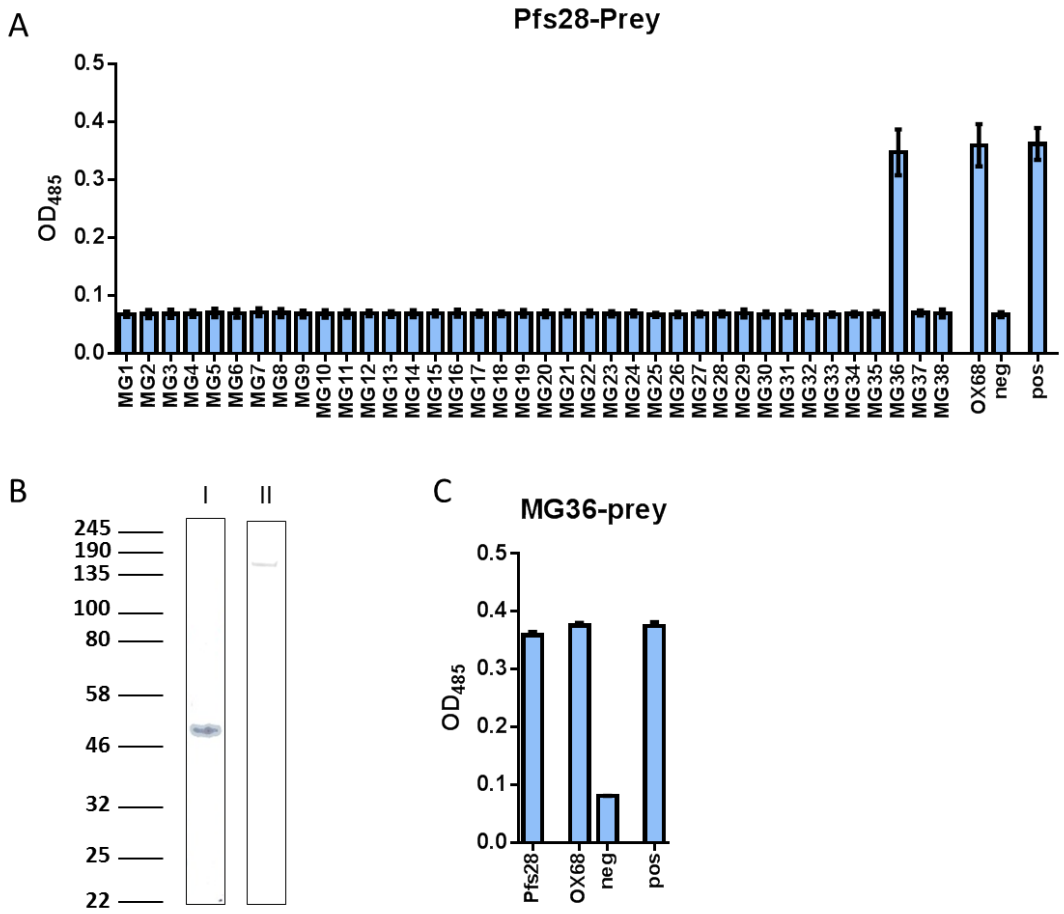

Figure 5.10: Confirmation of the Pfs28-MG36 interaction. **A** The Ook12 (Pfs28) AVEXIS was repeated two more times and the data pooled with the first AVEXIS to confirm the interaction between Pfs28 and MG36. Bars show mean of three replicates, error bars show standard deviation. **B** Western blot of Pfs28-bait and MG36-prey. Pfs28-bait (lane I) and MG36-prey (lane II) were electrophoresed on a 4-12% bis-Tris SDS polyacrylamide gel and detected by anti CD4-Tag Western blot. **C** Pfs28-MG36 reverse orientation AVEXIS. Monobiotinylated Pfs28-bait was coupled to a streptavidin coated microtire plate and probed with pentameric MG36-prey. Nitrocefin hydrolysis catalysed by the beta-lactamase of MG36-prey was assessed by measuring OD485 2 hours after addition of substrate to the plate. Biotinylated OX68 was coupled to the plate to confirm the presence of MG36-prey. As a negative control (neg) Bait+ was coupled to the plate and probed with MG36-prey. As a positive control (pos) Bait+ was coupled to the plate and probed with Prey+.

5.2.4 Characterisation of the Pfs28-MG36 interaction

To further characterise the interaction between Pfs28 and MG36, the two proteins were expressed as His-tagged monomeric proteins by subcloning them into the pExpreS2-KanPac-BirA-His backbone. After purification of the His-tagged proteins from the supernatant of transiently transfected S2 cells by immobilised metal ion affinity

chromatography (IMAC) followed by size exclusion chromatography (SEC) both proteins could be obtained at high purity as assessed by coomassie staining of polyacrylamide gels (***Figure 5.11*** **A**).

To quantify the interaction by surface plasmon resonance (SPR), monobiotinylated Pfs28-bait was coated to a CAP chip and purified MG36 was flowed over the chip at decreasing concentrations (***Figure 5.11*** **B**). The assay was performed three times using protein from two different batches of expression and purification. Analysis of the steady state signal revealed an affinity in the lower range of physiological interactions (K_D = 12.8 ± 1.8 µM) (***Figure 5.11*** **C**). The kinetics of the interaction could not be determined from the obtained data set, due to the high amount of immobilised ligand.

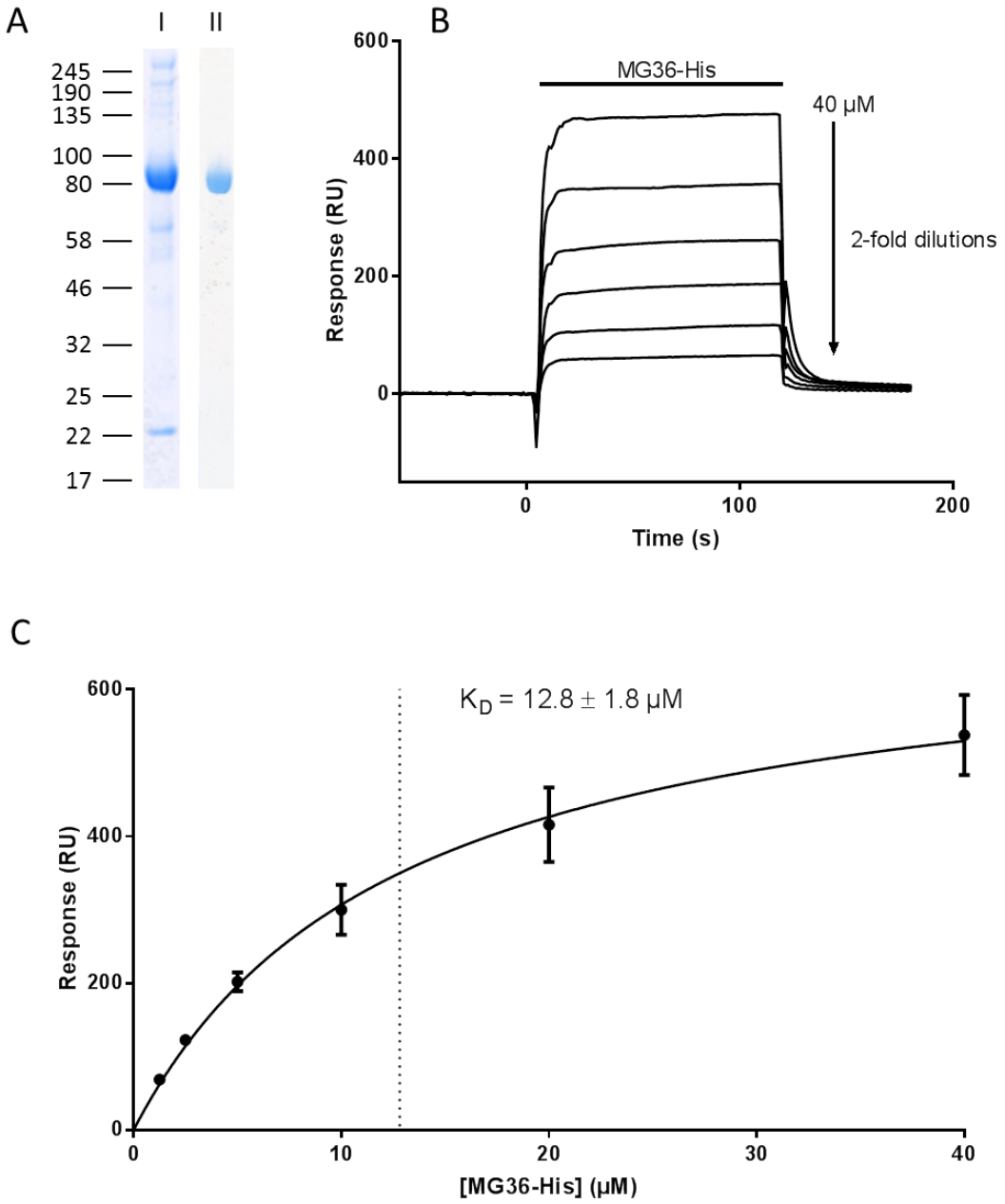

Figure 5.11: Characterisation of the Pfs28-MG36 interaction. **A** Coomassie gel of MG36-His. MG36-His after Ni-NTA chromatography (lane I) and after SEC (lane II) was electrophoresed on a 4-12% bis-Tris SDS polyacrylamide gel and then stained with Coomassie stain. **B** SPR sensograms of MG36-Pf28 interaction. Purified MG36-His was flowed over a CAP chip coated with monobiotinylated Pfs28-bait. Response is the difference in signal between MG36-His flowed over Pfs28 coupled to the CAP chip and MG36-His flowed over the chip without any coupled protein. **C** Steady state affinity analysis of the Pfs28-MG36 interaction. Response units at steady state were plotted against the concentration of MG36-His to determine the affinity of the interaction. Data points show mean of three replicates, error bars show standard deviation. KD was determined by fitting the data as One-site specific-binding in GraphPad Prism7.

5.2.5 Pfs28 only binds to full length MG36, not to either of its two transferrin like domains

Sequence homology and structure prediction of MG36 by Phyre2 revealed that its ectodomain comprises two transferrin like (TFL) domains (***Figure 5.12***). The two TFL domains make up most of the whole protein, which is anchored within the membrane by a single transmembrane helix at the extreme C-Terminus with only 3 amino acids protruding into the cytosol. To determine whether the binding to Pfs28 was facilitated through one of these two domains, both TFLs were expressed as bait proteins to analyse binding to Pfs28-prey by AVEXIS.

Both proteins could be expressed from transiently transfected S2 cells and expression level was determined by anti-CD4 Tag ELISA (Table 5.5). Subsequent analysis by Western blot using streptavidin conjugated alkaline phosphatase detected a band at around 70 kDa for TFL1-bait and a band of around 80 kDa for TFL2-bait. The MW of TFL1-bait without N-glycans was calculated to be 61 kDa and the MW of TFL2-bait without N-glycans was calculated to be 67 kDa. As TFL1 contains two and TFL2 contains three N-glycosylation sites the detected bands are likely to contain the two proteins (***Figure 5.12*** **D**).

Table 5.5: Relative expression level and molecular weight of MG36-TFL-bait proteins

sample	dilution factor	MW [Dalton]
MG36-TFL1-bait	100	60918
MG36-TFL2-bait	100	67254

Surprisingly, despite binding full length MG36 to similar signal intensity as observed in the positive control interaction, no interaction could be detected between Pfs28 and

any of the individual TFL domains (***Figure 5.12***). This indicates that both TFL domains are required together to efficiently bind Pfs28.

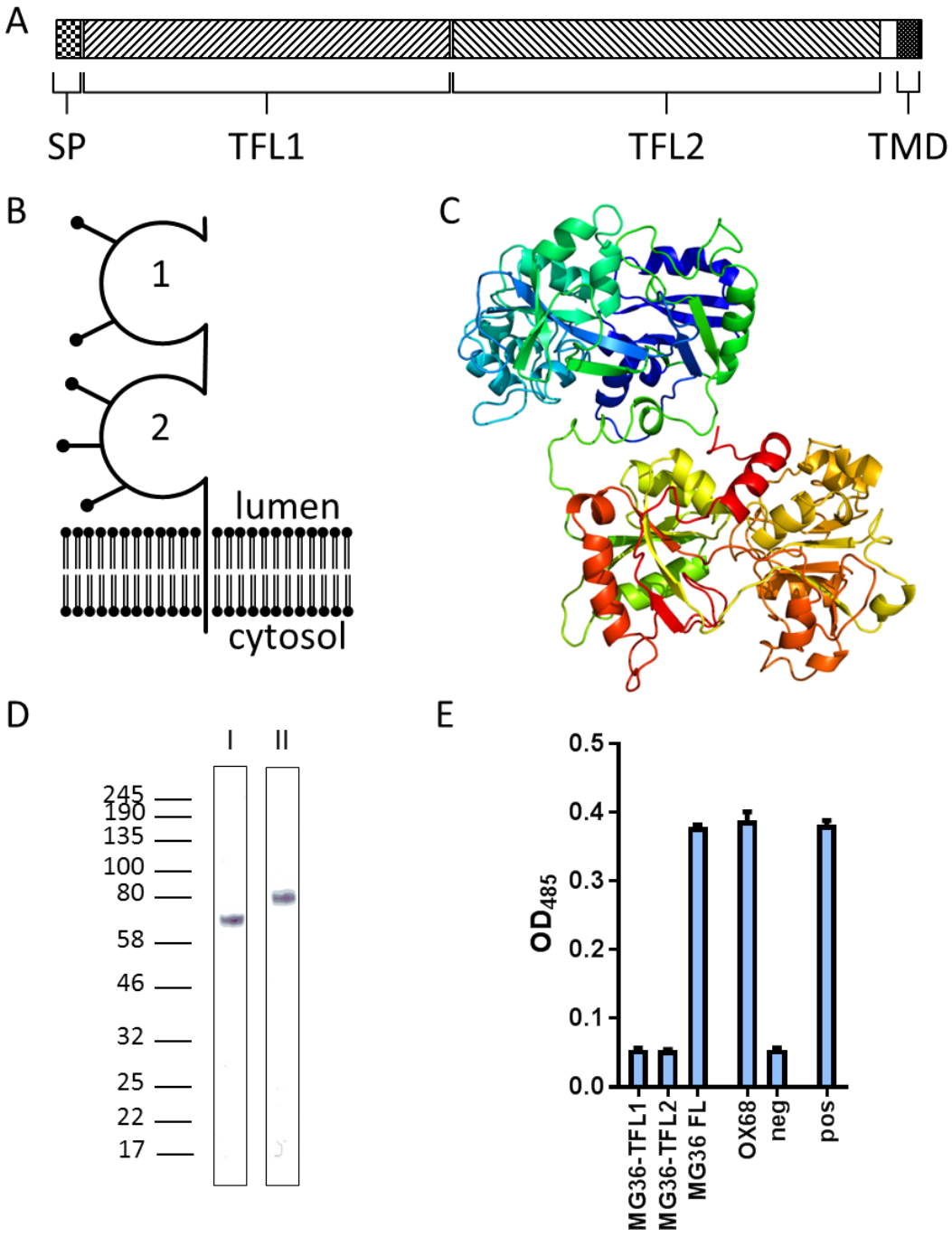

Figure 5.12: MG36 is made up of two Transferrin like domains, which are both required for binding of Pfs28. **A** Linear domain structure of MG36, bars are proportional to number of amino acids in each domain. SP = signal peptide, TFL = Transferrin like domain, TMD = Transmembrane domain. **B** Cartoon depiction of MG36 and its orientation in the membrane of the midgut epithelium. TFL domains are depicted as loops, balls and sticks indicate potential N-glycosylation sites. **C** 3D structure model of MG36 by homology modelling using Phyre2. **D** Western blot of TFL1 and TFL2 bait proteins. TFL1-bait

(lane I) and TFL2-bait (lane II) were electrophoresed on a 4-12% bis-Tris SDS polyacrylamide gel and detected by Western blot using streptavidin conjugated alkaline phosphatase. **E** Pfs28-MG36-TFL-domain AVEXIS. Monobiotinylated TFL1- and TFL2-bait was coupled to a streptavidin coated microtire plate and probed with pentameric Pfs28-prey. Nitrocefin hydrolysis catalysed by the beta-lactamase of Pfs28-prey was assessed by measuring OD485 2 hours after addition of substrate to the plate. Biotinylated OX68 was coupled to the plate to confirm the presence of Pf28-prey. As a negative control (neg) Bait+ was coupled to the plate and probed with Pfs28-prey. As a positive control (pos) Bait+ was coupled to the plate and probed with Prey+.

5.2.6 The interaction of Pfs28 and MG36 can be specifically inhibited by anti-Pfs28 antibodies

To assess whether the transmission blocking activity of anti-Pfs28 antibodies could be due to their ability to inhibit binding of Pfs28 to MG36, AVEXIS was performed in the presence of increasing concentrations of anti-Pfs28 IgG from a rabbit that had previously shown transmission blocking activity in SMFA. Whole IgG was purified over a protein G column from serum of a rabbit immunised with one dose of AdCh63-Pfs28 followed by one dose of MVA-Pfs28 and the concentration determined by measuring absorption at 280 nm. The ability of the purified IgG to interfere with the interaction of Pfs28 and MG36 was used in an IgG competition AVEXIS. This showed that anti-Pfs28 antibodies inhibited the interaction of Pfs28 and MG36 in a dose dependent manner, while having no effect on the interaction of the two AVEXIS control proteins (***Figure 5.13*** **A**). To confirm the transmission blocking activity of the rabbit IgG used in this experiment it was tested in SMFA (***Figure 5.13*** **B**). Interestingly an IgG concentration of 166 µg/ml was sufficient to completely block all interaction between MG36 and Ook12 in AVEXIS, while an IgG concentration of 1500 µg/ml only reduced the number of oocysts in SMFA by 67%. Nonetheless, this gives a first indication that interference with the binding of Pfs28 to MG36 could be partially responsible for the transmission blocking activity of anti-Pfs28 antibodies.

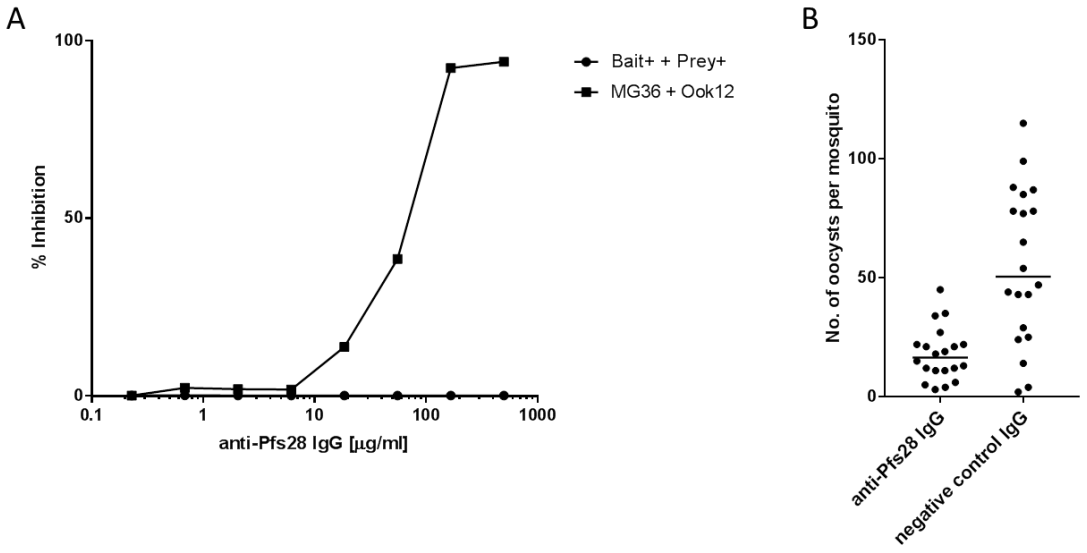

Figure 5.13: Anti-Pfs28 antibodies specifically inhibit the interaction of Pfs28 with MG36. **A** Anti-Pfs28 SMFA. Total IgG was purified from serum of a rabbit immunised with one dose of AdCh63-Pfs28 followed by one dose of MVA-Pfs28 and then tested in SMFA. IgG from a rabbit immunized with viral vectors encoding an irrelevant antigen (PfRH4) was used as negative control. **B** Anti Pfs28 rabbit IgG AVEXIS. Monobiotinylated MG36-bait was coupled to a streptavidin coated microtire plate and probed with pentameric Pfs28-prey in the presence of increasing concentrations of anti-Pfs28 rabbit-IgG. As a negative control Bait+ was coupled to the plate and probed with Prey+ in the presence of identical concentrations of anti Pfs28-IgG. Nitrocefin hydrolysis catalysed by the beta-lactamase of Pfs28-prey was assessed by measuring OD485 2 hours after addition of substrate to the plate. Inhibition was calculated as the reduction in signal intensity relative to the signal in the absence of anti-Pfs28 IgG.

5.2.7 Assessment of MG36 as a novel target for transmission blocking vaccines

As transmission blocking anti-Pfs28 antibodies interfered with the interaction between Pfs28 and MG36, it was assessed whether antibodies against MG36 exhibited transmission blocking activity of their own. Two groups of BALB/c mice (n = 5 per group) were primed by intramuscular administration of 3 µg Pfs28 or 3 µg MG36 in Addavax, respectively. 21 and 42 days later mice were boosted with the same vaccine formulation. Serum samples were collected on day 20 (prime), day 41 (1st boost) and day 63 (2nd boost) and the immune response assessed over the course of immunisation by ELISA (***Figure 5.14***).

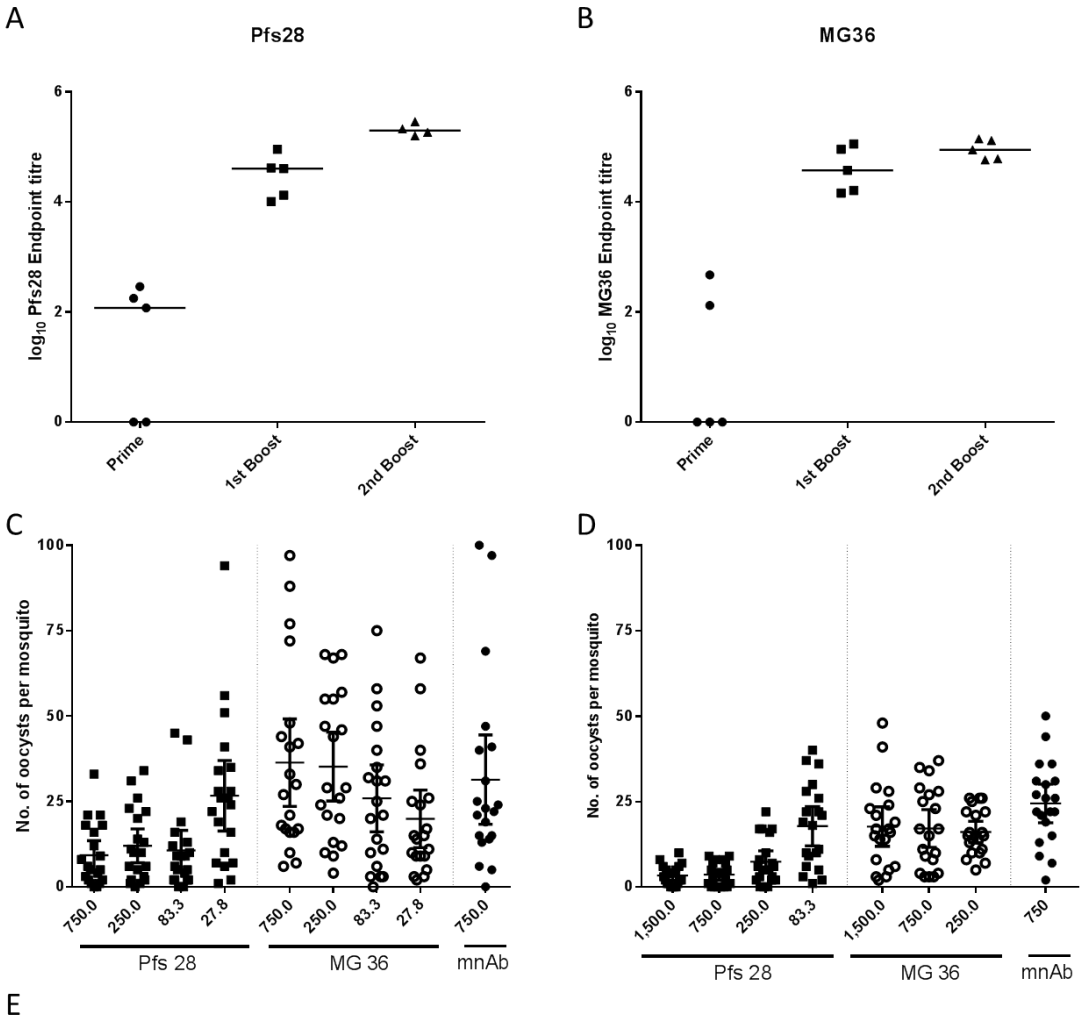

E

Sample name		Control	Pfs28					MG36				
IgG conc [ug/ml]		750	1500	750	250	83.3	27.8	1500	750	250	83.3	27.8
SMFA 1	Average Oocyst count	31.4		9.3	12.0	10.7	26.7		36.35	35.2	25.9	19.9
	TRA (%)			70.5	61.7	66.0	15.0		-15.9	-12.3	17.4	36.5
	p			0.005	0.019	0.010	0.671		0.713	0.765	0.672	0.268
SMFA 2	Average Oocyst count	24.5	3.4	3.6	7.4	17.8		17.7	17.1	16.1		
	TRA (%)		86.3	85.3	69.7	27.2		27.8	30.1	34.2		
	p		0.001	0.001	0.005	0.439		0.436	0.356	0.274		

Figure 5.14: Assessment of MG36 as a novel target for transmission blocking vaccines. **A** The total IgG response against Pfs28 in mice immunised with Pfs28 was assessed by Pfs28 endpoint ELISA. **B** The total IgG response against MG36 in mice immunised with MG36 was assessed by MG36 endpoint ELISA. **C** To assess the transmission blocking activity of the induced antibodies, total IgG was purified from pooled day 63 serum samples and tested in SMFA. **D** The SMFA was repeated once at higher IgG concentrations to confirm the results of the first assay. Data points show the number of oocysts in individual mosquitoes and the lines show the median. Mouse normal antibody was used as negative control. **E** Average number of oocysts per mosquito and percentage of transmission reducing activity. The p-value is in respect to the negative control.

Immunisation with both antigens induced a detectable antibody response in some of the mice after the first, and in all mice after the second immunisation, which was further increased by the third immunisation (***Figure 5.14*** **A,B**). As antibody responses against both antigens were high, IgG purified from pooled serum from after the second boost was assessed for transmission blocking activity by SMFA (***Figure 5.14*** **C,D**). As expected, antibodies against Pfs28 showed significant transmission blocking activity at higher IgG concentrations over both feeds. Unfortunately, antibodies against MG36 did not show any significant transmission blocking activity even at the highest tested IgG concentration of 1.5 mg/ml.

The inability of anti-MG36 antibodies to reduce mosquito infection by *P. falciparum* ookinetes could be due to a number of factors. The most likely ones are, the MG36 antibodies being unable to interfere with the Pfs28-MG36 interaction, MG36 being too highly expressed on the midgut epithelium to be completely blocked by anti-MG36 antibodies or the MG36-Pfs28 interaction being redundant for mosquito infection *in vivo*. To discern whether the first or any of the other two hypotheses were responsible for the observed absence of blocking, the IgG competition AVEXIS, previously performed with rabbit anti-Pfs28 IgG, was repeated using anti-Pfs28 and anti-MG36 IgG from the Pfs28/MG36 mouse study (***Figure 5.15***).

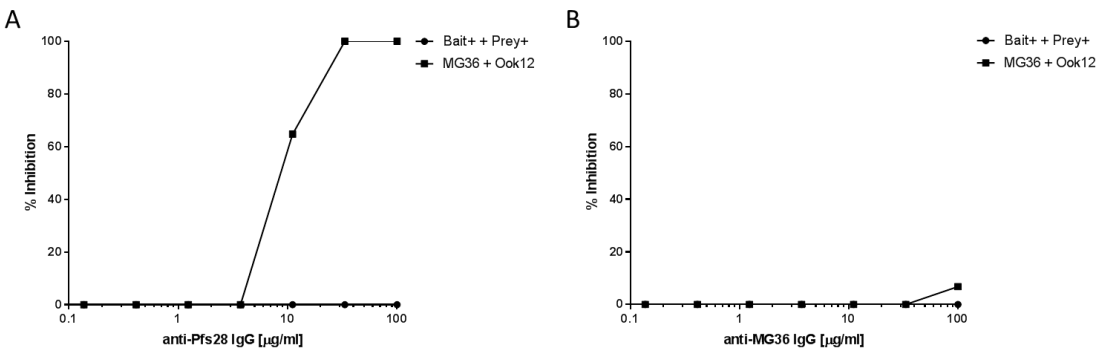

Figure 5.15: Anti-MG36 antibodies are less capable of blocking interaction between MG36 and Pfs28 than anti-Pfs28 antibodies. **A** Anti-Pfs28 mouse IgG AVEXIS. Monobiotinylated MG36-bait was coupled to a streptavidin coated microtire plate and probed with pentameric Pfs28-prey in the presence of increasing concentrations of anti-Pfs28 mouse-IgG. As a negative control Bait+ was coupled to the plate and probed with Prey+ in the presence of identical concentrations of anti Pfs28-IgG. Nitrocefin hydrolysis catalysed by the beta-lactamase of Pfs28-prey was assessed by measuring OD485 2 hours after addition of substrate to the plate. Inhibition was calculated as the reduction in signal intensity relative to the signal in the absence of anti-Pfs28 IgG. **B** Anti-MG36 mouse IgG AVEXIS. Monobiotinylated MG36-bait was coupled to a streptavidin coated microtire plate and probed with pentameric Pfs28-prey in the presence of increasing concentrations of anti-MG36 mouse-IgG. As a negative control Bait+ was coupled to the plate and probed with Prey+ in the presence of identical concentrations of anti MG36-IgG. Nitrocefin hydrolysis catalysed by the beta-lactamase of the prey proteins was assessed by measuring OD485 2 hours after addition of substrate to the plate. Inhibition was calculated as the reduction in signal intensity relative to the signal in the absence of anti-MG36 IgG.

Interestingly, while anti-Pfs28 IgG showed 100% inhibition at 33 µg/ml, even at 100 µg/ml anti-MG36 IgG only showed 6% inhibition. This suggests that antibodies directed against MG36 interfere with the interaction between MG36 and Pfs28 much less efficiently than antibodies directed against Pfs28, explaining why no transmission blocking activity could be detected in SMFA when anti-MG36 IgG tested.

5.2.8 Knockdown of *MG36* in mosquitoes reduces their susceptibility to malaria infection

To determine the importance of the interaction between Pfs28 and MG36 for infection of the mosquito by *P. falciparum in vivo*, *MG36* was knocked down in *A.gambiae*

mosquitoes using RNAi, and the effect on the susceptibility of mosquitoes to malaria infection was assessed as described in 2.5.7.

The DNA template for the generation of *MG36*-dsRNA required for the knock down was generated by PCR from *A. gambiae* cDNA. Primers were designed using E-RNAi [264] to amplify a 520 nucleotide amplicon in the third exon of the *MG36* gene AGAP011453. Both primers contained a T7 promotor sequence to allow the generation of dsRNA from the PCR product using T7 RNA polymerase. Out of the 502 potential siRNAs that could be diced from the obtained dsRNA one was predicted to have off target activity, targeting gene products of AGAP003702. After purification of the dsRNA it was concentrated by vacuum centrifugation to a concentration of 3 ug/ul, and 69 nl were injected into mosquitoes using a microinjection pipet. *LacZ* dsRNA of a similar concentration was injected into negative control mosquitoes. Two days after injecting the dsRNA, midguts and whole bodies were collected from a fraction of the mosquitoes for RNA extraction and knock down quantification by qPCR (***Figure 5.16***). The remaining mosquitoes (n = 100 per group) were fed on *P. falciparum* NF54 cultured gametocytes through a membrane feeder. Mosquitoes were starved for 24 hours after the membrane feed to remove unfed mosquitoes. Seven days after the membrane feed midguts were dissected, stained with mercurochrome and oocysts were counted to assess the effect of the knock down on oocyst formation (***Figure 5.16***).

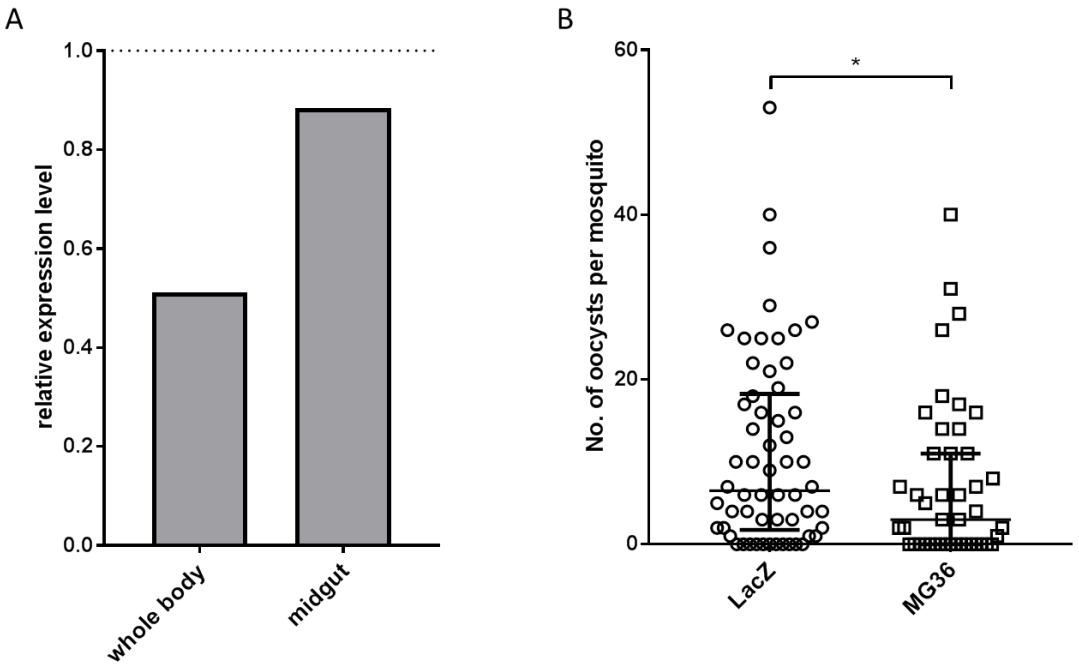

Figure 5.16: Knockdown of MG36 reduces the susceptibility to malaria infection in A. gambiae mosquitoes. **A** Relative expression levels of *MG36* in whole bodies and midguts after knockdown by RNAi. RNA was extracted from 15 whole mosquitoes and 15 midguts two days after injection with *MG36* and lacZ dsRNA, respectively. Relative expression was calculated as the ratio of mRNA in mosquitoes injected with *MG36* dsRNA and mosquitoes injected with lacZ dsRNA. **B** Effect of *MG36* knock down on oocyst formation in mosquito midguts. Mosquitoes were injected with *MG36* or lacZ dsRNA. Two days later mosquitoes were fed *P. falciparum* NF54 cultured gametocytes through a membrane feeder. Seven days after the feed midguts were dissected and oocysts counted.

At the time of feeding, mRNA levels of *MG36* were reduced by 49% in the whole body of mosquitoes, but only by 10% in the midgut (***Figure 5.16*** **A**). Nonetheless, even this modest knock down of *MG36* reduced the median number of oocysts in the mosquito midgut by 54% (***Figure 5.16*** **B**), indicating that MG36 plays an important role in the process of midgut infection by *P. falciparum* ookinetes.

5.2.9 The interaction of P28 and MG36 cannot be detected in other parasite-vector pairs

Considering that the interaction between Pfs28 and MG36 seems to play a role in the infection of A*. gambiae* by P*. falciparum*, it was assessed whether the interaction of these two proteins was conserved over orthologous vector-parasite pairs. Pfs28 is a highly conserved protein with an orthologue in all *Plasmodium* species listed in PlasmoDB. MG36 (AGAP011453) is also highly conserved, with orthologues in 17 out of the 18 *Anopheles* species listed in VectorBase. To initially assess whether the interaction between the two proteins constitutes a conserved mechanism for the infection of mosquito vectors by other P*lasmodium* parasites, it was assessed whether the interaction of the two proteins were also detected between *P. vivax* and *A. albimanus* as well as between *P. berghei* and *A. stephensi*. An alignment of the orthologous proteins showed the high degree of conservation in the sequences of the mosquito and parasite proteins (***Figure 5.17***). The optimised genes for expression in *Drosophila* cells for Pbs21, Pvs28 as well as *A. stephensi* and *A. albimanus* MG36 were synthesised by GeneArt and cloned into the AVEXIS prey and bait expression plasmids, respectively to screen for interactions between them by AVEXIS.



Figure 5.17: Sequence alignment of P28 and MG36 from three parasite-vector pairs. **A** Protein sequence alignment of MG36 from *A. albimanus* (top), *A. gambiae* (middle) and *A. stephensi* (bottom). **B** Protein sequence alignment of Pfs28 (*P. falciparum,* top), Pvs28 (*P. vivax, middle*) and Pbs21 (*P. berghei,* bottom). Black shading indicates sequence identity, grey shading indicates sequence similarity.

All four proteins could be expressed from transiently transfected S2 cells and were quantified by nitrocefin assay and CD4-Tag ELISA. Expression of the normalised proteins was confirmed by Western blot and the proteins then used in AVEXIS to screen for interactions between orthologues.

Table 5.6: Dilution factor and molecular weight of MG36 and Pfs28 orthologous proteins for AVEXIS

sample	dilution factor	MW [Dalton]
A. stephensi MG36-bait	50	105646
A. albimanus MG36-bait	50	104998
Pfs21-prey	100	76924
Pvs28-prey	100	78651

All bait and prey proteins were detected at the expected sizes in Western blot (***Figure 5.18*** **A**) and all prey proteins were captured in sufficient levels in the OX68 control wells on the AVEXIS plates but no interactions could be detected between any of the MG36 and Pfs28 orthologues (***Figure 5.18*** **B,C,D**).

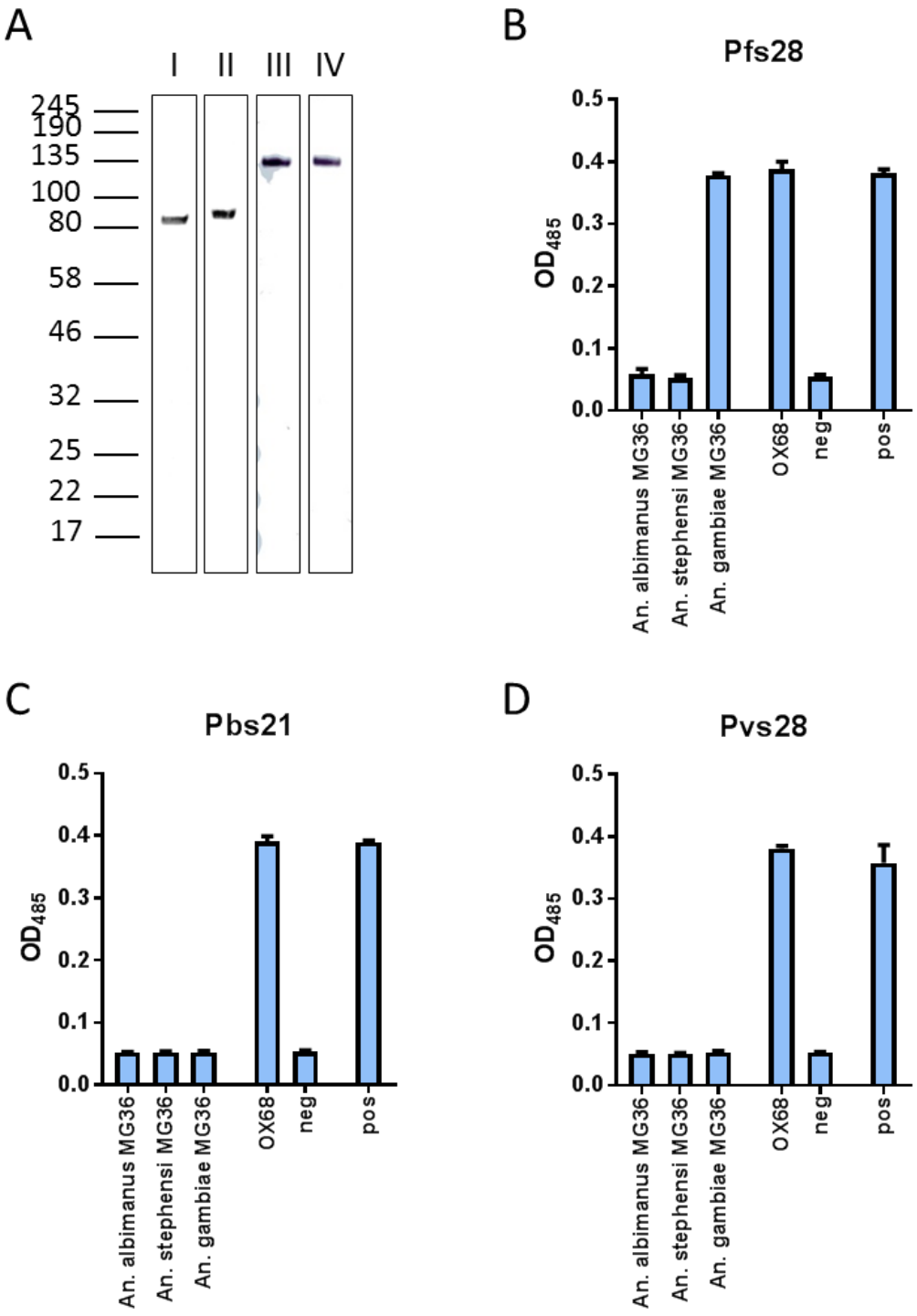

Figure 5.18: Interaction between P28 and MG36 were not detected in other parasite-vector pairs. **A** Western blot of MG36 and Pfs28 orthologous proteins used in AVEXIS. Pbs21-prey (lane I), Pvs28-prey (lane II) A. albimanus MG36-bait (lane III) and A. stephensi MG36-bait (lane IV) were electrophoresed on a 4-12% bis-Tris SDS polyacrylamide gel and detected by anti CD4-Tag western blot. **B,C,D** Orthologous Pfs28-MG36 AVEXIS. Monobiotinylated MG36-bait proteins were coupled to a streptavidin coated microtire plate and probed with pentameric Pfs28-prey proteins. Nitrocefin hydrolysis catalysed by the beta-lactamase of the Pfs28-prey was assessed by measuring OD485 2 hours after addition of substrate to the plate. Biotinylated OX68 was coupled to the plate to confirm the presence of Pf28-prey. As a negative control (neg) Bait+ was coupled to the plate and probed with Pfs28-prey. As a positive control (pos) Bait+ was coupled to the plate and probed with Prey+.

5.3 Discussion

Ligand receptor interactions are notoriously difficult to identify, often due to very low affinities and associated short half-lives of the interactions [265]. Because of this, entry pathways of *Plasmodium* motile lifecycle stages are to date poorly understood. Some progress has been made recently in identifying proteins involved in merozoite invasion of red blood cells, but hepatocyte traversal and invasion by sporozoites and mosquito midgut traversal by ookinetes are still largely not understood.

A breakthrough in understanding how merozoites invade erythrocytes was the identification of basigin as the receptor for the essential merozoite protein PfRH5 [63]. This discovery was enabled through the development of AVEXIS, a high throughput screening assay specifically designed to detect low affinity interactions [212]. Therefore, to identify ligand receptor pairs involved in mosquito midgut attachment and invasion, an AVEXIS screen was set up with proteins from the ookinete and the mosquito midgut surface. The screening approach widely followed a previously published method [214] but the assay was modified slightly. The biggest change to the experimental procedure was the use of an insect instead of a mammalian cell line for the expression of the AVEXIS proteins. S2 cells were chosen as we had previously used them successfully to express *Plasmodium* proteins that were challenging to express in other systems, such as Rh5 and Pfs48/45. Furthermore, it was hypothesised that glycosylation of mosquito proteins would be more natural when these proteins were expressed in insect cells, which could be important for correct conformation and recognition by potential ligands.

A library of 17 ookinete and 38 midgut surface proteins was compiled based on proteomic data and a review of available literature regarding the invasion and traversal of the mosquito midgut by *Plasmodium* ookinetes (Table 5.1 and Table 5.2). Upon expression in transiently transfected S2 cells biotinylated bait proteins were dialysed and then quantified by anti-CD4-Tag ELISA. Prey proteins were quantified by nitrocefin assay. Based on these quantifications, it appeared that all proteins could be expressed in sufficient quantities from a small culture (<25 ml). To further confirm expression, normalised quantities of the different bait and prey proteins were analysed by Western blot (***Figure 5.3***). Out of the 38 midgut proteins, 31 could be detected at the expected size or with only minor contaminating bands, most likely arising from aggregation or degradation of a small proportion of the protein. Contamination with other proteins non-specifically detected by the antibody is an unlikely cause for these bands, as they are not detected in other samples expressed under similar conditions. Results from AVEXIS using these proteins were considered as reliable. Out of the remaining seven bait proteins four showed signs of more pronounced degradation/aggregation and in three proteins preparations no band of the correct size could be detected. Results from AVEXIS using these proteins would have to be considered more carefully, as false positive results could arise from nonspecific binding to unfolded or aggregated proteins, and false negative results could arise from insufficient amounts or total absence of correctly folded full length protein. Expression of the parasite prey proteins was less successful than expression of the mosquito baits and more than half of them had to be concentrated to reach the required concentration for AVEXIS (in contrast to only 2 out of 38 bait proteins). Furthermore, only 10 out of 17 proteins could be detected in Western blot, three of

them very faintly. Interestingly, despite normalisation, expression levels correlated strongly with detection by Western blot. It is therefore conceivable that the process of concentrating interfered with detection in Western blot, either through loss of sample during the concentration process or through concentration of other factors in the undialysed supernatant. Despite the failure to detect more than a third of the prey-proteins, all of them were used in the following AVEXIS, under the premise that the potential for false negative results was strongly increased in interaction screens involving prey-constructs whose correct expression had not be confirmed by Western blot.

The AVEXIS screen of 646 potential interactions (***Figure 5.4*** - ***Figure 5.9***), identified a previously undescribed interaction between the well characterised transmission blocking antigen Pfs28 and a novel mosquito protein called AGAP011453-PA, or MG36 in the nomenclature of this interaction screen (***Figure 5.7***). The experiment was subsequently repeated in the same, as well as in reverse orientation with Pfs28 as bait and MG36 as prey protein, confirming the interaction between the two proteins *in vitro* (***Figure 5.10***).

To characterise the interaction further, monomeric His-tagged versions of the two proteins were expressed and purified. Pfs28-bait protein and monomeric MG36 were then used to determine the affinity of the interaction by SPR (***Figure 5.11***). The determined K_D of 12.8 ± 1.8 µM indicates a very weak interaction, but even weaker interactions, such as the rat CD2-CD48 interaction (K_D = 60-90 µM) have been shown to be of physiological relevance [266]. A number of factors further support the possibility that the Pfs28-MG36 interaction could be of importance for parasite

invasion of the mosquito midgut despite its high K_D. Pfs28 and its paralogue Pfs25, are the two most abundantly expressed protein on the ookinete surface [101] and transcriptomic data from adult mosquito tissues suggests that MG36 is highly expressed in the *A. gambiae* midgut [267]. The high abundance of both proteins on the respective surfaces could help overcome the low affinity by increasing the avidity of the interaction. Furthermore it has been reported that Pfs28 forms heterodimers with Pfs25 as well as homodimers, which could further increase the avidity of the interaction [242]. Finally, Pfs25 has been reported to form part of big extracellular multi-protein complexes including adhesive PfCCp proteins [104]. As Pfs25 forms dimers with Pfs28 involvement of the latter in such adhesion protein complexes is highly likely. Should the interaction of Pfs28 and MG36 occur in the context of such a complex, this could further help to overcome its low affinity.

In order to gain further insight into how Pfs28 interacts with MG36, the two transferrin like domains of MG36 were expressed individually as AVEXIS bait proteins and binding to Pfs28 was assessed (***Figure 5.12***). Surprisingly neither of the transferrin domains bound Pfs28 at a detectable level, indicating that both TFL domains a required and suggesting a complex interaction between the two proteins with amino acids from both TFL domains making contact with Pfs28 at the same time.

By performing AVEXIS between Pfs28 and MG36 in the presence of anti-Pfs28 IgG from an immunised rabbit it could be shown that the interaction can be inhibited by these antibodies (***Figure 5.13***). It is therefore possible that the well characterised transmission blocking activity of anti-Pfs28 antibodies is, at least partially, due to their ability to disrupt this interaction. Considering these results, it was expected that antibodies

directed against MG36 would exhibit transmission blocking activity of their own. To test this hypothesis and compare potential transmission blocking activity of anti-MG36 antibodies with the one of anti-Pfs28 antibodies, mice were immunised with purified, monomeric versions of the two proteins. Despite both proteins inducing strong antibody responses in immunised mice, only IgG purified from the serum of mice immunised with Pfs28 showed any transmission blocking activity in two independent SMFAs (***Figure 5.14***). Subsequent analysis of the interaction of Pfs28 and MG36 in the presence of antibodies directed against either of the two proteins revealed that anti-MG36 IgG blocks the interaction much less efficiently than anti-Pfs28 IgG, explaining the SMFA results (***Figure 5.15***). This data, as well as the inability of Pfs28 to bind any of the TFL domains of MG36 on their own, suggests a concealed binding site for Pfs28, inaccessible for antibodies and potentially located at the interface of the two TFL domains.

As the SMFA had failed to provide conclusive evidence that the interaction between MG36 and Pfs28 is of any physiological relevance for the infection of the mosquito midgut an RNAi experiment was conducted in *A. gambiae*. *MG36* was knocked down by injecting dsRNA into mosquitoes, and the effect on susceptibility was assessed by infecting the mosquitoes with *P. falciparum* through membrane feeding of cultured gametocytes two days later (***Figure 5.16***). Seven days after the feed, midguts were dissected and oocysts counted as a measure of infectivity. The off-target effect of one of the potential siRNAs was not considered to have any influence on the susceptibility of the mosquitoes, as AGAP003702 is not reported to be strongly expressed in the midgut [267].

Unfortunately, while mRNA levels could be reduced by 50% in the whole body of the mosquito, the knock down was much less pronounced in the midgut. Nonetheless, even a reduction of mRNA levels by only 10% had a substantial and statistically significant effect on the ability of *P. falciparum* ookinetes to form oocysts in the midguts of *A. gambiae* mosquitoes, reducing the number of oocysts per mosquito by more than 50%. This indicates that MG36 plays an important role in midgut traversal by ookinetes. Taking into account the other findings of this chapter, it is very likely that this role is dependent on the interaction with Pfs28 on the ookinete surface, facilitating contact between the midgut epithelium and the parasite.

Given the apparent importance of the MG36-Pfs28 interaction in *A. gambiae* infection with *P. falciparum* and the high level of conservation over multiple mosquito and parasite species (***Figure 5.17***), in a final experiment it was assessed whether the interaction was conserved in orthologous vector-parasite pairs (***Figure 5.18***). However, no further interaction could be detected by AVEXIS between any combination of *A. albimanus*, *A. gambiae* or *A. stephensi* MG36 and Pvs28, Pfs28 or Pbs21. This suggests that either the interaction is unique to the *P. falciparum-A. gambiae* parasite- vector pair, or the complex nature of the Pfs28-MG36 interaction prevents is detection in other parasite-vector pairs by AVEXIS.

In summary, work conducted as part of this thesis chapter resulted in the discovery of a novel ligand receptor pair. The interaction of Pfs28 with MG36 is only the second interaction between the surface of the P. *falciparum ookinete* and the *A. gambiae* midgut epithelium ever to be described, and the first one for which physiological importance could be demonstrated *in vivo*. Its discovery could therefore be an

important milestone in unravelling the poorly understood process of midgut epithelium traversal by *Plasmodium* ookinetes, and facilitate the discovery of novel interventions targeting this natural bottleneck in the parasite's life cycle.

Chapter 6 - Concluding remarks and future directions

6.1 Summary of findings

Membrane traversal is an essential step in multiple processes during all lifecycle stages, when the parasite switches from extracellular to intracellular location and vice versa. Results from this thesis led to the indication of novel ways to interfere with membrane traversal by examination of different vaccination strategies, as well as the detection of a previously undescribed protein-protein interaction with an important role during the traversal of the mosquito midgut epithelium by ookinetes.

6.1.1 Novel vaccination strategies to target membrane traversal

An effective vaccine would undoubtedly greatly facilitate efforts to eliminate and eventually eradicate malaria. It is widely agreed that such a vaccine would have to have two characteristics, prevent illness as well as impact disease transmission [239, 240]. The assessment of a combination of the currently most advanced malaria vaccine candidate RTS,S with Pfs25-IMX-313 in mice, is to my knowledge the first study to show pre-clinically that it is possible to combine RTS,S with a transmission blocking vaccine without affecting their immunogenicity or the *ex vivo* functionality of the induced antibodies. Combination of RTS,S with vaccines targeting other lifecycle stages has long been proposed as a way to generate an effective multi-stage malaria vaccine [268]. Here I have shown that the effect RTS,S naturally has on malaria transmission by preventing blood stage parasitaemia and therefore gametocytogenesis, can likely be increased by adding a transmission blocking component to a vaccine formulation. In

addition to this, the addition of an transmission blocking vaccine to RTS,S could help reduce the emergence of escape mutants, by preventing the spread of parasites that have evolved to not be effected by RTS,S. Pfs25-IMX313 is currently being developed for production under good manufacturing process (GMP) standards. Therefore a translation of these pre-clinical findings into clinical trials is possible and likely in the near future. In the field, a combination of RTS,S and a transmission blocking vaccine could be of great value, particularly in local malaria eradication campaigns.

Other work conducted as part of this thesis facilitated the production of R21, an alternative to RTS,S, to GMP standards and therefore its subsequent assessment in clinical trials. The use of C-Tag affinity chromatography for the purification of Hepatitis B surface antigen (HBsAg) virus like particles (VLPs) has widely been adapted by groups at the Jenner Institute and was essential for the development of a number of vaccines currently under pre-clinical evaluation, including a *P. vivax* variant of R21 (Rv21) [269], and VLPs displaying Spy- or SnoopCatcher. Pre-clinical comparisons of R21 and RTS,S furthermore revealed that lower vaccine doses correlate with higher vaccine efficacy in mice for both vaccines, a finding that has subsequently been assessed in recent clinical trials with promising results. Finally, assessment of R21 as a component of a triple vaccine combination, alongside the blood stage vaccine Rh5 and the transmission blocking vaccine Pfs25-IMX313, delivered first proof of concept of the possibility to combine these three components in a malaria vaccine targeting each stage of the *Plasmodium* lifecycle, albeit with a moderate cost to immunogenicity of one of the components. Combinations of antigens from all three lifecycle stages have been tested previously and were found to be effective in *ex vivo* assays [230], but this

is the first time a vaccine combination was tested where each component is already available as a GMP product, or will be available soon, theoretically allowing for this study to be replicated in clinical trials in the near future.

This thesis furthermore contains the first work on HBsAg VLPs displaying two different antigens at N- and C-terminus, respectively. In the case of R21-SPECT1, this resulted in a single component vaccine that elicited functional antibodies against both antigens. For R21-Pfs25 however, the presence of a C-terminal antigen reduced yields to an extent were the pre-clinical assessment of the VLP as a vaccine candidate was not possible. Subsequent generation of a CSP-Pfs25 dual antigen HBsAg VLP using Spy/Snoop technology and its assessment as a vaccine candidate in mice is the first description of a VLP vaccine targeting antigens of two distinct *Plasmodium* lifecycle stages. The only previous study to combine antigens against two lifecycle stages in a single vaccine used a monomeric fusion protein of the transmission blocking antigen Pfs48/45 and the asexual blood stage antigen GLURP [270]. While the role that dual antigen VLPs might play for future vaccine development depends on the results of further experiments, work from this part of this thesis facilitated research on other projects and helped establish new methods in the group. Particle maturation by KSCN and heat treatment has since been made a routine procedure during HBsAg VLP production, irrespective of the displayed antigens. Furthermore the generation of monomeric SPECT1 protein for ELISA, allowed the characterisation of immune responses to viral vectors expressing SPECT1 and comparing them to immune responses induced upon immunisation with protein in adjuvant (Ahmed Salman, manuscript in preparation).

6.1.2 Identification of novel protein-protein interaction involved in midgut traversal

The interaction between Pfs28 and the mosquito midgut protein MG36 is, to my knowledge, the first protein-protein interaction identified between the *P. falciparum* ookinete and the *A. gambiae* midgut epithelium for which a direct involvement in ookinete to oocyst development could be demonstrated. Previously described interactions in other parasite-vector pairs were either never shown to be of physiological relevance, like the interaction of *P. vivax* Pvs25 with *A. albimanus* calreticulin, or were only of importance for ookinete to oocyst development in a sub-population of parasites, like the binding of *P. berghei* enolase to *A. stephensi* enolase binding protein (EBP) [106]. The identified interaction of Pfs28 with MG36 could therefore have far reaching implications for the understanding of ookinete mosquito invasion and the development of novel drug or vaccine interventions.

6.1.2.1 A new hypothesis for the role of Pfs28 during midgut traversal

While the precise role that the interaction between Pfs28 and MG36 plays in the process of midgut traversal by the ookinete still has to be characterised in more detail, it allows a fresh view on a number of previous observations and unanswered questions. Whether specific interactions between the midgut epithelium and the ookinete are necessary for midgut traversal, and particularly whether either of the two predominant proteins on the ookinete surface, Pfs28 and Pfs25, are involved in the process is still a matter of debate [102], but findings from this thesis strongly argue in favour of it. Interestingly, in the same paper that proposed the time bomb model of mosquito invasion by ookinetes, it was observed that Pbs21, the *P. berghei* orthologue

of Pfs28, is deposited at the site of entry into the *A. stephensi* midgut [113]. Attachment and subsequent cleavage of adhesins is a conserved mechanism in cell traversal of *Plasmodium* motile lifecycle stages. During hepatocyte traversal by sporozoites, CSP is specifically cleaved at the site of entry in a process essential for sporozoite infectivity [43]. Similarly, during invasion of erythrocytes, the merozoite surface protein MSP1 is proteolytically processed by a subtilisin like protease secreted from the merozoite [271, 272]. This cleavage results in a short protein fragment (MSP1(19)) that remains attached to the merozoite and contains multiple epidermal growth factor (EGF) domains, and a larger fragment that is released as part of a multi-protein complex (MSP1(33)). Given the similarities observed between membrane traversal events in different lifecycle stages, it can be theorised that Pfs28 plays a similar role during midgut traversal as CSP does during traversal of hepatocytes or MSP1 during erythrocyte invasion. According to this theory Pfs28 would bind to its receptor on the midgut epithelium, now identified to be MG36, and then be released from the ookinete membrane, possibly through proteolytic cleavage by subtilisin 2, which is secereted by the ookinete during midgut traversal [113]. *Plasmodium* mosquito stage surface proteins have been shown to form multi-protein complexes [104], and although its involvement has not yet been directly demonstrated it is highly conceivable that Pfs28 forms a component of such complexes. The Pbs21 deposits detected at the site of midgut penetration by Han et al. [113] could therefore be multi-protein attachment and invasion complexes, guided to their location through the interaction of Pbs21 with its midgut receptor. In the *P. falciparum - A. gambiae* parasite-vector pair, MG36 could therefore present the gateway that is the first point of contact for ookinete cell invasion machinery on the mosquito midgut.

6.2 Future directions

6.2.1 Prospects of multi-antigen malaria vaccines

Experts in the field of malaria vaccinology have over the last few years come to the conclusion that a multi-antigen, multi- stage vaccine is most likely to be successful in the fight against malaria [228-230, 268]. Work conducted in this thesis demonstrated the potential combinations of different vaccines have, but also showed some of the problems that might be encountered. Future work should focus on how to balance the individual antigens in a multi component vaccine and correlate immune responses to functional *ex vivo* assays such as inhibition of sporozoite invasion, hepatocyte traversal and gliding motility assays for sporozoite antigens, growth inhibition assays for blood stage antigens and standard membrane feeding assays for sexual stage antigens [230]. Furthermore, it should be assessed to what extent mixtures of proteins in adjuvant, as tested as part of this thesis, can be combined with viral vectors targeting intrahepatic forms of the pre-erythrocytic parasite, as has previously been done in combination with R21 alone [222]. Once an optimal formulation has been determined, these findings should be translated into clinical trials as soon as possible to test the efficacy of a multi-component vaccine in humans. Some of these studies using mixtures of the individual components are already planned.

While multi-antigen fusion VLPs still hold some promise as highly efficacious vaccine candidates, their potential assessment in clinical trials is not as imminent. This is not last due to the detrimental effect that the expression of a second antigen on the C-terminus has on the particle yield, making production of a product to GMP standards

extremely challenging. This problem might be circumnavigated by the use of Spy/Snoop technology as has been demonstrated in this thesis. Nonetheless, there is an increased level of complexity compared to simply mixing multiple antigens in a multi-component vaccine. Future work on dual-antigen VLPs should therefore focus on carefully dissecting the advantages and disadvantages over a multi-component vaccine, both in terms of the induced immune responses as well as the feasibility of production to GMP standards at a large scale.

6.2.2 Defining the role of the Pfs28-MG36 interaction during midgut traversal

The identification of the interaction between Pfs28 and MG36 as the first protein-protein interaction between the ookinete and the mosquito midgut epithelium with a clear implication for midgut traversal is a significant first step in understanding this still largely enigmatic process, but a lot of questions remain unanswered. Future work should aim at understanding the role this newly described interaction plays *in vivo*. Given the low efficiency of the RNAi knockdown of *MG36* in the midgut during experiments in this thesis, the generation of a *MG36* knockout mosquito would be an invaluable tool in this endeavour. A first step in confirming the earlier described hypothesis for the role of Pfs28 during midgut traversal would be to replicate the findings of Han et al. that led to the formulation of the time bomb theory of mosquito invasion [113], in the *P. falciparum* - *A. gambiae* parasite-vector pair. As part of this work it should furthermore be determined whether Pfs28 is deposited at the site of entry into the mosquito midgut as part of a multi-protein complex or in isolation. If these experiments were performed in wild type *A. gambiae* mosquitoes, as well as in

mosquitoes in which *MG36* has been knocked out, this should give a good indication of the physiological role of this interaction.

Knock out experiments in *P. berghei* have shown Pfs28 and Pfs25 to be partially redundant and to have widely overlapping functions [101]. It is therefore surprising that Pfs25 was found not to interact with MG36 while Pfs28 did. To obtain a more complete picture of the processes during midgut traversal it would therefore be important, in addition to understand the role of Pfs28, to identify if there is an interaction partner for Pfs25. As the AVEXIS screen performed as part of this thesis failed to detect a midgut receptor for Pfs25, an alternative strategy was devised that entailed the use of BioID to detect proteins found in close proximity to Pfs25. BioID takes advantage of a promiscuous biotin ligase that, in presence of its substrates biotin and ATP, indiscriminately biotinylates protein in its proximity [273-275]. Biotinylated proteins can then be enriched using streptavidin coated beads and identified by mass spectrometry. To apply this assay to the identification of Pfs25 interacting proteins, a transgenic *P. berghei* parasite was generated expressing a fusion protein of Pbs25 and the biotin ligase BioID2. These parasites should be fed to *A. stephensi* mosquitoes by a membrane feed in the presence of excess amounts of biotin and ATP. Initial experiments with these parasites give cause to cautious optimism, but were not appropriately controlled and lacked signal intensity, which prevented detection of proteins by mass spectrometry. Future experiments will need to incorporate additional controls as well as improve the signal strength. The latter should be achievable through feeding cultured gametocytes rather than blood from infected mice, which should increase the intensity of infection, as well as through optimising

the enrichment process. Mosquito as well as parasite proteins identified in this assay could then be confirmed to interact with Pbs25 by AVEXIS and surface plasmon resonance. The same methods could then be used to determine whether the interaction is conserved between *P. falciparum* and *A. gambiae*.

If the proposed experiments were to be completed successfully, they could help to drastically increase our current understanding of the mosquito midgut traversal by ookinetes, the narrowest bottleneck in the *Plasmodium* life cycle and therefore an immensely attractive target for interventions aiming at disrupting malaria transmission.

6.3 Conclusion

Malaria is one of the world's most ancient human pathogens. It therefore had millions of years to adapt to its human and mosquito host, resulting in efficient evasion of the human and mosquito immune response. A vaccine against malaria therefore has to be able to surpass naturally acquired immunity, an exquisitely difficult task that can only be successful if the right antigens are identified and combined in a highly immunogenic vaccine. It is therefore of the utmost importance to understand the processes underlying key steps in the *Plasmodium* lifecycle at molecular detail, so that targets for efficient intervention can be identified. Work conducted in this thesis, identified a novel protein-protein interaction at a natural bottle neck in the *Plasmodium* lifecycle and assessed new strategies to efficiently deliver antigens as vaccines. I am therefore hopeful that information from this thesis can be built on and contribute to the endeavour of developing a vaccine capable of eradicating malaria.

References

1. Escalante, A.A. and F.J. Ayala, *Phylogeny of the malarial genus Plasmodium, derived from rRNA gene sequences.* Proc Natl Acad Sci U S A, 1994. **91**(24): p. 11373-7.

2. Hay, S.I., et al., *The global distribution and population at risk of malaria: past, present, and future.* Lancet Infect Dis, 2004. **4**(6): p. 327-36.

3. Sinka, M.E., et al., *A global map of dominant malaria vectors.* Parasit Vectors, 2012. **5**: p. 69.

4. Sutherland, C.J., et al., *Two nonrecombining sympatric forms of the human malaria parasite Plasmodium ovale occur globally.* J Infect Dis, 2010. **201**(10): p. 1544-50.

5. White, N.J., et al., *Malaria.* Lancet, 2014. **383**(9918): p. 723-35.

6. World-Health-Organisation, *World Malaria Report 2017*. 2017.

7. Bynum, W.F., *Ronald Ross and the malaria-mosquito cycle.* Parassitologia, 1999. **41**(1-3): p. 49-52.

8. Najera, J.A., M. Gonzalez-Silva, and P.L. Alonso, *Some lessons for the future from the Global Malaria Eradication Programme (1955-1969).* PLoS Med, 2011. **8**(1): p. e1000412.

9. Alonso, P.L., et al., *A research agenda to underpin malaria eradication.* PLoS Med, 2011. **8**(1): p. e1000406.

10. World-Health-Organisation, *Eliminating Malaria*. 2016.

11. Ashley, E.A., et al., *Spread of artemisinin resistance in Plasmodium falciparum malaria.* N Engl J Med, 2014. **371**(5): p. 411-23.

12. Noedl, H., et al., *Evidence of artemisinin-resistant malaria in western Cambodia.* N Engl J Med, 2008. **359**(24): p. 2619-20.

13. Dondorp, A.M., et al., *Artemisinin resistance in Plasmodium falciparum malaria.* N Engl J Med, 2009. **361**(5): p. 455-67.

14. Phyo, A.P., et al., *Emergence of artemisinin-resistant malaria on the western border of Thailand: a longitudinal study.* Lancet, 2012. **379**(9830): p. 1960-6.

15. Ranson, H., et al., *Pyrethroid resistance in African anopheline mosquitoes: what are the implications for malaria control?* Trends Parasitol, 2011. **27**(2): p. 91-8.

16. Ungureanu, E., et al., *Prepatent periods of a tropical strain of Plasmodium vivax after inoculations of tenfold dilutions of sporozoites.* Trans R Soc Trop Med Hyg, 1976. **70**(5-6): p. 482-3.

17. Amino, R., et al., *Quantitative imaging of Plasmodium transmission from mosquito to mammal.* Nat Med, 2006. **12**(2): p. 220-4.

18. Shin, S.C., J.P. Vanderberg, and J.A. Terzakis, *Direct infection of hepatocytes by sporozoites of Plasmodium berghei.* J Protozool, 1982. **29**(3): p. 448-54.

19. Opitz, C. and D. Soldati, *'The glideosome': a dynamic complex powering gliding motion and host cell invasion by Toxoplasma gondii.* Mol Microbiol, 2002. **45**(3): p. 597-604.

20. Sultan, A.A., et al., *TRAP is necessary for gliding motility and infectivity of plasmodium sporozoites.* Cell, 1997. **90**(3): p. 511-22.

21. Stewart, M.J. and J.P. Vanderberg, *Malaria sporozoites release circumsporozoite protein from their apical end and translocate it along their surface.* J Protozool, 1991. **38**(4): p. 411-21.

22. Vanderberg, J.P., *Studies on the motility of Plasmodium sporozoites.* J Protozool, 1974. **21**(4): p. 527-37.

23. Russell, D.G. and R.E. Sinden, *The role of the cytoskeleton in the motility of coccidian sporozoites.* J Cell Sci, 1981. **50**: p. 345-59.

24. Blackman, M.J. and V.B. Carruthers, *Recent insights into apicomplexan parasite egress provide new views to a kill.* Curr Opin Microbiol, 2013. **16**(4): p. 459-64.

25. Aikawa, M., et al., *Erythrocyte entry by malarial parasites. A moving junction between erythrocyte and parasite.* J Cell Biol, 1978. **77**(1): p. 72-82.

26. Mordue, D.G., et al., *Toxoplasma gondii resides in a vacuole that avoids fusion with host cell endocytic and exocytic vesicular trafficking pathways.* Exp Parasitol, 1999. **92**(2): p. 87-99.

27. Amino, R., et al., *Host cell traversal is important for progression of the malaria parasite through the dermis to the liver.* Cell Host Microbe, 2008. **3**(2): p. 88-96.

28. Frevert, U., et al., *Intravital observation of Plasmodium berghei sporozoite infection of the liver.* PLoS Biol, 2005. **3**(6): p. e192.

29. Tavares, J., et al., *Role of host cell traversal by the malaria sporozoite during liver infection.* J Exp Med, 2013. **210**(5): p. 905-15.

30. Mota, M.M., et al., *Migration of Plasmodium sporozoites through cells before infection.* Science, 2001. **291**(5501): p. 141-4.

31. Bhanot, P., et al., *A surface phospholipase is involved in the migration of plasmodium sporozoites through cells.* J Biol Chem, 2005. **280**(8): p. 6752-60.

32. Kariu, T., et al., *CelTOS, a novel malarial protein that mediates transmission to mosquito and vertebrate hosts.* Mol Microbiol, 2006. **59**(5): p. 1369-79.

33. Ishino, T., et al., *Cell-passage activity is required for the malarial parasite to cross the liver sinusoidal cell layer.* PLoS Biol, 2004. **2**(1): p. E4.

34. Ishino, T., Y. Chinzei, and M. Yuda, *A Plasmodium sporozoite protein with a membrane attack complex domain is required for breaching the liver sinusoidal cell layer prior to hepatocyte infection.* Cell Microbiol, 2005. **7**(2): p. 199-208.

35. Yang, A.S.P., et al., *Cell Traversal Activity Is Important for Plasmodium falciparum Liver Infection in Humanized Mice.* Cell Rep, 2017. **18**(13): p. 3105-3116.

36. Risco-Castillo, V., et al., *Malaria Sporozoites Traverse Host Cells within Transient Vacuoles.* Cell Host Microbe, 2015. **18**(5): p. 593-603.

37. Cha, S.J., et al., *Identification of GAPDH on the surface of Plasmodium sporozoites as a new candidate for targeting malaria liver invasion.* J Exp Med, 2016. **213**(10): p. 2099-112.

38. Cha, S.J., et al., *CD68 acts as a major gateway for malaria sporozoite liver infection.* J Exp Med, 2015. **212**(9): p. 1391-403.

39. Mota, M.M., J.C. Hafalla, and A. Rodriguez, *Migration through host cells activates Plasmodium sporozoites for infection.* Nat Med, 2002. **8**(11): p. 1318-22.

40. Carrolo, M., et al., *Hepatocyte growth factor and its receptor are required for malaria infection.* Nat Med, 2003. **9**(11): p. 1363-9.

41. Coppi, A., et al., *Heparan sulfate proteoglycans provide a signal to Plasmodium sporozoites to stop migrating and productively invade host cells.* Cell Host Microbe, 2007. **2**(5): p. 316-27.

42. Frevert, U., et al., *Malaria circumsporozoite protein binds to heparan sulfate proteoglycans associated with the surface membrane of hepatocytes.* J Exp Med, 1993. **177**(5): p. 1287-98.

43. Coppi, A., et al., *The Plasmodium circumsporozoite protein is proteolytically processed during cell invasion.* J Exp Med, 2005. **201**(1): p. 27-33.

44. Silvie, O., et al., *Hepatocyte CD81 is required for Plasmodium falciparum and Plasmodium yoelii sporozoite infectivity.* Nat Med, 2003. **9**(1): p. 93-6.

45. Rodrigues, C.D., et al., *Host scavenger receptor SR-BI plays a dual role in the establishment of malaria parasite liver infection.* Cell Host Microbe, 2008. **4**(3): p. 271-82.

46. Yalaoui, S., et al., *Scavenger receptor BI boosts hepatocyte permissiveness to Plasmodium infection.* Cell Host Microbe, 2008. **4**(3): p. 283-92.

47. Manzoni, G., et al., *Plasmodium P36 determines host cell receptor usage during sporozoite invasion.* Elife, 2017. **6**.

48. Labaied, M., et al., *Plasmodium yoelii sporozoites with simultaneous deletion of P52 and P36 are completely attenuated and confer sterile immunity against infection.* Infect Immun, 2007. **75**(8): p. 3758-68.

49. VanBuskirk, K.M., et al., *Preerythrocytic, live-attenuated Plasmodium falciparum vaccine candidates by design.* Proc Natl Acad Sci U S A, 2009. **106**(31): p. 13004-9.

50. Kaushansky, A., et al., *Malaria parasites target the hepatocyte receptor EphA2 for successful host infection.* Science, 2015. **350**(6264): p. 1089-92.

51. Dvorak, J.A., et al., *Invasion of erythrocytes by malaria merozoites.* Science, 1975. **187**(4178): p. 748-50.

52. Gilson, P.R. and B.S. Crabb, *Morphology and kinetics of the three distinct phases of red blood cell invasion by Plasmodium falciparum merozoites.* Int J Parasitol, 2009. **39**(1): p. 91-6.

53. Baldwin, M.R., et al., *Merozoite surface protein 1 recognition of host glycophorin A mediates malaria parasite invasion of red blood cells.* Blood, 2015. **125**(17): p. 2704-11.

54. Lin, C.S., et al., *The merozoite surface protein 1 complex is a platform for binding to human erythrocytes by Plasmodium falciparum.* J Biol Chem, 2014. **289**(37): p. 25655-69.

55. Das, S., et al., *Processing of Plasmodium falciparum Merozoite Surface Protein MSP1 Activates a Spectrin-Binding Function Enabling Parasite Egress from RBCs.* Cell Host Microbe, 2015. **18**(4): p. 433-44.

56. O'Donnell, R.A., et al., *Antibodies against merozoite surface protein (MSP)-1(19) are a major component of the invasion-inhibitory response in individuals immune to malaria.* J Exp Med, 2001. **193**(12): p. 1403-12.

57. Kana, I.H., et al., *Naturally Acquired Antibodies Target the Glutamate-Rich Protein on Intact Merozoites and Predict Protection Against Febrile Malaria.* J Infect Dis, 2017. **215**(4): p. 623-630.

58. Theisen, M., et al., *The glutamate-rich protein (GLURP) of Plasmodium falciparum is a target for antibody-dependent monocyte-mediated inhibition of parasite growth in vitro.* Infect Immun, 1998. **66**(1): p. 11-7.

59. Boyle, M.J., et al., *Human antibodies fix complement to inhibit Plasmodium falciparum invasion of erythrocytes and are associated with protection against malaria.* Immunity, 2015. **42**(3): p. 580-90.

60. Harris, P.K., et al., *Molecular identification of a malaria merozoite surface sheddase.* PLoS Pathog, 2005. **1**(3): p. 241-51.

61. Dasgupta, S., et al., *Membrane-wrapping contributions to malaria parasite invasion of the human erythrocyte.* Biophys J, 2014. **107**(1): p. 43-54.

62. Cowman, A.F., et al., *The Molecular Basis of Erythrocyte Invasion by Malaria Parasites.* Cell Host Microbe, 2017. **22**(2): p. 232-245.

63. Crosnier, C., et al., *Basigin is a receptor essential for erythrocyte invasion by Plasmodium falciparum.* Nature, 2011. **480**(7378): p. 534-7.

64. Reddy, K.S., et al., *Multiprotein complex between the GPI-anchored CyRPA with PfRH5 and PfRipr is crucial for Plasmodium falciparum erythrocyte invasion.* Proc Natl Acad Sci U S A, 2015. **112**(4): p. 1179-84.

65. Chen, L., et al., *An EGF-like protein forms a complex with PfRh5 and is required for invasion of human erythrocytes by Plasmodium falciparum.* PLoS Pathog, 2011. **7**(9): p. e1002199.

66. Volz, J.C., et al., *Essential Role of the PfRh5/PfRipr/CyRPA Complex during Plasmodium falciparum Invasion of Erythrocytes.* Cell Host Microbe, 2016. **20**(1): p. 60-71.

67. Weiss, G.E., et al., *Revealing the sequence and resulting cellular morphology of receptor-ligand interactions during Plasmodium falciparum invasion of erythrocytes.* PLoS Pathog, 2015. **11**(2): p. e1004670.

68. Lamarque, M., et al., *The RON2-AMA1 interaction is a critical step in moving junction-dependent invasion by apicomplexan parasites.* PLoS Pathog, 2011. **7**(2): p. e1001276.

69. de Koning-Ward, T.F., et al., *Plasmodium species: master renovators of their host cells.* Nat Rev Microbiol, 2016. **14**(8): p. 494-507.

70. Su, X.Z., et al., *The large diverse gene family var encodes proteins involved in cytoadherence and antigenic variation of Plasmodium falciparum-infected erythrocytes.* Cell, 1995. **82**(1): p. 89-100.

71. Deitsch, K.W. and T.E. Wellems, *Membrane modifications in erythrocytes parasitized by Plasmodium falciparum.* Mol Biochem Parasitol, 1996. **76**(1-2): p. 1-10.

72. McMillan, P.J., et al., *Spatial and temporal mapping of the PfEMP1 export pathway in Plasmodium falciparum.* Cell Microbiol, 2013. **15**(8): p. 1401-18.

73. Pain, A., et al., *Platelet-mediated clumping of Plasmodium falciparum-infected erythrocytes is a common adhesive phenotype and is associated with severe malaria.* Proc Natl Acad Sci U S A, 2001. **98**(4): p. 1805-10.

74. Miller, L.H., et al., *The pathogenic basis of malaria.* Nature, 2002. **415**(6872): p. 673-9.

75. Maier, A.G., et al., *Exported proteins required for virulence and rigidity of Plasmodium falciparum-infected human erythrocytes.* Cell, 2008. **134**(1): p. 48-61.

76. Bruce, M.C., et al., *Cellular location and temporal expression of the Plasmodium falciparum sexual stage antigen Pfs16.* Mol Biochem Parasitol, 1994. **65**(1): p. 11-22.

77. Kafsack, B.F., et al., *A transcriptional switch underlies commitment to sexual development in malaria parasites.* Nature, 2014. **507**(7491): p. 248-52.

78. Sinha, A., et al., *A cascade of DNA-binding proteins for sexual commitment and development in Plasmodium.* Nature, 2014. **507**(7491): p. 253-257.

79. Dyer, M. and K.P. Day, *Commitment to gametocytogenesis in Plasmodium falciparum.* Parasitol Today, 2000. **16**(3): p. 102-7.

80. Dantzler, K.W., et al., *Ensuring transmission through dynamic host environments: host-pathogen interactions in Plasmodium sexual development.* Curr Opin Microbiol, 2015. **26**: p. 17-23.

81. Hawking, F., M.E. Wilson, and K. Gammage, *Evidence for cyclic development and short-lived maturity in the gametocytes of Plasmodium falciparum.* Trans R Soc Trop Med Hyg, 1971. **65**(5): p. 549-59.

82. Sinden, R.E., et al., *Gametocyte and gamete development in Plasmodium falciparum.* Proc R Soc Lond B Biol Sci, 1978. **201**(1145): p. 375-99.

83. Aguilar, R., et al., *Molecular evidence for the localization of Plasmodium falciparum immature gametocytes in bone marrow.* Blood, 2014. **123**(7): p. 959-66.

84. Joice, R., et al., *Plasmodium falciparum transmission stages accumulate in the human bone marrow.* Sci Transl Med, 2014. **6**(244): p. 244re5.

85. Billker, O., et al., *Identification of xanthurenic acid as the putative inducer of malaria development in the mosquito.* Nature, 1998. **392**(6673): p. 289-92.

86. Sinden, R.E. and N.A. Croll, *Cytology and kinetics of microgametogenesis and fertilization in Plasmodium yoelii nigeriensis.* Parasitology, 1975. **70**(1): p. 53-65.

87. Janse, C.J., et al., *DNA synthesis in gametocytes of Plasmodium falciparum.* Parasitology, 1988. **96 (Pt 1)**: p. 1-7.

88. Wirth, C.C., et al., *Perforin-like protein PPLP2 permeabilizes the red blood cell membrane during egress of Plasmodium falciparum gametocytes.* Cell Microbiol, 2014. **16**(5): p. 709-33.

89. Rener, J., et al., *Target antigens of transmission-blocking immunity on gametes of plasmodium falciparum.* J Exp Med, 1983. **158**(3): p. 976-81.

90. Vermeulen, A.N., et al., *Sequential expression of antigens on sexual stages of Plasmodium falciparum accessible to transmission-blocking antibodies in the mosquito.* J Exp Med, 1985. **162**(5): p. 1460-76.

91. Sinden, R.E., *The cell biology of malaria infection of mosquito: advances and opportunities.* Cell Microbiol, 2015. **17**(4): p. 451-66.

92. Kumar, N., *Target antigens of malaria transmission blocking immunity exist as a stable membrane bound complex.* Parasite Immunol, 1987. **9**(3): p. 321-35.

93. Kumar, N. and B. Wizel, *Further characterization of interactions between gamete surface antigens of Plasmodium falciparum.* Mol Biochem Parasitol, 1992. **53**(1-2): p. 113-20.

94. Liu, Y., et al., *The conserved plant sterility gene HAP2 functions after attachment of fusogenic membranes in Chlamydomonas and Plasmodium gametes.* Genes Dev, 2008. **22**(8): p. 1051-68.

95. Janse, C.J., et al., *Rapid repeated DNA replication during microgametogenesis and DNA synthesis in young zygotes of Plasmodium berghei.* Trans R Soc Trop Med Hyg, 1986. **80**(1): p. 154-7.

96. Shao, L., M. Devenport, and M. Jacobs-Lorena, *The peritrophic matrix of hematophagous insects.* Arch Insect Biochem Physiol, 2001. **47**(2): p. 119-25.

97. Dessens, J.T., et al., *Knockout of the rodent malaria parasite chitinase pbCHT1 reduces infectivity to mosquitoes.* Infect Immun, 2001. **69**(6): p. 4041-7.

98. Duffy, P.E. and D.C. Kaslow, *A novel malaria protein, Pfs28, and Pfs25 are genetically linked and synergistic as falciparum malaria transmission-blocking vaccines.* Infect Immun, 1997. **65**(3): p. 1109-13.

99. Ghosh, A.K., et al., *Plasmodium ookinetes coopt mammalian plasminogen to invade the mosquito midgut.* Proc Natl Acad Sci U S A, 2011. **108**(41): p. 17153-8.

100. Armistead, J.S., et al., *Antibodies to a single, conserved epitope in Anopheles APN1 inhibit universal transmission of Plasmodium falciparum and Plasmodium vivax malaria.* Infect Immun, 2014. **82**(2): p. 818-29.

101. Tomas, A.M., et al., *P25 and P28 proteins of the malaria ookinete surface have multiple and partially redundant functions.* EMBO J, 2001. **20**(15): p. 3975-83.

102. Baton, L.A. and L.C. Ranford-Cartwright, *Do malaria ookinete surface proteins P25 and P28 mediate parasite entry into mosquito midgut epithelial cells?* Malar J, 2005. **4**: p. 15.

103. Baton, L.A. and L.C. Ranford-Cartwright, *How do malaria ookinetes cross the mosquito midgut wall?* Trends Parasitol, 2005. **21**(1): p. 22-8.

104. Simon, N., et al., *Adhesion protein complexes of malaria gametocytes assemble following parasite transmission to the mosquito.* Parasitol Int, 2016. **65**(1): p. 27-30.

105. Vlachou, D., et al., *Anopheles gambiae laminin interacts with the P25 surface protein of Plasmodium berghei ookinetes.* Mol Biochem Parasitol, 2001. **112**(2): p. 229-37.

106. Vega-Rodriguez, J., et al., *Multiple pathways for Plasmodium ookinete invasion of the mosquito midgut.* Proc Natl Acad Sci U S A, 2014. **111**(4): p. E492-500.

107. Scally, S.W., et al., *Molecular definition of multiple sites of antibody inhibition of malaria transmission-blocking vaccine antigen Pfs25.* Nat Commun, 2017. **8**(1): p. 1568.

108. Zieler, H., et al., *Adhesion of Plasmodium gallinaceum ookinetes to the Aedes aegypti midgut: sites of parasite attachment and morphological changes in the ookinete.* J Eukaryot Microbiol, 1998. **45**(5): p. 512-20.

109. Dinglasan, R.R., et al., *Plasmodium falciparum ookinetes require mosquito midgut chondroitin sulfate proteoglycans for cell invasion.* Proc Natl Acad Sci U S A, 2007. **104**(40): p. 15882-7.

110. Shahabuddin, M. and P.F. Pimenta, *Plasmodium gallinaceum preferentially invades vesicular ATPase-expressing cells in Aedes aegypti midgut.* Proc Natl Acad Sci U S A, 1998. **95**(7): p. 3385-9.

111. Shahabuddin, M., *Do Plasmodium ookinetes invade a specific cell type in the mosquito midgut?* Trends Parasitol, 2002. **18**(4): p. 157-61.

112. Sinden, R.E. and P.F. Billingsley, *Plasmodium invasion of mosquito cells: hawk or dove?* Trends Parasitol, 2001. **17**(5): p. 209-12.

113. Han, Y.S., et al., *Molecular interactions between Anopheles stephensi midgut cells and Plasmodium berghei: the time bomb theory of ookinete invasion of mosquitoes.* EMBO J, 2000. **19**(22): p. 6030-40.

114. Zieler, H. and J.A. Dvorak, *Invasion in vitro of mosquito midgut cells by the malaria parasite proceeds by a conserved mechanism and results in death of the invaded midgut cells.* Proc Natl Acad Sci U S A, 2000. **97**(21): p. 11516-21.

115. Vlachou, D., et al., *Real-time, in vivo analysis of malaria ookinete locomotion and mosquito midgut invasion.* Cell Microbiol, 2004. **6**(7): p. 671-85.

116. Ecker, A., et al., *Plasmodium berghei: plasmodium perforin-like protein 5 is required for mosquito midgut invasion in Anopheles stephensi.* Exp Parasitol, 2007. **116**(4): p. 504-8.

117. Kadota, K., et al., *Essential role of membrane-attack protein in malarial transmission to mosquito host.* Proc Natl Acad Sci U S A, 2004. **101**(46): p. 16310-5.

118. Angrisano, F., et al., *Malaria parasite colonisation of the mosquito midgut--placing the Plasmodium ookinete centre stage.* Int J Parasitol, 2012. **42**(6): p. 519-27.

119. Nikolaeva, D., et al., *Functional characterization and comparison of Plasmodium falciparum proteins as targets of transmission-blocking antibodies.* Mol Cell Proteomics, 2017.

120. Stanisic, D.I., et al., *Robert Koch redux: malaria immunology in Papua New Guinea.* Parasite Immunol, 2010. **32**(8): p. 623-32.

121. Cohen, S., G.I. Mc, and S. Carrington, *Gamma-globulin and acquired immunity to human malaria.* Nature, 1961. **192**: p. 733-7.

122. Owusu-Agyei, S., et al., *Incidence of symptomatic and asymptomatic Plasmodium falciparum infection following curative therapy in adult residents of northern Ghana.* Am J Trop Med Hyg, 2001. **65**(3): p. 197-203.

123. Sokhna, C.S., et al., *Host factors affecting the delay of reappearance of Plasmodium falciparum after radical treatment among a semi-immune population exposed to intense perennial transmission.* Am J Trop Med Hyg, 2000. **62**(2): p. 266-70.

124. Triller, G., et al., *Natural Parasite Exposure Induces Protective Human Anti-Malarial Antibodies.* Immunity, 2017.

125. John, C.C., et al., *Antibodies to the Plasmodium falciparum antigens circumsporozoite protein, thrombospondin-related adhesive protein, and liver-stage antigen 1 vary by ages of subjects and by season in a highland area of Kenya.* Infect Immun, 2003. **71**(8): p. 4320-5.

126. Connelly, M., et al., *T-cell immunity to peptide epitopes of liver-stage antigen 1 in an area of Papua New Guinea in which malaria is holoendemic.* Infect Immun, 1997. **65**(12): p. 5082-7.

127. Sedegah, M., et al., *Naturally acquired CD8+ cytotoxic T lymphocytes against the Plasmodium falciparum circumsporozoite protein.* J Immunol, 1992. **149**(3): p. 966-71.

128. Bull, P.C., et al., *Parasite antigens on the infected red cell surface are targets for naturally acquired immunity to malaria.* Nat Med, 1998. **4**(3): p. 358-60.

129. Goel, S., et al., *RIFINs are adhesins implicated in severe Plasmodium falciparum malaria.* Nat Med, 2015. **21**(4): p. 314-7.

130. Khattab, A., et al., *Plasmodium falciparum variant STEVOR antigens are expressed in merozoites and possibly associated with erythrocyte invasion.* Malar J, 2008. **7**: p. 137.

131. Winter, G., et al., *SURFIN is a polymorphic antigen expressed on Plasmodium falciparum merozoites and infected erythrocytes.* J Exp Med, 2005. **201**(11): p. 1853-63.

132. Chan, J.A., F.J. Fowkes, and J.G. Beeson, *Surface antigens of Plasmodium falciparum-infected erythrocytes as immune targets and malaria vaccine candidates.* Cell Mol Life Sci, 2014. **71**(19): p. 3633-57.

133. Bengtsson, A., et al., *A novel domain cassette identifies Plasmodium falciparum PfEMP1 proteins binding ICAM-1 and is a target of cross-reactive, adhesion-inhibitory antibodies.* J Immunol, 2013. **190**(1): p. 240-9.

134. Tebo, A.E., P.G. Kremsner, and A.J. Luty, *Fcgamma receptor-mediated phagocytosis of Plasmodium falciparum-infected erythrocytes in vitro.* Clin Exp Immunol, 2002. **130**(2): p. 300-6.

135. Hviid, L. and A. Salanti, *VAR2CSA and protective immunity against pregnancy-associated Plasmodium falciparum malaria.* Parasitology, 2007. **134**(Pt 13): p. 1871-6.

136. Salanti, A., et al., *Evidence for the involvement of VAR2CSA in pregnancy-associated malaria.* J Exp Med, 2004. **200**(9): p. 1197-203.

137. Claessens, A., et al., *Generation of antigenic diversity in Plasmodium falciparum by structured rearrangement of Var genes during mitosis.* PLoS Genet, 2014. **10**(12): p. e1004812.

138. Frank, M., et al., *Frequent recombination events generate diversity within the multi-copy variant antigen gene families of Plasmodium falciparum.* Int J Parasitol, 2008. **38**(10): p. 1099-109.

139. Ofori, M.F., et al., *Malaria-induced acquisition of antibodies to Plasmodium falciparum variant surface antigens.* Infect Immun, 2002. **70**(6): p. 2982-8.

140. Kinyanjui, S.M., et al., *Protection against clinical malaria by heterologous immunoglobulin G antibodies against malaria-infected erythrocyte variant surface antigens requires interaction with asymptomatic infections.* J Infect Dis, 2004. **190**(9): p. 1527-33.

141. Gupta, S., et al., *Immunity to non-cerebral severe malaria is acquired after one or two infections.* Nat Med, 1999. **5**(3): p. 340-3.

142. Bull, P.C., et al., *Plasmodium falciparum-infected erythrocytes: agglutination by diverse Kenyan plasma is associated with severe disease and young host age.* J Infect Dis, 2000. **182**(1): p. 252-9.

143. Lindenthal, C., P.G. Kremsner, and M.Q. Klinkert, *Commonly recognised Plasmodium falciparum parasites cause cerebral malaria.* Parasitol Res, 2003. **91**(5): p. 363-8.

144. Nielsen, M.A., et al., *Plasmodium falciparum variant surface antigen expression varies between isolates causing severe and nonsevere malaria and is modified by acquired immunity.* J Immunol, 2002. **168**(7): p. 3444-50.

145. Druilhe, P. and S. Khusmith, *Epidemiological correlation between levels of antibodies promoting merozoite phagocytosis of Plasmodium falciparum and malaria-immune status.* Infect Immun, 1987. **55**(4): p. 888-91.

146. Osier, F.H., et al., *Breadth and magnitude of antibody responses to multiple Plasmodium falciparum merozoite antigens are associated with protection from clinical malaria.* Infect Immun, 2008. **76**(5): p. 2240-8.

147. Egan, A.F., et al., *Clinical immunity to Plasmodium falciparum malaria is associated with serum antibodies to the 19-kDa C-terminal fragment of the merozoite surface antigen, PfMSP-1.* J Infect Dis, 1996. **173**(3): p. 765-9.

148. Jaschke, A., et al., *Merozoite Surface Protein 1 from Plasmodium falciparum Is a Major Target of Opsonizing Antibodies in Individuals with Acquired Immunity against Malaria.* Clin Vaccine Immunol, 2017. **24**(11).

149. Metzger, W.G., et al., *Serum IgG3 to the Plasmodium falciparum merozoite surface protein 2 is strongly associated with a reduced prospective risk of malaria.* Parasite Immunol, 2003. **25**(6): p. 307-12.

150. Tran, T.M., et al., *Naturally acquired antibodies specific for Plasmodium falciparum reticulocyte-binding protein homologue 5 inhibit parasite growth and predict protection from malaria.* J Infect Dis, 2014. **209**(5): p. 789-98.

151. Niang, M., et al., *STEVOR is a Plasmodium falciparum erythrocyte binding protein that mediates merozoite invasion and rosetting.* Cell Host Microbe, 2014. **16**(1): p. 81-93.

152. Kumaratilake, L.M., et al., *Effects of cytokines, complement, and antibody on the neutrophil respiratory burst and phagocytic response to Plasmodium falciparum merozoites.* Infect Immun, 1992. **60**(9): p. 3731-8.

153. Osier, F.H., et al., *Opsonic phagocytosis of Plasmodium falciparum merozoites: mechanism in human immunity and a correlate of protection against malaria.* BMC Med, 2014. **12**: p. 108.

154. Kennedy, A.T., et al., *Recruitment of Factor H as a Novel Complement Evasion Strategy for Blood-Stage Plasmodium falciparum Infection.* J Immunol, 2016. **196**(3): p. 1239-48.

155. Murungi, L.M., et al., *Targets and Mechanisms Associated with Protection from Severe Plasmodium falciparum Malaria in Kenyan Children.* Infect Immun, 2016. **84**(4): p. 950-63.

156. Healer, J., A. Graszynski, and E. Riley, *Phagocytosis does not play a major role in naturally acquired transmission-blocking immunity to Plasmodium falciparum malaria.* Infect Immun, 1999. **67**(5): p. 2334-9.

157. Sutherland, C.J., *Surface antigens of Plasmodium falciparum gametocytes--a new class of transmission-blocking vaccine targets?* Mol Biochem Parasitol, 2009. **166**(2): p. 93-8.

158. Gebru, T., et al., *Recognition of Plasmodium falciparum mature gametocyte-infected erythrocytes by antibodies of semi-immune adults and malaria-exposed children from Gabon.* Malar J, 2017. **16**(1): p. 176.

159. Mulder, B., et al., *Malaria transmission-blocking activity in experimental infections of Anopheles gambiae from naturally infected Plasmodium falciparum gametocyte carriers.* Trans R Soc Trop Med Hyg, 1994. **88**(1): p. 121-5.

160. Ouedraogo, A.L., et al., *Naturally acquired immune responses to Plasmodium falciparum sexual stage antigens Pfs48/45 and Pfs230 in an area of seasonal transmission.* Infect Immun, 2011. **79**(12): p. 4957-64.

161. Healer, J., et al., *Complement-mediated lysis of Plasmodium falciparum gametes by malaria-immune human sera is associated with antibodies to the gamete surface antigen Pfs230.* Infect Immun, 1997. **65**(8): p. 3017-23.

162. Clyde, D.F., et al., *Immunization of man against sporozite-induced falciparum malaria.* Am J Med Sci, 1973. **266**(3): p. 169-77.

163. Spring, M., et al., *First-in-human evaluation of genetically attenuated Plasmodium falciparum sporozoites administered by bite of Anopheles mosquitoes to adult volunteers.* Vaccine, 2013. **31**(43): p. 4975-83.

164. Bijker, E.M., et al., *Protection against malaria after immunization by chloroquine prophylaxis and sporozoites is mediated by preerythrocytic immunity.* Proc Natl Acad Sci U S A, 2013. **110**(19): p. 7862-7.

165. Epstein, J.E., et al., *Protection against Plasmodium falciparum malaria by PfSPZ Vaccine.* JCI Insight, 2017. **2**(1): p. e89154.

166. Mordmuller, B., et al., *Sterile protection against human malaria by chemoattenuated PfSPZ vaccine.* Nature, 2017. **542**(7642): p. 445-449.

167. Yoshida, N., et al., *Hybridoma produces protective antibodies directed against the sporozoite stage of malaria parasite.* Science, 1980. **207**(4426): p. 71-3.

168. Sherwood, J.A., et al., *Plasmodium falciparum circumsporozoite vaccine immunogenicity and efficacy trial with natural challenge quantitation in an area of endemic human malaria of Kenya.* Vaccine, 1996. **14**(8): p. 817-27.

169. Rutgers, T., et al., *Hepatitis B Surface Antigen as Carrier Matrix for the Repetitive Epitope of the Circumsporozoite Protein of Plasmodium Falciparum.* Bio/Technology, 1988. **6**: p. 1065.

170. Cohen, J., et al., *From the circumsporozoite protein to the RTS, S/AS candidate vaccine.* Hum Vaccin, 2010. **6**(1): p. 90-6.

171. Vanloubbeeck, Y., et al., *Comparison of the immune responses induced by soluble and particulate Plasmodium vivax circumsporozoite vaccine candidates formulated in AS01 in rhesus macaques.* Vaccine, 2013. **31**(52): p. 6216-24.

172. Gomes, A.C., M. Mohsen, and M.F. Bachmann, *Harnessing Nanoparticles for Immunomodulation and Vaccines.* Vaccines (Basel), 2017. **5**(1).

173. Mohsen, M.O., et al., *Major findings and recent advances in virus-like particle (VLP)-based vaccines.* Semin Immunol, 2017. **34**: p. 123-132.

174. RTS,S Clinical Trials Partnership, *Efficacy and safety of the RTS,S/AS01 malaria vaccine during 18 months after vaccination: a phase 3 randomized, controlled trial in children and young infants at 11 African sites.* PLoS Med, 2014. **11**(7): p. e1001685.

175. RTS,S Clinical Trials Partnership, *Efficacy and safety of RTS,S/AS01 malaria vaccine with or without a booster dose in infants and children in Africa: final results of a phase 3, individually randomised, controlled trial.* Lancet, 2015. **386**(9988): p. 31-45.

176. Hoffman, S.L., et al., *Sporozoite vaccine induces genetically restricted T cell elimination of malaria from hepatocytes.* Science, 1989. **244**(4908): p. 1078-81.

177. Rodrigues, M.M., et al., *CD8+ cytolytic T cell clones derived against the Plasmodium yoelii circumsporozoite protein protect against malaria.* Int Immunol, 1991. **3**(6): p. 579-85.

178. Romero, P., et al., *Cloned cytotoxic T cells recognize an epitope in the circumsporozoite protein and protect against malaria.* Nature, 1989. **341**(6240): p. 323-6.

179. Schofield, L., et al., *Gamma interferon, CD8+ T cells and antibodies required for immunity to malaria sporozoites.* Nature, 1987. **330**(6149): p. 664-6.

180. Weiss, W.R., et al., *CD8+ T cells (cytotoxic/suppressors) are required for protection in mice immunized with malaria sporozoites.* Proc Natl Acad Sci U S A, 1988. **85**(2): p. 573-6.

181. Liu, M.A., *Immunologic basis of vaccine vectors.* Immunity, 2010. **33**(4): p. 504-15.

182. Dunachie, S.J., et al., *A DNA prime-modified vaccinia virus ankara boost vaccine encoding thrombospondin-related adhesion protein but not circumsporozoite protein partially protects healthy malaria-naive adults against Plasmodium falciparum sporozoite challenge.* Infect Immun, 2006. **74**(10): p. 5933-42.

183. McConkey, S.J., et al., *Enhanced T-cell immunogenicity of plasmid DNA vaccines boosted by recombinant modified vaccinia virus Ankara in humans.* Nat Med, 2003. **9**(6): p. 729-35.

184. Ewer, K.J., et al., *Protective CD8+ T-cell immunity to human malaria induced by chimpanzee adenovirus-MVA immunisation.* Nat Commun, 2013. **4**: p. 2836.

185. Rampling, T., et al., *Safety and High Level Efficacy of the Combination Malaria Vaccine Regimen of RTS,S/AS01B With Chimpanzee Adenovirus 63 and Modified Vaccinia Ankara Vectored Vaccines Expressing ME-TRAP.* J Infect Dis, 2016. **214**(5): p. 772-81.

186. Baruch, D.I., et al., *Immunization of Aotus monkeys with a functional domain of the Plasmodium falciparum variant antigen induces protection against a lethal parasite line.* Proc Natl Acad Sci U S A, 2002. **99**(6): p. 3860-5.

187. El Sahly, H.M., et al., *Safety and immunogenicity of a recombinant nonglycosylated erythrocyte binding antigen 175 Region II malaria vaccine in healthy adults living in an area where malaria is not endemic.* Clin Vaccine Immunol, 2010. **17**(10): p. 1552-9.

188. Elias, S.C., et al., *Assessment of immune interference, antagonism, and diversion following human immunization with biallelic blood-stage malaria viral-vectored vaccines and controlled malaria infection.* J Immunol, 2013. **190**(3): p. 1135-47.

189. Jepsen, M.P., et al., *The malaria vaccine candidate GMZ2 elicits functional antibodies in individuals from malaria endemic and non-endemic areas.* J Infect Dis, 2013. **208**(3): p. 479-88.

190. McCarthy, J.S., et al., *A phase 1 trial of MSP2-C1, a blood-stage malaria vaccine containing 2 isoforms of MSP2 formulated with Montanide(R) ISA 720.* PLoS One, 2011. **6**(9): p. e24413.

191. Palacpac, N.M., et al., *Phase 1b randomized trial and follow-up study in Uganda of the blood-stage malaria vaccine candidate BK-SE36.* PLoS One, 2013. **8**(5): p. e64073.

192. Sagara, I., et al., *A randomized controlled phase 2 trial of the blood stage AMA1-C1/Alhydrogel malaria vaccine in children in Mali.* Vaccine, 2009. **27**(23): p. 3090-8.

193. Douglas, A.D., et al., *The blood-stage malaria antigen PfRH5 is susceptible to vaccine-inducible cross-strain neutralizing antibody.* Nat Commun, 2011. **2**: p. 601.

194. Douglas, A.D., et al., *Neutralization of Plasmodium falciparum merozoites by antibodies against PfRH5.* J Immunol, 2014. **192**(1): p. 245-58.

195. Reddy, K.S., et al., *Bacterially expressed full-length recombinant Plasmodium falciparum RH5 protein binds erythrocytes and elicits potent strain-transcending parasite-neutralizing antibodies.* Infect Immun, 2014. **82**(1): p. 152-64.

196. Vaccines, m.C.G.o., *A research agenda for malaria eradication: vaccines.* PLoS Med, 2011. **8**(1): p. e1000398.

197. Niederwieser, I., I. Felger, and H.P. Beck, *Limited polymorphism in Plasmodium falciparum sexual-stage antigens.* Am J Trop Med Hyg, 2001. **64**(1-2): p. 9-11.

198. Sinden, R.E., et al., *The design and interpretation of laboratory assays measuring mosquito transmission of Plasmodium.* Trends Parasitol, 2012. **28**(11): p. 457-65.

199. Miura, K., et al., *Qualification of standard membrane-feeding assay with Plasmodium falciparum malaria and potential improvements for future assays.* PLoS One, 2013. **8**(3): p. e57909.

200. Wu, Y., et al., *Phase 1 trial of malaria transmission blocking vaccine candidates Pfs25 and Pvs25 formulated with montanide ISA 51.* PLoS One, 2008. **3**(7): p. e2636.

201. Shimp, R.L., Jr., et al., *Development of a Pfs25-EPA malaria transmission blocking vaccine as a chemically conjugated nanoparticle.* Vaccine, 2013. **31**(28): p. 2954-62.

202. Talaat, K.R., et al., *Safety and Immunogenicity of Pfs25-EPA/Alhydrogel(R), a Transmission Blocking Vaccine against Plasmodium falciparum: An Open Label Study in Malaria Naive Adults.* PLoS One, 2016. **11**(10): p. e0163144.

203. Cheru, L., et al., *The IC(50) of anti-Pfs25 antibody in membrane-feeding assay varies among species.* Vaccine, 2010. **28**(27): p. 4423-9.

204. Li, Y., et al., *Enhancing immunogenicity and transmission-blocking activity of malaria vaccines by fusing Pfs25 to IMX313 multimerization technology.* Sci Rep, 2016. **6**: p. 18848.

205. MacDonald, N.J., et al., *Structural and Immunological Characterization of Recombinant 6-Cysteine Domains of the Plasmodium falciparum Sexual Stage Protein Pfs230.* J Biol Chem, 2016. **291**(38): p. 19913-22.

206. Theisen, M., M.M. Jore, and R. Sauerwein, *Towards clinical development of a Pfs48/45-based transmission blocking malaria vaccine.* Expert Rev Vaccines, 2017. **16**(4): p. 329-336.

207. Salazar, C.E., et al., *Sequence of a cDNA from the mosquito Anopheles gambiae encoding a homologue of human ribosomal protein S7.* Nucleic Acids Res, 1993. **21**(17): p. 4147.

208. Morefield, G.L., et al., *Role of aluminum-containing adjuvants in antigen internalization by dendritic cells in vitro.* Vaccine, 2005. **23**(13): p. 1588-95.

209. Didierlaurent, A.M., et al., *Adjuvant system AS01: helping to overcome the challenges of modern vaccines.* Expert Rev Vaccines, 2017. **16**(1): p. 55-63.

210. Bengtsson, K.L., et al., *Matrix-M adjuvant: enhancing immune responses by 'setting the stage' for the antigen.* Expert Rev Vaccines, 2013. **12**(8): p. 821-3.

211. Fang, J.-H. and M. Hora, *The Adjuvant MF59: A 10-Year Perspective Gary Ott, Ramachandran Radhakrishnan*, in *Vaccine Adjuvants: Preparation Methods and Research Protocols*, D.T. O'Hagan, Editor. 2000, Springer New York: Totowa, NJ. p. 211-228.

212. Bushell, K.M., et al., *Large-scale screening for novel low-affinity extracellular protein interactions.* Genome Res, 2008. **18**(4): p. 622-30.

213. Cohen, S.N., A.C. Chang, and L. Hsu, *Nonchromosomal antibiotic resistance in bacteria: genetic transformation of Escherichia coli by R-factor DNA.* Proc Natl Acad Sci U S A, 1972. **69**(8): p. 2110-4.

214. Kerr, J.S. and G.J. Wright, *Avidity-based extracellular interaction screening (AVEXIS) for the scalable detection of low-affinity extracellular receptor-ligand interactions.* J Vis Exp, 2012(61): p. e3881.

215. Miura, K., et al., *Functional comparison of Plasmodium falciparum transmission-blocking vaccine candidates by the standard membrane-feeding assay.* Infect Immun, 2013. **81**(12): p. 4377-82.

216. Nardin, E.H., et al., *Circumsporozoite proteins of human malaria parasites Plasmodium falciparum and Plasmodium vivax.* J Exp Med, 1982. **156**(1): p. 20-30.

217. Gordon, D.M., et al., *Safety, immunogenicity, and efficacy of a recombinantly produced Plasmodium falciparum circumsporozoite protein-hepatitis B surface antigen subunit vaccine.* J Infect Dis, 1995. **171**(6): p. 1576-85.

218. Leach, A., et al., *Design of a phase III multicenter trial to evaluate the efficacy of the RTS,S/AS01 malaria vaccine in children across diverse transmission settings in Africa.* Malar J, 2011. **10**: p. 224.

219. Rts, S.C.T.P., et al., *A phase 3 trial of RTS,S/AS01 malaria vaccine in African infants.* N Engl J Med, 2012. **367**(24): p. 2284-95.

220. European Medicines Agency, *First malaria vaccine receives positive scientific opinion from EMA*. 2015: London, United Kingdom.

221. World-Health-Organisation, *Malaria vaccine: WHO position paper – January 2016*. 2016.

222. Collins, K.A., et al., *Enhancing protective immunity to malaria with a highly immunogenic virus-like particle vaccine.* Sci Rep, 2017. **7**: p. 46621.

223. White, M.T., et al., *Immunogenicity of the RTS,S/AS01 malaria vaccine and implications for duration of vaccine efficacy: secondary analysis of data from a phase 3 randomised controlled trial.* Lancet Infect Dis, 2015. **15**(12): p. 1450-8.

224. Jin, J., et al., *Accelerating the clinical development of protein-based vaccines for malaria by efficient purification using a four amino acid C-terminal 'C-tag'.* Int J Parasitol, 2017. **47**(7): p. 435-446.

225. Phogat, S., et al., *Analysis of the human immunodeficiency virus type 1 gp41 membrane proximal external region arrayed on hepatitis B surface antigen particles.* Virology, 2008. **373**(1): p. 72-84.

226. Lell, B., et al., *A randomized trial assessing the safety and immunogenicity of AS01 and AS02 adjuvanted RTS,S malaria vaccine candidates in children in Gabon.* PLoS One, 2009. **4**(10): p. e7611.

227. Aide, P., et al., *Four year immunogenicity of the RTS,S/AS02(A) malaria vaccine in Mozambican children during a phase IIb trial.* Vaccine, 2011. **29**(35): p. 6059-67.

228. Hill, A.V., et al., *Towards a multi-antigen multi-stage malaria vaccine.* Malaria Journal, 2014. **13**(1): p. O31.

229. Tran, T.M., et al., *Malaria Vaccines: Moving Forward After Encouraging First Steps.* Curr Trop Med Rep, 2015. **2**(1): p. 1-3.

230. Boes, A., et al., *Analysis of a Multi-component Multi-stage Malaria Vaccine Candidate--Tackling the Cocktail Challenge.* PLoS One, 2015. **10**(7): p. e0131456.

231. Kaiser, K., et al., *A member of a conserved Plasmodium protein family with membrane-attack complex/perforin (MACPF)-like domains localizes to the micronemes of sporozoites.* Mol Biochem Parasitol, 2004. **133**(1): p. 15-26.

232. Kaslow, D.C., et al., *Saccharomyces cerevisiae recombinant Pfs25 adsorbed to alum elicits antibodies that block transmission of Plasmodium falciparum.* Infect Immun, 1994. **62**(12): p. 5576-80.

233. Nikolaeva, D., S.J. Draper, and S. Biswas, *Toward the development of effective transmission-blocking vaccines for malaria.* Expert Rev Vaccines, 2015. **14**(5): p. 653-80.

234. Zhao, Q., et al., *Maturation of recombinant hepatitis B virus surface antigen particles.* Hum Vaccin, 2006. **2**(4): p. 174-80.

235. Veggiani, G., et al., *Programmable polyproteams built using twin peptide superglues.* Proc Natl Acad Sci U S A, 2016. **113**(5): p. 1202-7.

236. Zakeri, B., et al., *Peptide tag forming a rapid covalent bond to a protein, through engineering a bacterial adhesin.* Proc Natl Acad Sci U S A, 2012. **109**(12): p. E690-7.

237. Brune, K.D., et al., *Dual Plug-and-Display Synthetic Assembly Using Orthogonal Reactive Proteins for Twin Antigen Immunization.* Bioconjug Chem, 2017. **28**(5): p. 1544-1551.

238. Brune, K.D., et al., *Plug-and-Display: decoration of Virus-Like Particles via isopeptide bonds for modular immunization.* Sci Rep, 2016. **6**: p. 19234.

239. malERA Consultative Group on Vaccines, *A research agenda for malaria eradication: vaccines.* PLoS Med, 2011. **8**(1): p. e1000398.

240. malERA Refresh Consultative Panel on Tools for Malaria Elimination, *malERA: An updated research agenda for diagnostics, drugs, vaccines, and vector control in malaria elimination and eradication.* PLoS Med, 2017. **14**(11): p. e1002455.

241. Zahid, M., H. Lunsdorf, and U. Rinas, *Assessing stability and assembly of the hepatitis B surface antigen into virus-like particles during down-stream processing.* Vaccine, 2015. **33**(31): p. 3739-45.

242. Siden-Kiamos, I., et al., *Distinct roles for pbs21 and pbs25 in the in vitro ookinete to oocyst transformation of Plasmodium berghei.* J Cell Sci, 2000. **113 Pt 19**: p. 3419-26.

243. Trottein, F., T. Triglia, and A.F. Cowman, *Molecular cloning of a gene from Plasmodium falciparum that codes for a protein sharing motifs found in adhesive molecules from mammals and plasmodia.* Mol Biochem Parasitol, 1995. **74**(2): p. 129-41.

244. Li, F., et al., *Plasmodium ookinete-secreted proteins secreted through a common micronemal pathway are targets of blocking malaria transmission.* J Biol Chem, 2004. **279**(25): p. 26635-44.

245. Dessens, J.T., et al., *SOAP, a novel malaria ookinete protein involved in mosquito midgut invasion and oocyst development.* Mol Microbiol, 2003. **49**(2): p. 319-29.

246. Ecker, A., et al., *Reverse genetics screen identifies six proteins important for malaria development in the mosquito.* Mol Microbiol, 2008. **70**(1): p. 209-20.

247. Dinglasan, R.R., et al., *Disruption of Plasmodium falciparum development by antibodies against a conserved mosquito midgut antigen.* Proc Natl Acad Sci U S A, 2007. **104**(33): p. 13461-6.

248. Kotsyfakis, M., et al., *Plasmodium berghei ookinetes bind to Anopheles gambiae and Drosophila melanogaster annexins.* Mol Microbiol, 2005. **57**(1): p. 171-9.

249. Lavazec, C., et al., *cpbAg1 encodes an active carboxypeptidase B expressed in the midgut of Anopheles gambiae.* Insect Mol Biol, 2005. **14**(2): p. 163-74.

250. Gonzalez-Lazaro, M., et al., *Anopheles gambiae Croquemort SCRBQ2, expression profile in the mosquito and its potential interaction with the malaria parasite Plasmodium berghei.* Insect Biochem Mol Biol, 2009. **39**(5-6): p. 395-402.

251. Rodriguez Mdel, C., et al., *The surface protein Pvs25 of Plasmodium vivax ookinetes interacts with calreticulin on the midgut apical surface of the malaria vector Anopheles albimanus.* Mol Biochem Parasitol, 2007. **153**(2): p. 167-77.

252. Wass, M.N., et al., *Proteomic analysis of Plasmodium in the mosquito: progress and pitfalls.* Parasitology, 2012. **139**(9): p. 1131-45.

253. Petersen, T.N., et al., *SignalP 4.0: discriminating signal peptides from transmembrane regions.* Nat Methods, 2011. **8**(10): p. 785-6.

254. Krogh, A., et al., *Predicting transmembrane protein topology with a hidden Markov model: application to complete genomes.* J Mol Biol, 2001. **305**(3): p. 567-80.

255. Sonnhammer, E.L., G. von Heijne, and A. Krogh, *A hidden Markov model for predicting transmembrane helices in protein sequences.* Proc Int Conf Intell Syst Mol Biol, 1998. **6**: p. 175-82.

256. Eisenhaber, B., P. Bork, and F. Eisenhaber, *Sequence properties of GPI-anchored proteins near the omega-site: constraints for the polypeptide binding site of the putative transamidase.* Protein Eng, 1998. **11**(12): p. 1155-61.

257. Eisenhaber, B., P. Bork, and F. Eisenhaber, *Prediction of potential GPI-modification sites in proprotein sequences.* J Mol Biol, 1999. **292**(3): p. 741-58.

258. Sunyaev, S.R., et al., *PSIC: profile extraction from sequence alignments with position-specific counts of independent observations.* Protein Eng, 1999. **12**(5): p. 387-94.

259. Foth, B.J., et al., *Dissecting apicoplast targeting in the malaria parasite Plasmodium falciparum.* Science, 2003. **299**(5607): p. 705-8.

260. Emanuelsson, O., et al., *Predicting subcellular localization of proteins based on their N-terminal amino acid sequence.* J Mol Biol, 2000. **300**(4): p. 1005-16.

261. Hernandez-Romano, J., et al., *Conserved peptide sequences bind to actin and enolase on the surface of Plasmodium berghei ookinetes.* Parasitology, 2011. **138**(11): p. 1341-53.

262. Kelley, L.A., et al., *The Phyre2 web portal for protein modeling, prediction and analysis.* Nat Protoc, 2015. **10**(6): p. 845-58.

263. Parish, L.A., et al., *Ookinete-interacting proteins on the microvillar surface are partitioned into detergent resistant membranes of Anopheles gambiae midguts.* J Proteome Res, 2011. **10**(11): p. 5150-62.

264. Horn, T. and M. Boutros, *E-RNAi: a web application for the multi-species design of RNAi reagents--2010 update.* Nucleic Acids Res, 2010. **38**(Web Server issue): p. W332-9.

265. Wright, G.J., *Signal initiation in biological systems: the properties and detection of transient extracellular protein interactions.* Mol Biosyst, 2009. **5**(12): p. 1405-12.

266. van der Merwe, P.A., et al., *Affinity and kinetic analysis of the interaction of the cell adhesion molecules rat CD2 and CD48.* EMBO J, 1993. **12**(13): p. 4945-54.

267. Baker, D.A., et al., *A comprehensive gene expression atlas of sex- and tissue-specificity in the malaria vector, Anopheles gambiae.* BMC Genomics, 2011. **12**: p. 296.

268. Heppner, D.G., Jr., et al., *Towards an RTS,S-based, multi-stage, multi-antigen vaccine against falciparum malaria: progress at the Walter Reed Army Institute of Research.* Vaccine, 2005. **23**(17-18): p. 2243-50.

269. Salman, A.M., et al., *Rational development of a protective P. vivax vaccine evaluated with transgenic rodent parasite challenge models.* Sci Rep, 2017. **7**: p. 46482.

270. Theisen, M., et al., *A multi-stage malaria vaccine candidate targeting both transmission and asexual parasite life-cycle stages.* Vaccine, 2014. **32**(22): p. 2623-30.

271. Blackman, M.J. and A.A. Holder, *Secondary processing of the Plasmodium falciparum merozoite surface protein-1 (MSP1) by a calcium-dependent membrane-bound serine protease: shedding of MSP133 as a noncovalently associated complex with other fragments of the MSP1.* Mol Biochem Parasitol, 1992. **50**(2): p. 307-15.

272. Holder, A.A., et al., *A malaria merozoite surface protein (MSP1)-structure, processing and function.* Mem Inst Oswaldo Cruz, 1992. **87 Suppl 3**: p. 37-42.

273. Roux, K.J., D.I. Kim, and B. Burke, *BioID: a screen for protein-protein interactions.* Curr Protoc Protein Sci, 2013. **74**: p. Unit 19 23.

274. Roux, K.J., et al., *A promiscuous biotin ligase fusion protein identifies proximal and interacting proteins in mammalian cells.* J Cell Biol, 2012. **196**(6): p. 801-10.

275. Kim, D.I., et al., *An improved smaller biotin ligase for BioID proximity labeling.* Mol Biol Cell, 2016. **27**(8): p. 1188-96.